

BIOCHEMISTRY OF TOPOISOMERASE INHIBITION AND  
CELLULAR MECHANISMS OF ANTHRAQUINONE-AMINO ACID  
CONJUGATES *IN VITRO*

A THESIS SUBMITTED IN PARTIAL FULFILLMENT OF THE REQUIREMENTS  
OF NAPIER UNIVERSITY FOR THE DEGREE OF DOCTOR OF PHILOSOPHY

BY

**SUSANNE PETTERSSON**

MARCH 2004

## ABSTRACT

NU:UB compounds are novel spacer-linked amino acid substituted anthraquinone derivatives; several of these, including an *in vivo*-active lead compound NU:UB 31, are cytotoxic *in vitro* in a range of human and animal cancer cell lines, with selectivity for melanoma and colon cancers. Topoisomerase enzymes have proved to be valid targets for anti-cancer therapeutics. The NU:UB compounds were designed to be inhibitors of DNA topoisomerase I and II enzymes.

This study has focused on NU:UB 31 (and, in part, on structural analogues) to investigate the mechanism of action of this compound *in vitro*. NU:UB 31 was cytotoxic in the low micro-molar range in human leukaemia, as well as in colon cancer cell lines, as early as 4h following treatment. NU:UB 31, exhibited DNA intercalation and minor groove binding properties (that are thought to facilitate interactions with topoisomerase II and topoisomerase I respectively). Topoisomerase I-mediated DNA relaxation (of supercoiled plasmid) was inhibited completely by NU:UB 31 at 50 $\mu$ M. Topoisomerase II $\alpha$  and II $\beta$  inhibition was achieved by NU:UB 31 concentrations of 25 $\mu$ M and 20 $\mu$ M respectively. NU:UB 31 also induced drug-stabilised topoisomerase I and II ( $\alpha$  and  $\beta$  isoforms) cleavable complex formation in intact HL60 cells determined by immunoband depletion of the Western blot protein signals. Therefore, unlike most clinically used chemotherapeutics that act via one type of topoisomerase, there was evidence to suggest that NU:UB 31 was a dual topoisomerase inhibitor, which may explain observations that NU:UB 31 can circumvent drug resistance mediated by altered topoisomerase expression, levels and functions.

Cellular, morphological and biochemical apoptotic changes were investigated following NU:UB 31 treatment. In HL60 cells caspase activation, indicative of apoptosis induction, was recorded after 4h 20 $\mu$ M NU:UB 31 treatment; DNA fragmentation was evident following 6h NU:UB 31 treatment. Furthermore, the amount of cells with DNA content less than G1 had more than doubled following 1h of NU:UB 31 treatment. Additionally, over 20% of HL60 cells showed apoptotic morphology following 8h NU:UB 31 treatment. Although the tumour suppressor p53 protein levels were significantly increased following 3h of NU:UB 31 (at 20  $\mu$ M) treatment of p53+ HCT116 cells, there was also evidence to suggest that p53-independent apoptotic pathways could play a part in NU:UB cytotoxicity. NU:UB compounds had equipotent GI<sub>50</sub> values in NCI p53 wild type and p53 mutant cell lines, suggesting a p53-independent mechanism together with, or in place of, a p53-dependent mechanism of action. Confocal microscopic drug accumulation observations revealed a significant cytosolic (in particular lysosomal) localisation of NU:UB 31. This, in addition to NCI drug target Compare data suggested that mitochondria may be an additional NU:UB compound target. Collectively, these findings support the prediction that molecular events triggered via topoisomerase enzymes lead to NU:UB 31-induced apoptosis, and further identify mitochondria as a putative additional molecular target of NU:UB 31.

# CONTENTS

Acknowledgements	i
Preface	ii
List Of Abbreviations	vi
List Of Figures	viii
List Of Tables	xiv
HYPOTHESIS	1
AIMS	1
CHAPTER 1 GENERAL INTRODUCTION	2
1.1 CANCER	3
1.2 DNA TOPOISOMERASES	5
1.2.1 Topoisomerase I	7
1.2.2 Topoisomerase II	8
1.3 INHIBITION OF TOPOISOMERASES	12
1.3.1 Inhibitors and Poisons	12
1.3.2 DNA Binding Mode	14
1.3.3 Anti-topoisomerase Drugs And Their Side Effects	15
1.4 DRUG RESISTANCE	18
1.4.1 Multi Drug Resistance And Transporter Proteins	18
1.5 NU:UB COMPOUNDS	20
1.6 THE CELL CYCLE	24
1.6.1 Cell Cycle Phases And Checkpoints	24
1.6.2 Cell Cycle Regulation	25
1.6.3 The Cell Cycle And Topoisomerases	29
1.7 APOPTOSIS	30
1.7.1 Characteristic Features Of Apoptotic Cells	31
1.7.1a Morphological Changes	31
1.7.1b Biochemical Changes	33
1.7.2 Necrosis	34
1.7.3 Apoptosis And Therapeutics	35
1.8 P21	36
1.8.1 P21 In Cell Cycle Arrest And Apoptosis	38
1.9 P53	40
1.9.1 Cell Cycle Arrest Or Apoptosis?	42
1.9.2 P53 In Cell Cycle Arrest	43
1.9.3 P53 In Apoptosis	43
1.9.4 P53 Mutations	46
1.9.5 P53 Interactions With Topoisomerases	47
1.9.6 P53 And Therapeutics	48
1.10 MDM2	51
1.11 CASPASES	55
1.11.1 Caspases In Apoptosis	55
1.11.1a Initiation	57
1.11.1b Commitment	58

1.11.1c	Amplification	58
1.11.1d	Demolition	59
1.11.2	Caspase-3	61
1.11.3	Apoptosis In Resistant Cells Via Caspase Activation	62
1.12	MITOCHONDRIA	63
1.12.1	Mitochondrial Structure	63
1.12.2	Mitochondrial Function	64
1.12.2a	ATP Production	64
1.12.2b	Mitochondria And Calcium	65
1.12.2c	Mitochondria And Apoptosis	66
1.12.3	Mitochondria As Potential Drug Targets	68
CHAPTER 2		70
2.1	MATERIALS AND GENERAL METHODS	71
2.1.1	Anti-cancer Agents	71
2.1.2a	Materials For Cell Culture	71
2.1.2b	Method For Cell Culture	72
2.1.3	Materials For Cytotoxicity Assays	72
2.1.4	Materials For DNA Mobility Assays	73
2.1.5a	Materials For Lysing Cells	73
2.1.5b	Method For Lysing Cells With Protease Inhibitors	74
2.1.6a	Materials For Bicinchoninic Acid Protein Assays	74
2.1.6b	Method For Bicinchoninic Acid Protein Assays	74
2.1.7a	Materials For Western Blotting And Immunostaining	75
2.1.7b	Antibodies And Probes	78
2.1.7c	Method For Western Blotting	78
2.1.7d	Dot Blot Assay For Determining The Primary Antibody Concentration To Be Used In The Western Blotting Experiments	80
2.1.7e	Stripping Solution For Western Blot Membranes	80
2.1.8	Materials For Apoptotic Investigations	81
2.1.9	Equipments	81
CHAPTER 3		83
3.1	ANTI-TOPOISOMERASE ACTIVITY	84
3.2	METHODS	87
3.2.1	DNA Binding Mode Of NU:UB 31 In Relation To The Comparative Intercalator, Mitoxantrone And The Minor Groove Binder, Netropsin.	87
3.2.1a	Treatment Of Results	88
3.2.2	Topoisomerase I And Topoisomerase II ( $\alpha$ And $\beta$ ) Relaxation Assays	89
3.2.3	Topoisomerase I And Topoisomerase II Immunoband Depletion Assays	90
3.2.4	Topoisomerase I And Topoisomerase II ( $\alpha$ And $\beta$ ) Relaxation Assays	91
3.3	RESULTS	94

3.3.1	DNA Binding Mode Of NU:UB 31 In Relation To Comparative Drugs (Mitoxantrone And Netropsin)	94
3.3.2	Topoisomerase Relaxation Assays	95
3.3.2a	Topoisomerase I Relaxation Assays	95
3.3.2b	Topoisomerase II Relaxation Assays	96
3.3.3	Topoisomerase Cleavage Assays	97
3.3.3a	Topoisomerase I Cleavage Assays	97
3.3.3b	Topoisomerase II Cleavage Assays	98
3.3.4	Topoisomerase Immunoband Depletion Assays	99
3.3.4a	Topoisomerase I Immunoband Depletion Assays	99
3.3.4b	Topoisomerase II Immunoband Depletion Assays	100
3.4	DISCUSSION	111
CHAPTER 4		121
4.1	CYTOTOXICITY	122
4.2	METHODS	125
4.2.1	Growth Curve Of HL60 Cells	125
4.2.2	Cytotoxicity Investigations With The MTT Assay, Preparation And Treatment Of Cells With Anti-cancer Agents	125
4.2.3	Addition Of MTT	126
4.2.3a	Treatment Of Results	126
4.2.4	Cytotoxicity Investigations With Nigrosin Exclusion Cell Count	127
4.2.4a	Treatment Of Results	127
4.3	RESULTS	128
4.3.1	Growth Curve Of HL60 Cells	128
4.3.2	MTT Cytotoxicity Assay Of NU:UB And Standard Drugs Using HL60, HCT116 And HT29 Cells	128
4.3.3	Nigrosin Exclusion Assay Of NU:UB And Standard Drugs Using HL60 Cells	130
4.4	DISUSSION	136
CHAPTER 5		143
5.1	INVESTIGATION OF CELL CYCLE DISTURBANCES FOLLOWING NU:UB TREATMENT	144
5.2	METHODS	146
5.2.1	Growth Curve Of HL60 Cells	146
5.2.2	Analysis Of The Cell Cycle Using Flow Cytometry	146
5.2.2a	Treatment Of Results	148
5.2.3	Analysis Of Apoptosis Using Flow Cytometry	148
5.2.3a	Treatment Of Results	149
5.3	RESULTS	150
5.3.1	Growth Curve Of HL60 Cells	150
5.3.2	Cell Cycle Analysis	150
5.3.2a	Cell Cycle Analysis Of HL60 Cells Following 1h Treatment With NU:UB 31 Or Standard Drugs	150
5.3.2b	Cell Cycle Analysis Of HL60 Cells Following 4h Treatment With NU:UB 31	152

5.3.3	Analysis Of The Sub G1 Population	153
5.4	DISCUSSION	171
CHAPTER 6		178
6.1	INVESTIGATION OF APOPTOTIC CELL DEATH	179
6.2	METHODS	182
6.2.1	Morphology Studies In HL60 Cells Following Treatment With NU:UB Compounds	182
6.2.1a	Treatment Of Results	183
6.2.2	Additional Experiments	183
6.2.3	DNA Laddering Studies Following Treatment With NU:UB Compounds	183
6.2.4	Caspase Activation Studies Following Treatment With NU:UB Compounds	185
6.2.4a	Treatment Of Results	187
6.3	RESULTS	188
6.3.1	Morphology Studies In HL60 Cells Following Treatment With NU:UB Compounds, Camptothecin Or Etoposide	188
6.3.2	Hoechst Staining Of HL60 Cells	189
6.3.3	DNA Laddering Studies Following Treatment With NU:UB Compounds Or Camptothecin	189
6.3.4	Caspase Activation Studies Following Treatment With NU:UB Compounds Or Camptothecin Using The Flow Cytometry	191
6.3.5	Caspase Activation Studies Following Treatment With NU:UB Compounds Or Camptothecin Using The Fluorescent Microscope	192
6.4	DISCUSSION	219
CHAPTER 7		223
7.1	PROTEIN STUDIES	224
7.2	METHODS	227
7.2.1	Investigation Of The P53 Protein Content In HCT116, HT29 And HL60 Cells	227
7.2.2	Investigation Of P53 Protein Levels In HCT116 Cells Treated With NU:UB Compounds Or Doxorubicin	228
7.2.2a	Treatment Of Results	228
7.2.3	P53 protein Immunostaining Of HCT116 Cells Treated With NU:UB Compounds Or Doxorubicin	229
7.2.4	Investigation Of Mdm2 Protein Levels In HCT116 Cells Treated With NU:UB Copmpounds Or Doxorubicin	230
7.2.4a	Treatment Of Results	231
7.2.5	Investigation Of P21 Levels In HCT116 Cells Treated With NU:UB 31 Or Doxorubicin	231
7.2.6	Investigation Of Procaspace-3 Levels In HL60 And HCT116 Cells Treated With NU:UB Compounds, Doxorubicin Or Camptothecin	232
7.3	RESULTS	233
7.3.1	P53 Protein	233

7.3.1a	P53 Protein Contents In HL60, HCT116 And HT29 Cells	233
7.3.1b	Time Course Of P53 Protein Levels In HCT116 Cells	234
7.3.1c	Immunostaining Of HCT116 Cells Treated With NU:UB 31, NU:UB 51 Or Doxorubicin	234
7.3.1d	Relationship Between Drug Sensitivity And P53 Status In NCI Cell Lines	235
7.3.2	Mdm2 Protein	236
7.3.2a	Time Course Of Mdm2 Protein Levels In HCT116 Cells	236
7.3.3	P21 Protein	236
7.3.3a	P21 Levels In HCT116 Cells Treated With NU:UB Compound Or Doxorubicin	236
7.3.3b	HCT116 Cells Grown In Culture Medium Supplemented With 1, 5 Or 10% FBS Concentrations	237
7.3.3c	Time Course Of P21 Levels In HCT116 Cells	237
7.3.4	Procaspase-3 Cleavage In HCT116 And HL60 Cells	238
7.4	DISCUSSION	255
CHAPTER 8		264
8.1	INTRACELLULAR DRUG ACCUMULATION STUDIES	265
8.2	METHODS	268
8.2.1	NU:UB And Doxorubicin Distribution In HL60 Cells	268
8.2.2	Localisation Of The Nucleus In HL60 Cells Treated With NU:UB 31 Or Doxorubicin	268
8.2.3	MitoTracker Green And Hoechst Staining Of NU:UB 31 Treated HL60 Cells	269
8.2.4	Investigation Of Mitochondria Disruption In HL60 Cells With MitoCapture Kit	270
8.2.5	LysoTracker Green And Hoechst Staining Of NU:UB 31 Treated HL60 Cells	272
8.3	RESULTS	273
8.3.1	Time Course Of NU:UB 31, NU:UB 80 And Doxorubicin Treated HL60 Cells	273
8.3.2	Hoechst Staining Of NU:UB 31 Treated HL60 Cells To Visualise Nucleus	273
8.3.3	MitoTracker Green And Hoechst Staining Of NU:UB 31 Treated Cells	274
8.3.4	Investigation Of Mitochondria Disruptions In HL60 Cells With MitoCapture	275
8.3.5	LysoTracker Green And Hoechst Staining Of NU:UB 31 Treated HL60 Cells	276
8.4	DISCUSSION	291
CHAPTER 9		303
9.0	SUMMARY DISCUSSION	304
CONCLUSION AND FURTHER RESEARCH		316
REFERENCES		320

## **DECLARATION**

The work presented in this thesis was carried out under the supervision of Dr. David Mincher, Cancer Research Group, Napier University, Edinburgh. This work was carried out independently and has not been submitted for any other degree.

## **ACKNOWLEDGEMENTS**

I would like to acknowledge my supervisor Dr David Mincher who I am indebted for his guidance throughout the course of my studies. I am also grateful for the encouragement from everybody else in the Cancer Research Group at Napier University.

From the Biomedicine Research Group at Napier University, I would like to thank my second supervisor Dr Keith Guy for the time he has dedicated to my work, and of course, thanks to everybody else working in the biomedicine lab.

I am appreciative for the opportunity I got to spend at the Cancer Research Unit in Bradford. I particularly want to thank David Swaine who was of great help with the FACS and confocal work, and my third supervisor Professor Mike Bibby for his advice and guidance.

Finally, much appreciation goes to my friends, partner and family for their support, patience and constant belief in me, without them much of what follows would not have been possible.

## PREFACE

Anthraquinone-based compounds, shown to target DNA topoisomerase enzymes, have been used in the cancer clinic for many years. The clinical use of these agents is unfortunately, limited due to dose-limiting toxic side effects associated with non-topoisomerase, secondary mechanisms of action and the development of drug resistance. In this research programme novel spacer-linked anthraquinone-amino acid conjugates (code named NU:UB and represented by the lead compound NU:UB 31, a novel anthraquinone-L-proline amino acid conjugate), initially developed to exert cytotoxicity by selectively inhibiting topoisomerase enzymes, were investigated for their mechanism of action *in vitro*.

Chapter 1 gives a general introduction to topoisomerases and topoisomerase inhibition. The problems of toxic side effects and resistance to current drugs is introduced. Furthermore, drug induced cell cycle disruptions and apoptotic cell death, as well as apoptotic related proteins including p53 and caspases are discussed, since these are important determinants of the outcome of chemotherapeutic treatments and were properties investigated in respect of the novel agents used in this research programme.

The materials and general methods for the experiments performed in this study are detailed in Chapter 2; the data obtained and the discussion of the results are contained within Chapters 3 to 8.

Firstly, results from the study of anti-topoisomerase activity, with investigations of the topoisomerase (I, II $\alpha$  and II $\beta$ ) inhibition and poisoning activity of the NU:UB drugs (focusing on NU:UB 31) are given in Chapter 3.

Chapter 4 goes on to discuss data to establish the cytotoxicity of NU:UB agents in human cancer cell lines. Following this, cell cycle disruption studies in cell lines exposed to NU:UB 31 in comparison with known topoisomerase inhibitors have been presented in Chapter 5.

Chapter 6 presents data of investigations into morphological and biochemical evidence of induction of apoptotic cell death following NU:UB treatment of human cancer cells. These apoptotic studies included DNA laddering using agarose gel electrophoresis, and caspase activation using UV fluorescent microscopy and flow cytometry.

Alterations in protein levels involved in the regulation of the cell cycle (notably including p21, p53 and mdm-2) and apoptotic cell death have been investigated following NU:UB treatments and the results are presented in Chapter 7.

Chapter 8 contains the observations of a confocal microscopic study of the sub-cellular localisation of NU:UB 31 in cells.

Chapter 9 affords a summary discussion of the collated results (of the separate studies compiled in Chapters 3 to 8), that highlights the key findings for the NU:UB agents in the setting of contemporary topoisomerase-targeting drugs and incorporates conclusions and suggestions for future work with the NU:UB agents that are identified as important for their continuing pre-clinical development.

Results from this research programme have been reported, in part, in the following publications:

Novel dual topoisomerase (I and II) inhibitors displaying high selectivity in colon carcinoma. Mincher DJ, Turnbull A, **Pettersson S**, Bibby MC, Double JA, Br. J. Cancer, (2000), 83(Suppl. 1), P162.

NU:UB 31: A novel *in vivo*-active dual topoisomerase I and II inhibitor with high selectivity in colon carcinoma. Mincher DJ, Turnbull A, **Pettersson S**, Bibby MC, Double JA, Clinical Cancer Research, (2000), 6(Suppl.), 249.

Design of new topoisomerase I inhibitors: Synthesis and *in vitro* activity. Mincher DJ, Kay G, **Pettersson S**, Turnbull A, Bibby MC, B. J. Cancer, (2001), 85(Suppl. 1), 92.

*In vitro* and *in vivo*-active anthraquinone peptide conjugates: A putative pharmacophore for colon specificity. **Pettersson S**, Turnbull A, Kay G, Bibby MC, Double JA, Mincher DJ, Br. J. Cancer, (2001), 85(Suppl. 1), 92.

NU:UB 199, a new colon selective agent that targets topoisomerase I and II. Mincher DJ, Turnbull A, Kay G, Young L, **Pettersson S**, Bibby MC, Double JA, Clinical Cancer Research, (2001), 7(11)(Suppl.), 452.

Mincher DJ, Turnbull A, Kay G, Young L, **Pettersson S**, Bibby MC, Double JA. NU:UB 199, a new dual inhibitor of topoisomerase I and II with selectivity for colon carcinoma, Proceedings of the American Association for Cancer Research, (2002), 43, 1157.

NU:UB 199: A new colon selective agent that targets topoisomerase I and the beta-isoform of topoisomerase II. Young L, Mincher DJ, Turnbull A, Kay G, **Pettersson S**, Bibby MC, Double JA, Br. J. Cancer, (2002), 86(Suppl. 1), P230.

## LIST OF ABBREVIATIONS

AIF	Apoptosis inducing factor
APS	Ammonium persulphate
ATP	Adenosine triphosphate
BSA	Bovine serum albumin
Caspases	<u>Cysteine-Aspartate Proteases</u>
Cdk	Cyclin dependent kinase
CHO	Chinese hamster ovary (cell line)
Cip1	Cdk-interacting protein
CKI	Cyclin dependent kinase inhibitors
CMT	Camptothecin
CO <sub>2</sub>	Carbon dioxide
DMSO	Dimethyl sulphoxide
DNA	Deoxyribonucleic acid
DNase	Deoxyribonuclease
Dox	Doxorubicin
ECL	Enhanced chemiluminescence
EDTA	Ethylene diamine tetraacetic acid
Em	Emission
Etp	Etoposide
Ex	Excitation
FBS	Foetal Bovine Serum
H <sub>2</sub> O	Water
H <sub>2</sub> O <sub>2</sub>	Hydrogen peroxide
HBSS	Hanks buffered salt solution
Hdm2	Human double minute 2
IMM	Inner mitochondrial membrane
M	Molar
MDR	Multi drug resistance
Mdm2	Murine double minute 2
MRP	Multidrug resistance protein
MTT	3-(4,5-dimethylthiazol-2-yl)-2,5-diphenyltetrazolium bromide
NCI	National Cancer Institute (US)
NU:UB	Napier University:University of Bradford
O <sub>2</sub> <sup>-</sup>	Superoxide (radical anion)
OD	Optical density
<sup>•</sup> OH	Hydroxyl radical
OMM	Outer mitochondrial membrane
PARP	poly(ADP-ribose) polymerase
PBS	Phosphate buffered saline
PI	Propidium iodide
Pic1	P53-regulated inhibitor of cdks
P-gp	P-glycoprotein
PCNA	Proliferating cell nuclear antigen
ROS	Reactive oxygen species
SD	Standard deviation
Sdi1	Senescent cell derived inhibitor

SDS	Sodiumdodecyl sulphate
SEM	Standard error of mean
Topo	Topoisomerase
UV	Ultraviolet
Waf1	Wild-type p53 activated fragment

## LIST OF FIGURES

Fig. 1.1	Illustration of the topoisomerase I mediated DNA cleavage reaction.	11
Fig. 1.2	Illustration of the topoisomerase II mediated DNA cleavage reaction.	11
Fig. 1.3a	General structure of the NU:UB compounds.	22
Fig. 1.3b	Chemical structure of NU:UB 31.	22
Fig. 1.4	Diagram representing the cell cycle phases and a histogram of DNA content, measured with flow cytometry analysis of propidium iodide (PI) fluorescence.	27
Fig. 1.5	Representation of the role of cdks in the cell cycle.	28
Fig. 1.6	Typical morphological features of Jurkat cells undergoing apoptosis.	32
Fig. 1.7	Schematic illustration how DNA damage causes disruption in the mdm2-p53 interaction.	54
Fig. 1.8	Representation of the cellular death programme phases, initiation, commitment, amplification and demolition.	60
Fig. 3.1a-d	Graphs of DNA/binder fluorescence versus drug concentration reflecting an agents DNA intercalating/groove binding capacity.	102
Fig. 3.2a	Topoisomerase I relaxation assay of NU:UB 31.	103
Fig. 3.2b	Topoisomerase I relaxation assay of NU:UB 80.	103
Fig. 3.2c	Topoisomerase I relaxation assay of NU:UB 81.	103
Fig. 3.3	Topoisomerase II $\alpha$ relaxation assay of NU:UB 31.	104
Fig. 3.4	Topoisomerase II $\beta$ relaxation assay of NU:UB 31.	104
Fig. 3.5	Topoisomerase I cleavage assay of NU:UB 31.	105
Fig. 3.6	Topoisomerase II $\alpha$ cleavage assay of NU:UB 31.	106
Fig. 3.7	Topoisomerase II $\beta$ cleavage assay of NU:UB 31.	106
Fig. 3.8a	Topoisomerase I immunodepletion assay of NU:UB 31 and NU:UB 51.	107
Fig. 3.8b	Topoisomerase I immunodepletion assay of NU:UB 81.	107
Fig. 3.8c	Topoisomerase I immunodepletion assay of NU:UB 150.	107
Fig. 3.9a	Topoisomerase II $\alpha$ immunoband depletion assay of NU:UB 31.	108
Fig. 3.9b	Topoisomerase II $\beta$ immunoband depletion assay of NU:UB 31.	108
Fig. 3.10	Chemical structure of the minor groove binder netropsin.	112
Fig. 3.11	Chemical structure of the minor groove binder Hoechst 33258.	112
Fig. 3.12	Chemical structure of the DNA intercalator mitoxantrone.	112
Fig. 3.13	Chemical structure of the DNA intercalator ethidium bromide.	113

Fig. 4.1	Growth curve of HL60 cells grown in 96 well plates.	132
Fig. 4.2a	Nigrosin exclusion counts of HL60 cells following 4h drug treatment.	134
Fig. 4.2b	Nigrosin exclusion counts of HL60 cells following 8h drug treatment.	134
Fig. 4.2c	Nigrosin exclusion counts of HL60 cells following 24h drug treatment.	135
Fig. 4.2d	Nigrosin exclusion counts of HL60 cells following 48h drug treatment.	135
Fig. 5.1	Growth curve of HL60 cells in culture.	156
Fig. 5.2a-c	Representative histograms and respective cytograms of the cell cycle distribution in HL60 cells treated for 1h and left to recover for 4h.	157
Fig. 5.2d-f	Representative histograms and respective cytograms of the cell cycle distribution in HL60 cells treated for 1h and left to recover for 4h.	158
Fig. 5.2g	Summary histogram of the cell cycle phase distribution in HL60 cells treated for 1h and left to recover for 4h.	159
Fig. 5.3a-c	Representative histograms and respective cytograms of the cell cycle distribution in HL60 cells treated for 1h and left to recover for 24h.	160
Fig. 5.3d-f	Representative histograms and respective cytograms of the cell cycle distribution in HL60 cells treated for 1h and left to recover for 24h.	161
Fig. 5.3g	Summary histogram of the cell cycle phase distribution in HL60 cells treated for 1h and left to recover for 24h.	162
Fig. 5.4a-c	Representative histograms with respective cytograms of flow cytometry analysis of the cell cycle in HL60 cells treated for 4h.	163
Fig. 5.4d-f	Representative histograms with respective cytograms of flow cytometry analysis of the cell cycle in HL60 cells treated for 4h and left to recover for 4h.	164
Fig. 5.4g-h	Representative histograms with respective cytograms of flow cytometry analysis of the cell cycle in HL60 cells. Cells treated for 4h and left to recover for 24h.	165
Fig. 5.4i	Summary of flow cytometry analysis of cell cycle in HL60 cells treated for 4h, left to recover for 0, 4 or 24h.	166
Fig. 5.5	Summary of flow cytometry analysis of sub G1 material in HL60 cell samples treated for 1h and left to recover for 4h.	167
Fig. 5.6	Summary of flow cytometry analysis of sub G1 material in HL60 cell samples treated for 1h and left to recover for 24h.	168
Fig. 5.7	Summary of flow cytometry analysis of sub G1 material in HL60 cell samples treated for 4h and left to recover for 0h, 4h or 24h.	169

Fig. 5.8	Representative confocal image of camptothecin treated HL60 cells from the sub-G1 fraction of the cell population.	170
Fig. 6.1a-b	Drug treated Diff Quick stained HL60 cells visualized in light microscope.	194
Fig. 6.1c-d	Drug treated Diff Quick stained HL60 cells visualized in light microscope.	195
Fig. 6.1e-f	Drug treated Diff Quick stained HL60 cells visualized in light microscope.	196
Fig. 6.1g-h	Drug treated Diff Quick stained HL60 cells visualized in light microscope.	197
Fig. 6.1i-j	Drug treated Diff Quick stained HL60 cells visualized in light microscope.	198
Fig. 6.1k-l	Drug treated Diff Quick stained HL60 cells visualized in light microscope.	199
Fig. 6.1m	Drug treated Diff Quick stained HL60 cells visualized in light microscope.	200
Fig. 6.2a-b	Percentages of HL60 cells with apoptotic morphology following drug treatment.	201
Fig. 6.3a-b	UV fluorescent microscope images of drug treated Hoechst stained HL60 cells.	202
Fig. 6.3c-d	UV fluorescent microscope images of drug treated Hoechst stained HL60 cells.	203
Fig. 6.3e-f	UV fluorescent microscope images of drug treated Hoechst stained HL60 cells.	204
Fig. 6.3g-h	UV fluorescent microscope images of drug treated Hoechst stained HL60 cells.	205
Fig. 6.4a-b	DNA ladder assay of drug treated Jurkat cells.	206
Fig. 6.5	DNA ladder assay of drug treated HL60 cells, 6 and 24h.	207
Fig. 6.6	DNA ladder assay of drug treated HL60 cells, 6h.	207
Fig. 6.7a-c	Flow cytometer cytograms and corresponding histograms of caspase activation in HL60 cells following 4h treatment.	208
Fig. 6.7d-f	Flow cytometer cytograms and corresponding histograms of caspase activation in HL60 cells following 24h treatment.	209
Fig. 6.8a-b	General caspase activation in HL60 cells.	210
Fig. 6.9a-b	General caspase activation in HCT116 cells.	211
Fig. 6.10a-b	Caspase-3 activation in HL60 cells.	212
Fig. 6.11-13	UV fluorescent microscope images of drug treated HL60 cells stained with Hoechst stain and general caspase inhibitor.	213
Fig. 6.14-16	UV fluorescent microscope images of drug treated HL60 cells stained with Hoechst stain and general caspase inhibitor.	214

Fig. 6.17-18	UV fluorescent microscope images of drug treated HL60 cells stained with Hoechst stain and general caspase inhibitor.	215
Fig. 6.19-21	UV fluorescent microscope images of drug treated HL60 cells stained with Hoechst stain and caspase-3 inhibitor.	216
Fig. 6.22-24	UV fluorescent microscope images of drug treated HL60 cells stained with Hoechst stain and caspase-3 inhibitor.	217
Fig. 6.25-27	UV fluorescent microscope images of drug treated HL60 cells stained with Hoechst stain and caspase-3 inhibitor.	218
Fig 7.1	Western blot of p53 protein contents in untreated HL60, HCT116 and HT29 cells, or following 24h treatment with doxorubicin.	239
Fig 7.2a	Time course Western blot image of p53 levels in HCT116 following NU:UB 31 or doxorubicin treatment.	239
Fig 7.2b	Time course Western blot image of p53 levels in HCT116 following NU:UB 51 or doxorubicin treatment.	239
Fig 7.3a	Graph of p53 protein levels in HCT116 cells treated with NU:UB 31.	240
Fig 7.3b	Graph of p53 levels in HCT116 cells treated with NU:UB 51.	241
Fig 7.3c	Graph of p53 protein levels in HCT116 cells treated with doxorubicin.	242
Fig. 7.4a-d	P53 immunostaining of drug treated HCT116 cells.	243
Fig. 7.5a	Relationship between NCI cell line sensitivity to drugs and expression of wild type or mutated p53, doxorubicin.	244
Fig. 7.5b	Relationship between NCI cell line sensitivity to drugs and expression of wild type or mutated p53, NU:UB 31.	245
Fig. 7.5c	Relationship between NCI cell line sensitivity to drugs and expression of wild type or mutated p53, NU:UB 43.	246
Fig. 7.5d	Relationship between NCI cell line sensitivity to drugs and expression of wild type or mutated p53, NU:UB 80.	247
Fig. 7.5e	Relationship between NCI cell line sensitivity to drugs and expression of wild type or mutated p53, NU:UB 81.	248
Fig 7.6a	Time course Western blot image of mdm2 levels in HCT116 cells following NU:UB 31 treatment.	249
Fig 7.6b	Time course Western blot image of mdm2 levels in HCT116 cells following NU:UB 51 treatment.	249
Fig 7.7a	Graph over mdm2 levels in HCT116 cells treated with NU:UB 31.	250
Fig 7.7b	Graph over mdm2 levels in HCT116 cells treated with NU:UB 51.	251
Fig. 7.8a	Western blot of p21 levels in HCT116 following 24h NU:UB 31 treatment.	252

Fig. 7.8b	Western blot of p21 levels in HCT116 following 24h NU:UB 31 or doxorubicin treatment. Cells grown in 1%, 5% or 10% FBS supplemented culture medium.	252
Fig 7.8c	Time course Western blot of p21 levels in HCT116 following NU:UB 31 treatment.	252
Fig 7.8d	Time course Western blot of p21 levels in HCT116 following NU:UB 51 treatment.	252
Fig. 7.9a	Time course Western blot of procaspase-3 levels in HCT116 cells following NU:UB 31 or doxorubicin treatment.	253
Fig. 7.9b	Time course Western blot of procaspase-3 levels in HCT116 cells following NU:UB 51 or doxorubicin treatment.	253
Fig. 7.9c	Time course Western blot of procaspase-3 levels in HL60 cells following NU:UB 31, NU:UB 51 or camptothecin treatment.	254
Fig. 8.1a-c	Confocal images of a time course of NU:UB 31 treated HL60 cells.	277
Fig. 8.1d-e	Confocal images of a time course of NU:UB 31 treated HL60 cells.	278
Fig. 8.2a-f	Confocal images of a time course of NU:UB 80 treated HL60 cells.	279
Fig. 8.3a-b	Confocal images of doxorubicin treated HL60 cells.	280
Fig. 8.4a-b	Confocal images of NU:UB 31 treated and Hoechst stained HL60 cells.	281
Fig. 8.5	Confocal microscope image (60x magnification, 4x zoom) of MitoTracker green and Hoechst stained HL60 cells.	282
Fig. 8.6a-d	Confocal microscope images (60x magnification) of NU:UB 31 treated HL60 cells stained with MitoTracker green and Hoechst stain.	283
Fig. 8.7	Confocal microscope image (60x magnification, 4x zoom) of NU:UB 31 treated HL60 cells stained with MitoTracker green and Hoechst stain.	284
Fig. 8.8a-d	Flow cytometer cytograms of 1h NU:UB 31 treated MitoCapture stained HL60 cells.	285
Fig. 8.9a-d	Flow cytometer cytograms of betulinic acid treated MitoCapture stained HL60 cells.	286
Fig. 8.10a-c	Flow cytometer cytograms of 4h NU:UB 31 treated MitoCapture stained HL60 cells.	287
Fig. 8.11	Confocal microscope image (60x magnification, 4x zoom) of LysoTracker green and Hoechst stained HL60 cells.	288
Fig. 8.12a-d	Confocal microscope images (60x magnification) of NU:UB 31 treated HL60 cells stained with LysoTracker green and Hoechst stain.	289

Fig. 8.13	Confocal microscope image (60x magnification, 4x zoom) of NU:UB 31 treated HL60 cells stained with LysoTracker green and Hoechst stain.	290
Fig. 9.1	Chemical structure of DACA.	306
Fig. 9.2	Chemical structure of TAS-103.	307

## LIST OF TABLES

Table 1.1	UK cancer mortality numbers in males and females from 2001 for the four most common cancer types.	4
Table 1.2	Spacer and peptide motifs of NU:UB compounds.	23
Table 2.1	Polyacrylamide concentration (protein separation range) in relation to protein size.	76
Table 2.2	Components for the making of SDS-polyacrylamide separating gel solutions.	77
Table 2.3	Components for the making of SDS-polyacrylamide stacking gel solutions.	77
Table 3.1	Topoisomerase I and II relaxation assay components.	89
Table 3.2	Topoisomerase I and II cleavage assay components.	90
Table 3.3	Table of DNA binding, topoisomerase relaxation and topoisomerase cleavage assay results.	109
Table 3.4	Table of topoisomerase immunoband depletion results.	110
Table 4.1	MTT assay results expressed as IC <sub>50</sub> values in $\mu$ M.	133

## **HYPOTHESIS**

Anthraquinone-based compounds have successfully been used in the cancer clinic for several years; doxorubicin and mitoxantrone are notable examples that, after their introduction, were shown to target DNA topoisomerase enzymes as a key component of their cytotoxic action. Clinical application of these agents is, however, restricted due to acute toxicity and side effects associated with non-topoisomerase, secondary mechanisms of action and the development of altered topoisomerase drug resistance and multidrug resistance. In this research programme, it was hypothesised that lead compounds from a novel series [code named NU:UB] of spacer-linked anthraquinone- amino acid conjugates would act as 'clean' inhibitors of DNA topoisomerase enzymes, and as a consequence, these anti-topoisomerase properties would, in part, contribute to their mechanism of cytotoxic action.

## **AIMS**

The principal aim of the project was to investigate the biochemical effects of selected conjugates, focused on the L-proline candidate NU:UB 31, in cancer cell lines and cell-free systems *in vitro* to elucidate mechanisms of cytotoxic action. Specific aims were to establish whether or not the novel agents inhibited topoisomerase I and II enzymes and affected apoptotic mechanisms in relation to their pattern of cell kill, in comparison with standard topoisomerase inhibitors, in order to contribute to the rational design of more selective drugs to target topoisomerase proteins.

## **CHAPTER 1**

### **GENERAL INTRODUCTION**

## 1.1 CANCER

It is estimated that one in three people will be diagnosed with cancer during their lifetime and that one in four people will die from cancer. Much of the problem in curing cancer lies in the fact that cancer is not just one, but a whole family of diseases, classified according to tissue type of origin, all with somewhat different behaviour and prognosis. There are over 200 different kinds but four types, lung, breast, prostate and colorectal cancers make up the majority of cancers, together accounting for half of all diagnosed cases. Table 1.1 displays UK cancer mortality numbers in males and females from 2001 for the four most common cancer types ([www.cancerresearchuk.org](http://www.cancerresearchuk.org)).

Although there are several types of cancers, they all begin when a single host cell loses its control mechanisms and starts to grow and divide abnormally. Eventually the cancerous cells get so numerous that they interfere with the normal functions of the tissues and organs where the tumour is located. In addition, tumour cells can also undergo metastasis, which is a mechanism for the cancer cells to relocate to other sites within the host. If the cancer cannot be eradicated it will eventually cause the death of the host. The progressive and uncontrollable growth in cancers is a result of damage to cellular growth control mechanisms, processes that are governed by our genes to maintain the correct numbers of cells for homeostasis and proper function. Genetic damage is accumulated over time and cancers are therefore more often seen with increasing age (Thibodeau and Patton, 1992; Campell, 1993; [www.cancerresearchuk.org](http://www.cancerresearchuk.org)).

<b>Breast Cancer</b>	<b>Mortality Numbers</b>
Male	90
Female	12 994
Total	13 084
<b>Prostate Cancer</b>	
Male	9887
<b>Lung Cancer</b>	
Male	20 348
Female	13 038
Total	33 386
<b>Colorectal Cancer</b>	
Male	8524
Female	7628
Total	16 152

**Table 1.1** UK mortality numbers in males and females from 2001. Adapted from [www.cancerresearchuk.org](http://www.cancerresearchuk.org)

Characteristically, cancer cells have damaged (mutated) genes involved in the control of the cell cycle and also in the apoptotic pathway(s). Such genes are often referred to as proto-oncogenes and tumour suppressor genes. Normally proto-oncogenes regulate cell growth but when damaged (mutated) these become so-called oncogenes and as a result their gene products (onco proteins) may stimulate excessive cell growth. Several genes have now been found to be proto-oncogenes, including genes belonging to the growth factor, growth factor receptor, transcription factor, cyclin and cyclin dependent kinase (cdk) families. Tumour suppressor genes usually act to slow cellular growth, inhibiting cell division making sure each step is completed before growth is

continued. Damage to tumour suppressor genes will therefore remove the natural constraints on the cell cycle allowing for continued cell growth (Thibodeau and Patton, 1992; Campell, 1993). P53 is the most studied tumour suppressor gene, activating genes that promote cell cycle arrest or apoptosis.

## **1.2 DNA-TOPOISOMERASES**

Screening against tumour models in animals originally identified the potential of the majority of clinically used drugs. However, the drug target(s) as well as the molecular basis of these types of animal models were in many cases undefined. Enzymes referred to as DNA-topoisomerases have now been identified as targets of several of the anti-cancer drugs used clinically today and these enzymes may also provide important and valid targets for new chemotherapeutic agents. The topoisomerases and the inhibition of these enzymes are discussed in this section.

DNA supercoiling is an essential feature that enables the long DNA helix to be stored within the nucleus of the cell. At the same time this presents a problem when it comes to DNA metabolism, including replication and other processes that require that the DNA molecule is uncoiled (Wang, 1996; Nitiss, 1998). An enzyme that was able to alter the topology of superhelical DNA was reported by Wang (1971). Since then, more of these types of enzymes have been identified and the name DNA-topoisomerase has been introduced to describe

this class of enzymes (Wang and Liu, 1979). It is now realised that the activities of topoisomerase enzymes, to deal with the topological problems associated with DNA metabolism, are essential in all living cells. One of the major roles of topoisomerase enzymes is to prevent excessive supercoiling of DNA. Both positive and negative supercoils may be generated by a number of processes, including replication and transcription, in which macromolecular assemblies move along DNA (Gellert, 1981; Nitiss, 1994a; Postow *et al.*, 1999). Topoisomerase enzymes change the conformation of DNA by a complex catalytic process involving DNA strand cleavage, strand passage and finally religation of the DNA strands and can do all this without even leaving a trace in the DNA. Although these enzymes in themselves are fascinating, the huge interest and intense studies in this area are more likely due to the realisation that topoisomerases appear to be the primary targets for a range of clinically used cytotoxic drugs (Nelson *et al.*, 1984; Tewey *et al.*, 1984a; Tewey *et al.*, 1984b; Zunino and Capranico, 1990; Hwang and Hwong, 1991; Chen and Liu, 1994). Since then, these enzymes have also become the main targets for rational drug design of novel anti-cancer drugs.

The DNA topoisomerases in humans have been divided into three sub-groups and this classification has been based on their respective protein structures and on their mechanism to alter DNA topology. These sub-groups are: type IA enzymes (represented by topoisomerase III $\alpha$  and III $\beta$ ), type IB enzymes (topoisomerase I and mitochondrial topoisomerase I) and finally type II enzymes (topoisomerase II $\alpha$  and II $\beta$ ) (Wang, 1994; Zhang *et al.*, 2001; Wang *et al.*, 2002). Why there are so many kinds of topoisomerase enzymes is not

known but there must be a requirement for them and these various enzymes have been discussed by Wang (1991). With continued research into this field even more topoisomerases may be identified, but so far it is topoisomerase I and II that have been mostly studied in relation to human cancers.

### **1.2.1 Topoisomerase I**

The gene for topoisomerase I has been mapped to chromosome 20q12-13.2 (Juan *et al.*, 1988). The topoisomerase I gene product is a 100kDa monomeric protein that requires phosphorylation for full activity (Pommier *et al.*, 1990). This protein is most abundant in the nucleus but also found in nucleoplasm and in mitochondria (Fleischmann *et al.*, 1984; Zhang *et al.*, 2001; Christensen *et al.*, 2002; Wang *et al.*, 2002). Characteristic of topoisomerase I is that it requires no cofactor in its catalysis of DNA strand breakage and rejoining, the energy for this reaction is instead derived from that stored in the supercoiled DNA. In the breakage reaction, a hydroxyl group of an amino acid, tyrosine located in the active site of topoisomerase I, attacks DNA. This results in the formation of a covalent bond between the topoisomerase and DNA, where the active site tyrosine of topoisomerase I is attached to the 3' phosphoryl end of the cleaved DNA molecule and the other DNA end has a hydroxyl group on its sugar. This cleavage of DNA is however only a transient arrangement allowing for DNA strand passage, relaxation of supercoiled DNA, and rejoining of the DNA strand as soon as all this has been accomplished. When topoisomerase I performs these catalytic reactions it has been suggested by Berger (1998) to look like a hand holding on to, and

entirely enclosing DNA. In this 'hand', DNA lies between the fingers (topoisomerase I subdomains I and II) and the palm (III and the C-terminal domain). The thumb is made up of the linker domain and has not much contact with DNA, it instead helps in its rotation. DNA is cleaved when it is locked between the fingers and the palm, and the rotation of DNA to relax it may occur by slightly loosening the grip (Berger, 1998; Stewart *et al.*, 1998). For an illustration of the topoisomerase I mediated cleavage reaction see Fig. 1.1.

### **1.2.2 Topoisomerase II**

Topoisomerase II is, in some capacity, thought to be involved in chromosome condensation and decondensation and is found to play an important part in chromosome structure. It is believed that topoisomerase II partly makes up the chromosome scaffold and the nuclear matrix. The chromosome scaffold is the protein structure that remains after DNA and histones have been removed from chromosomes in mitotic cells, and the nuclear matrix is a similar preparation from cells in interphase (Berezney and Coffey, 1974; Adolphs *et al.*, 1977; Nitiss, 1998). Two isoforms of the topoisomerase II enzyme have been identified; these are 170 and 180kDa in size and have been referred to as topoisomerase II $\alpha$  and topoisomerase II $\beta$  respectively (Drake *et al.*, 1987; Stacey *et al.*, 2000). The topoisomerase II $\alpha$  gene is located on chromosome 17q21-22 and the topoisomerase II $\beta$  gene on the 3p24 chromosome (Tan *et al.*, 1992). These two gene product isoenzymes have different localisation and expression patterns, which would imply that they differ in their cellular

functions (Stacey *et al.*, 2000). Topoisomerase II $\alpha$  is localised in the nucleoplasm, while topoisomerase II $\beta$  is found in the nucleolus (Cummings and Smyth 1993; Zini *et al.*, 1992). Drake *et al.* (1989) compared biochemical and pharmacological properties between the two topoisomerase II isoforms and found that while there were some similarities between these, they had also many unique biochemical properties and differential pharmacological sensitivities to several drugs.

In contrast to topoisomerase I catalysed reactions, topoisomerase II cuts both strands of DNA, passing an intact helix through this double stranded cut and reseals the cut. To do so, topoisomerase II utilises ATP. While topoisomerase I was likened to a hand holding onto and cleaving one strand of DNA, topoisomerase II has been thought of as a pair of closable jaws coupled by a set of hinges. For an illustration of this see Fig. 1.2, adapted from Berger (1998). In this arrangement, one set of jaws is responsible for gripping and cleaving a DNA duplex. A second DNA duplex and ATP also bind to the enzyme, this will result in closure of the jaws, trapping of the second DNA strand (sometimes described as the closed-clamp conformation), and cleavage of the first DNA strand allowing the second to pass through the break in the first one (Lindsley and Wang, 1991; Roca and Wang, 1992). In common with topoisomerase I, it is a tyrosine in the cleavage site of topoisomerase II that is important as the nucleophile in attacking the DNA strand, but the enzyme becomes attached to DNA through a 5'-phosphotyrosine linkage rather than through 3'-linkage, which is the case following topoisomerase I cleavage (Berger, 1998). In addition to the function of topoisomerase II in relaxing DNA

(functions that can also be performed by topoisomerase I), topoisomerase II is the only enzyme capable of separating interlocked double stranded daughter chromosomes that are formed during replication, a process referred to as decatenation (Chen and Liu, 1994). In summary, while there are some features of topoisomerase I and II that are shared; for example, both types relax positive and negative supercoils and form covalent links to DNA, topoisomerase I attaches to the 3' end of DNA whereas topoisomerase II links to the 5' end. Topoisomerase II but not topoisomerase I, requires ATP and is able to catenate and decatenate DNA (Cummings and Smyth, 1993).

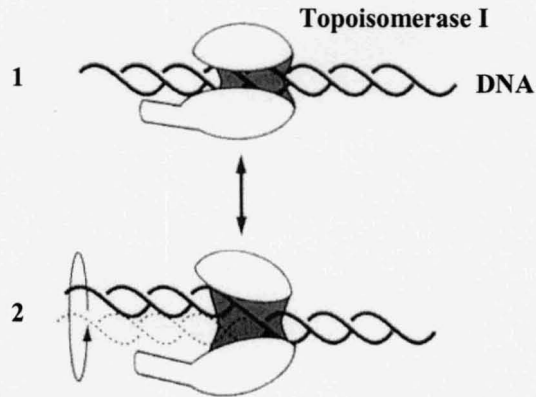


**Fig. 1.1** Schematic illustration of the topoisomerase I mediated cleavage reaction. Topoisomerase I binds DNA (1). One of the DNA strands is cleaved by topoisomerase I and following cleavage the topoisomerase I-DNA interaction is loosened slightly allowing for one end of the DNA to rotate (2). Figure adapted from Berger, 1998.

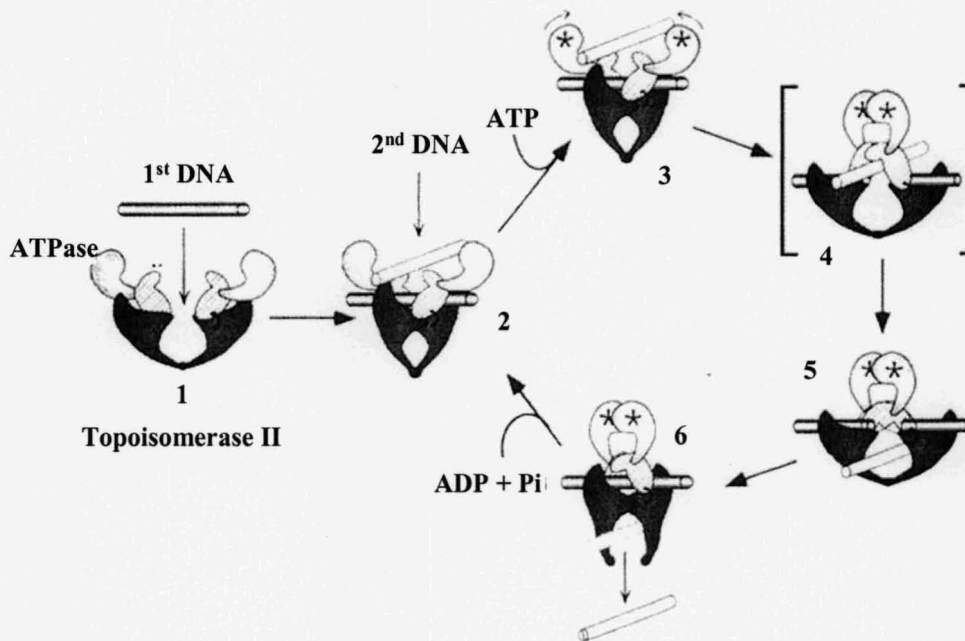


**Fig. 1.2** Representation of the topoisomerase II catalysed cleavage reaction. Topoisomerase II binds first to DNA (1). A second DNA duplex and ATP bind to topoisomerase II (2,3). Cleavage of the first DNA duplex and transport of the second one through the break (4,5). Religation of the cleaved DNA duplex and release of DNA(6). Figure adapted from Berger, 1998.

## **1.3 INHIBITION OF TOPOISOMERASES**

Since tumour cells in many cases are highly proliferative cells and topoisomerases are involved in replication and proliferation processes, the levels of these enzymes are often increased in growing cancer cells compared to normal cells. Several tumours have been shown to have increased levels of topoisomerases promoting further DNA separation and growth. For example, colorectal tumours show a 5 to 35-fold increase in topoisomerase I compared to normal colon tissue (Larsen and Skladanowski, 1998). Furthermore, overexpression of topoisomerase II has been noted in human cervix, lung and colon cancers (McLeod *et al.*, 1994). If topoisomerases in tumour cells could be inhibited, then unwinding, strand separation and reproduction of DNA would be prevented. For drugs selectively targeting the topoisomerase enzymes, the increased levels found in many tumours could provide some degree of tumour cell selectivity that would hopefully decrease the DNA damage to normal tissue and thereby reduce side effects.

### **1.3.1 Inhibitors And Poisons**

Drugs are thought to work as anti-topoisomerase agents mainly by two mechanisms. They can act as pure catalytic inhibitors of topoisomerases or as topoisomerase poisons (although the name topoisomerase inhibitors often in the literature refers to both types). Topoisomerase inhibitors either bind to topoisomerases directly or bind to DNA, changing its structure so that it can

no longer be recognised by the topoisomerases. Drugs trapping topoisomerases in what is referred to as cleavable complexes (drug-stabilised intermediates) are called topoisomerase poisons. Topoisomerase poisons normally do not inhibit the catalytic activity of topoisomerases; these agents instead take advantage of the DNA cleavage reaction by topoisomerases and increase the concentrations of the drug-stabilised cleavable complexes to levels that cells can no longer tolerate (Froelich-Ammon and Osheroff, 1995). When DNA is to be replicated, there are a lot of cleavable complexes formed and this process is likely to be the main cellular process that drives the conversion of transient cleavable complexes into lethal lesions following treatment with for example the topoisomerase I poison camptothecin. Cellular processes other than replication may however also be of importance for the cell kill mechanism of these types of drugs. For the pure inhibitors of topoisomerase II, mitosis may be the cellular process whereby the damage is instigated; proceeding through this stage of the cell cycle when topoisomerase II is inhibited can result in aneuploidy and chromosomal breakage (Wang, 1994). Whereas for topoisomerase poisons, the sensitivity to these drugs increases with over-expression of the topoisomerase enzymes, thus increasing the level of cleavable complexes that can be formed per cell (Nitiss *et al.*, 1992; Wang, 1994), for pure topoisomerase inhibitors sensitivity should be the other way around.

### 1.3.2 DNA Binding Mode

Several of the agents acting as poisons are known to be DNA binders and these can be further subdivided into intercalators, groove binders and mixed-modal binding agents (with features of both intercalators and groove binders). Thus, anti-tumour agents may be classified not only as poisons or inhibitors, or according to which topoisomerase enzyme they act on, but also according to their DNA binding mode. The binding mode of anthracyclines (e.g. doxorubicin, daunorubicin and idarubicin) and anthracenediones (e.g. mitoxantrone) has largely been considered to be by pure intercalation. Studies of intercalators have however revealed that many of these have a side chain that allows for a direct contact with the topoisomerase protein, and thus a groove-binding moiety may also be important for their topoisomerase poisoning activity (Capranico *et al.*, 1997; Capranico and Binaschi, 1998). Camptothecin and etoposide are examples of topoisomerase poisons that are not believed to be intercalators or DNA binders, but instead bind only to the DNA-topoisomerase cleavage complex and interfere with the religation steps (Hertzberg *et al.*, 1990; Hwang and Hwang, 1991). Anthracenediones generally have a high affinity constant of DNA binding, which alone may be responsible for conferring catalytic inhibitory properties (in addition to poisoning actions). Whereas at low drug concentrations these may stimulate DNA cleavage, at high enough concentrations these could inhibit the catalytic activity without stimulating cleavage. This type of behaviour will generate a bell shaped dose-response curve of DNA cleavage stimulation (Capranico *et al.*, 1997; Capranico and Binaschi, 1998). Properties of this type have been

observed amongst members of the NU:UB compound series (Mincher D.J. *personal communications*). However, strong DNA binders can also induce adverse toxicity as these may non-selectively inhibit the activity of other DNA dependent enzymes.

### **1.3.3 Anti-topoisomerase Drugs And Their Side Effects**

Chemotherapy and radiation therapies have for some cancers been very successful, with the survival figures for certain types of cancers having greatly improved over the years. Despite this, the treatment of the most common forms of cancers such as lung, breast and bowel carcinomas is still troublesome, since these types of cancers in many cases are more or less resistant to current therapies. In addition, the effectiveness of the currently used chemotherapy regimens has also been limited by the side effects of these drugs.

Camptothecin and its more soluble derivatives target topoisomerase I. Several camptothecin analogues, including 9-aminocamptothecin, topotecan and irinotecan (CPT-11) have been developed and put through clinical trials (Takimoto and Thomas, 2000; Kohn and Pommier, 2000). In addition, the homocamptothecin (hCPT) derivative BN80915, containing a seven-membered (instead of the conventional six-membered) lactone ring, is a potent topoisomerase I compound. This agent has reached phase I clinical trials and appears to be a promising addition to the camptothecin drug family (Lansiaux *et al.*, 2001). While licensed topoisomerase I poisons so far only

include the camptothecin derivatives, there are several topoisomerase II poisons available. Topoisomerase II anti-cancer agents are among the most effective drugs available for cancer treatment. Agents found to interfere with topoisomerase II include doxorubicin (adriamycin), daunorubicin and idarubicin, as well as mitoxantrone. Etoposide (VP-16) was the first cancer drug to be demonstrated to work through inhibition of topoisomerase II and teniposide (VM-26) belongs to the same family as etoposide (Hande, 1998). The chemical structures for some of the anti-topoisomerase drugs and other types of drugs available and referred to in this project have been collated in Appendix 1.

The side effects from the camptothecins, irinotecan and topotecan are of a similar nature and comprise nausea, hairloss, bone marrow toxicities and diarrhoea. While irinotecan is used for the treatment of bowel cancers, topotecan is most commonly used when treating ovarian cancers, but also in the treatment of small cell lung cancer and acute myeloid leukaemia. The primary use for doxorubicin is in the treatment of lymphomas, breast cancer, sarcomas, ovarian and bladder cancer. Side effects of doxorubicin include suppression of white blood cells, inflammation of mucus membranes, hair loss and more severely, heart damage. Daunorubicin and idarubicin are used in treating leukaemias and their toxicities are similar to those of doxorubicin. Mitoxantrone is mainly used for the treatment of breast cancer, prostate cancer, leukaemia and lymphoma. Mitoxantrone has perhaps overall slightly less antitumour activity compared to doxorubicin, but although of a similar nature, the side effects from mitoxantrone are less severe than following

doxorubicin treatment. Etoposide is active against several cancers including lung, testicular and stomach cancers, leukaemias, KS, non-Hodgkin's lymphomas, neuroblastoma and sarcomas. Toxicities include bone marrow suppression, nausea and hair loss ([www.cancerresearchuk.org](http://www.cancerresearchuk.org); Hande, 1998).

Many of the currently used topoisomerase agents have not been specifically designed to target topoisomerases and it has been realised that they are not 'clean' topoisomerase inhibitors. For example doxorubicin, in addition to targeting topoisomerase II, is also known to generate free radicals in its mechanisms of action, contributing to its high degree of host toxicity. The mechanisms involved in doxorubicin-mediated toxicities including free radical formation, have recently been reviewed by Jung and Reszka (2001). Many topoisomerase II drugs may also induce sister chromatid exchange and illegitimate recombinations and these effects are thought to reflect the capacity of topoisomerase II to induce double strand breaks (Chen and Liu, 1994). It is important to understand this, and the extent of genetic rearrangements induced by drugs targeting topoisomerases, since agents that stabilise cleavable DNA-topoisomerase complexes such as etoposide and doxorubicin may increase the risk of secondary malignancies (Morgan and Rubin, 1998; Turner *et al.*, 2001).

## **1.4 DRUG RESISTANCE**

In addition to the side effects from chemotherapeutics, the effectiveness of current agents is also hampered by resistance, a major problem and cause of treatment failure. Natural resistance is resistance present prior to treatment, whereas acquired drug resistance is developed as a result of drug treatment. Both natural and acquired resistance restrict the clinical efficacy of chemotherapy. Larsen and Skladanowski (1998) stated that the same molecular mechanisms are nearly always involved in natural and acquired resistance, and these mechanisms are also always multi-factorial in nature. The molecular mechanisms involved in resistance, from drug uptake to cell death were reviewed here and divided into: pre-target events (including drug accumulation, distribution and metabolism), drug-target interactions (chromatin structure, topoisomerase levels, activity, localisation and mutations), and post-target events (macromolecular synthesis, mechanisms involved in the regulation of DNA repair/recombination, cell cycle progression and of cell death). Additionally, in an article by Hannun (1997), the mechanisms involved in chemotherapy induced cell death, and in resistance to chemotherapeutics have been outlined in relation to apoptosis.

### **1.4.1 Multi Drug Resistance And Transporter Proteins**

There are many and complex factors involved in the development of resistant cells, including pre-target events where increased drug efflux results in less

drug-target interactions since many agents are substrates for the protein transporters associated with multi drug resistance (MDR).

MDR defines a resistance phenotype where cells, even though they have been selected for resistance to a single agent are also cross-resistant to a range of agents with different structures and molecular targets. A gene product, making up a 170kDa glycoprotein transporter responsible for MDR has been described. This transporter has been given the names, P-glycoprotein (P-gp), P-170 or MDR-associated glycoprotein. Transfection experiments with drug sensitive cells have shown that P-gp expression could result in a MDR phenotype (Gros *et al.*, 1986; Ueda *et al.*, 1987). In addition to P-gp, another protein transporter associated with resistance has also been identified, the multidrug resistance protein (MRP) (Cole *et al.*, 1992). MRP is a 190kDa protein that has several substrates in common with P-gp and the simultaneous activity of these is thought to be important in resistant cells (Legrand *et al.*, 1999). These types of resistance transporters can be expressed on the plasma membrane and also on vesicular membranes (Feller *et al.*, 1995; Flens *et al.*, 1996) with decreased intracellular drug levels as a result of their actions. However, to establish the combined importance of the expression of MDR-related transporters in chemotherapy failure, more studies of P-gp and MRP expression in tumour samples from patients undergoing chemotherapy will be required (Legrand *et al.*, 1999).

In summary, there are a range of mechanisms such as, increased drug efflux, altered intracellular drug distribution, diminished drug-target interaction,

altered cell cycle regulation, and uncoupling of the pathways linking cellular damage with apoptosis involved in resistance (Larsen and Skladanowski, 1998). These resistance mechanisms are still major obstacles for today's anti-topoisomerase based cancer treatments and provide a valid reason for the development of new and more effective topoisomerase targeting drugs. In addition to the limitations linked to resistance, there are also other reasons as to why there is a need for research into the development of more anti-topoisomerase agents. Topoisomerases are the targets of the most active cancer drugs currently used in clinics. The fact that new topoisomerase enzymes have recently been discovered, which could possibly be explored as therapeutic targets, makes a strong case for topoisomerases still being valid targets even though there is already a range of anti-topoisomerase drugs available in the clinics. Arguments for the need for more topoisomerase drugs have been outlined by Pommier (1999).

## **1.5 NU:UB COMPOUNDS**

The NU:UB compounds have been synthesised and developed so that via selective topoisomerase inhibition they will act as improved anti-cancer agents. Computerised molecular modelling and structure activity investigations are beginning to reveal the molecular requirements for formation of cleavable complexes between drug, DNA and protein. For this kind of cleavable complex formation a polycyclic ring system is thought necessary for the drug to intercalate into DNA. To interact with the protein, a

hydroxy or amino moiety is thought to be required to reach out from the site of intercalation into the grooves of DNA (Cummings *et al.*, 1996). For the design of the NU:UB compounds an anthraquinone was the ring system of choice to potentially confer DNA intercalation properties. To the anthraquinone, a spacer arm was linked, to which amino acids were added, providing the amino moiety that was thought to be required for enzyme interaction. The type of spacer, as well as the composition and sequence of the amino acids, was then altered to achieve different modes of interactions with the target proteins, and to provide chemical diversity in the attempts to design efficient anti-topoisomerase agents. Compounds of this type were thought to have a low affinity for DNA, yet they still appear to possess anti-topoisomerase activity. The low level of DNA interaction of these types of compounds was hoped to limit the overall level of DNA damage, which would hopefully result in fewer side effects than with conventional anti-cancer drugs. In addition these types of compounds *in vivo* are highly unlikely to undergo bioreduction and induce toxicity through formation of free radicals (Mincher D.J., *personal communications*) due to unfavourable quinone one-electron reduction potentials.

Six NU:UB compounds, numbered NU:UB 31, 43, 51, 73, 80 and 81 have recently been in focus when studying cytotoxicity and anti-topoisomerase activity of the NU:UB agents. These agents represent a novel class of anti-topoisomerase agents that are believed to act through either cleavable complex formation, or through pure topoisomerase inhibition. NU:UB 31 was chosen as the lead compound for the investigations in this project. The

chemical structures of each of the NU:UB compounds mentioned above can be found in Appendix 1. Fig. 1.3a represents a general structure of the NU:UB compounds and Fig. 1.3b represents NU:UB 31. Table 1.2 summarises the spacer and peptide motifs of the NU:UB compounds referred to in this thesis.

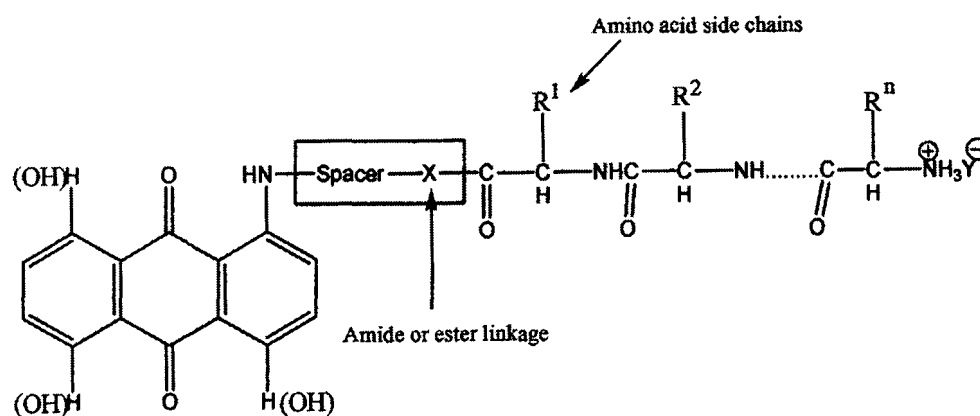


**Fig. 1.3a** General structure of the NU:UB compounds

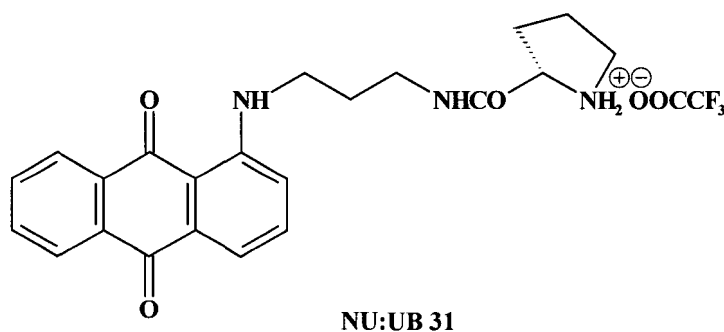


**Fig. 1.3b** Structure of NU:UB 31.

Compound	Spacer Descriptor	Spacer Structure	Peptide Motif
NU:UB 31	Propyl		L-Pro
NU:UB 43	Butyl		L-Pro
NU:UB 51	Propyl (AQ4,8 di-OH)		Gly
NU:UB 73	Butoxy		L-Ala
NU:UB 80	Butyl		D-Val
NU:UB 81	Butyl		L-Val
NU:UB 150	1,4-diaminocyclohexyl		L-Phe

**Table. 1.2** Spacer and peptide motifs of NU:UB compounds.

## **1.6 THE CELL CYCLE**

### **1.6.1 Cell Cycle Phases And Checkpoints**

The period following one cell division, mitotic phase (M-phase) to the next division is referred to as the cell cycle. The cell cycle can be divided into different phases called M, G1, S and G2 phases. In addition, a quiescent cell that is not involved in division is in a G0 state. Most studies have been performed on immortalised cells in culture and for cultured mammalian cells the cycle typically lasts about 18-24 hours. If division is triggered, the cell first enters the G1 phase, during which RNA and certain proteins essential for DNA replication are made. When the cell starts to make new DNA it has entered the S-phase of the cycle. During this phase the DNA content of the cell increases until it has doubled. At this point DNA synthesis ceases and the cell is in the G2 phase, where the cell cycle can be arrested if DNA is damaged, to allow time for repair before M-phase. Finally the cell will enter M-phase and divide thereby returning to G1 if cell division is to be sustained, or to G0. In the M-phase two main processes take place, nuclear division (called mitosis) and subsequent division of the cytoplasm. If growing cells are starved of nutrients they will arrest in G1, and this leads to the identification of a point of no return in the late G1-phase. This point has been referred to as a restriction point and cells that pass this point are obliged to divide. Two other check points also exist: one at the G2-phase and another within the M-phase (Becker *et al.*, 1996; Tannock and Hill, 1998). With regard to DNA content, cells in G2 and M phases of the cell cycle have double the DNA content of

those in G<sub>0</sub> and G<sub>1</sub>, and cells in S phase have a DNA content somewhere in between. If the DNA content of cells is to be measured, using for example a flow cytometer and a DNA binding probe, a histogram of the number of cells against DNA content can be plotted reflecting the cell cycle state of the cell population (Fig. 1.4).

### **1.6.2 Cell Cycle Regulation**

The molecular basis of cell cycle regulation has been heavily researched and an understanding of this will hopefully give an insight into how cancer cells manage to escape normal control mechanisms. The cell cycle regulation is very likely to involve complex protein cascades and although these cascades are yet to be clearly defined, the regulation of the cycle appears to rely on specific cyclin and kinase complexes (Becker *et al.*, 1996). The cell cycle and its regulation via various cyclins and kinases is a complicated issue indeed, discussed in detail by Sherr *et al.* (1993). Briefly, cyclins and cyclin dependent kinases (cdks) are key regulators of the cell cycle, and what governs the correct progression of cells through the cycle appears to be the activation and subsequent inactivation of cyclin-cdk complexes. During the course of the cell cycle, the level of various cyclins acting as positive regulatory subunits for a series of cdks, increase and subsequently decrease in a defined order. The increase and decrease of cyclins is striking since most proteins like cdks have relatively constant levels in cells, but this will confer substrate and thereby also cell cycle specificity upon the cdks. The various types of cdks and cyclins act in different combinations and at different stages of the cell cycle controlling

the G1/S and G2/M transitions (Lee and Fukushima, 1998; Tannock and Hill, 1998; Chetty, 2002). For an illustration of the cdks in the cell cycle see Fig.1.5.

In addition to the positive regulation of the cell cycle by activation of cyclin-cdk complexes, negative regulation also occurs at the cell cycle checkpoints. Feedback mechanisms act here to prevent cells from entering the next stage of the cell cycle, before the molecular events required for such a transition have been completed and the cell is ready for the next phase. If proper control is not maintained, the cell cycle progression may become insensitive to DNA damage. The negative regulators include tumour suppressor proteins such as Rb and p53 as well as the cyclin dependent kinase inhibitors (CKIs) including p21 (Lee and Fukushima, 1998; Tannock and Hill, 1998). P21 and p53 will be discussed in more detail in sections 1.8 and 1.9 respectively.

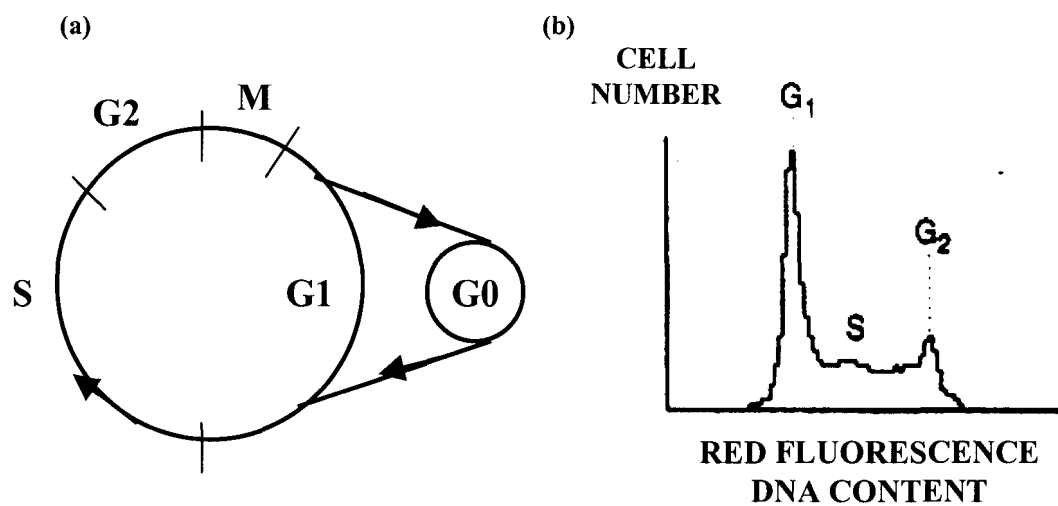


**Fig. 1.4** Diagram representing the cell cycle phases (a). Histogram of DNA content measured with flow cytometry analysis of propidium iodide (PI) fluorescence (b). Cells are stained with PI that intercalates into DNA to give a linear relationship between red fluorescence and cellular DNA content. The fluorescence i.e. the DNA content of each cell is measured and reflects the cell cycle position. Figure represents a normal population of cells. The G<sub>1</sub>-phase is the period between the previous nuclear division and the beginning of DNA synthesis. S-phase, DNA synthesis phase during which chromosomal DNA replicates. G<sub>2</sub>-phase represent the time between DNA replication and nuclear division and finally the M-phase (mitosis) which is the nuclear division phase where two daughter cells are produced. Cells in G<sub>2</sub>/M phase have double the amount of DNA compared to cells in G<sub>0</sub>/G<sub>1</sub> phase and S-phase cells have intermediate DNA content. The diagram of the cell cycle and a DNA histogram were adapted from Ormerod, 2000.

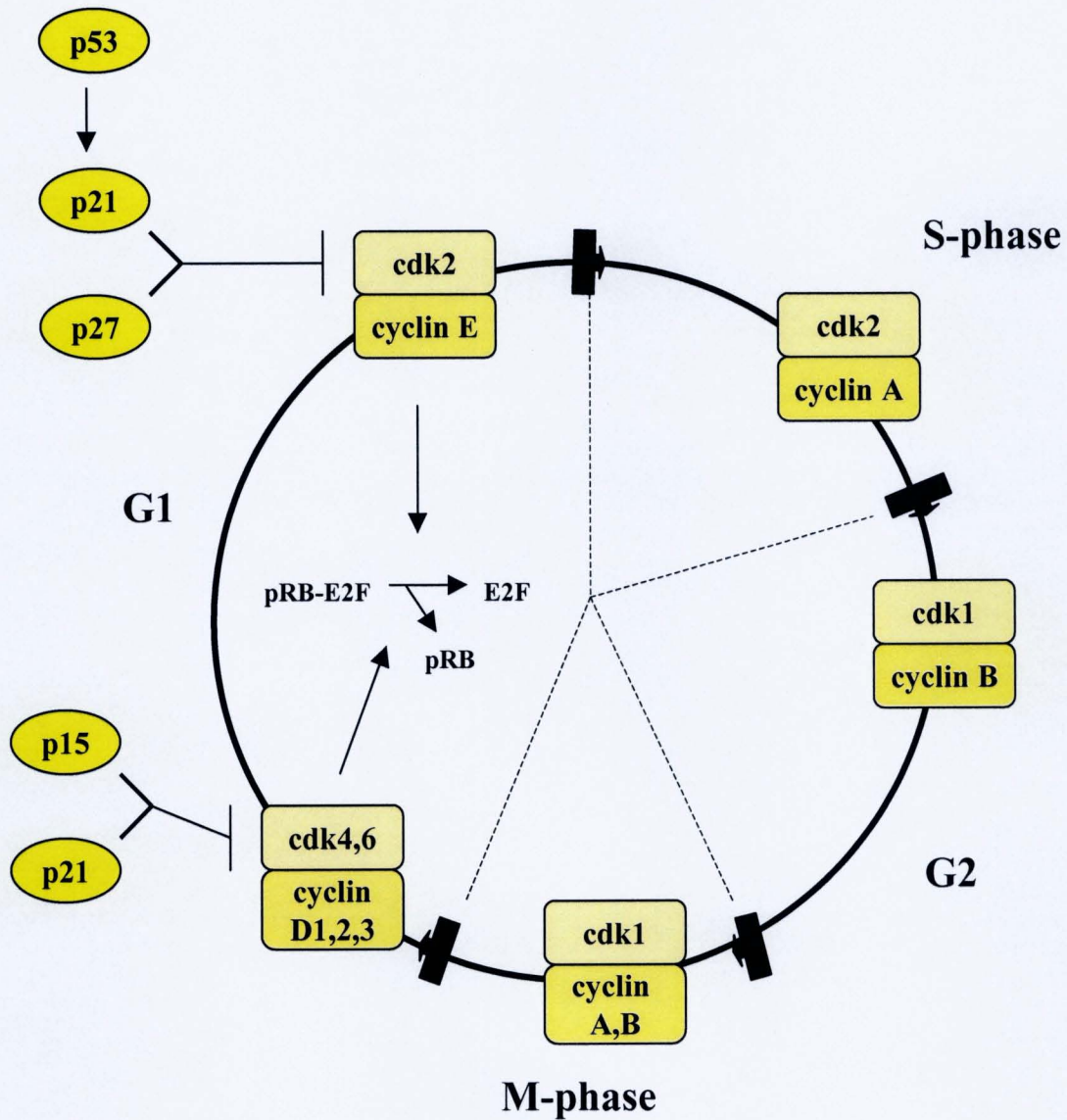


**Fig. 1.5** Schematic representation of the role of cdks in the cell cycle. The various types of cdks and cyclins act in different combinations and at different stages of the cell cycle. Cdk1 together with cyclin A and B seem to be involved at G2 and M-phase. Cdk4 and cdk6 complex with D-type cyclins, and cdk2 with cyclin E, and these complexes appear to be required for the progression through G1. The cdk2-cyclin A complex, controls the progression through S-phase. Figure adapted from Chetty, 2002.

### 1.6.3 The Cell Cycle And Topoisomerases

It has been suggested that the action of some anti-cancer drugs in part is cell cycle dependent, such that there could be a link between the efficiencies of these drugs and the cell cycle phase of the cells being targeted. This may partly be due to variations in topoisomerase enzyme activity between different phases of the cell cycle. In a study by Heck *et al.* (1988), immunoblotting was performed for the examination of topoisomerase (I and II) levels in cells. It was found that while there were no differences in stability of topoisomerase I in normal compared to transformed cells, for topoisomerase II the half-life was shorter in normal than in transformed cells. Topoisomerase I and topoisomerase II also appeared to have distinct functions in the cell cycle process. Whereas topoisomerase I expression levels appeared stable, topoisomerase II levels underwent cell cycle dependent fluctuations, reaching higher levels in proliferating cells, with topoisomerase II peaking at G2. Thus, topoisomerase II might have a regulatory role during the G2-phase of the cell cycle. Furthermore, there are also different expression patterns between the two isoforms of topoisomerase II. Whereas the topoisomerase II $\beta$  isoform is present in G0 cells and expressed at constant levels throughout the cell cycle, topoisomerase II $\alpha$  expression levels fluctuate over the course of the cell cycle. Topoisomerase II $\alpha$  proteins do not appear to be present in G0 cells and cells in exponential growth have more topoisomerase II $\alpha$  protein, whereas cells having reached a growth plateau phase have higher levels of the II $\beta$  protein (Woessner *et al.*, 1991; Hwang and Hwong, 1991; Cummings and Smyth, 1993; Poot *et al.*, 1995; Valkov *et al.*, 2000).

## 1.7 APOPTOSIS

Apoptosis can be defined as a form of cell death in which the cell is destroyed from within (Kerr *et al.*, 1972; Wyllie *et al.*, 1980). The word 'apoptosis' stems from the classical Greek 'apo' that means apart and 'ptosis' meaning falling. Apoptosis is a morphological descriptor of cell death that was first described in the 1970s by Kerr *et al.* (1972). Apoptotic cell death is continually taking place in both slowly and rapidly proliferating tissues. While past research has identified regulation of cell proliferation as a key element in tumour growth and spread, it is now thought that improper regulation of growth arrest and apoptosis are implicated in the development of cancers, and that apoptotic cell kill is also considered important in the treatment of cancers (Kerr *et al.*, 1994). Evidence in the past few years has revealed that many chemotherapeutics kill cells *in vitro* and *in vivo* through apoptosis. An understanding of how apoptosis is engaged following treatment with chemotherapeutic agents and why it fails to get engaged in some cases, may offer novel approaches to overcoming the clinical problem of drug resistance (Makin and Hickman, 2000).

Apoptosis is different from the other major form of cell death, necrosis. These two types of cell death can be induced by different stimuli, although it has also been realised that the same stimulus may induce apoptosis or necrosis in a cell depending on the dose of a given agent used to induce cell death. Thus, whereas mild injury might induce apoptosis, exposure to high doses inducing severe damage leads directly to cell death by necrosis (Anselmi *et al.*, 2002).

The situation is however, more complicated, a process starting with very specific changes may end non-specifically when the cell loses the ability to maintain homeostasis. This will complicate the identification of apoptotic cells since apoptosis quite often ends in secondary necrosis, at least *in vitro*, where the removal of apoptotic cells is inefficient or nonexistent (Squir *et al.*, 1995). Some of the most characteristic features of apoptotic cell death will be outlined below.

### **1.7.1 Characteristic Features Of Apoptotic Cells**

Whereas necrotic cell death appears to be accidental, apoptosis is a genetically programmed mechanism of cell death that can be triggered by a variety of external and internal stimuli (Tortora and Grabowski, 2000). For apoptotic changes to occur, new gene expression is in many cases needed. Apoptosis is thereby an active process in which synthesis of proteins is likely to take place (this is however, not the case in all cell lines e.g. HL60). Many morphological and biochemical changes triggered during apoptosis appear to be similar.

#### **1.7.1a Morphological Changes**

Characteristic apoptotic events at the cellular level include both morphological and biochemical changes. Morphologically, nuclear size is reduced and there is typically shrinkage of total cell volume. In early apoptosis there are plasma membrane changes that shift phospholipid distribution between the inner and

outer leaflets and this may also contribute to the plasma membrane blebbing. There is also evidence that exposure of phospholipids, phosphatidylserines (PS) on the surface of apoptotic cells may lead to their specific recognition by macrophages. This is a mechanism that appears to happen early *in vivo*, and when using vital dyes, cells appear to be phagocytosed whilst still viable. Other morphological features include dilation of the endoplasmic reticulum, chromatin condensation, increase in cell density, nuclear fragmentation, and constriction of both the nucleus and the cytoplasm into multiple, small, membrane-bound apoptotic bodies (Cohen, 1993; Kerr *et al.*, 1994; Studzinski, 1995; Squir, 1995; Cima and Brunner, 2003). Fig. 1.6 shows typical morphological features of cells undergoing apoptosis.

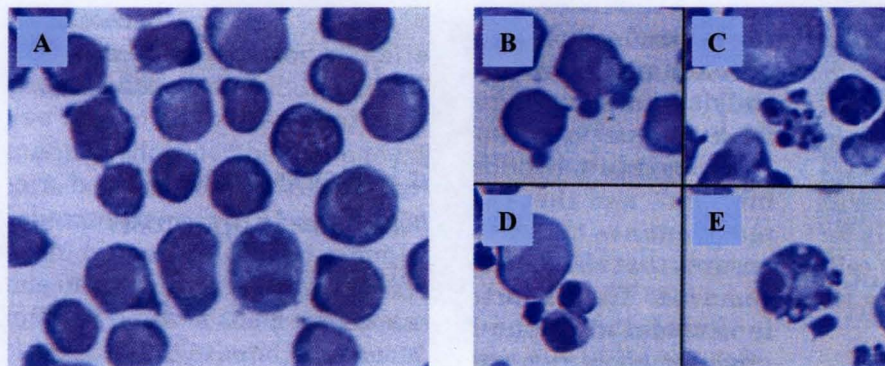


**Fig. 1.6** Morphological changes in Jurkat cells undergoing apoptosis following UV irradiation. Normal cells (A). Membrane blebbing in early apoptotic cells (B). Apoptotic bodies (C). Cellular and nuclear condensation (D). Nuclear fragmentation (E). Figure adapted from Cima and Brunner, 2003.

### 1.7.1b Biochemical Changes

An established hallmark of apoptotic cell death is internucleosomal DNA cleavage, generating a characteristic ladder formation on agarose gels following electrophoresis. This process is thought to proceed in two steps: there is first an infrequent DNA cutting that results in the generation of fragments of 300-50 kilo base pairs. The enzymes responsible for this have not yet been clearly identified. Secondly, in some (but not all) cell types, the DNA degradation proceeds with more specific DNA scission, producing fragments of DNA that are multiples of 180-200 base pairs. This is the length of DNA wrapped around histones in a nucleosome, which indicates that the chromatin is being cleaved at the linker DNA between nucleosomes (Wyllie, 1980). However, the cleavage occasionally may be delayed or absent in cell death that appears by other criteria to be apoptotic (Cohen *et al.*, 1992; Ucker *et al.*, 1992; Falcieri *et al.*, 1993; Pandey *et al.*, 1994; Sleiman, 1998). Although DNA fragmentation is an indicator of apoptosis, many researchers prefer to investigate caspase-3 activation, which is considered to be a reliable hallmark of apoptosis. So far it is not fully understood how the caspases cleave their cellular protein targets and thereby induce cell death, but three mechanisms have been suggested; inactivation of proteins that protect cells from apoptosis; destruction of nuclear lamina and other vital cell structures; and indirect cleavage of proteins involved in cytoskeleton regulation (Thornberry and Lazebnik, 1998).

## 1.7.2 Necrosis

There are some features that distinguish necrosis from apoptosis. Cell death by necrosis is a passive process that can be sustained by hyperthermia, severe physical or chemical trauma. The early event of necrosis is a change in mitochondrial shape and function and the cell rapidly becomes unable to maintain homeostasis. The plasma membrane may however be the major site of damage (Majno and Joris, 1995), no longer maintaining the proper regulation of osmotic pressure. This results in swelling of the cell, and rupture with spilled cell contents provoking inflammation. An inflammatory response following extensive injury can be beneficial, efficiently clearing away debris so that the repair process can begin. An inflammatory response may however not be desirable following *in vivo* chemotherapy treatments as this can result in severe side effects, and thus an apoptotic response with no inflammation is more desirable. Furthermore, the nuclear morphology of necrotic cells never separates into discrete membrane enclosed fragments that in apoptotic cell death are referred to as apoptotic bodies (Kerr *et al.*, 1994). Whereas there is DNA fragmentation in apoptosis, the DNA degradation in necrosis does not occur to the same extent. During the necrotic process lysosomes may rupture and with the escape of lysosomal enzymes, DNA and other cellular components get digested. DNA is then cleaved into fragments that are heterogeneous in size and therefore do not form discrete bands, but rather smears, upon agarose gel electrophoresis. The release of these lysosomal hydrolases is further thought to rapidly accelerate the cellular disintegration in late necrosis (Schwartzmann and Cidlowski, 1993). The above characteristics

distinguish necrotic cells from apoptotic ones, but there are sometimes similarities between these two types of cell death so conclusive evidence of apoptosis therefore has to include more than one morphological or biochemical criterion (Studzinski, 1995).

### **1.7.3 Apoptosis And Therapeutics**

Dysregulation of apoptotic cell death has been suggested to play a role in the pathogenesis of a variety of human diseases. Defects in genes that control apoptosis can result in too little apoptosis and the survival of cells that under normal conditions would be destroyed; this can promote cancer development (Tannock and Hill, 1998). Hence, a way to stimulate apoptosis in malignant cells would be therapeutically valuable. The observation that apoptosis is a programmed process in which gene transcription may be required is encouraging, so it may be possible to control this process by developing drugs to act against the molecular components in the apoptotic pathway. A wide range of agents are thought to induce apoptosis (Shellhaas and Zuckerman, 1995; Kaufmann and Earnshaw, 2000), a summary of anti-cancer treatments that induce apoptosis *in vitro* has been given by Kaufmann and Earnshaw (2000). This list includes the intercalating agents, doxorubicin and mitoxantrone, the topoisomerase I poisons, camptothecin and topotecan as well as the topoisomerase II poisons etoposide and teniposide. Etoposide, camptothecin, doxorubicin and several other agents have been found to induce DNA fragmentation (Kaufmann, 1989; Onishi *et al.*, 1993). It has also been proposed that apoptosis might proceed through mechanisms that vary

according to cell type or apoptotic inducer. The topoisomerase inhibitors, camptothecin and etoposide that were potent apoptotic inducers in HL60 cells, induced only a weak apoptotic response in Syrian hamster embryo (SHE) cells. In both cell lines condensation of chromatin and DNA fragmentation were observed, but whereas caspase-3 was activated and poly(ADP-ribose)polymerase (PARP) cleaved in HL60 cells, caspase-3 activation was not observed in SHE cells. SHE cells did however show increased p53 levels following topoisomerase inhibitor treatments, which would indicate that DNA damage is induced, but despite this there were no massive apoptotic responses (Alexandre *et al.*, 2000). The way in which various anticancer drugs induce apoptosis has not been fully established, but apoptosis is likely to be an important part for chemotherapy to be successful. Cellular transformations that decrease the ability to activate the apoptotic machinery might play a role in the resistance observed with many drugs (Kaufmann and Earnshaw, 2000).

## **1.8 P21**

There are various reasons for thinking of apoptosis as a cell cycle phenomenon, and some of these have been discussed by Meikrantz and Schlegel (1995). In brief, apoptosis is mainly found in proliferating tissues. Depending on the point of arrest, the manipulation of the cell cycle can either prevent or potentiate apoptosis. By premature activation of cdks it is possible

to induce apoptosis, but also premature mitosis, often referred to as mitotic catastrophe.

P21 is a cell cycle regulation protein and this cdk inhibitor has, following its identification in the early 1990's, also been given several other names as it has been cloned independently by different routes. Cip1 (cdk-interacting protein) (Harper *et al.*, 1993), was identified with a screen for human proteins that interact with cdk2. Sdi1 (senescent cell derived inhibitor) (Noda *et al.*, 1994) was identified in a search for expression to prevent growing cells from entering S-phase. In addition, WAF1 (wild-type p53 activated fragment) (El-Deiry *et al.*, 1993), was discovered in identifying genes stimulated by wild-type p53 but not mutant p53. Pic1 (p53-regulated inhibitor of cdk) is another acronym that has been suggested by Xiong *et al.* (1992) and Zhang *et al.* (1993) that is based on the p53-mediated induction of WAF1 as well as the ability of cip1 to inhibit cdk-cyclin activity. Localisation studies of p21 proteins have revealed that these proteins formed quaternary complexes with cyclins (A, B, D or E), cdk (cdk2 or cdk4) and proliferating cell nuclear antigen (PCNA), a protein important in DNA replication and DNA repair (Xiong *et al.*, 1992; Zhang *et al.*, 1993; Waga *et al.*, 1994). The fact that p21 associates with PCNA makes it different from other cdk inhibitors. The interaction of p21 with cdk-cyclin complexes is thought to result in arrest of the cell cycle in G1, whereas the effects on cell cycle progression from interactions of p21 with PCNA have not been clearly defined. The p21-PCNA interaction possibly plays a part in both G1 and G2 arrest (Cayrol *et al.* 1998). More detailed

information about the identification of p21 and inhibition of cyclin-cdk complexes in cell cycle control can be found in a review by Hunter (1993). An overview of p21 functions and its relation to malignancies has been given by Harada and Ogden (2000).

### **1.8.1 P21 In Cell Cycle Arrest And Apoptosis**

Cells may respond to DNA damage by either arresting the cell cycle (G1 and G2 arrest) or by instructing the cell to die. The p21 protein is thought to mediate some of the effects of p53, mainly the G1 cell cycle arrest in response to DNA damage, but a role of the p21 protein in G2 arrest has also been suggested (Cayrol *et al.* 1998; Rigberg *et al.*, 1999). Since p21 appears to be directly activated by p53, and a major part of p53 mediated growth arrest is thought to proceed through the induction of this cdk inhibitor, its identification was considered to provide a direct link between growth suppression by p53 and cell cycle regulation by cdks (Hunter, 1993; Evan and Littlewood, 1998). However, there appear to be at least two separate pathways of p21 induction: a p53-dependent pathway activated by DNA damage that leads to cell cycle arrest, and a p53-independent pathway associated with cell growth that is activated by growth factors at the entry into the cell cycle.

Whereas growth arrest is elicited in some cells following p21 expression (Di Leonardo *et al.*, 1994) apoptosis may occur in others (El-Deiry *et al.*, 1994). It is further suggested that if sufficient levels of p21 are not expressed, the cell

cycle arrest may be converted into apoptotic cell death and this protein may thereby be a critical checkpoint protein for both cell cycle arrest and apoptosis in response to DNA damage (Waldmann *et al.*, 1996). The role of p21 in apoptosis is, however, controversial and p21 induction might take place under different physiological situations. Gamma radiation that induced p21 via p53 in p53 positive cells did not induce p21 expression in HL60 cells, as these are p53 negative (Serrano *et al.*, 1993). However Steinman *et al.* (1994) showed that p21 upregulation was evident in HL60 cells that were induced to differentiate, but when HL60 cells were induced to undergo apoptosis there was (as in the study above) no p21 increase in this cell line. Therefore it appears that expression of p21 is neither necessary nor sufficient for apoptosis in p53 negative cells. Using urothelial carcinoma cells, it was proposed that while p21 inhibits proliferation by p53-dependent or p53-independent mechanisms, p21 does not mediate p53-induced apoptosis in these cells. The results in this study therefore suggested that the function of p21 in p53 mutant urothelial carcinoma cells appears to be restricted to the regulation of cell proliferation (Makri *et al.*, 1998). Furthermore, p53-dependent apoptosis does occur in cells lacking p21 following DNA damage (Waldmann *et al.*, 1996). In different experiments performed by El-Deiry *et al.* (1994), p21 was up-regulated in cells undergoing p53 associated G1 arrest and apoptosis but not in cells induced to arrest or undergo apoptosis by p53 independent mechanisms. This suggests that p53 is required for p21 to be induced following DNA damage and this is supported by studies of wild type and mutant p53 containing cells, where p21 was only induced in the wild type p53 cell line upon DNA damage. To summarise the findings from the above

mentioned studies, it seems that while p21 mediates the growth inhibitory effects of p53 in response to DNA damage, it is not clear what role, if any, it plays in p53-mediated apoptosis. Data exist supporting both pro- and anti-apoptotic functions, and p21 involvement in apoptosis may vary depending on cell type and physiological situation.

## **1.9 P53**

Despite the large number of different cancers and the heterogeneity among malignant diseases affecting different tissues, there seem to be alterations in a certain protein, involved directly or indirectly in many of these, suggesting that there might be one pathway for controlling abnormal growth (Vogelstein and Kinzler, 1992). P53 is a likely candidate considering that this protein has tumour suppressive activity and that loss of wild type p53 function takes place in almost all human cancers (Hollstein *et al.*, 1991). It is now well established that p53 plays a highly important role in preventing cancer development by arresting or killing potential tumour cells, and impaired p53 function has been associated with loss of normal cell cycle control and diminished apoptosis, as well as genomic instability.

P53 was originally identified towards the end of the 1970s in co-immunoprecipitations with the SV40 T antigen (Linzer and Levine, 1979; Lane and Crawford, 1979) and was initially thought to have dominant oncogenic activity. However, later studies demonstrated that it is mutant p53 that has

dominant oncogenic activity, and wild type p53 is instead a tumour suppressor (Lane and Benchimol, 1990). To highlight this, the rate of spontaneous tumours in p53 deficient mice (Donehower *et al.*, 1992) is increased and these high rates may partially result from a lack of p53-induced apoptosis.

P53 proteins are capable of integrating a variety of stress signals and following these, bind to specific DNA sequences. The binding of p53 to DNA will activate corresponding genes and via these gene products the cells are hopefully enabled to respond to the signals accordingly (Hall *et al.*, 1996; Hall, 1998). In normal cells p53 monitors the integrity of the genome and responses initiated via the p53 pathway may lead to cell growth inhibition by arresting proliferation and allowing time for repair, or to apoptosis if the damage is extensive (Lane, 1992). These responses thereby prevent the propagation of cells that may be undergoing malignant transformation. The favoured response will however depend on factors such as cell type and environment (Vousden, 2000; 2002). In contrast to cell cycle arrest, the pathway of p53-mediated apoptosis is less well defined, with the induction of many specific target genes (Sabbatini *et al.*, 1995; Attardi *et al.*, 1996) that appear to differ from those applied in growth arrest (Friedlander *et al.*, 1996a). Studies have revealed proteins with which p53 may interact, but in many cases the functional consequences of such interactions are yet to be established. Genes with p53-responsive elements include p21, mdm2 and many others. Mdm2 was the first p53 partner to be identified (Oliner *et al.*, 1992). It has been found that overexpression of this protein may affect cells in a similar manner

as mutations of the p53 gene, and the realisation that mdm2 could be an important oncogene stepped up the search for other p53 associating proteins.

### **1.9.1 Cell Cycle Arrest Or Apoptosis?**

It is not clear how a cell makes the choice between arrest and apoptosis following damage-induced p53 expression. It is also uncertain whether or not p53 mediates apoptosis by separate mechanisms from which it regulates cell cycle arrests. It has been suggested that p53 inhibits progression of the cell cycle, but in certain contexts such as over expression of oncogenes, simultaneous inhibition and stimulatory signals may clash and result in apoptosis (Shiamura and Fisher, 1996). On the other hand it is likely that cell cycle arrest and apoptosis are different separable functions of p53; that p53 differentially controls cell cycle arrest and apoptosis depending on which target genes it activates (Rowan *et al.*, 1996; Chen *et al.*, 1996; Ryan and Vousden 1998). Furthermore, the extent of DNA damage and possibly the level of p53 may affect the choice between cell cycle arrest and apoptosis (Chen *et al.*, 1996). However, to contradict this, the basal levels of p53 in some cells are higher than the stimulated levels reached in others following DNA damage (O'Connor *et al.*, 1997). These observations thereby suggest that whether or not apoptosis occurs depends more on the cellular context such as cell type, cellular environment or whether the cell has sustained other oncogenic alterations, than on the level of p53 (Fojo, 2002; Vousden, 2002).

### **1.9.2 P53 In Cell Cycle Arrest**

Cells containing functional p53 are, after DNA damage, likely to undergo cell cycle arrest. Following such damage there is a rapid increase in p53 protein levels. This rapid increase is thought to be due to post-translational changes in p53 stability and leads to transcriptional activation of certain target genes. P53 mediated cell cycle arrest is thought to proceed via the cdk inhibitor p21 and also via Gadd45 and 14-3-3 $\sigma$ . The p21 upregulation prevents cells from entering S-phase by arresting in G1, and p21 is also thought to bind PCNA and via this interaction prevents DNA replication (Pines, 1994). While p21 is predominantly implicated in G1 arrest, Gadd45 is one of the mediators thought to be involved in the G2/M-phases (Kastan *et al.*, 1992; El-Deiry *et al.*, 1993). Gadd45 is induced by p53 following DNA damage, at which point it binds PCNA and this is thought to stimulate DNA damage repair, indicating that p53 may be involved in controlling the DNA repair machinery (Smith *et al.*, 1994). Therefore p53 mediated induction of both p21 and Gadd45 may make it possible for p53 to inhibit DNA replication and simultaneously propagate DNA repair.

### **1.9.3 P53 In Apoptosis**

Apoptosis plays an important part in normal cellular homeostasis, and early studies restoring p53 function to p53 deficient cells resulting in rapid apoptosis, provided evidence that p53 may control apoptosis (Yonish-Rouach *et al.*, 1991). The occurrence of tumour cells with deficient p53 functions

possibly reflects a growth advantage and damaged apoptotic responses, compared to normal wild type p53 containing cells. It has also been shown that lack of p53 is linked to resistance, whereas wild type p53 cells are more sensitive. Initially it may seem strange that cells containing no p53 and therefore incapable of properly repairing damaged DNA, would be more resistant. However, p53 can also affect a cell's susceptibility to apoptotic cell death and this would provide an explanation for this phenomenon. It has been shown that the absence of proper p53 function confers chemotherapy resistance (Lowe *et al.*, 1993a; Blandino *et al.*, 1999). The cellular effect of p53 disruptions may however vary between cell lines and this could possibly be explained by differences in the apoptotic regulatory signals. Adverse alterations in other proteins along the p53 mediated pathway(s), either before or after p53 tumour suppressor activity, can potentially be equivalent to inactivation of p53 itself. This could disrupt all, or part of the p53 pathway, and lead to disruptions in cell cycle check points, genomic instability and possibly tumourigenesis as a result (Agarwal *et al.*, 1998). Various anti-cancer agents are known to induce DNA damage, resulting in apoptosis. P53 may, however, also modulate apoptosis from other stresses that do not induce DNA damage, and the variety of stimuli that are able to induce apoptosis via the p53 pathway, indicate that p53 activation might be a general stress response (Wagner *et al.*, 1994; Hermeking and Eick, 1995).

DNA damage induces p53 and apoptosis, but the pathway whereby p53 leads to execution of apoptosis is not well characterised. It was initially thought that pro-apoptotic bax was the main effector of p53 in apoptosis. The p53-bax

pathway involves translocation of bax from the cytosol to mitochondrial membranes. The resulting release of cytochrome c from mitochondria activates initiator caspase-9, setting off the caspase cascade. However, these days it is thought that there must be effector proteins other than bax involved in p53-mediated apoptosis and several apoptosis related genes that are transcriptionally regulated by p53 have now been identified (Miyashita and Reed, 1995; Oda *et al.*, 2000; Nakano and Vousden, 2001; Polyak *et al.*, 1997).

P53-responding caspases include caspase-9, caspase-3 and caspase-8, which suggest that the p53-mediated apoptotic pathway(s) converge on initiator as well as effector caspase activation (Fischer *et al.*, 2003). Caspase-3 is a general executioner that is involved in many apoptotic pathways. It has been proposed that the p53-mediated cellular destruction in apoptosis could be carried out via activation of caspase-3 (Cregan *et al.*, 1999; Hietanen *et al.*, 2000; Schuler 2000). However, the mechanism by which p53 activates the caspases and if these are required in p53-mediated apoptosis is still to be deduced.

While a crucial role for the p53 tumour suppressor gene in the execution of some forms of apoptosis has been demonstrated, other studies have reported that not all forms of apoptosis require p53 and data have been gathered showing evidence of p53-independent apoptosis (Lowe *et al.*, 1993b; Clarke *et al.*, 1993; Liu *et al.*, 2002). HL60 cells containing no p53 are indeed capable of dying by apoptosis independently of p53-mediated transcription, and DNA

damage may also kill cells with mutant p53 proteins, unable to trans-activate target genes. Thus cells that sustain sufficient damage may undergo apoptosis regardless of their p53 status. In addition, apoptosis that continually occurs during development appears to take place in p53 knockouts (Lowe *et al.*, 1993b).

#### **1.9.4 P53 Mutations**

To date several tumour suppressor genes and oncogenes that are in mutated form in human cancers have been identified, with cancers being derived from some combination of these mutant genes. P53 is a nuclear phosphoprotein and the core of p53 can fold to form a domain that can bind to double stranded DNA in a sequence specific manner (Kern *et al.*, 1991; Bargonetti *et al.*, 1991; Hall, 1998). Crystal structures of this DNA binding configuration have indeed revealed a highly folded and conformationally complex architecture (Cho *et al.*, 1994). The complexity of the interaction(s) between p53 and DNA is likely to make this protein sensitive to mutations, and a number of these have been reported (Halevy *et al.*, 1990; Blandino *et al.*, 1999; Fojo, 2002). In fact, p53 is the single most common molecular abnormality in human cancers. Overall it is estimated that as many as 40-50% of all cancers have p53 mutations, and whereas only 10-20% of prostate cancers and leukaemias have mutated p53, as many as 60-70% of head and neck, colon and lung carcinomas express mutant p53 (Fojo *et al.*, 2002). The problem in tumour cells with mutated p53 is that these are not capable of proper cell cycle arrest. Due to this, these cells are often genetically unstable

and therefore readily accumulate mutations and abnormal chromosomal rearrangements resulting in malignancies. Studies of mice containing no p53 confirm this. These mice developed normally, but did indeed have an increased incidence of tumours (Donehower *et al.*, 1992). Cells undergoing p53 mutation or loss would therefore have a selective advantage during tumour progression, but it is not only the increased incidence of mutations and the occurrence of tumours that will be a problem associated with mutant p53; as mentioned above, loss of p53 activity may also be related to resistance. Tumour cells may acquire drug resistance through p53 mutations disrupting the apoptotic pathway. Thus, the presence of p53 may in some cases be required for efficient activation of apoptosis following chemotherapy, whereas the absence of p53 confers resistance (Lowe *et al.*, 1993a; Blandino *et al.*, 1999).

### **1.9.5 P53 Interactions With Topoisomerases**

It is not clear how the cell allocates all the topoisomerase tasks involved in DNA metabolism between different cellular topoisomerases. More answers as to how a cell divides up the tasks to the different types of topoisomerases, possibly lie in the identification of other proteins such as chromosomal proteins or transcription factors with which the topoisomerases interact. P53 is an example of a tumour suppressor with which topoisomerases are thought to interact. Both topoisomerase I and topoisomerase II have been found in complexes with p53 and it has been reported that p53 stimulates the enzyme activity of topoisomerase I *in vitro* (Gobert *et al.*, 1996; Albor *et al.*, 1998). It

was suggested by Cowell *et al.* (2000) that topoisomerase II generates a background level of DNA strand breaks that can be tolerated in cells if repaired. Further, an interaction between topoisomerase II and p53 may be required for these breaks to be realised and repaired. Thus, this interaction between topoisomerase II and p53 may be important in providing cells a surveillance mechanism for topoisomerase II mediated genomic damage. This group also found that both topoisomerase II $\alpha$  and topoisomerase II $\beta$  interact with p53 *in vitro* in plasmids and *in vivo* using human mammary carcinoma (MCF7) cells. Overexpression of topoisomerase II is common in many cancers and topoisomerase II binding to p53 may be involved in inhibiting p53 mediated apoptosis in cells. Faults in this regulation could possibly help to explain the early stages of carcinogenesis when p53 mutations are rare (Yuwen *et al.*, 1997).

### **1.9.6 P53 And Therapeutics**

The cellular targets for many anti-cancer drugs have been identified, but less is known about the mechanisms leading to cell death of cancer cells (Dive and Hickman, 1991). A major goal is to identify features unique to tumour cells that can act as targets for new drug discovery. A number of genes, and in particular p53, are thought to be important for efficient induction of apoptosis. Many anti-cancer agents are thought to activate a so called "intrinsic" apoptotic pathway (Fuchs *et al.*, 1997; Sun *et al.*, 1999). The events before mitochondrial cytochrome c release and caspase activation in this intrinsic pathway are not well understood, but are thought to involve bax. It

could be that p53 increases bax transcription, or p53 may induce conformational changes and mitochondrial targeting of bax, or this pathway may go via different so far unidentified mediators (Schuler *et al.*, 2000). When the p53 pathway(s) and the relationship between p53 status and therapeutic response to chemotherapy have been completely deduced, analysis of p53 protein may provide some prediction of therapeutic responses, or p53 could provide a target for more tailored cancer treatments (Lowe *et al.*, 1993a).

Several mechanisms are now being explored with regard to the knowledge of p53 and p53-mediated pathways in an attempt to kill tumour cells (Vogelstein and Kinzler, 2001). For example it may be beneficial to stimulate p53 functions in cells that retain their wild type p53, but are defective in their ability to activate this protein, or to re-introduce wild type p53 into p53 mutant tumours. This could reverse the malignant phenotype, or enhance cellular sensitivity to the drugs used in treatment. A number of researchers have claimed to be able to regain at least some wild type functions from mutant p53 proteins, and *in vitro* data do suggest that this may be possible. Different strategies have recently been developed in an attempt to kill cancer cells with deficiencies in their p53 pathways, for example, the transfer of wild type p53 into cancer cells with gene replacement therapy using adenovirus vectors (Liu *et al.*, 1994; Gomez-Manzano *et al.*, 1996; Hitt *et al.*, 1997). Another virus-based approach uses a mutant human adenovirus that has been designed for viral replication in p53 mutant cells but not in wild type containing cells. Thus, normal cells will be resistant to cytolysis whereas the virus replicates and kills tumour cells with mutant p53. Additionally, destroyed cells will release more

viruses capable of infecting other p53-mutant containing tumour cells (Bischoff *et al.*, 1996).

Targeting other p53 interacting/controlling proteins is also being investigated. For example mdm2 proteins play an essential part in normalising p53 levels following its activation and this interaction could in theory make a target (Bottger *et al.*, 1997). In wild type p53-containing tumours inactivated by faulty mdm2 proteins, restoration of p53 activity can be achieved by anti-sense approaches decreasing levels or blocking undesired interactions.

Another approach (that may be relevant to the NU:UB category of compounds studied in this research project, discussed in Chapter 7) is the identification and design of small molecules with therapeutic, stabilising potential against mutant p53, restoring their wild type activities in cancer cells (Foster *et al.*, 1999). For example, compared to approaches using viral delivery systems that have disadvantages such as inefficiency of gene transfer and risk of toxicity and immunoresponses to viral antigens, the use of synthetic compounds provides low toxicity upon administration and ease of entry into tumour cells due to small size.

In summary, various therapeutic strategies have been attempted to restore p53 function to cancerous cells. The above-mentioned therapies and others have recently been described by Willis and Chen (2002), and by Lane and Lain (2002).

## 1.10 MDM2

It is essential for the organism that apoptosis is properly regulated, being initiated when required but not otherwise. The understanding of how apoptosis is regulated will have great implications in the cancer area, as well as in other areas. From the above information it is clear that p53 is implicated in both cell growth and apoptosis, so the regulation of p53 activity is therefore critical to allow for both normal cell division and tumour suppression. Thus, p53 function must be dampened sufficiently to allow normal growth and development, while retaining the capacity for rapid induction in response to stresses associated with tumourigenesis. P53 is subject to a diverse range of regulatory mechanisms which keep it in check until needed and, in addition to synthesis and degradation of p53, other mechanisms are also involved. For example: protein-protein interactions, post-translational modifications as well as regulation of the subcellular localisation of p53 (Levine, 1997; Agarwal *et al.*, 1998; Vousden, 2002).

With regard to regulation of p53 degradation, this process is mainly initiated by mdm2. Mdm2 is the abbreviation for murine double minute 2 and the human analogue of this gene is named hdm2 accordingly. The human mdm2 can be found on 12q13-q14 where it encodes a 90kDa, 491 amino acid nuclear phosphoprotein and this protein has further been identified as a dominant transforming oncogene (Fakharzadeh *et al.*, 1991). Activation of p53 requires post-transcriptional modifications of the protein by, for example phosphorylations and acetylations. These modifications contribute to the

dramatic increase in the half-life of p53 and the fine-tuning of its transcriptional activities, and mdm2 appears to be of importance in these aspects of p53 regulation. Thus, the relationship between mdm2 and p53 is thought to be carefully controlled by complex post-translational modifications, determining the stability and activity of p53 and mdm2. In normal unstressed cells mdm2 maintains low levels of inactive wild type p53. However, in response to various stimuli p53 accumulates inducing cell cycle arrest and/or apoptosis (Levine, 1997). Stress dissociates mdm2 from p53 and this stabilises p53 and increases transcription of p53 target genes. Fig. 1.7 schematically shows how DNA damage causes disruption in the mdm2-p53 interaction and stabilisation of the p53 protein (Colman *et al.*, 2000). The mdm2 gene itself is a transcriptional target of p53, and accumulation of mdm2 protein could be important for cellular recovery once the cell damage has been repaired (Daujat *et al.*, 2001; Vousden, 2002). The interval between p53 activation and consequent mdm2 accumulation defines the time window during which p53 exerts its effects. During recovery from DNA damage, maximal mdm2 induction coincides with rapid p53 loss. Results by Haupt *et al.* (1997) showed that mdm2 could significantly reduce p53 levels and that binding of mdm2 to p53 is important for this effect. In their study, p53 peaked within 1h of radiation then decreased over the next 2h, whereas mdm2 peaked 1.5-2h post irradiation coinciding with the subsequent p53 loss. Furthermore, earlier research had also determined that whereas p53 stimulates synthesis of mdm2 proteins, mdm2 can in turn inhibit p53 activation by binding to the transcriptional domain of p53, so in this way p53 and mdm2 form an interrelationship (Chen *et al.*, 1993; Picksley and Lane, 1993,

Vousden 2002). The complex interrelationship between mdm2 and p53 is thought to involve mdm2 binding to the transcriptional N-terminal region of p53. Thus mdm2 counteracts p53 activity not only by mediating its degradation (acting as a shuttling protein, inducing nuclear export of p53 for ubiquitination and degradation), but mdm2 also interferes with the transactivation of p53 by blocking its transcriptional activation domain (Haupt *et al.*, 1997; Kubbutat *et al.*, 1997; reviewed by Vousden 2002).

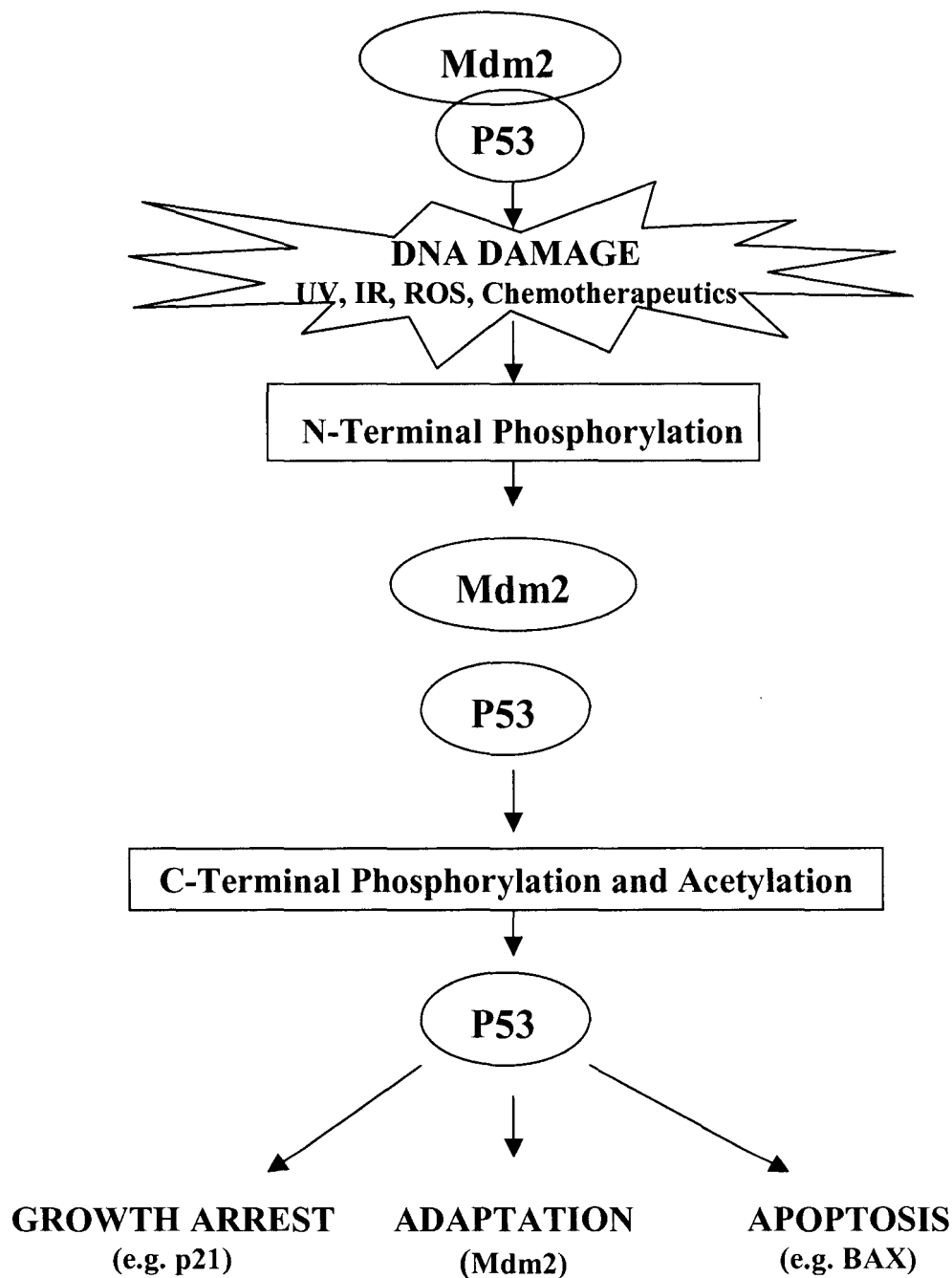


**Fig 1.7** Activation of p53-mediated gene expression in response to DNA damage. Various types of DNA damage trigger the phosphorylation of the p53 N-terminus, which stabilised the p53 protein via disruption of the mdm2-p53 interaction. Activation of the latent DNA-binding activity of p53 is facilitated through the phosphorylation-acetylation cascade at the p53 C-terminus. Integration of signals by p53 culminates in growth arrest, apoptosis, or adaptation to DNA damage. Figure adapted from Colman *et al.*, 2000.

## 1.11 CASPASES

Activation of a family of proteases is thought to be central to the apoptotic pathway. These types of proteases, now named caspases appear to be responsible for many of the characteristics of apoptotic cell death. The name caspase was based on two catalytic properties of these enzymes. The 'c' refers to a cysteine present in the active site of these proteases, and 'aspase' refers to their most distinctive catalytic feature, i.e. to cleave substrates after aspartic acids (Caspases=Cysteine-Aspartate Proteases). The caspases are first synthesised as pro-enzymes and these inactive precursors are named pro-caspase-1, pro-enzyme-3 accordingly (Alnemri *et al.*, 1996). The mammalian caspase family is growing and currently contains 14 members. Most of the so far identified caspases participate either in the activation of pro-inflammatory cytokine pathways, or in the promotion of apoptotic cell death pathways (Salvesen and Dixit, 1997). Caspase -2, -3, -6, -7, -8, -9 and -10 are involved in apoptosis, while caspase -1, -4, -5 and -11 are mainly involved in cytokine processing. Not much is known about the latter caspase group, involved in cytokine processing, and in addition caspase -12, -13, and 14 have been identified but not yet characterised.

### 1.11.1 Caspases In Apoptosis

In this project we investigated apoptotic caspase activation in cancer cells in response to NU:UB compound exposure. Goyal (2001) compared the apoptotic dismantling of cells with the implosion of a building that depends on

the precise detonation of explosives where the explosives would be represented by the caspases in an apoptotic cell. The caspase enzymes make up a so called, caspase cascade that is triggered in response to pro-apoptotic signals and culminates in cleavage of proteins that result in the disassembly of the cell. Caspases involved in mediating apoptotic cell death have been subdivided into upstream signalling initiator caspases and downstream effector caspases. This was mainly based on their structure and length of their respective pro-domain. Long pro-domain caspases include caspase-2, -8, -9 and -10. These are typically recruited into membrane complexes by adaptor proteins, initiating the caspase cascade and thereby activating other caspases. The effector caspases, caspase-3, -6 and -7 have short pro-domains and are presumed to dismantle the cell. This model of initiating and effector type caspases gives an understanding of the caspase cascade, but the cellular situation is often more complex, as caspases further down the cascade can amplify the response by feeding back on caspases further up. An example of this is caspase-3; following its activation by an initiator, caspase-9, this effector caspase-3 can feed back on caspase-9 thereby amplifying the cascade (Slee *et al.*, 1996). Inactive pro-caspases can be activated by proteolytic cleavage and are usually activated at conserved Asp residues, therefore, most activated caspases can process their own (auto catalysis triggered by e.g. cofactor binding) as well as other caspase precursors (Salvesen, 1997). Furthermore, large amounts of pro-enzymes can be made and accumulated in advance and then activated when required (Thornberry and Lazebnik, 1998).

While many caspases are localised in the cytosol, many of their substrates are contained within the nucleus or other cellular compartments and there is therefore likely to be some delay between caspase activation and the proteolytic attack of the target (Slee *et al.*, 1996). Caspase activity is however thought to be an early event, possibly preceding phospholipid (PS) externalisation. PS externalisation observed in response to several agents is thought to be one of the earliest indications of apoptosis, preceding nuclear changes associated with apoptotic cell death. Studies of caspase inhibition however blocked the externalisation of membrane PS, which would indicate that the loss of membrane phospholipid asymmetry is a downstream event of caspase activation (Pervaiz *et al.*, 1998).

Caspases participate in apoptotic control on several levels, as triggers of the death machinery, as regulatory elements within it and also as effectors of the machinery itself. The cellular death programme can be divided into different phases: initiation, commitment, amplification and demolition. These phases have been depicted in Fig. 1.8 (Slee *et al.*, 1996).

#### 1.11.1a Initiation

In the initiation phase the cell receives signals and these may result in the activation of cell death. The initiators can be further divided into three categories: death receptor signals, contents of cytotoxic T and NK cell granules and stimuli such as cytotoxic drugs and radiation that provoke generalised cellular damage.

### 1.11.1b Commitment

The commitment phase is the point at which the death signals become irreversible and here the mitochondria appear to be an important sensor of cellular damage. Several pro-apoptotic stimuli provoke changes in the permeability of the outer membrane of the mitochondria permitting the escape of proteins such as AIF and cytochrome c. These can be released in a caspase dependent or a caspase independent manner (via unknown effectors). Which it is, most likely depends on the nature of the pro-apoptotic stimulus. AIF exerts its effects in a caspase independent manner by translocating to the nucleus and triggering chromatin collapse and fragmentation into high molecular weight fragments that is commonly observed during apoptosis. When cytochrome c is released from mitochondria it regulates activities of Apaf-1 and the so called apoptosome is formed. The apoptosome is a large protein complex of approximately 700-1400 kDa that is composed of several Apaf-1 molecules, that each has a bound caspase-9 molecule and dATP is also involved (Cain *et al.*, 2002). The apoptosome recruits and activates caspase-9 that drives the next, amplification phase of the caspase cascade.

### 1.11.1c Amplification

In the amplification phase, multiple caspases are activated in a cascade to cooperate in the destruction of the cell. The caspase activation events driven by caspase-9 appear to be simultaneously the activation of caspase-3 and -7.

Caspase-3 then drives the activation of caspases-2 and caspase-6 followed by activation of caspase-8 and caspase-10.

#### 1.11.1d Demolition

Finally, when the caspases that are necessary for proper execution of the death programme are activated, the final demolition phase begins. In the demolition phase, caspases destroy cellular structures and inactivate various proteins directly, or via the activation (or inactivation) of other enzymes (Slee *et al.*, 1996). Thus, caspases are thought to be involved in all the phases of cell death and play a central role in the complex demolition process of apoptosis. Caspases are for example involved in reorganising the cytoskeleton, disrupting the nuclear structure, shutting down DNA replication and repair, interrupting splicing and disintegrating the cell into apoptotic bodies (Salvesen, 1997; Thornberry and Lazebnik, 1998; Cima and Brunner, 2003).

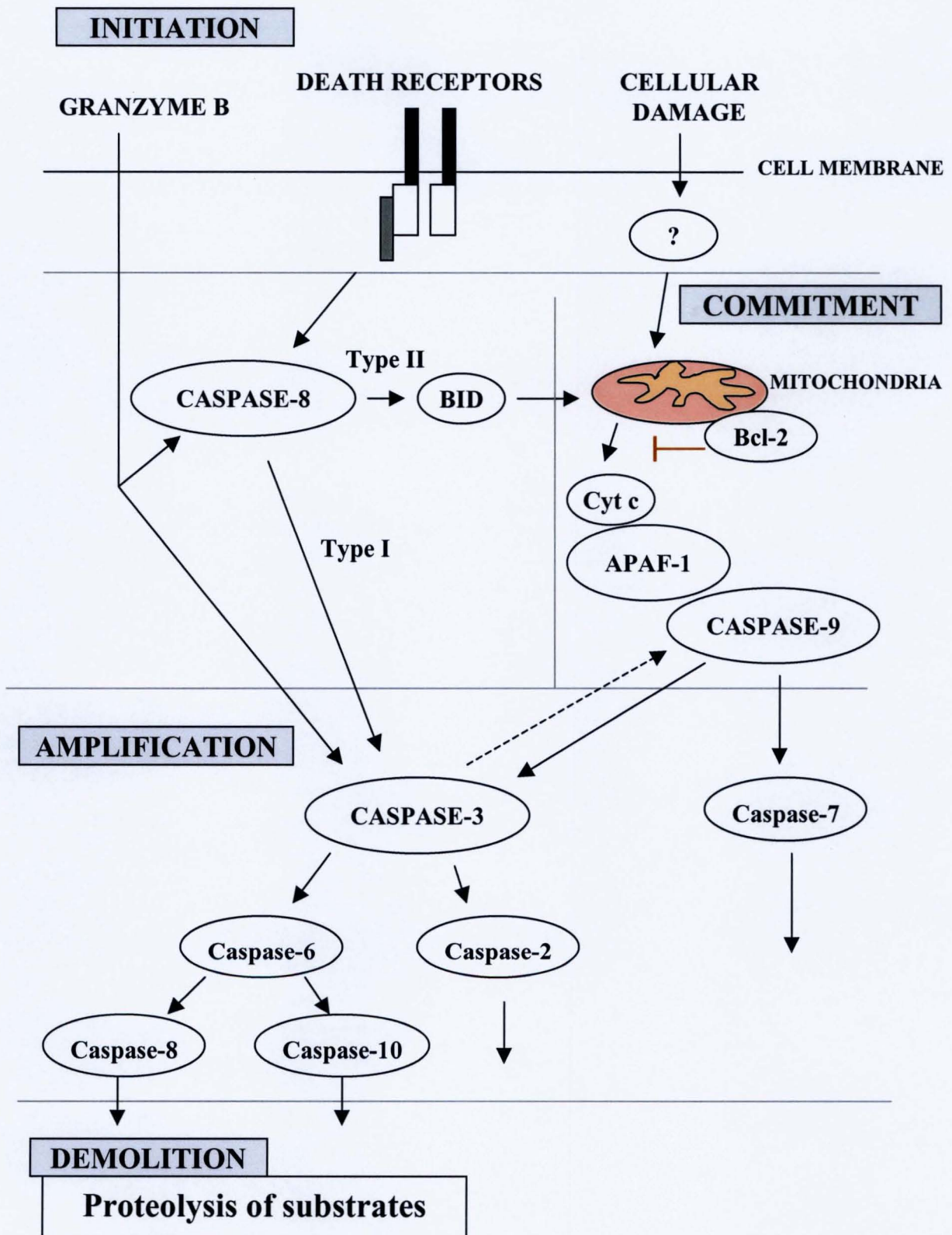


Fig 1.8 Representation of the routes to caspase activation. Figure adapted from Slee *et al.*, 1999.

### 1.11.2 Caspase-3

It is predominantly caspase-3 which has been in focus in apoptotic studies. This enzyme exists in the cytosol as a 33kD inactive pro-enzyme that is cleaved and activated in apoptotic cells. Caspase-3 cleaves PARP and is activated in HL60 cells by a number of agents. For example a study by Zhu *et al.* (2002) showed that squamocin induced apoptosis in HL60 cells. In their studies, a caspase-3 activation assay and Western blotting of caspase-3 (using time points from 2-6h) were performed. The results showed that caspase-3 was involved in the apoptosis induction since caspase-3 inhibitors prevented apoptosis. Furthermore, caspase-3 activation appears to be initiated by the release of cytochrome c from mitochondria (Martins *et al.*, 1997). However, it has been proved that apoptotic cell death does not require caspase-3, so although caspase-3 is considered to be important in the apoptotic cascade, MCF-7 human breast cancer cells that do not express caspase-3 can be made to undergo apoptosis after treatment with a variety of stimuli. Therefore, that MCF-7 cells, without caspase-3 undergo morphological and physiological apoptosis, suggests that they have an alternative pathway. With the use of caspase inhibitors, enzyme specific chromogenic substrates and antibodies it was determined that apoptosis in these cells proceeds via caspase-9, caspase-7 and caspase-6 (Liang *et al.*, 2001).

### 1.11.3 Apoptosis In Resistant Cells Via Caspase Activation

The major challenge in treating cancer is to kill cells that have become resistant to available chemotherapy. Failure to undergo apoptosis is associated with drug resistance, and different rational strategies have been identified during the last decade to re-sensitise resistant tumours. In particular, restoration of p53 has been an attractive target (discussed previously in 1.9). However, mutations of the p53 downstream effectors such as caspases might undermine such p53-targeted efforts (Pruschy *et al.*, 2001). Therefore direct activation of caspases in cancer cells may be an effective strategy to kill resistant cells (Salvesen and Dixit, 1997). When apoptotic signals in cells are uncoupled from caspase activation, the transformed cells survive. If these signals could be re-coupled to caspase activation this might provide an opportunity to selectively kill transformed cells. One possibility may be to activate death receptor complexes directly linked to initiator caspases but this should only happen in cancer cells and not in normal cells (Thornberry and Lazebnik, 1998). Furthermore, caspase-independent activation of apoptosis may be another way to induce apoptosis in cells with defects in their caspase cascade, and agents with caspase independent pathways may be useful for treatment of cancers resistant to usual chemotherapy. Though many anti-cancer drugs are known to induce apoptosis in tumour cells, few are reported to be independent of caspases. The means of caspase independent induction of apoptosis is so far uncertain, but a mitochondrial protein AIF could be connected to this pathway (Kawagoe *et al.*, 2002).

## **1.12 MITOCHONDRIA**

Mitochondria are indeed important organelles in cells and are involved in the regulation of several aspects of cell biology, including energy production, molecular metabolism e.g. fatty acid oxidation and purine and pyrimidine metabolism, redox status, calcium signalling and apoptosis. With so many and important functions, the estimation that 75-100 human disorders have improper mitochondrial function implicated at some point in their pathogenesis comes as no surprise. A recent area of research is the role of mitochondrial function in cancers and in the treatment of cancers. Gathered information of cancer drugs and their mechanism(s) of action have now revealed that several agents may have significant mitochondrial effects, even though these agents were not originally developed to act on mitochondrial targets (Howell *et al.*, 2003).

### **1.12.1 Mitochondrial Structure**

The mitochondria are approximately 1µm in diameter, elongated, thread like, differing in length and make up approximately 15% of the total cellular protein. The mitochondria are thought to have originated from protobacteria that have been taken up by nucleated cells. It is therefore possible that the inner mitochondrial membrane (IMM) originally stems from bacteria, whereas the outer mitochondrial membrane (OMM) is derived from a nucleated cell. Mitochondria can be divided into four parts, each with different compositions and functions: the OMM which is fairly porous, the IMM which is a highly

convoluted structure containing the enzymes of oxidative phosphorylation and a range of metabolite carrier proteins. Whereas the OMM is relatively permeable, the IMM is more impermeable and there is therefore a complex machinery involved to transport molecules across this membrane. The space in between these two membranes (OMM and IMM) is referred to as the intermembrane space and contains a number of specialised proteins. In the centre of mitochondria, enclosed by the IMM, is the mitochondrial matrix, this compartment contains mitochondrial DNA, ribosomes and enzymes used for many different pathways (e.g. for the urea cycle, the citric acid cycle and for fatty acid oxidation). Mitochondria contain their own DNA and all but 13 proteins (components of the respiratory chain or ATP synthase) of the hundreds of mitochondrial proteins, are encoded by nuclear DNA. This confirms that mitochondria do require nucleated encoded proteins for proper function (reviewed by Alberts *et al.*, 1998; Preston *et al.*, 2001; Murphy and Smith, 2000).

## **1.12.2 Mitochondrial Function**

### **1.12.2a ATP Production**

One of the main functions of mitochondria is to generate energy in the form of ATP, a process also referred to as respiration. To accommodate the enzyme complexes required for this ATP production a large surface area is required which is why the IMM has to be highly folded. One of the proteins in mitochondria involved in the production of energy is cytochrome c, which

transfers electrons in the electron transport chain. As electrons are transported along the chain, protons are pumped out of the matrix. This creates a negative potential called mitochondrial transmembrane potential wherein ATP synthase converts ADP to ATP (Waterhouse *et al.*, 2002; Custido *et al.*, 2001).

In the conversion of oxygen to energy (ATP) in mitochondrial respiration, reactive oxygen species (ROS, e.g. superoxide  $O_2^{\cdot-}$ , hydrogen peroxide  $H_2O_2$ , hydroxyl radical OH) are generated and mitochondria are therefore continuously exposed to ROS, which can have damaging consequences to the cell (Ames *et al.*, 1993; Shigenaga *et al.*, 1994; Wallace, 1999). For protection of cellular components, cells have developed antioxidant mechanisms for example glutathione GSH and superoxide dismutase SOD (Oberley and Oberley, 1997).

### 1.12.2b Mitochondria And Calcium

In addition to the major function of mitochondria, to provide ATP by oxidative phosphorylation, mitochondria have also a role in the modulation of intracellular calcium concentrations. If there is disruption of mitochondria calcium metabolism this may both interfere with cellular calcium signalling and make cells in danger of calcium overload and necrosis. Mitochondria may thus act as a safeguard to increased cytosolic calcium levels, in a mechanism to protect cells. The responses to high calcium levels in mitochondria depends on the duration of the calcium signal (Cano-Abad *et al.*, 2001) and on cell type

(Andreyev and Fiskum, 1999). Increased cellular calcium levels can be the result of exposure to chemicals; calcium accumulation in mitochondria may increase ROS production, cytochrome c release and result in cell death. Thus, calcium regulation by mitochondria seems to play a part in apoptotic cell death and therefore, adjusting the amount of calcium in mitochondria and the cytosol may inhibit or induce apoptosis (Parone *et al.*, 2002).

### 1.12.2c Mitochondria And Apoptosis

Mitochondria are thought to regulate apoptosis in cells since they store a range of apoptogenic proteins. These include Smac/Diablo (Du *et al.*, 2000; Verhagen *et al.*, 2000), AIF (apoptosis inducing factor, that is not thought to activate caspases directly but instead moves to and induces apoptosis via the nucleus) (Daugas *et al.*, 2000; Joza *et al.*, 2001), several caspases [pro-(2, 3, 8 and 9)] and cytochrome c. Cytochrome c appears to play a dual role in cells, it is a trigger of apoptosis but also in viable cells as mentioned above, a vital component of the respiratory chain.

In apoptosis, mitochondria may be integrating a range of apoptotic downstream signalling cascades. Several factors may be capable of transmitting death signals from e.g. DNA damage, radiation or oxidative stress to the mitochondria. For example bcl-2 and bax are found to translocate from the cytosol to mitochondria when exposed to apoptotic stimuli. Bid, another bcl-2 family member, is thought to mediate the death response from cell surface death receptors (via caspase-8) (Desagher *et al.*, 1999; Luo *et al.*,

1998). In response to nuclear DNA damage P53 is thought to be able to directly insert into mitochondria, activating caspases without causing release of cytochrome c. Furthermore, PUMA or Noxa (Nakano and Vousden, 2001; Oda *et al.*, 2000) have also been found to be involved in the p53-dependent death response to DNA damage, moving to mitochondria, and via Bcl-2 sub-families inducing the release of apoptogenic factors such as cytochrome c and other apoptotic proteins, for example pro-caspases and AIF. Thus, the mitochondria indeed seem to play a key role in the apoptotic processes linking the apoptotic mediators (e.g. bcl-2 proteins) with the effector molecules (caspases) (Parone *et al.*, 2002). In addition to apoptotic cell death, mitochondria also seem to be a factor in necrosis. Apoptotic cell death requires ATP, whereas extensive mitochondrial damage following ATP depletion and calcium overload results in uncontrolled necrotic cell death. Furthermore, if the ATP level falls below a critical threshold after initiation of the apoptotic pathway, this is aborted and the cell dies by necrosis (Leist and Nicotera, 1997; 1998).

Thus, mitochondria have been proposed to have a role(s) in cell death. However, the role(s) is controversial where several aspects of mitochondrial functions including generation of ROS, calcium overload and permeability transition and others have been implied. This area of research has recently been reviewed by Newmeyer and Ferguson-Miller (2003).

### 1.12.3 Mitochondria As A Potential Drug Target

Due to the fact that mitochondrial damage contributes to a range of human diseases, and because mitochondrial function is important in apoptosis, this organelle is potentially a promising intracellular target for drug delivery. The mitochondrial DNA is surrounded by the IMM where the electron transport chain generates ROS and these ROS species cause significant mitochondrial DNA damage, which is more common than nuclear DNA damage (Yakes and Vanhouten, 1997). The lack of introns in mitochondrial DNA further increases the probability that any mutation will be damaging to the mitochondrial DNA and this, together with the limited capacity for repair (Singh and Maniccia-Bozzo, 1990; Driggers *et al.*, 1996), makes mitochondria sensitive targets. In addition, the lack of histones makes mitochondrial DNA more susceptible to covalent binding by alkylating agents than nuclear DNA (Allen and Coombs, 1980). Mitochondria are thought to have a large membrane potential and lipophilic cations would therefore readily accumulate within mitochondria. Some cancer cells have been found to have elevated mitochondrial transmembrane potentials; therefore, if critical differences between the mitochondrial permeability transition pore of certain cancer cells and untransformed cells can be identified and targeted, this may provide a feasible target to enhance tumour destruction. Improved understanding of mitochondrial permeability transition pore agents and their functions may therefore prove useful for treatments. Additionally, therapeutics to prevent mitochondrial damage from free radicals, from mitochondrial DNA mutations,

or to genetically correct mutated mitochondrial DNA could possibly be useful in the future (reviewed by Murphy and Smith, 2000; Preston *et al.*, 2001).

## **CHAPTER 2**

### **MATERIALS AND GENERAL METHODS**

## 2.1 MATERIALS AND GENERAL METHODS

### 2.1.1 Anti-cancer Agents

A series of NU:UB compounds including NU:UB 31, 51, 43, 80, 81, and 150 were available in the host laboratory. Camptothecin (36,563-7, Aldrich); Doxorubicin (86036-0, Aldrich); Etoposide (E1383, Sigma); m-AMSA (A9809, Sigma).

The NU:UB compounds were dissolved in DMSO to make a stock solution of 10mM. From each stock, serial dilutions were made in suitable cell culture medium, making sure that DMSO concentration in cell treatments did not exceed 0.1%.

#### 2.1.2a Materials For Cell Culture

RPMI 1640 (without L-glutamine), McCoy's 5a, penicillin-streptomycin, foetal bovine serum (FBS), Hanks balanced salt solution (HBSS), trypsin, trypsin/EDTA (prepared by diluting 10x solution in sterile saline, the resulting 1x solution stored at  $-20^{\circ}\text{C}$ ) all obtained from Sigma. L-glutamine 2mM (Gibco); freezing medium (8% DMSO in FBS, filter sterilised and stored at  $-20^{\circ}\text{C}$ ); HL60 cells (human Caucasian promyelocytic leukaemia cells, ECACC, 85011431); HCT116 (human colon carcinoma cells, obtained from Bradford

University); HT29 (human colon adenocarcinoma cells, from Napier University); inverted light microscope, Axiovert 25 (Zeiss).

### 2.1.2b Methods For Cell Culture

HL60 cells were grown in suspension and were kept in RPMI 1640 medium supplemented with 2mM L-glutamine, 1% penicillin-streptomycin and 10% heat inactivated FBS.

The HCT116 and HT29 cells were both epithelial, adherent cell lines. HCT116 and HT29 were maintained in McCoy's 5a with the addition of 2mM glutamine, 1% penicillin-streptomycin and 10% heat inactivated FBS. These cell lines were passaged by trypsinisation.

All cell cultures were kept in a humidified incubator at 37°C with 95% air and 5% CO<sub>2</sub>. The cell lines were regularly examined under an inverted light microscope, Axiovert 25 (Zeiss).

### 2.1.3 Materials For Cytotoxicity Assays

Dimethyl Sulphoxide (DMSO), MTT (3-(4,5-dimethylthiazol-2-yl)-2,5-diphenyltetrazoliumbromide), Nigrosin (Sigma); Dynatech MRX microplate reader (Dynex Technologies).

## 2.1.4 Materials For DNA Mobility Assays (Topoisomerase Relaxation And Cleavage Assays)

Ethidium bromide, agarose, proteinase K, SDS, TBE buffer (10x, running buffer) (Sigma); plasmid pBR322 DNA (BDH); topoisomerase I (Amersham); topoisomerase II $\alpha$  and topoisomerase II $\beta$  (provided by Dr Caroline Austin, University of Newcastle upon Tyne); 10x running buffer (Tris Borate 0.89M, EDTA 0.02M); Proteinase K (5mg/ml); 10x topoisomerase I buffer (used for topoisomerase I relaxation and cleavage assay, 100mM Tris-HCl pH 7.9, 500mM KCl, 1mM EDTA, 50mM MgCl<sub>2</sub>, 150  $\mu$ g/ml BSA); 10x topoisomerase II buffer [used for ( $\alpha$  and  $\beta$ ) relaxation and cleavage assay, 100mM Tris-HCl pH 7.9, 500mM NaCl, 500mM KCl, 1mM EDTA, 50mM MgCl<sub>2</sub>, 150  $\mu$ g/ml BSA, 10mM ATP]; loading buffer (SDS 5%, Bromophenol Blue 0.25mg/ml, Glycerol 25%); mini horizontal submarine unit HE 33 (Hoefer).

### 2.1.5a Materials For Lysing Cells

Complete mini protease inhibitor cocktail tablets (1836170, Roche); lysing buffer (0.5% NP40 in PBS); 1% SDS lysis buffer in PBS (Boege *et al.*, 1996); 4M deionized urea (2.4g), 2% SDS (0.2g), 62.5mM Tris-HCl pH 6.8 (0.0985g), 1mM EDTA (3.7mg) in 10ml dH<sub>2</sub>O (Kaufman and Svingen, 1999).

### 2.1.5b Methods For Lysing Cells With Protease Inhibitors

Each protease inhibitor tablet was diluted in 1.5ml PBS to make up a 10x stock, which was aliquoted and stored at  $-80^{\circ}\text{C}$ . For use, each aliquot was diluted 1:10 in lysing buffer and put on ice. Cells were washed twice in ice cold PBS, pelleted by centrifugation at  $500 \times g$  for 5 mins at  $4^{\circ}\text{C}$ . Cells were immediately lysed with protease inhibitor lysing solution for 30 mins on ice, and centrifuged at  $15\,000 \times g$  for 20 mins at  $4^{\circ}\text{C}$ . Following centrifugation the supernatants were aliquoted and either stored at  $-80^{\circ}\text{C}$  until required, or protein content determined with the bicinchoninic protein assay and samples used immediately.

### 2.1.6a Materials For Bicinchoninic Acid Protein Assay

Protein (Bovine serum albumin) standard (P-O14), bicinchoninic acid, copper (II) sulphate (Sigma); BCA working reagent [copper (II) sulphate 4%(v/v) solution was added to bicinchoninic acid solution in the ratio 1:50 immediately prior to use].

### 2.1.6b Method For Bicinchoninic Acid Protein Assay

Total protein concentration in each sample was determined by the bicinchoninic acid protein (BCA) assay according to Smith *et al.* (1985). A serial doubling dilution of BSA standard 1mg/ml in PBS was prepared ranging from 1mg/ml to  $7.8\mu\text{g/ml}$ . These were stored at  $-80^{\circ}\text{C}$  and defrosted when

needed. 10µl of each sample and BSA standard were added to individual wells on a 96 well microtitre plate and 190µl working reagent was added. This was carried out in duplicate for standards and triplicates for samples. Blank wells, containing 190µl of working reagent and 10µl diluent were included in each analysis. The plate was covered and incubated at 37°C for 30 mins, after which the absorbance was measured at 570nm in a Dynatech MRX microplate reader. Using blank corrected mean absorbance values over the range of BSA standards, concentrations in the unknown samples were determined.

#### 2.1.7a Materials For Western Blotting And Immunostaining

PBS tablets, TEMED, ammonium persulphate, colour markers, SDS (Sigma); acrylamide mix 30% (BioRad); biotinylated markers (BioRad); 0.5M Tris pH 6.8 (30.4g Trizma base was dissolved in 400ml dH<sub>2</sub>O, pH was adjusted to 6.8 and the volume was made up to 500ml); 1.5M Tris pH 8.8 (91.2g Trizma base was dissolved in 400ml dH<sub>2</sub>O, the pH was adjusted to 8.8 and the volume made up to 500ml); 10% ammonium persulphate (50mg ammonium persulphate was dissolved in 500µl dH<sub>2</sub>O); 10% SDS (50g SDS was dissolved in 400ml dH<sub>2</sub>O and made up to 500 ml); separating gel (see table 2.2); stacking gel (see table 2.3); sample buffer (prepared by mixing 4.0ml dH<sub>2</sub>O, 1.0ml Trizma base 0.5M pH 6.8, 0.8ml glycerol, 1.6ml SDS (10%), 0.2ml bromophenol blue 0.05%); DTT 1M (1.54g DTT dissolved in 10ml dH<sub>2</sub>O to make a 10x stock, stored frozen. For use, DTT was diluted 1:10 in sample buffer); electrophoresis buffer (A 10x stock solution of electrophoresis buffer

was prepared by dissolving 30.3g Trizma base, 144.4g glycine and 10g SDS in dH<sub>2</sub>O, the volume was made up to 1L. For use 10x stock solution was made up to 1x in dH<sub>2</sub>O); transfer buffer (30.3g Trizma base and 144g glycine was dissolved in 4L of water, 2L of methanol was added and the volume was made up to 10L, pH 8.1-8.3, buffer stored at room temperature); blocking buffer (Marvel non-fat milk powder 5% was dissolved in 0.05% Tween, 0.1% NP-40 PBS solution); wash buffer (0.25% Tween, 0.1% NP-40 in PBS); nitrocellulose Protan (SLS); enhanced chemiluminescence reagents, ECL (Amersham Pharmacia); hyperfilm (Amersham Pharmacia); developing solution and fixer (HA West); mighty small electrophoresis apparatus (Hoefer); mini Trans Blot transfer apparatus (BioRad); Scotts Tapwater (potassium hydrogen carbonate, 2g, magnesium sulphate 7-hydrate, 20g and sodium azide, 1g were added to 1L tapwater).

% Polyacrylamide	Protein size (kDa)
15	12-43
10	16-68
8	36-94
6	57-212

**Table 2.1** Polyacrylamide concentration (protein separation range) in relation to protein size

For 10ml separating gel solution the following were added (volumes in ml):

	6%	8%	10%	12%	15%
<b>dH<sub>2</sub>O</b>	5.3	4.6	4.0	3.3	2.3
<b>30% acrylamide mix</b>	2.0	2.7	3.3	4.0	5.0
<b>1.5M Tris (pH 8.8)</b>	2.5	2.5	2.5	2.5	2.5
<b>10% SDS</b>	0.1	0.1	0.1	0.1	0.1
<b>10% APS</b>	0.1	0.1	0.1	0.1	0.1
<b>TEMED</b>	0.008	0.006	0.004	0.004	0.004

**Table 2.2** Components for the making of SDS-polyacrylamide separating gel solutions

APS and TEMED were added to the separating gel solution immediately prior to the gel being made up.

For 10ml stacking gel solution the following were added (volumes in ml):

<b>dH<sub>2</sub>O</b>	6.8
<b>30% acrylamide mix</b>	1.7
<b>0.5M Tris (pH 6.8)</b>	1.25
<b>10% SDS</b>	0.1
<b>10% APS</b>	0.1
<b>TEMED</b>	0.01

**Table 2.3** Components for the making of SDS-polyacrylamide stacking gel solutions

APS and TEMED were added to the stacking gel solution immediately prior to the gel being made up.

## 2.1.7b Antibodies And Probes

Human polyclonal anti-topo I antibody (2012, 1:10 000 dilution) from TopoGEN; monoclonal anti-topo II $\alpha$  (1:75 dilution); monoclonal anti-topo II $\beta$  antibody (1:100 dilution), monoclonal anti-p53 antibody (NCLp53DO1, 1:1000 dilution), vectastain ABC mouse IgG (PK6102) all from Novo Castra; monoclonal anti-WAF1 (p21) antibody (Ab-4, OP76, 1:100 dilution) Oncogene Research Products; monoclonal anti-mdm2 antibody (Sc965, 1:500 dilution), monoclonal anti-caspase-3 antibody (Sc7272, 1:200 dilution) from Santa Cruz (Autogen Bioclear); DAB (SK-4100, Vector); biotinylated anti-mouse IgG (1:250 dilution), biotinylated anti-human IgG (1:250 dilution), streptavidin horseradish peroxidase (1:250 dilution) were purchased from Amersham Pharmacia; lysoTracker green DND-26 (L-7526, Molecular Probes); MitoTracker green FM (M-7514, Molecular Probes).

## 2.1.7c Methods For Western Blotting

SDS-polyacrylamide gels were prepared with a separating gel of the appropriate concentration and a 10 well stacking gel. The separating gel was allowed to polymerise for 1h before adding the stacking gel, which was polymerised for at least 30 mins at room temperature. The use of a stacking gel, which is of low acrylamide concentration, allows relatively large samples to be concentrated before reaching the separating gel, increasing resolution of the bands. The samples were diluted in sample buffer so that the total volume (30 $\mu$ l sample + buffer) contained 30 $\mu$ g of total protein. Each sample was then

boiled for 3 mins and immediately cooled on ice. Molecular weight markers (rainbow markers and biotinylated markers), in sample buffer (total volume of 30 $\mu$ l) were also included on each gel and were treated in the same way as the samples. The proteins in each sample and markers were separated at 40mA for approximately 40 mins on an electrophoresis apparatus until the blue dye front reached the bottom of the gel. The proteins were transferred onto membranes for 1h at 100V with cooling using a transfer apparatus.

Membranes were immersed in blocking buffer for 1h at room temperature with shaking or left in the fridge overnight. The immunostaining was performed at constant shaking. Membranes were stained with primary antibody for 1-2h at room temperature. Residues were washed off by wash buffer 2 x 5 mins and the primary antibodies were bound by secondary biotinylated antibody for 30 mins. Membranes were washed 2 x 5 mins and Streptavidin horseradish peroxidase was added to the membranes for 30 mins. After the final washing steps (2 x 5 mins wash buffer, 1 x 5 mins PBS), the membranes were incubated in ECL according to the manufacturer's instructions and the topoisomerase proteins visualised on Hyperfilm.

#### 2.1.7d Dot Blot Assay For Determining The Primary Antibody Concentration To Be Used In The Western Blotting Experiments

Nitrocellulose membrane was cut into pieces. Sample, 2 $\mu$ l at the protein concentration to be used in the Western blot experiment was blotted onto the membrane pieces in duplicate. The membranes were air dried and blocked in marvel solution. The primary antibody was diluted in blocking buffer in a range of concentrations (1/10 000, ....1/100). Each membrane was labelled with one of these concentrations, and was then immersed in corresponding primary antibody concentration. The blotted membranes were incubated with primary antibody for 1h. Primary antibody residues were washed off with wash buffer (2 x 5 mins) and the membranes were incubated for 30 mins with the secondary biotinylated antibody at the concentration to be used in Western blot experiments. Following washing the membranes (2 x 5 mins), these were incubated 30 mins in streptavidin horseradish peroxidase. The membranes were finally washed in wash buffer (2 x 5 mins), and in PBS (1 x 5 mins), and a photograph was taken using the ECL technique.

#### 2.1.7e Stripping Solution For Western Blot Membranes

Glycine, 1.5g (0.2M) and SDS, 1g (1%) were dissolved in 100ml dH<sub>2</sub>O. HCl was used to adjust the pH to 2.5. To strip the Western blot membranes from antibodies, the membranes were soaked in stripping solution for 45 mins, on a shaker, at room temperature. After this the strip solution was poured off and membranes were washed in wash buffer 2 x 5 mins. Membranes could then

be re-used immediately, or were wrapped in cling film and foil, and stored in air-tight containers kept in the fridge.

## 2.1.8 Materials For Apoptotic Investigations

ApoTarget Quick Apoptotic DNA ladder detection kit (KHO1021, BioSource); RAPI-DIFF stain pack for rapid Romanowsky staining (Raymond A Lamb Limited); CaspaTag<sup>TM</sup>Fluorescein Caspase Assay kit (VAD, S7300, Intergen); CaspaTag<sup>TM</sup>Fluorescein Caspase-3 Assay kit (DEVD, S7301, Intergen); MitoCapture kit (K250-25-100, BioVision); Sørensens buffered water (KH<sub>2</sub>PO<sub>4</sub> 9.1g/L (solution A) and NaHPO<sub>4</sub> 9.5g/L (solution B) were made up separately. To make a 10x buffer, 50.8ml of solution A was mixed with 49.2ml of solution B. 1x Sørensens buffered water was obtained by adding 50ml stock to 950ml dH<sub>2</sub>O).

## 2.1.9 Equipment

Fluorescence spectrophotometer (Perkin Elmer LF50B); mini horizontal submarine unit HE 33 (Hoefer); SynGene Digital Imager (SynGene); mighty small electrophoresis apparatus (Hoefer); Dynatech MRX microplate reader (Dynex Technologies); mini Trans Blot transfer apparatus (BioRad); Cytospin3 (Shandon); light microscope, Axioskop (Zeiss); inverted light microscope, Axiovert 25 (Zeiss); FACSCalibur flow cytometer, equipped with a 15mW argon-ion air-cooled laser with excitation wavelength 488nm (Becton Dickinson Immunocytometry Systems, BDIS); UV fluorescent microscope,

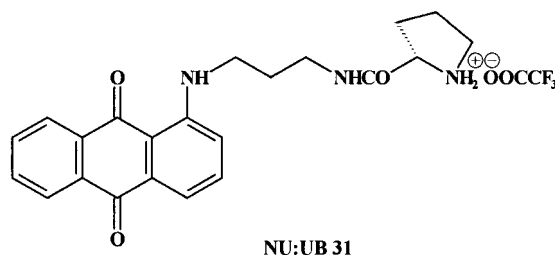
fitted with JVC colour video camera (KY-F55B) (Leica DMRB); Confocal microscope(NikonEclipseTE2000-U).

## **CHAPTER 3**

### **ANTI-TOPOISOMERASE ACTIVITY**

### 3.1 ANTI-TOPOISOMERASE ACTIVITY

Rational drug design typically starts with a molecule that has some degree of pharmacological activity, perhaps a lead compound, or less commonly a biochemical target, usually an enzyme or receptor with known molecular architecture. The chemistry of the lead molecule is then optimised to fit a potential target (e.g. the topoisomerase-DNA cleavable complex), whilst retaining the pharmacological potential of the molecule (Monks *et al.*, 1997). The NU:UB agents were rationally designed to selectively target DNA topoisomerase enzymes; the anti-topoisomerase activities of these compounds have been investigated in this research programme and presented within this chapter. The focus was put on the lead compound NU:UB 31, to determine whether or not it bound to DNA and whether or not it interfered with the DNA cleavage and relaxation activities of topoisomerase enzymes *in vitro*. Although the focus has been on NU:UB 31, other NU:UB compounds have also been included in some of the assays. The topoisomerase I and topoisomerase II poisons camptothecin and etoposide (respectively) have further been included for comparison.



As tumour cells in many cases are highly proliferative cells and topoisomerases are involved in the processes of DNA metabolism, the levels

and activities of these types of enzymes are often increased in proliferating tumour cells compared to normal cells. If topoisomerases in tumour cells could be inhibited, then unwinding, strand separation and reproduction of DNA would be prevented. With the discovery that several, currently used chemotherapeutics act on topoisomerases, these enzymes have become popular and validated targets for therapeutic intervention. The increased topoisomerase levels found in many tumours would then provide some degree of tumour cell specificity for these topoisomerase-targeting agents that should hopefully limit the side effects. Drugs can work as anti-topoisomerase agents mainly by two mechanisms. They can act as pure catalytic inhibitors of topoisomerases or as topoisomerase poisons. Pure topoisomerase inhibitors either bind to topoisomerases directly or bind to DNA, changing its structure so that it can no longer be recognised by the topoisomerases. Drugs trapping topoisomerases in what is referred to as cleavable complexes are called topoisomerase poisons. Topoisomerase poisons do not inhibit the catalytic activity of these enzymes, but instead take advantage of the DNA cleavage by topoisomerases, increasing the concentration of the ternary drug-stabilised cleavable complexes to levels which a cell can no longer tolerate. Agents that are able to form stable, relatively long-lived complexes with DNA and topoisomerase may confer yet improved cytotoxicity.

The ability of the NU:UB compounds to inhibit topoisomerase enzymes, and possibly form cleavable complexes was investigated. We chose to study drug inhibition of topoisomerase I and topoisomerase II-mediated DNA relaxation using a supercoiled (pBR322) plasmid DNA. NU:UB compounds were also

found to stabilize topoisomerase-DNA cleavable complexes in cell free assays using plasmid DNA with purified enzymes. Furthermore, we wanted to find out whether or not NU:UB compounds were able to form such cleavable complexes in living cells, which we achieved using topoisomerase immunoband depletion assays after incubation of intact tumour cells with a given drug. The topoisomerase inhibition and cleavable complex formation investigations were performed using DNA gel mobility assays, on agarose gels for the relaxation experiments (Keller, 1975) and cleavable complex formation assays (Boege *et al.* 1996), and on SDS polyacrylamide gels according to Boege *et al.* (1996) for the topoisomerase immunoband depletion investigations. The principle of these techniques relies on the fact that compact nucleic acid structures move faster through a gel than more open conformations. Thus, supercoiled DNA generally migrates faster through an agarose gel compared to DNA with a more open and relaxed conformation. Topoisomerase (I or II) protein moves more readily through a SDS polyacrylamide gel compared to topoisomerase that has been trapped by drug (topoisomerase poison) in a ternary DNA-topoisomerase-drug cleavable complex forming the basis of the immunoband depletion assay. Hence, the topoisomerase relaxation assay provided an indication of whether or not compounds were pure catalytic topoisomerase inhibitors, binding directly to topoisomerase (or DNA) preventing topoisomerase from relaxing the supercoiled plasmid DNA. The topoisomerase immunoband depletion assays like the topoisomerase cleavage assay provided information on whether or not compounds acted as topoisomerase poisons, by the mechanism of stabilising cleavable complexes with DNA and topoisomerases in the cell.

## 3.2 METHODS

### 3.2.1 DNA Binding Mode Of NU:UB 31 In Relation To The Comparative Intercalator, Mitoxantrone And The Minor Groove binder, Netropsin

The displacement of known DNA binders was detected by measuring the fluorescence of a fluorescent DNA-bound reporter molecule complex. The reporter molecules, ethidium bromide and Hoechst dye 33258 strongly intercalate or bind to the minor groove of DNA respectively. Stock solutions of these dyes were prepared at 60 $\mu$ M, reaching a final concentration of 2 $\mu$ M once added to the 3ml standard quartz cuvette. For this assay calf thymus DNA (molar extinction coefficient 6600, 260nm) was used. A DNA solution at 20 $\mu$ M was prepared in buffer (10mM Tris-HCl, pH7.5) and water was added to the assay to make up a total volume of 3ml. Once ethidium bromide or Hoechst stain had been added, the fluorescence of the DNA-bound complex was measured using a fluorescence spectrometer (Perkin Elmer LF50B) and recorded as the maximum fluorescence for ethidium bromide (E) or Hoechst dye (H).

In this study, the DNA binding characteristics of NU:UB 31 were related to mitoxantrone and netropsin using these as comparator molecules for intercalation and groove-binding, respectively. The methods used were essentially adaptations of the procedures according to Bailly *et al.* (1989).

Each test compound was prepared for assay by making up a stock solution of 60 $\mu$ M concentration. Subsequent dilutions were made to obtain a range of concentrations for the total volume of 3ml to be analysed using a standard cuvette in the spectrometer. The addition of NU:UB 31 or comparator drug to the DNA-dye (ethidium bromide or Hoechst stain) solution displaced the dye depending on the strength and mode of DNA binding (intercalation or groove binding) and thus reduced the fluorescence accordingly of the fluorescent DNA-bound dye complex.

### 3.2.1a Treatment Of Results

The mode of DNA binding by NU:UB 31 (or comparative agent) was quantified by determining the reduction in fluorescence of the reporter fluorophore upon treatment with a given concentration of the analysed compound. A competitive displacement graph for each drug (mitoxantrone, netropsin and NU:UB 31) with each dye was plotted from the mean fluorescence intensity values at each drug concentration of 3 separate experiments  $\pm$  SD. The measure of the ability to bind to DNA was then expressed as  $Q_{50}$  values: the concentration required to reduce the fluorescence intensity of the DNA-bound ethidium bromide ( $QE_{50}$ ) or Hoechst stain ( $QH_{50}$ ) complexes by 50%.

### 3.2.2 Topoisomerase I And Topoisomerase II ( $\alpha$ And $\beta$ )

#### Relaxation Assays

Stock solution, 100 $\mu$ M and 1000 $\mu$ M of NU:UB compound was made up in DMSO/dH<sub>2</sub>O. Plasmid pBR322 DNA, was diluted in dH<sub>2</sub>O to 40ng/ $\mu$ l. To make up a total volume of 20 $\mu$ l, buffer, DNA, dH<sub>2</sub>O and compound solution were added to eppendorf tubes as follows.

	DNA Control	Topoisomerase Control	10 $\mu$ M Compound	25 $\mu$ M Compound	50 $\mu$ M Compound
Buffer (I or II)	2	2	2	2	2
DNA	10	10	10	10	10
dH <sub>2</sub> O	8	7.8	5.8	2.8	6.8
Topoisomerase (I, II $\alpha$ or II $\beta$ )	-	0.2	0.2	0.2	0.2

**Table 3.1** Topoisomerase I and II relaxation assay components (volumes in  $\mu$ l)

Finally, topoisomerase I (2 units) was added and the contents of the tubes were mixed. Samples were incubated for 30 mins in a waterbath at 37°C. The reaction was terminated by addition of 4 $\mu$ l loading buffer. The plasmid samples were separated on an agarose gel (0.8%) by 1 x TBE at 50V for 2h, or overnight at 16V. DNA was stained in ethidium bromide (1 $\mu$ g/ml in 1 x TBE) for 1h and was then destained in dH<sub>2</sub>O water for another hour to reduce background fluorescence. The gel was viewed in UV light and photographed.

The topoisomerase II relaxation assay protocol was the same as the above topoisomerase I relaxation assay protocol, but the topoisomerase I buffer was exchanged for the topoisomerase II buffer and topoisomerase II ( $\alpha$  or  $\beta$ , 2 units) replaced topoisomerase I.

### 3.2.3 Topoisomerase I and Topoisomerase II ( $\alpha$ And $\beta$ ) Cleavage Assays

NU:UB compound stock solutions were prepared. Plasmid pBR322 DNA was prepared at 40ng/ $\mu$ l. Buffer, DNA, dH<sub>2</sub>O and compound were added to an eppendorf as depicted in Table 3.2.

	DNA Control	Topoisomerase Control	10 $\mu$ M Compound	50 $\mu$ M Compound	100 $\mu$ M Compound
Buffer (I or II)	2	2	2	2	2
DNA	10	10	10	10	10
dH <sub>2</sub> O	8	4	2	3	2
Compound	-	-	2 (at 100 $\mu$ M)	1 (at 1000 $\mu$ M)	2 (at 1000 $\mu$ M)
Topoisomerase (I, II $\alpha$ or II $\beta$ )	-	4	4	4	4

**Table 3.2** Topoisomerase I and II cleavage assay components (volumes in  $\mu$ l)

Topoisomerase I (50 units) was added and samples were left in a waterbath at 37°C for 45mins. SDS (10%), (2.2 $\mu$ l) was added and samples left for 30 sec. Proteinase K (5mg/ml), (2.4 $\mu$ l) was added and the samples were incubated in the waterbath, at 37°C for 1h. Loading buffer, 4 $\mu$ l was added to

each sample. Samples were loaded onto an agarose gel (0.8%). The gel was electrophoresed in 1 x TBE buffer with ethidium bromide, 0.5µg/ml at 50V for 2h or overnight at 16V. The gel was de-stained in dH<sub>2</sub>O for 1h in darkness, viewed in UV light and photographed.

The topoisomerase II ( $\alpha$  and  $\beta$ ) cleavage assay was performed by a similar procedure to the topoisomerase I cleavage assay. The topoisomerase II buffer was used and suitable topoisomerase II enzyme. Furthermore, following the addition of SDS, the tubes were left for 30 seconds followed by the addition of 1.5µl of 250mM Na<sub>2</sub>EDTA. Proteinase K, 2µl was then added at 0.8mg/ml and the tubes were incubated for 1h at 45° C. Loading buffer, 4µl was added to each sample to terminate the reaction. The samples were then separated on an agarose gel as described above. The electrophoresis was performed in the absence of ethidium bromide and, under these conditions, evidence of cleavable complex formation was detected by the formation of a band of linear DNA that has previously been shown to run between the supercoiled plasmid and the retarded nicked/relaxed DNA bands. The methods were adapted from Austin *et al.* (1995).

### **3.2.4 Topoisomerase I and II Immunoband Depletion Assays**

The samples were lysed under denaturing conditions without being washed to prevent reversion of the cleavable complexes formed. Therefore, to avoid contamination with serum proteins from the culture medium, cells were resuspended in serum-free medium prior to the start of the assay. HL60 cells

were recovered from culture, washed and resuspended in FBS free, RPMI 1640 HEPES medium at a density of  $20 \times 10^4$  cells/ml. Cells were untreated (solvent only), or treated with NU:UB compounds, or standard drugs. The topoisomerase immunoband depletion assay requires the formation of large numbers of topoisomerase-DNA complexes to produce band depletion, whereas cytotoxicity can result from a small number of cleavable complexes being converted into permanent cytotoxic lesions. Thus for these assays, high drug concentrations, 100-1000-fold higher than those used to produce cytotoxicity have been suggested. Camptothecin was recommended to be used at  $50\mu\text{M}$ , and etoposide at up to  $700\mu\text{M}$  was reported to partially deplete topoisomerase II ( $\alpha$  and  $\beta$ ). The drug incubation time suggested for topoisomerase immunoband depletion assays was 30-60 mins (Kaufman and Svingen, 1999), but longer incubation times have been used. Boege *et al.* (1996) used a 2h incubation time in their topoisomerase I depletion study of flavones. In our assays NU:UB compounds were used over a concentration range of  $50\mu\text{M}$ ,  $100\mu\text{M}$ ,  $200\mu\text{M}$ ,  $300\mu\text{M}$  and up to  $400\mu\text{M}$ . As a positive topoisomerase I depletion control camptothecin was used at  $50\mu\text{M}$ . Etoposide was used at  $100\text{-}700\mu\text{M}$ . Cells were treated with agents for 45 mins. Following this exposure time, cells were counted, cell density adjusted to  $1 \times 10^6$  cells/ml and the samples were then pelleted by centrifugation at  $500 \times g$  for 5 mins at  $4^\circ\text{C}$ . To prevent lysosomal proteases from degrading the topoisomerase enzymes, cell lysis was performed rapidly. The cells were lysed in a SDS containing buffer according to Boege *et al.* (1996). Further improvements to the topoisomerase immunoband depletion assay and the sample preparation for this assay have been suggested by Kaufman and

Svingen (1999). Lysate samples were aliquoted and used immediately, or stored at  $-80^{\circ}\text{C}$  until analysis could be performed.

The lysate samples were loaded onto a SDS polyacrylamide gel and the proteins separated by electrophoresis. When large proteins, such as topoisomerase II $\alpha$  and topoisomerase II $\beta$  were transferred, a greater transfer was achieved by the addition of SDS (0.02%) to the transfer buffer. Western blotting using human anti-human topoisomerase I antibody, mouse monoclonal anti-topoisomerase II $\alpha$  or mouse monoclonal anti-topoisomerase II $\beta$  were performed and topoisomerase bands photographed and identified. For the detailed Western blot protocol see materials and general methods section in Chapter 2.

## 3.3 RESULTS

### 3.3.1 DNA Binding Mode Of NU:UB 31 In Relation To Comparative Drugs (Mitoxantrone And Netropsin)

DNA interacting studies were performed using calf thymus DNA. Mitoxantrone is a molecule which is known to be a good intercalator, and NU:UB 31 was therefore compared to mitoxantrone in order to determine if it was a DNA intercalating compound. Fig. 3.1a shows mitoxantrone displacement of ethidium bromide. The ethidium bromide fluorescence decreased with increased mitoxantrone concentration. Mitoxantrone had a  $QE_{50}$  value of approximately  $0.5\mu\text{M}$ , which is the concentration where ethidium bromide fluorescence had dropped 50%. Netropsin is a potent minor groove binder and for this reason, netropsin was used as a comparator compound. NU:UB 31 was compared to netropsin, in order to determine if it was able to bind to DNA by a groove-binding mechanism. Fig. 3.1b displays Hoechst dye fluorescence versus netropsin concentration. Netropsin had a  $QH_{50}$  value of  $0.67\mu\text{M}$ . The same measurements were performed with NU:UB 31, replacing mitoxantrone and netropsin. Fig 3.1c and Fig. 3.1d shows ethidium bromide fluorescence against NU:UB 31 concentration and Hoechst dye against NU:UB 31 concentration respectively. NU:UB 31 gave a  $QE_{50}$  value of  $0.79\mu\text{M}$  and a  $QH_{50}$  value of  $0.42\mu\text{M}$ . The  $QE_{50}$  and  $QH_{50}$

values of mitoxantrone, netropsin and NU:UB 31 have been summarised in Table 3.3.

### **3.3.2 Topoisomerase Relaxation Assays**

#### **3.3.2a Topoisomerase I Relaxation Assays**

These experiments assessed the capacity of NU:UB compounds to inhibit topoisomerase I-mediated relaxation of DNA. When the plasmid DNA was treated with topoisomerase I enzyme, supercoils were removed, resulting in a more relaxed (conformationally flexible) structure, which was retarded on the gel compared to the supercoiled DNA. Fig. 3.2a shows a relaxation assay of plasmid by NU:UB 31. In lane 1 (DNA) the main band is the supercoiled plasmid DNA. In lane 2 (DNA + topoisomerase I) relaxed DNA bands appeared, and the supercoiled DNA band disappeared. This meant that topoisomerase I had converted the previously supercoiled DNA into relaxed topoisomers, which were retarded to various degrees on the agarose gel. Treatment with 10 $\mu$ M or 25 $\mu$ M NU:UB 31 resulted in partial inhibition of the topoisomerase I mediated DNA relaxation (lane 3 and 4). At a concentration of 50 $\mu$ M NU:UB 31, complete inhibition of topoisomerase I-mediated relaxation was observed (lane 5). Relaxation assays of the close analogues NU:UB 80 and NU:UB 81 can be seen in Fig. 3.2b and Fig. 3.2c. The topoisomerase I relaxation assay results have been summarised in table 3.3 (p109), and suggest that NU:UB 31 and to some degree NU:UB 80 inhibited topoisomerase I mediated DNA relaxation, possibly by binding directly to

topoisomerase I, or to DNA changing the conformation of DNA so that it is no longer recognised (nor consequently cut) by topoisomerase I. The latter is a more likely process since NU:UB 31 has been shown to bind to DNA. In contrast, NU:UB 81 did not appear to inhibit topoisomerase I mediated DNA relaxation despite having a broadly similar chromophore (cationically-charged and hydrophobic) and comparable antitumour potency and selectivity (anti-melanoma and colon sub-panel selectivity) in the cytotoxicity data from NCI (see Appendix 2).

### 3.3.2b Topoisomerase II Relaxation Assays

In an analogous manner to the action of topoisomerase I, the individual isoforms ( $\alpha$  and  $\beta$ ) of human topoisomerase II are capable of converting supercoiled plasmid DNA into relaxed topoisomers. Inhibition of topoisomerase II $\alpha$  or topoisomerase II $\beta$  mediated relaxation of supercoiled plasmid DNA was investigated following NU:UB 31 treatments. Fig 3.3 is representative of the topoisomerase II $\alpha$  relaxation assays of plasmid DNA by NU:UB 31. A NU:UB 31 concentration of 10 $\mu$ M was sufficient to partially inhibit topoisomerase II $\alpha$ -mediated DNA relaxation (lane 5). At the higher concentrations 25 $\mu$ M and 50 $\mu$ M, complete inhibition of topoisomerase II $\alpha$  was evident (lane 6-7). Similarly to topoisomerase II $\alpha$ , inhibition of topoisomerase II $\beta$ -mediated DNA relaxation was also observed following 10 $\mu$ M NU:UB 31 treatment (lane 4), with the higher NU:UB 31 concentrations resulting in complete inhibition (lane 5-7) of topoisomerase II $\beta$  catalytic activity (Fig. 3.4).

### 3.3.3 Topoisomerase Cleavage Assays

#### 3.3.3a Topoisomerase I Cleavage Assays

The formation of drug-stabilised topoisomerase I–DNA cleavable complexes were investigated with the topoisomerase I cleavage assay. Fig 3.5 shows a topoisomerase I cleavage assay of NU:UB 31 using camptothecin as a positive control. Upon visualisation supercoiled plasmid DNA appeared as one band, travelling far down the gel due to its compact size (lane 1). For this assay more topoisomerase was used than in the relaxation assay in order to induce a high degree of cleavable complex formation. In contrast to relaxation gels, the conditions for running the DNA gels under cleavage conditions required the use of ethidium bromide in the gel matrix in addition to the running buffer; in this way, the fully relaxed plasmid topoisomers migrated as a single band ahead of the supercoiled band, thereby allowing resolution of the retarded nicked plasmid from relaxed forms. Topoisomerase I–DNA complexes are trapped and stabilized by anti-topoisomerase drugs, including the anti-topoisomerase I standard agent camptothecin. Treatment with camptothecin resulted in increased levels of cleavable complex formation, resulting in open-circular (or nicked) DNA plasmids that were severely retarded on the gel (lane 3). The cleavage induced by camptothecin and NU:UB were observed as an increase in the intensity of the open-circular band compared to the background cleavage with topoisomerase I treated DNA. At low concentrations (0.1µM, 1µM, 5µM and 10µM) NU:UB 31 showed stimulation of topoisomerase I induced cleavage, whereas the high

concentration (100 $\mu$ M) NU:UB 31 appeared to antagonise its own cleavage reaction (self-inhibition). In contrast to camptothecin (lane 3, apparently complete disappearance of supercoiled plasmid), only partial cleavable complex formation by NU:UB 31 was produced at a concentration of 5 $\mu$ M. Nevertheless, the cleavage assay results indicated that NU:UB compounds, like camptothecin, to some degree stabilise ternary topoisomerase I-DNA-drug complexes in cell-free *in vitro* systems.

### 3.3.3b Topoisomerase II Cleavage Assays

The ability of NU:UB 31 to stabilise DNA-topoisomerase cleavable complexes was investigated by comparison of the individual isoforms of (recombinant) human topoisomerase II, with the topoisomerase II poison, m-AMSA. A range of experiments was performed to find the optimum levels of cleavage by the test and comparator compound; a representative gel is shown in Fig. 3.6. When the enzymes were used at levels of 50 units (considerably higher than those required to effect relaxation), m-AMSA at 100 $\mu$ M gave largely nicked plasmid (lane 1); a concentration of 50 $\mu$ M was found to reproducibly induce the formation of a band corresponding to linear DNA (shown in lane 2). Comparable levels of linear DNA formation were obtained with the  $\beta$ -isoform at the same concentration (data not shown); earlier studies (Marsh *et al.*, 1996) had demonstrated that m-AMSA promoted drug-stabilised cleavable complex formation equally well with  $\beta$  and  $\alpha$ -isoforms of topoisomerase II. NU:UB 31, at an optimal concentration of 25 $\mu$ M, produced comparable linear DNA band formation to m-AMSA at 50 $\mu$ M with each of the  $\alpha$ - and  $\beta$ -isoforms

of topoisomerase II (Fig. 3.6, lane 3 and Fig. 3.7, lane 4), representing drug-stabilised cleavable complex formation compared to drug-free enzyme-only controls wherein supercoiled plasmid was notably converted to some of the nicked form at the high concentrations of enzyme used.

### **3.3.4 Topoisomerase Immunoband Depletion Assays**

#### **3.3.4a Topoisomerase I Immunoband Depletion Assays**

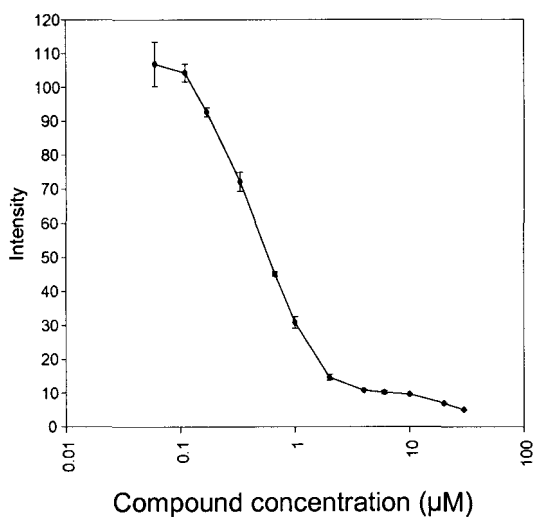
The inhibition of the religation step during the processing of DNA topoisomerases is believed to be the molecular basis of the anti-tumour activity of topoisomerase I poisons including camptothecin and its derivatives irinotecan (CPT 11) and topotecan. Inhibition of religation can be detected in drug treated cells by immunoband depletion assays. Whereas topoisomerase will migrate at the molecular weight of the topoisomerase molecule on SDS-polyacrylamide gels, the covalent topoisomerase-DNA complexes are larger in size and will exhibit a lower mobility. In untreated cells, there are few and probably short-lived covalent topoisomerase-DNA complexes. Drug treatment of cells may however increase the number of covalent topoisomerase-DNA complexes. Thus, the degree of topoisomerase I immunoband depletion will reflect the drugs' capacity to stabilise topoisomerase I-DNA cleavable complexes by depleting the Western blot topoisomerase I signal. HL60 cells were treated with 50 $\mu$ M, 100 $\mu$ M, 200 $\mu$ M and 300 $\mu$ M NU:UB compound for 45 mins. In the topoisomerase I band depletion assay, 50 $\mu$ M camptothecin treatment resulted in a weaker topoisomerase I signal because the

topoisomerase I enzymes became covalently trapped by the drug. The NU:UB compounds, except NU:UB 80 and NU:UB 81 (Fig. 3.8b) also induced topoisomerase I immunoband depletion, albeit at higher concentrations than were used for camptothecin. The topoisomerase I signal was not depleted by 50 $\mu$ M of any of the NU:UB compounds. For NU:UB 31, the topoisomerase I band intensity was notably diminished at 100 $\mu$ M (Fig. 3.8a). Treatment with the more hydrophobic and conformationally restricted analogue NU:UB 150 at 200 $\mu$ M also resulted in partial depletion of the topoisomerase I bands (Fig. 3.8c). The topoisomerase I immunoband depletion results have been summarised in Table 3.4.

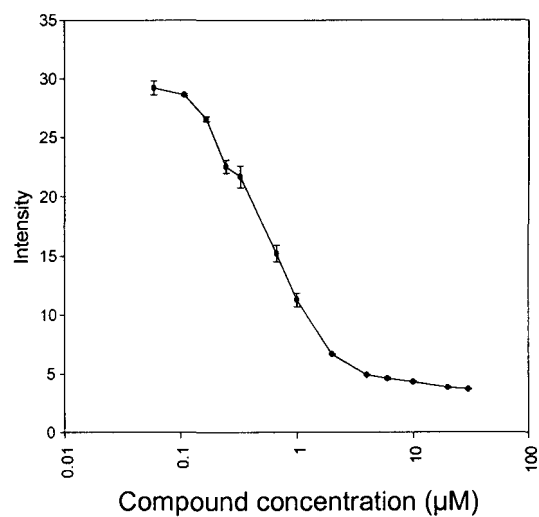
### 3.3.4b Topoisomerase II Immunoband Depletion Assays

To investigate whether or not NU:UB compounds bind and form cleavable topoisomerase II complexes in HL60 cells, topoisomerase II immunoband depletion assays were performed using isoform-specific antibodies. The topoisomerase II depletion assays used the same principle as the above topoisomerase I depletion assay. The electrophoretic properties of the human topoisomerase II $\alpha$  and topoisomerase II $\beta$ , migrating as proteins of 170kDa and 180kDa respectively on SDS-polyacrylamide gels were studied. The degree of topoisomerase II ( $\alpha$  and/or  $\beta$ ) immunoband depletion reflects the capacity of the NU:UB compound to stabilise cleavable complexes with DNA and topoisomerase II $\alpha$  and/or topoisomerase II $\beta$ , trapping the proteins and thus decreasing the topoisomerase II ( $\alpha$  and/or  $\beta$ ) Western blot signal. HL60 cells were treated with NU:UB 31. Following 200 $\mu$ M, no band depletion was

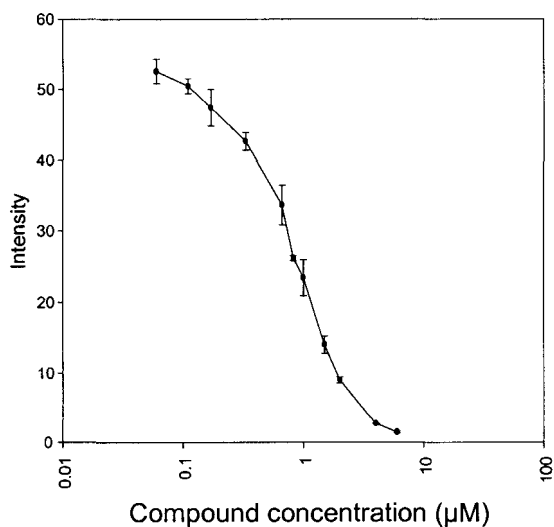
observed but the topoisomerase II $\alpha$  signal was weakened at 300 $\mu$ M (Fig. 3.9a). At 200 $\mu$ M partial depletion of the topoisomerase II $\beta$  signal was evident when compared to the control (Table 3.4, p110). The signal was also depleted following 300 $\mu$ M and 400 $\mu$ M NU:UB 31 treatment (Fig. 3.9b). It has to be noted that problems were encountered in getting the positive etoposide control to work in these assays. However, using camptothecin (topoisomerase I poison) as a negative control it was confirmed that camptothecin did not, as expected, deplete the topoisomerase II signal.



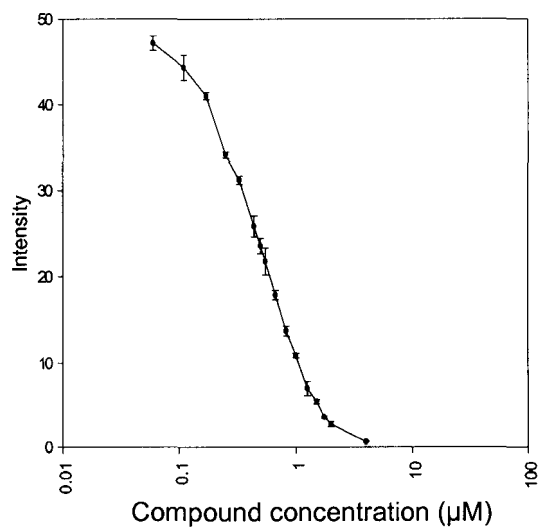
(a) DNA binding, mitoxantrone with ethidium bromide,  $QE_{50}$  value  $\sim 0.5\mu\text{M}$



(b) DNA binding, netropsin with Hoechst dye,  $QH_{50}$  value  $\sim 0.67\mu\text{M}$



(c) DNA binding, NU:UB 31 with ethidium bromide,  $QE_{50}$  value  $\sim 0.79\mu\text{M}$



(d) DNA binding, NU:UB 31 with Hoechst dye,  $QH_{50}$  value  $\sim 0.42\mu\text{M}$

**Fig. 3.1** Graphs of DNA/binder fluorescence versus drug concentration reflecting the DNA intercalating capacity of mitoxantrone (a), minor groove binding capacity of netropsin (b) and the intercalation and groove binding capacities of NU:UB 31 (c and d).  $QE_{50}$  and  $QH_{50}$  representing the concentration of compound that has displaced 50% of fluorescence of ethidium bromide and Hoechst stain respectively. The graphs represents mean intensity  $\pm$  SD where  $n=3$ .

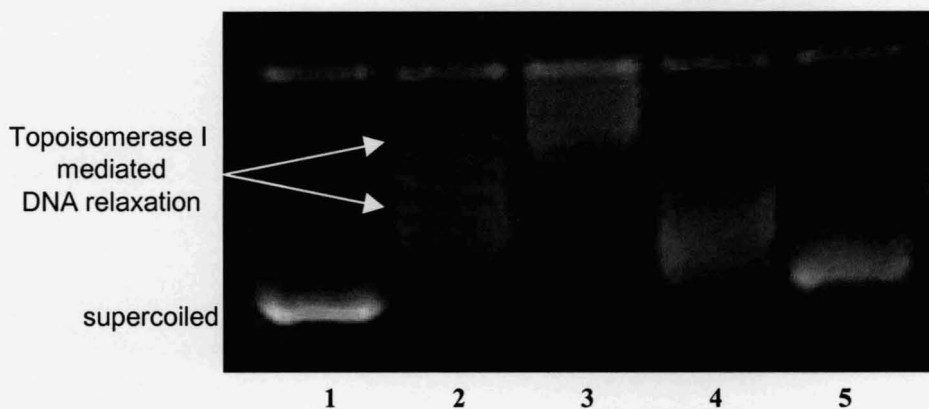


**Fig. 3.2a** Topoisomerase I relaxation assay of NU:UB 31. DNA (lane 1), DNA + Topoisomerase I (lane 2), DNA + Topoisomerase I + NU:UB 31 at 10 $\mu$ M, 25 $\mu$ M and 50 $\mu$ M (lane 3, 4 and 5). Fig. is representative of a series of separate experiments.

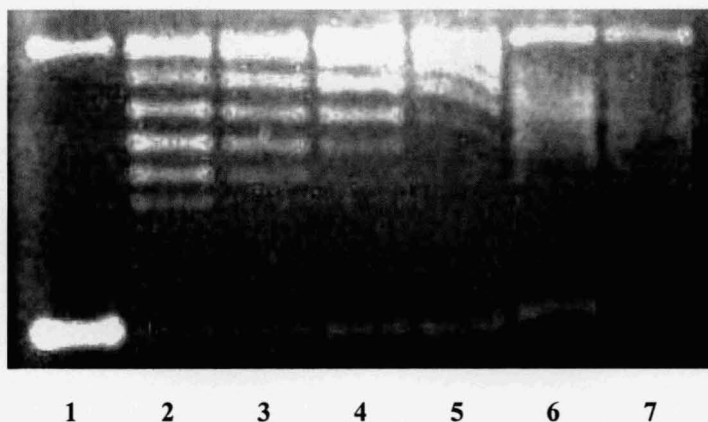


**Fig. 3.2b** Representative figure of the NU:UB 80 topoisomerase I relaxation assay. DNA (lane 1), DNA + topoisomerase I (lane 2), DNA + topoisomerase I + NU:UB 80 at 5 $\mu$ M, 10 $\mu$ M, 25 $\mu$ M, 50 $\mu$ M and 100 $\mu$ M (lane 3-7).

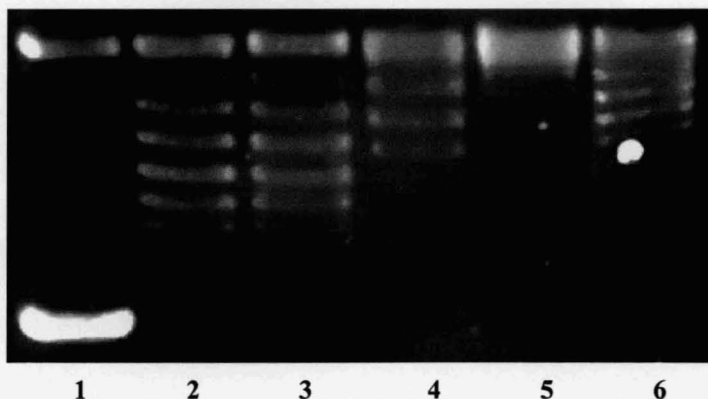


**Fig. 3.2c** Representative figure of the NU:UB 81 topoisomerase I relaxation assay. DNA (lane 1), DNA + topoisomerase I (lane 2), DNA + topoisomerase I + NU:UB 81 at 5 $\mu$ M, 10 $\mu$ M, 25 $\mu$ M and 50 $\mu$ M (lane 3-6).

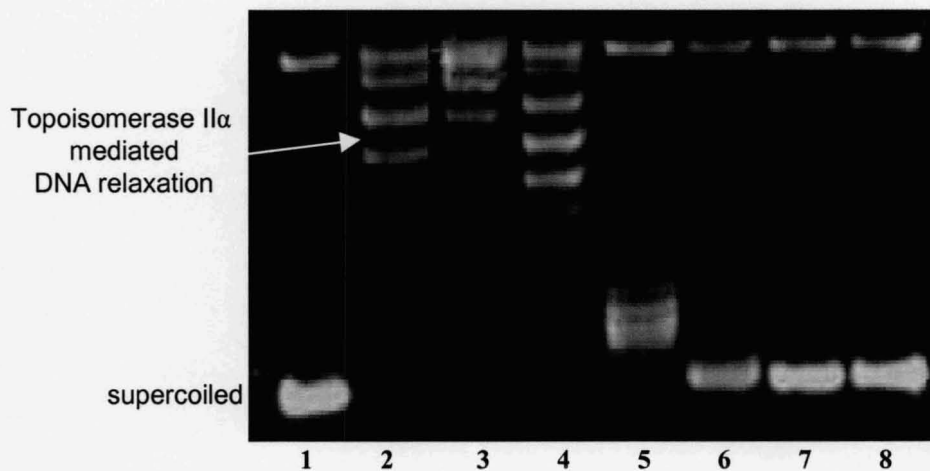


**Fig. 3.3** Topoisomerase II $\alpha$  relaxation assay of NU:UB 31. DNA (lane 1), DNA + topoisomerase II $\alpha$  (lane 2), DNA + topoisomerase II $\alpha$  + NU:UB 31 at 1 $\mu$ M, 5 $\mu$ M, 10 $\mu$ M, 25 $\mu$ M and 50 $\mu$ M (lane 3-7), DNA + NU:UB 31 at 50 $\mu$ M (lane 8). The figure is representative of a series of separate experiments.

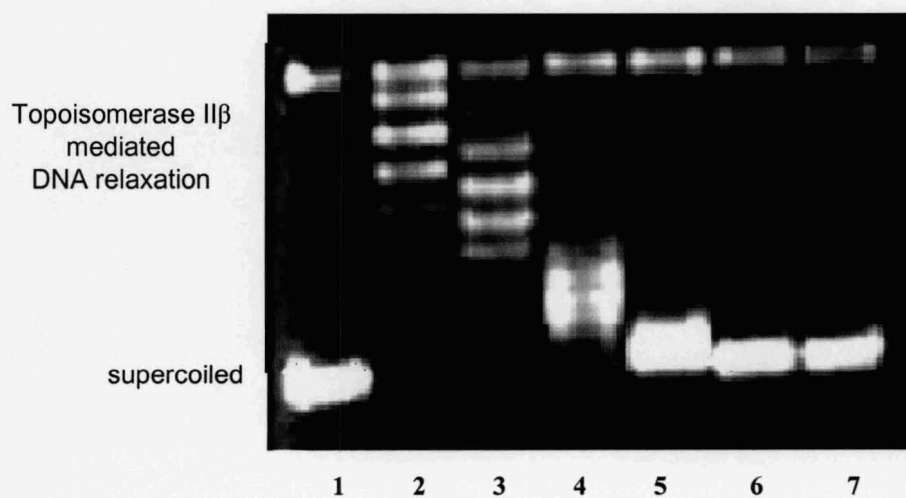


**Fig. 3.4** Topoisomerase II $\beta$  relaxation assay of NU:UB 31. DNA (lane 1), DNA + topoisomerase II $\beta$  (lane 2), DNA + topoisomerase II $\beta$  + NU:UB 31 at 5 $\mu$ M, 10 $\mu$ M, 15 $\mu$ M, 20 $\mu$ M and 50 $\mu$ M (lane 3-7). The figure is representative of a series of separate experiments.

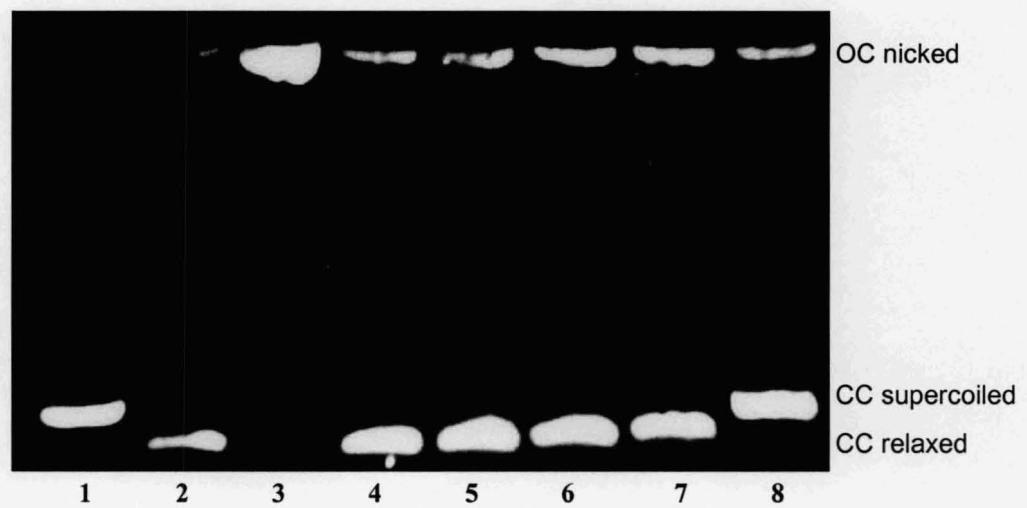


**Fig. 3.5** Topoisomerase I cleavage assay of NU:UB 31. DNA (lane 1), DNA + topoisomerase I (lane 2), DNA + topoisomerase I + camptothecin 10 $\mu$ M (lane 3), DNA + topoisomerase I + NU:UB 31, 0.1 $\mu$ M, 1 $\mu$ M, 5 $\mu$ M, 10 $\mu$ M and 100 $\mu$ M (lane 4-8). The figure is representative of a series of separate experiments.

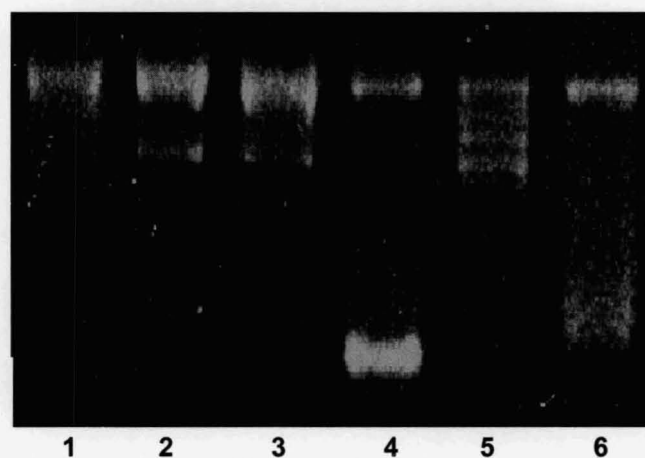


**Fig. 3.6** Topoisomerase II $\alpha$  cleavage assay of NU:UB 31. DNA + m-AMSA (100 $\mu$ M) + topoisomerase II $\alpha$  (lane 1), DNA + m-AMSA (50 $\mu$ M) + topoisomerase II $\alpha$  (lane 2), DNA + NU:UB 31 (25 $\mu$ M) + topoisomerase II $\alpha$  (lane 3), DNA (lane 4), relaxed DNA (lane 5), DNA + topoisomerase II $\alpha$  (lane 6). The figure is representative of a series of separate experiments.

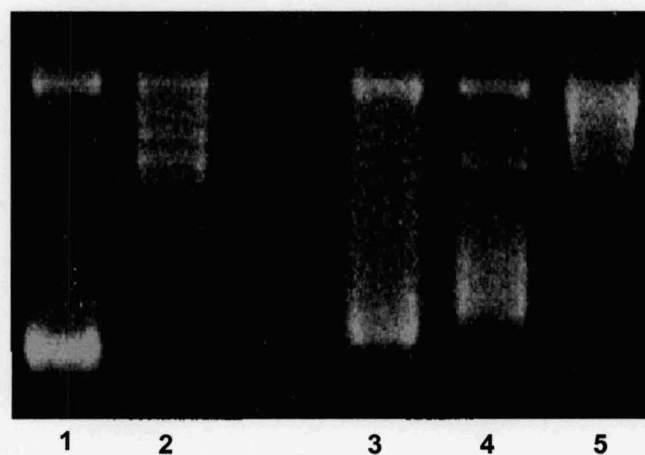


**Fig. 3.7** Topoisomerase II $\beta$  cleavage assay of NU:UB 31. DNA (lane 1), relaxed DNA (lane 2), DNA + topoisomerase II $\beta$  (lane 3), DNA + NU:UB 31 (25 $\mu$ M) + topoisomerase II $\beta$  (lane 4), DNA + mAMSA (100 $\mu$ M) + topoisomerase II $\beta$  (lane 5). The figure is representative of a series of separate experiments.

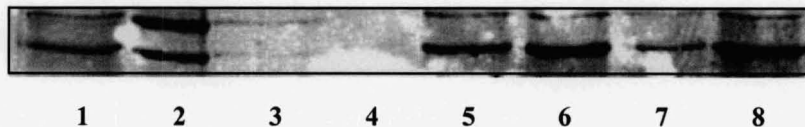


**Fig. 3.8a** Topoisomerase I immunodepletion assay of NU:UB 31 and NU:UB 51. Camptothecin 50 $\mu$ M (lane 1), Biotinylated marker (lane 2), empty (lane 3), NU:UB 51 300 $\mu$ M (lane 4), NU:UB 51 200 $\mu$ M (lane 5), NU:UB 31 300 $\mu$ M (lane 6), NU:UB 31 100 $\mu$ M (lane 7), solvent control (lane 8). The figure is representative of a series of separate experiments.



**Fig. 3.8b** Topoisomerase I immunodepletion assay of NU:UB 81 - No topoisomerase I immunoband depletion. Camptothecin 50 $\mu$ M (lane 1), solvent control (lane 2), NU:UB 81 300 $\mu$ M (lane 3), NU:UB 81 200 $\mu$ M (lane 4), NU:UB 81 100 $\mu$ M (lane 5), NU:UB 81 50 $\mu$ M (lane 6), empty (lane 7), solvent control (lane 8). The figure is representative of a series of separate experiments.

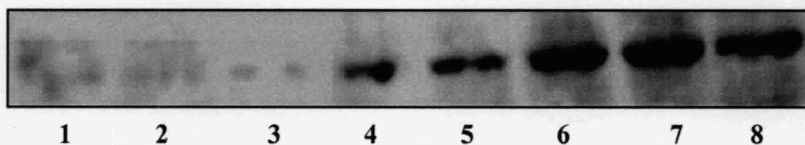


**Fig. 3.8c** Topoisomerase I immunodepletion assay of NU:UB 150. Camptothecin 50 $\mu$ M (lane 1), Camptothecin 50 $\mu$ M (lane 2), NU:UB 150 300 $\mu$ M (lane 3), NU:UB 150 200 $\mu$ M (lane 4), NU:UB 150 100 $\mu$ M (lane 5), NU:UB 150 50 $\mu$ M (lane 6), solvent control (lane 7), control (lane 8). The figure is representative of a series of separate experiments.

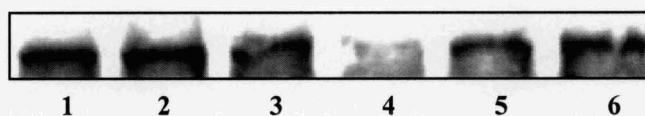


**Fig. 3.9a** Topoisomerase II $\alpha$  immunoband depletion assay of NU:UB 31. Solvent control (lane1), Etoposide 500 $\mu$ M (lane 2), NU:UB 31 200 $\mu$ M (lane 3), NU:UB 31 300 $\mu$ M (lane 4), solvent control (lane 5), Etoposide 500 $\mu$ M (lane 6). The figure is representative of a series of separate experiments.

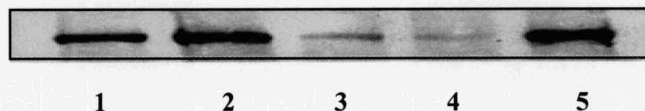


**Fig. 3.9b** Topoisomerase II $\beta$  immunoband depletion assay of NU:UB 31. Solvent control (lane 1), Camptothecin 50 $\mu$ M (lane 2), NU:UB 31 200 $\mu$ M (lane 3), NU:UB 31 300 $\mu$ M (lane 4), Etoposide 700 $\mu$ M (lane 5). The figure is representative of a series of separate experiments.

Treatment	Type Of Assay
	<b>DNA Binding Assay</b>
Mitoxantrone	QE <sub>50</sub> value ~ 0.50µM
Netropsin	QH <sub>50</sub> value ~ 0.67µM
NU:UB 31	QE <sub>50</sub> value ~ 0.79µM
NU:UB 31	QH <sub>50</sub> value ~ 0.42µM
	<b>Topoisomerase I Relaxation</b>
NU:UB 31	Partial at 10-25µM, Complete at 50µM
NU:UB 80	Partial at 25µM (n=2)
NU:UB 81	No inhibition
	<b>Topoisomerase IIα Relaxation</b>
NU:UB 31	Partial at 10µM, Complete at 25µM
	<b>Topoisomerase IIβ Relaxation</b>
NU:UB 31	Partial at 10µM, Complete at 15µM
	<b>Topoisomerase I Cleavage</b>
NU:UB 31	Optimum at 5µM
	<b>Topoisomerase IIα Cleavage</b>
NU:UB 31	Optimum at 25µM
	<b>Topoisomerase IIβ Cleavage</b>
NU:UB 31	Optimum at 25µM

**Table 3.3** Summary of DNA binding, topoisomerase relaxation and topoisomerase cleavage assay results. Concentration of mitoxantrone, netropsin and NU:UB 31 where ethidium bromide (QE<sub>50</sub>) and Hoechst dye (QH<sub>50</sub>) fluorescence have diminished by 50%. Concentrations at which NU:UB compounds inhibited topoisomerase I or topoisomerase II-mediated DNA relaxation or cleavage. Results were obtained from 3 or more separate experiments if not otherwise stated.

<b>Treatment</b>	<b>Type Of Assay</b>
	<b>Topoisomerase I Immunoband Depletion</b>
NU:UB 31	100µM
NU:UB 43	200µM
NU:UB 51	200µM
NU:UB 80	No depletion
NU:UB 81	No depletion (n=2)
NU:UB 150	200µM (n=2)
Camptothecin	50µM
	<b>Topoisomerase IIα Immunoband Depletion</b>
NU:UB 31	300µM
	<b>Topoisomerase IIβ Immunoband Depletion</b>
NU:UB 31	200µM

**Table 3.4** Topoisomerase immunoband depletion results. Drug concentration at which NU:UB compounds partially stabilised topoisomerase I-DNA or topoisomerase II-DNA cleavable complexes. Results were obtained from 3 separate experiments if not otherwise stated.

### 3.4 DISCUSSION

The DNA-binding properties of drug molecules are important factors that can contribute to cytotoxic potency, mutagenicity, or the ability to interact with DNA-processing enzymes including topoisomerases. Indeed, direct targeting of DNA or DNA-associated proteins have received great attention in the past and still figure prominently as viable approaches in cancer therapy strategies (Hurley, 2002). Reversible drug interactions with DNA take place in three primary ways (Neidle, 2002):

1. Non-specific interactions, involving electrostatic binding along the exterior of the helix.
2. Specific groove binding, involving interactions with the edges of base pairs in the major or minor grooves.
3. DNA intercalation that relies on insertion of a planar or approximately planar (aromatic) ring system between base pairs.

Strong correlations exist between chemical structure and DNA-binding properties. Groove binding molecules are generally crescent-shaped and incorporate an aromatic ring such as benzene, or heteroaromatic ring such as pyrrole, that is able to twist into the helical curve of the groove, with the displacement of water. Netropsin (Fig. 3.10) and Hoechst 33258 (Fig. 3.11) are typical minor groove binding molecules.

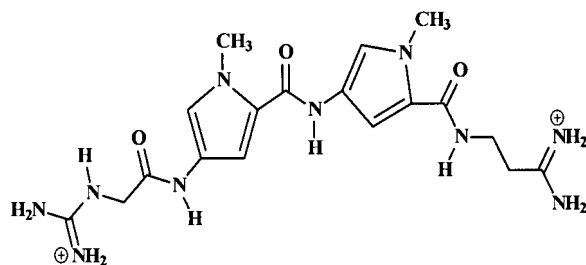


**Fig. 3.10** Chemical structure of the minor groove binder netropsin.

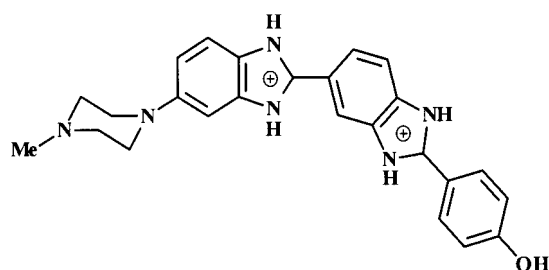


**Fig. 3.11** Chemical structure of the minor groove binder Hoechst 33258.

DNA intercalation typically displays an aromatic ring system that is planar and has the same thickness as the base pairs of DNA. Nucleic acid conformation is changed when intercalation takes place, which favours insertion of the flat molecules into DNA. Mitoxantrone (Fig. 3.12) and ethidium bromide (Fig. 3.13) are typical intercalating molecules.

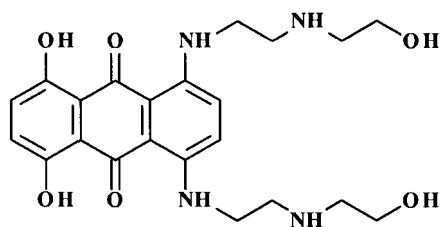


**Fig. 3.12** Chemical structure of the DNA intercalator mitoxantrone.

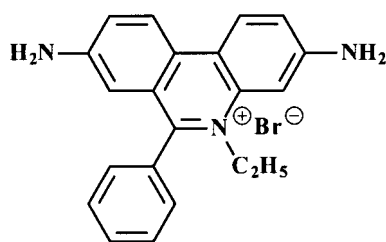


**Fig. 3.13** Chemical structure of the DNA intercalator ethidium bromide.

Competitive DNA-ethidium (or Hoechst dye) fluorescence quenching is a well established technique that has been applied to structurally diverse DNA binding ligands to give a measure of the relative strengths of binding of small molecules to DNA (McConnaughie and Jenkins, 1996). The aminoanthraquinone and topoisomerase inhibitor mitoxantrone was used as a comparator agent in order to probe the potential intercalative properties of NU:UB 31 by ethidium displacement. It is generally accepted that  $Q_{50}$  values  $> 1$  indicates poor intercalative capacity; mitoxantrone was determined to have a mean  $QE_{50}$  value of  $0.5\mu\text{M}$ , whereas NU:UB 31 was found to have a mean value of  $0.79\mu\text{M}$ , confirming that an intercalative component contributed to the process of DNA-binding by NU:UB 31; although it does not bind so tightly as the comparator compound. This observation is consistent with NU:UB 31 possessing a single cationic charge in contrast to the double cationic mitoxantrone, which through its two side chains has additional stabilisation of the intercalated complex. It is proposed that NU:UB 31 has a mixed-modal (part intercalative, part groove-binding) mechanism of binding to DNA, given the potent groove binding properties shown by the low mean  $QH_{50}$  value of  $0.42\mu\text{M}$  compared to the groove-binding comparator netropsin which had a mean  $QH_{50}$  value of  $0.67\mu\text{M}$ . Molecules with a planar chromophore

(that can insert into the hydrophobic space between base pairs in DNA) combined with positively charged side chains of appropriate length and conformation have been shown to have groove-binding contributions to the DNA-bound intercalation complex in which the charges act as anchor points to the negatively charged phosphodiester backbone in the nucleic acid, effectively slowing the dissociation kinetics and tethering the molecule firmly to DNA. Empirical observations have noted that intercalating compounds, including the anthracyclines and mitoxantrone, generally favour interaction with DNA topoisomerase II and often function as poisons, whereas crescent-shaped, groove binding molecules, including the camptothecins and Hoechst 33258 (pibenzimol), interact with topoisomerase I, also usually functioning as enzyme poisons. The mixed-modal DNA binding behaviour of NU:UB 31 is thus consistent with its proposed dual action on each of topoisomerase I and topoisomerase II.

Most clinically used anti-topoisomerase agents work via the formation of cleavable topoisomerase-DNA-drug complexes (the effect termed 'poisoning') rather than by inhibiting the catalytic activity of these enzymes. Drug-stabilised cleavable complexes commonly induce permanent damage to the structural integrity of DNA; the DNA lesions are considered to then trigger apoptotic mechanisms, leading to cell death. Resistance to topoisomerase inhibitors is still problematic in treating cancers and can be the result of various factors including disruptions in the interactions between drug, DNA and topoisomerase so that proper stabilisation of cleavable complexes by the drug is not achieved. Down-regulation of topoisomerases, or (compensating)

up-regulation of a topoisomerase enzyme that is not targeted by the drug, are mechanisms with implications for the efficacy of topoisomerase inhibitors (Larsen and Skladonovski, 1998; Pommier *et al.*, 1999). For example, alterations in topoisomerase I, due either to decreases in levels or qualitative changes of this enzyme which affect the interactions between topoisomerase I and camptothecins have been observed in cell lines resistant to camptothecin (Madelaine *et al.*, 1993; Chang *et al.*, 1992; Sorensen *et al.*, 1997). In experiments performed by Murren *et al.* (1996) camptothecin resistance was related to the down regulation of topoisomerase I. Enzyme concentrations were here determined in human nasopharyngeal (KB) cells by immunoblotting. The total amount of topoisomerase I in resistant KB cells was reduced compared to the parental KB cells and furthermore, in the resistant cells this topoisomerase I reduction was further associated with increased topoisomerase II levels (not related to proliferation differences). In cells made resistant to etoposide, the opposite was found; lower topoisomerase II and an increased amount of topoisomerase I enzyme. Thus, the reduction of one topoisomerase enzyme was associated with an increase in the other, but no collateral sensitivity to drugs (etoposide and camptothecin respectively) directed against this topoisomerase was observed.

Mutations in the topoisomerase enzyme targeted by the drug is yet another problem that can have implications for efficacy of drug regimens. Topoisomerase II mutations often make cells cross-resistant towards several of the topoisomerase II drugs. Moreover, alterations in topoisomerase localisation may be involved in development of resistance and treatment of

cells with topoisomerase inhibitors has been found to affect the localisation of these enzymes. Camptothecin treatment of human KB cells resulted in translocation of topoisomerase I from the nucleolus to other sites. Immunolocalisation of topoisomerase I by confocal microscopy revealed less intra-nuclear staining in camptothecin resistant cells and these observations further suggested a greater cytosolic topoisomerase I distribution in the resistant cells compared to the parental cell line (Murren *et al.*, 1996). How relevant this translocation is for the toxicity of camptothecin derivatives was however not established. Boege *et al.* (1993) reported on the existence of two types of topoisomerase II $\alpha$  enzymes and the possibility that cells may become more resistant by altering the levels of these. Mitoxantrone resistant HL60 cells expressed the nuclear 170 000 M<sub>r</sub>, and also a cytoplasmic 160 000 M<sub>r</sub> form of topoisomerase II $\alpha$  (Harker *et al.*, 1995). This shift of topoisomerases from the nucleus into cytoplasm may possibly be a way for cells to diminish the formation of drug-induced cleavable complexes (i.e. limiting DNA damage).

The drug-target mechanisms discussed above may confer resistance to a variety of drugs. However, a high level of resistance is likely to be associated with several of these target enzyme modifications as well as other pre- and post- target resistance mechanisms. In cases where resistance associated with topoisomerase levels/functions is a problem, treatment with new potent drugs with dual topoisomerase I and topoisomerase II inhibition capacity may be beneficial in circumventing these resistance mechanisms. Anthraquinone-based amino acid substituted drugs (NU/ICRF 600, 601 and 602) have been

investigated by Meikle *et al.* (1995) and were found to be dual inhibitors of the catalytic activity of topoisomerase I and topoisomerase II. Some of the NU:UB compounds investigated here and elsewhere also appeared to be dual topoisomerase I and II inhibitors (poisons). The mechanistic studies with topoisomerase I performed in this project included assays for the determination of drug-induced effects on topoisomerase I-mediated relaxation (topoisomerase I inhibition) of supercoiled DNA as well as cleavable complex formation studies, by *in vitro* topoisomerase I cleavage assays and topoisomerase I immunoband depletion assays in intact cells. The topoisomerase I inhibition studies of the NU:UB compounds showed that NU:UB 81 did not inhibit topoisomerase I activity in relaxation assays, whereas, inhibition of topoisomerase I-mediated relaxation of pBR322 plasmid was however evident in assays using NU:UB 31 and NU:UB 80 (the unnatural D-isomer of NU:UB 81).

In topoisomerase I cleavage assays using supercoiled plasmid DNA, NU:UB 31 was found to stabilize cleavable complexes. Additionally, NU:UB 31, 43, 51 and NU:UB 150, but not NU:UB 80 nor NU:UB 81, were active in the topoisomerase I immunoband depletion experiments confirming that these agents stabilised topoisomerase I-DNA complexes in whole HL60 cells. NU:UB 31 showed band depletion at 100 $\mu$ M but higher NU:UB 31 concentrations appeared to antagonise topoisomerase I band depletion (a phenomenon also reported at high NU:UB 31 concentrations in the topoisomerase I cleavage assay using plasmid DNA). The observation that NU:UB 31 antagonised its own topoisomerase I cleavage reaction (i.e. 'self

inhibition') with increased concentrations may be consistent with its properties of being a catalytic inhibitor and poison vested in the same molecule. Precedent exists for this type of behaviour and has notably been observed for the dual topoisomerase inhibitor, DACA that like NU:UB 31 possesses a planar (acridine) chromophore with a single, positively charged aminoalkyl side chain substituent (Bridewell *et al.*, 1999). Additionally, it is known that pure catalytic inhibitors can nullify the effects of known topoisomerase poisons. The poisoning activity of many topoisomerase inhibitors is known to be antagonised by co-incubation with pure catalytic inhibitors with consequent reduced levels of cleavable complex formation. Camptothecin was used as a positive control in these topoisomerase I immunoband depletion assays and efficiently depleted the topoisomerase I signal at 50 $\mu$ M. Although the NU:UB agents were less potent than camptothecin in forming cleavable complexes, NU:UB 31 and some of the other NU:UB compounds were also inhibitors of topoisomerase I mediated DNA relaxation. It should be noted that the cleavable complexes induced by camptothecin are *in vivo* highly reversible upon drug removal so if NU:UB compounds induce less cleavage complexes but these have longer half lives and they also act to inhibit topoisomerase I directly this may be beneficial for cytotoxicity *in vivo*.

The same experimental principles as for the topoisomerase I studies were used in the topoisomerase II studies, but instead of topoisomerase I, topoisomerase II $\alpha$  and topoisomerase II $\beta$  enzymes and antibodies were being used. Work involving topoisomerase II plasmid DNA relaxation assays suggested that NU:UB 31 was an inhibitor of topoisomerase II $\alpha$  and

topoisomerase II $\beta$  enzyme catalytic activities. Topoisomerase II $\alpha$  and topoisomerase II $\beta$  cleavage assays in cell-free purified enzyme systems indicated that NU:UB 31 effected approximately equivalent levels of linear DNA formation indicative of the formation of drug-stabilised cleavable complexes with either the  $\alpha$ - or  $\beta$ -isoforms. This result parallels the behaviour of m-AMSA, which has been shown not to discriminate between topoisomerase II isoforms (Marsh, 1996). These results supported the data from topoisomerase II $\alpha$  and topoisomerase II $\beta$  immunoband depletion assays in which NU:UB 31 was shown to cause topoisomerase II depletion. The topoisomerase II immunoband depletion experiments were however not conclusive as the positive control recommended for these assays, etoposide, was not successful in depleting topoisomerase II. Insolubility could have been a problem as concentrations of up to 700 $\mu$ M were recommended.

In summary, the DNA binding studies showed that NU:UB 31 bound DNA, via intercalation as well as through groove binding. The anti-topoisomerase investigations in this project together with earlier work implied that NU:UB compounds were active in topoisomerase assays using plasmid DNA as well as whole cells. For NU:UB 31 both topoisomerase I relaxation and cleavage complex formation were observed. Additionally anti-topoisomerase II ( $\alpha$  and  $\beta$ ) activities were also revealed. Thus, there is evidence to suggest that NU:UB 31 (and possibly other NU:UB compounds, Mincher D.J., *personal communications*) may have dual topoisomerase I and II activities and that NU:UB 31 could work via direct inhibition of enzyme function as well as acting as a topoisomerase poison. This may mean that the NU:UB 31 mechanism of

action is less specific than the action of a drug that only acts by poisoning topoisomerases. However, dual mechanisms may well prove to be beneficial *in vivo* considering reports of resistance where alterations in topoisomerase levels and functions are contributory factors.

## **CHAPTER 4**

### **CYTOTOXICITY**

## 4.1 CYTOTOXICITY

The cytotoxicity of NU:UB compounds, previously found to exert anti-topoisomerase activity (anti-topoisomerase data presented in Chapter 3) was investigated during this research programme. Standard anti-topoisomerase I and II drugs were also included in these studies for comparison.

The cytotoxic potency of an anti-cancer agent is an important consideration (not least from an *in vivo* perspective). Before we can expose cells to compounds for apoptotic, cell cycle and related studies, the cytotoxicities of these agents need to be established. The cytotoxicity induced over short and long drug exposure times in the cell lines that would be used in future experiments was assessed. This would further give an indication of stability of the NU:UB compounds over time *in vitro*. The cytotoxicity of the NU:UB compounds was studied with the 3-(4,5-dimethylthiazol-2-yl)-2,5-diphenyltetrazolium bromide (MTT) assay, which is a colorimetric-based assay for quantification of cell growth and viability. With this assay, cytotoxicity is expressed as IC<sub>50</sub> values. This is a measure representing the drug concentration at which 50% of the cells have survived the course of the treatment. The MTT assay was originally developed by Mosmann (1983) and has, in cancer research, become a tool for quantification of *in vitro* chemosensitivity in tumour cells. Denizot and Lang (1986) suggested modifications to the MTT assay to further improve reliability and sensitivity. Early studies suggested that MTT is reduced in mitochondria (at the

ubiquinone and cytochrome b and c sites of the mitochondrial electron transport system) (Slater *et al.*, 1963). Cleavage of MTT is thought to take place only in active, living cells and therefore the amount of formazan, and thus the intensity of blue colour produced should be proportional to the number of cells present (as well as the mitochondrial activity per cell) (Vistica *et al.*, 1991). In this MTT cytotoxicity study, three human cell lines were used; firstly, a leukaemia cell line, HL60 that was used for the immunoband depletion experiments (Chapter 3), and also for investigations of apoptosis (Chapter 6). The two other cell types chosen were the colon cell lines HCT116 and HT29, that have been reported to contain wild type and mutant p53 respectively (Chapter 7). The cytotoxicity at three time points, 4h, 24h and 96h was assessed. Cytotoxicity following 4h and 24h treatments was investigated since we wanted to determine whether or not the NU:UB agents had effect at short exposure times. If this was the case, the 4h and 24h time points would hopefully be suitable for the apoptotic investigations. A time point at 96h was also used since this is a standard time point used in the host laboratory and by collaborators at the Cancer Research Unit, Bradford University.

Cytotoxicity was also assessed by a second method, nigrosin exclusion cell counts. Nigrosin is a blue dye that is excluded from viable cells with intact membranes, but that can enter cells with compromised membranes and thereby distinguish between viable and dead cells. For this study HL60 cells were used and these were counted at various time points. NU:UB 31 was

used for this experiment, and known topoisomerase inhibitors (camptothecin and etoposide) were also included.

In addition, NU:UB compounds have been screened *in vitro* by NCI in a 60 cell line screen with the sulforhodamine B cytotoxicity assay, using 48h endpoints. The results from this screen are presented, in part, in mean graphs that can be found in Appendix 2. The activity of NU:UB agents (NU:UB 31 and NU:UB 51) *in vivo*, has also been investigated in NMRI mice bearing subcutaneous MAC 15A (murine adenocarcinoma) tumours. This work was performed by collaborators at the Cancer Research Unit, Bradford University and the results are presented in Appendix 3.

## **4.2 METHODS**

### **4.2.1 Growth Curve Of HL60 Cells**

HL60 cells were recovered from culture and washed. 180µl per well, of a cell suspension at  $1 \times 10^4$  cells/ml, was seeded into 96 well plates in all columns except column 1 (A1 to H1). Column 1 was used as a blank and contained medium only. For a 10 day growth curve, 10 plates were used and the plates were kept at 37°C, 5% CO<sub>2</sub>. Each day 20µl MTT (5mg/ml) was added and left to incubate for 4h. The optical density (OD) was measured at 540nm in a MRX Microplate Reader (Dynex Technologies).

### **4.2.2 Cytotoxicity Investigations With The MTT Assay, Preparation And Treatment Of Cells With Anti-Cancer Agents**

The cell solution was transferred to a sterile universal and centrifuged at 500 x g for 5 mins at 4°C. The supernatant was discarded and the cell pellet resuspended in fresh culture medium. Cell counts were performed using a haemocytometer. Cells were diluted to a density of  $1 \times 10^4$  cells/ml with culture medium for 96h MTT assay. The cell suspension was seeded into a 96 well plate (180µl cell solution per well) in all wells except A1 to H1 in column 1. Column 1 represented the blank, and medium only (180µl per well) was added to these wells. The plate was left to recover overnight, before being treated with NU:UB compounds or standard agents.

For each compound, serial dilutions were made in suitable culture medium from the 10mM stock solution. Drug solution, 20 $\mu$ l, was added per well from drug dilutions of 0.1 to 1000 $\mu$ M into columns 3 to 7. Thereby, the final concentrations ranged from 0.01 to 100 $\mu$ M with a total volume of 200 $\mu$ l per well. Columns 8 to 12 were used for a second compound in the same concentration range. Column 1 was left as a blank, and column 2 contained control cells, to which 20 $\mu$ l of medium was added. Treatments were carried out at 37°C, 5% CO<sub>2</sub>, for 96h.

### **4.2.3 Addition Of MTT**

Following treatments, 20 $\mu$ l MTT (5mg/ml in PBS) was added to each well of the 96 well plate, and the plate was then incubated at 37°C for 4 hours. When using non-adherent cells (HL60), the plates were centrifuged at 500 x g for 5 mins before removing the supernatant. Supernatants were removed and the purple formazan crystals were dissolved in 150 $\mu$ l of DMSO. OD was measured at 540nm in an MRX Microplate Reader (Dynex Technologies).

#### **4.2.3a Treatment Of Results**

The mean OD value of each column was obtained. The mean blank value, for medium only from column 1, was subtracted from all the other mean OD values. The results were expressed as percentage of survival, where any decrease from the control, 100% cell viability, would indicate cytotoxicity. The

concentration at which 50% of the cells had survived following treatment, relative to the control, was referred to as the IC<sub>50</sub> value. For each treatment the results have been expressed as the mean IC<sub>50</sub> value ± SEM.

#### **4.2.4 Cytotoxicity Investigations With Nigrosin Exclusion Cell Counts**

HL60 cells were recovered from suspension by centrifugation, 500 x g for 5 mins at 4°C, cells were washed, resuspended in fresh medium at 10 x 10<sup>4</sup> cells/ml in 10ml per sample and left overnight. Cells were treated with NU:UB 31 (5µM, 20µM, or 30µM), camptothecin (0.1µM or 5µM), etoposide (5µM) or with solvent (control). Cell viability was investigated over a time course of 4h, 8h, 24h and 48h treatments. Following treatments, cells were spun down at 500 x g for 5 mins at 4°C and were resuspended in 1ml medium. An aliquot of each sample was mixed 1:1 with 0.1% nigrosin and counted in a haemocytometer.

##### **4.2.4a Treatment of Results**

The experiment was performed in triplicate and the nigrosin negative (viable) cell counts were expressed as a percentage of total number of viable cells ± SEM. Tukey's one-way analysis of variance was used to evaluate significant differences between treated cells and control cells at each time point.

## **4.3 RESULTS**

### **4.3.1 Growth Curve Of HL60 Cells**

A growth curve of HL60 cells grown in 96 well plates, such as would be used for the MTT assay, was performed to make sure that the MTT assay conditions were suitable for this cell line. From this growth curve it was realised that a seeding density of  $1 \times 10^4$  cells/ml was suitable, and that cells grew exponentially from day 1-8 (Fig. 4.1). Thus, throughout the MTT assay, when cells will be seeded, left overnight and treated for 96h, the HL60 cells should grow exponentially.

### **4.3.2 MTT Cytotoxicity Assay Of NU:UB And Standard Drugs Using HL60, HCT116 And HT29 Cells**

Cells were exposed to NU:UB compounds or to standard anti-topoisomerase drugs (camptothecin, doxorubicin, etoposide) for 4h, 24h and 96h. After the exposure times the cell survival relative to the control was determined by addition of MTT. The cytotoxic potencies of the compounds at each time point expressed as  $IC_{50}$  values are shown in Table 4.1.

At the 4h time point, for all three cell lines, NU:UB compounds had  $IC_{50}$  values of less than  $39\mu\text{M}$ . At the 24h time point the  $IC_{50}$  mean values ranged from

1.7-26.5 $\mu$ M, where NU:UB 51 was the most cytotoxic of the NU:UB agents in all three cell lines. Additional hydroxy groups in the nucleus of the anthraquinone might be predicted to confer greater cytotoxic properties; in 1,4-bis-substituted (aminoalkylamino)anthraquinones, activity is greatly enhanced by inclusion of hydroxy groups at the 5- and 8- positions. Removal, for example, of the 5- and 8-hydroxy groups from mitoxantrone to afford ametantrone reduces activity 10-fold. The enhanced potency of hydroxylated aminoanthraquinones is believed to be due to their increased DNA-binding capacity (by intercalation) and to their increased propensity to result in free radical (ultimately hydroxy radical) formation (Cheng and Zee-Cheng, 1983).

The IC<sub>50</sub> values of the NU:UB compounds did not differ greatly over the 4h and 24h time points for these cell lines. This was not the case for the standard drugs, where camptothecin and doxorubicin had IC<sub>50</sub> values above 100 $\mu$ M (except camptothecin, 1.9 $\mu$ M in HL60 cells) in the 4h MTT assays. However in the 24h MTT assays, the standard drugs were more cytotoxic with IC<sub>50</sub> values between 0.02 $\mu$ M and 15.7 $\mu$ M. Thus, there were overall larger differences in the IC<sub>50</sub> values between the 4h to 24h time points for the standard drugs in HL60 and colon cells. For NU:UB compounds there were no differences or only up to 6-fold differences in the IC<sub>50</sub> values between the 4h and 24h time points. For the 96h time point the IC<sub>50</sub> values of the NU:UB compounds ranged from 0.3-4.2 $\mu$ M. In contrast, the IC<sub>50</sub> values of the known topoisomerase inhibitors were considerably lower for all cell lines, ranging from <0.01-0.4 $\mu$ M. Clearly for the NU:UB agents maximum cell death occurs early despite the lower intrinsic cytotoxic potency when compared to standard

agents. Cell death and the relationship to onset of apoptosis are discussed in Chapter 5 and 6.

### **4.3.3 Nigrosin Exclusion Assay Of NU:UB And Standard Drugs Using HL60 Cells**

The effect of NU:UB 31 on growth and viability was assayed by nigrosin exclusion cell counts. This assay distinguished viable and dead cells on the basis of cell membrane permeability of the nigrosin dye. NU:UB 31 was used in a concentration range of 5 $\mu$ M, 20 $\mu$ M and 30 $\mu$ M, camptothecin and etoposide were also included for comparison. Cell counts were carried out following 4h, 8h, 24h and 48h treatment. Nigrosin negative cells were considered to be viable in this experiment; negatively-stained and blue nigrosin positive (dead) cells were counted. Nigrosin negative (viable) cells were visualized by light microscopy. Whereas the cell numbers in the controls increased over the time course, 5 $\mu$ M NU:UB 31 resulted in growth inhibition compared to the control, however, there did not appear to be any significant cell kill with this concentration. At a concentration of 20 $\mu$ M there was some cell kill after 8h treatment, and cell growth was inhibited at the 24h and the 48h time points. Following 30 $\mu$ M NU:UB 31 treatment there were less viable cells at all time points compared to controls, including the first, 4h time point. In Fig 4.2 the nigrosin results have been expressed as percentages of viable cells in relation to total cell numbers. For the control, viability remained above 85% throughout the course of the experiment, confirming a healthy cell population. Fig. 4.2a indicates that the majority (>90%), of the cells were

viable, excluding the nigrosin dye at the 4h time point for all treatments. Following 8h, camptothecin (5 $\mu$ M) resulted in decreased viability (Fig. 4.2b). Fig. 4.2c shows that the control cells had >90% viability. NU:UB 31 at 20 $\mu$ M had effect on viability after 24h. Following NU:UB 31 (at 30 $\mu$ M), etoposide (5 $\mu$ M) and camptothecin (0.1 $\mu$ M and 5 $\mu$ M) treatment for 24h, significant differences from the control were reached. At 48h highly significant differences were reached compared to the control after NU:UB 31 (30 $\mu$ M), etoposide and camptothecin treatments ( $p < 0.001$ ) (Fig. 4.2d).

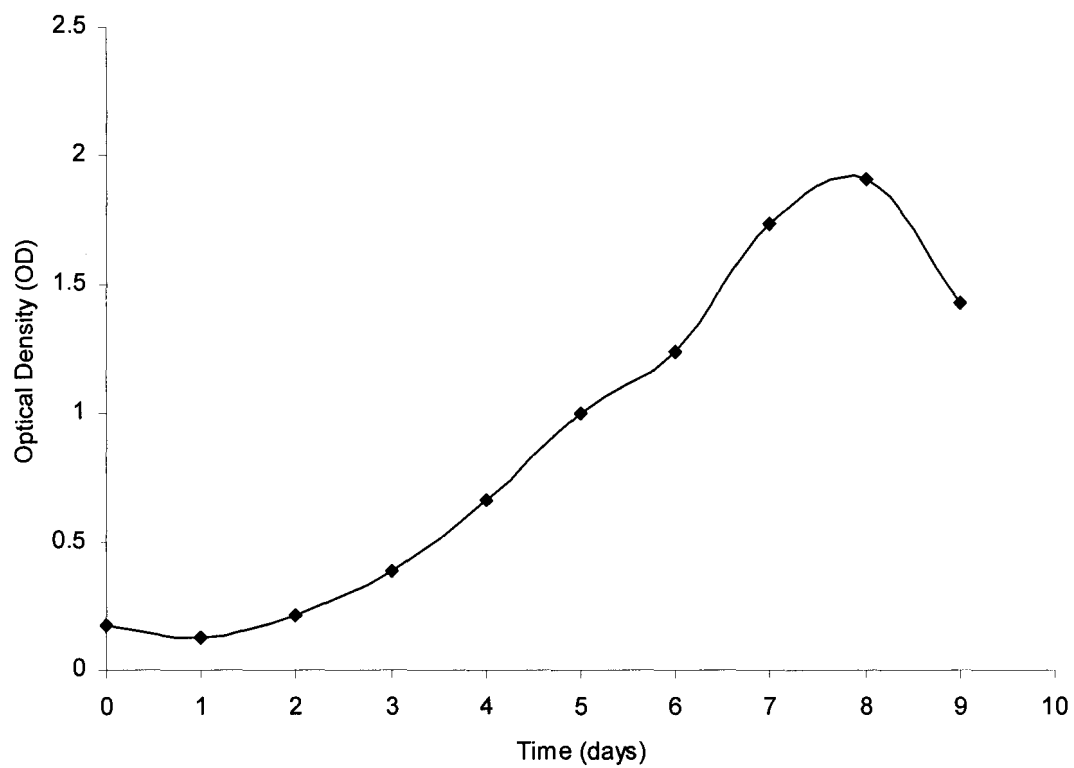
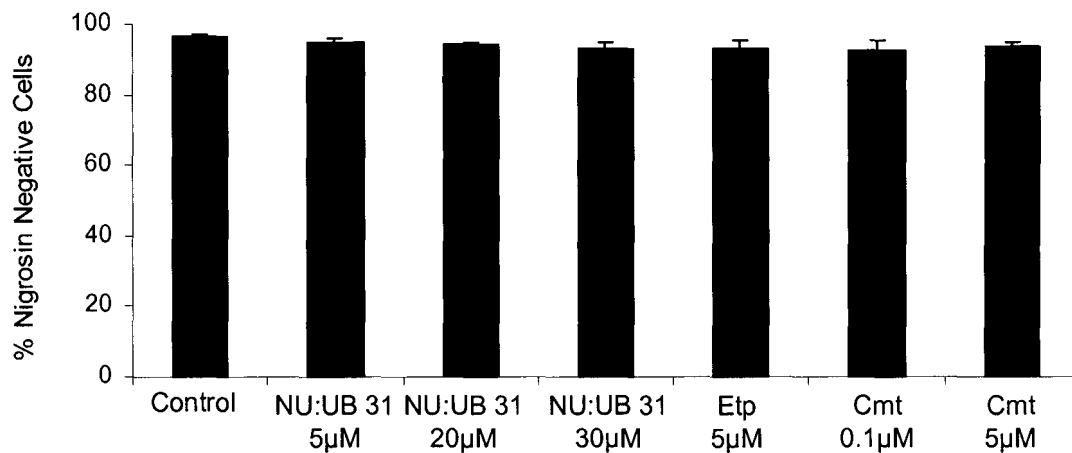


**Fig. 4.1** Growth curve of HL60 cells grown in 96 well plates. HL60 cells seeded at a density of  $1 \times 10^4$  cells/ml at day 0. Following addition of MTT the optical density in each well was measured at 540nm.

<b>HL60</b>	<b>4h</b>	<b>24h</b>	<b>96h</b>
NU:UB 31	27.5 ± 2.0	4.9 ± 0.5	3.1 ± 0.3
NU:UB 43	-	-	3.2 ± 0.2
NU:UB 51	4.0 ± 0.3	1.7 ± 0.2	0.3 ± 0.02
NU:UB 80	6.7 ± 0.6	2.9 ± 0.1	2.9 ± 0.3
NU:UB 81	-	-	4 (n=2)
Camptothecin	1.9 ± 0.2	0.02 ± 0.002	<0.01
Doxorubicin	> 100	0.3 ± 0.03	-
Etoposide	41.7 ± 1.7	1.0 ± 0.1	0.035 ± 0.005
<b>HCT116</b>	<b>4h</b>	<b>24h</b>	<b>96h</b>
NU:UB 31	30.0 ± 1.7	26.3 ± 2.4	2.8 ± 0.2
NU:UB 51	15.3 ± 1.5	3.8 ± 0.5	1.0 ± 0.07
NU:UB 80	38.5 ± 3.1	19.3 ± 1.8	2.9 ± 0.3
Camptothecin	> 100	0.1 ± 0.01	<0.01
Doxorubicin	> 100	0.9 ± 0.0	0.03 ± 0.003
Etoposide	-	-	0.4 ± 0.04
<b>HT29</b>	<b>4h</b>	<b>24h</b>	<b>96h</b>
NU:UB 31	33.5 ± 1.7	26.5 ± 1.9	4.2 ± 0.3
NU:UB 51	0.6 ± 0.1	2.2 ± 0.2	2.9 ± 0.3
NU:UB 80	29.5 ± 0.7	5.4 ± 0.5	2.6 ± 0.2
Camptothecin	> 100	15.7 ± 1.8	< 0.01
Doxorubicin	> 100	15.0 ± 4.5	0.06 ± 0.003
Etoposide	-	-	0.9 ± 0.09

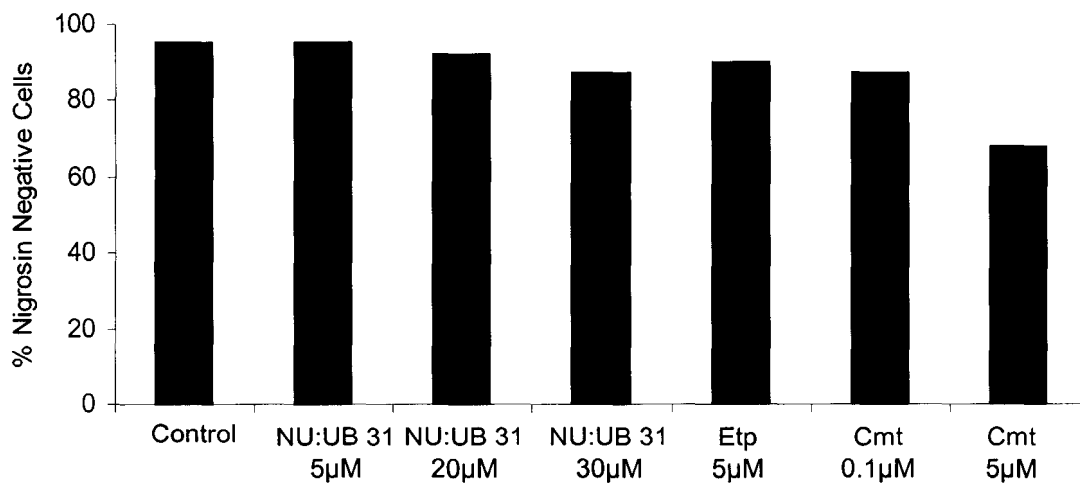
**Table 4.1** IC<sub>50</sub> values (µM) in cells exposed to standard drugs or NU:UB compounds for 4h, 24h, or 96h. Results are the mean IC<sub>50</sub> values ± SEM of 3 or more MTT assays.

Fig. 4.2a



4h Treatment

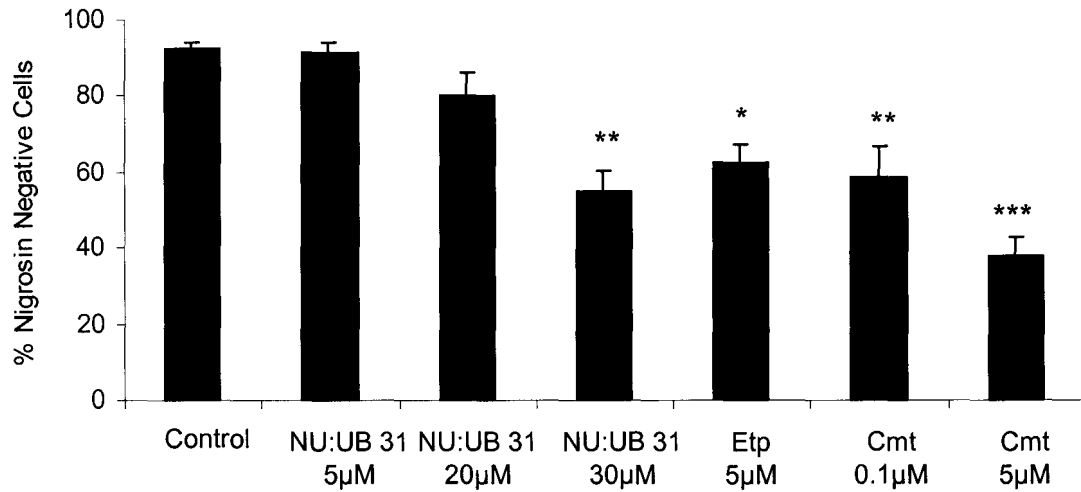
Fig. 4.2b



8h Treatment

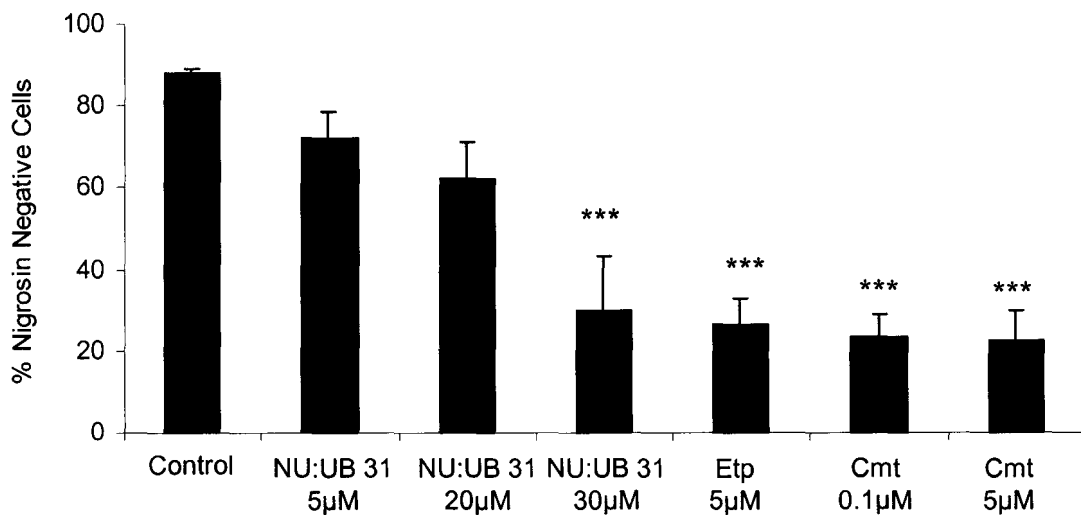
Fig. 4.2 (a and b). Nigrosin exclusion counts of HL60 cells following NU:UB 31, camptothecin (cmt) or etoposide (etp) treatment carried out for 4h (a) and 8h (b). Nigrosin negative (viable) cells expressed as a percentage of total (nigrosin negative + nigrosin positive) HL60 cells. Results are the mean of 3 separate experiments  $\pm$  SEM (except for the 8h time point (b) where n=2).

Fig. 4.2c



24h Treatment

Fig. 4.2d



48h Treatment

Fig. 4.2 (c and d). Nigrosin exclusion counts of HL60 cells following NU:UB 31, camptothecin (cmt) or etoposide (etp) treatment carried out for 4h 24h (c) and 48h (d). Nigrosin negative (viable) cells expressed as a percentage of total (nigrosin negative + nigrosin positive) HL60 cells. Results are the mean of 3 separate experiments  $\pm$  SEM. Asterisks denote significant differences from the control (\*  $p < 0.05$ , \*\*  $p < 0.01$ , \*\*\*  $p < 0.001$ ).

## 4.4 DISCUSSION

Toxicity of the standard agents, camptothecin, doxorubicin and etoposide is well documented in a range of cell lines and these known topoisomerase inhibitors were used as positive cytotoxicity controls. NU:UB 31, 43, 80 and 81 have previously, in a 60 cell line 48h sulforhodamine B cytotoxicity screen performed by NCI, shown exceptional profiles against refractory human colon carcinomas and malignant melanomas. Based on this, these compounds have therefore been chosen by NCI for complete biological evaluation as part of progression to clinical trials. In the NCI cell screen, different drugs are screened against a number of cell lines and to be able to compare these drugs, 'mean graphs' can be plotted. Mean graphs of the NU:UB agents can be found in Appendix 2. The NCI data include  $GI_{50}$  (mean concentration of drug which inhibits cell growth by 50%), TGI (mean concentration of drug which inhibits cell growth by 100%) and  $LC_{50}$  (mean concentration of drug which decreases protein stain absorbance by 50%) values, which are an effective indicator of cell kill, rather than growth inhibition. The effect of a compound on a specific cell line (or type of cell line, e.g. melanoma) can in these mean graphs be related to the mean effect on all screened cell lines, since these graphs display the mean of each cell line as a deflection from the overall calculated mean value. If the  $GI_{50}$  values of a cell line is to the right of the mean value, these cells are sensitive to the drug ( $GI_{50}$  values < the mean, sensitivity), whereas cells that are more resistant will be to the left ( $GI_{50}$  values > the mean, resistant). Screening drugs in this manner may be very useful

since a growth inhibitory response of a single cell line might give relatively little information about a particular drug, whereas a pattern of response by several cell lines (and groups of cell lines) can make up a "molecular fingerprint" that could aid in categorising drugs according to their mechanism(s) of action (Monks *et al.*, 1997).

In this study, a series of NU:UB compounds (NU:UB 31, 51 and 80) were screened with 96h MTT assays in the human HL60, HCT116 and HT29 cell lines. IC<sub>50</sub> values for these NU:UB agents ranged for the 96h time point from 0.3-4.0µM in HL60 cells, 1.0-2.9µM in HCT116 cells and 2.6-4.2µM in HT29 cells. Additionally, NU:UB 31 and NU:UB 80 have also been screened by NCI, and showed cytotoxicity. The MTT results together with the NCI data, indicated that the NU:UB compounds were cytotoxic at low, µM concentrations. The standard drugs camptothecin, doxorubicin and etoposide were (in the MTT assay) more cytotoxic at 96h than any of the NU:UB compounds. This was not the case at the short, 4h time point where NU:UB compounds were more potent than the standard drugs with IC<sub>50</sub> values at µM levels, compared to the standard drugs which had IC<sub>50</sub> values above 100µM in the colon cell lines. Thus the MTT data in the cell lines used, together showed that the NU:UB compounds were cytotoxic at low, µM concentrations at both long and short exposure times over a range of cell lines. Furthermore, the NU:UB IC<sub>50</sub> values did not decrease very much between the 4h and 24h time points, which was the case for standard drugs. From the MTT data it appeared that the NU:UB compounds were taken up by the cells and acted within the 4h exposure time. One major contributor to low potency of cytotoxic

agents is drug resistance commonly manifested through the expression of the MDR1 gene product, P-gp (classical multidrug resistance phenotypes); furthermore, many standard topoisomerase inhibitors are susceptible to P-gp- or the related MRP-mediated protein efflux mechanisms (Larsen and Skladanowski, 1998). The anthraquinone NU:UB 31 has, however, shown activity in a number of cell lines that are classically resistant to topoisomerase inhibitors; in the NCI screen, for example, NU:UB 31 showed only 1.3-fold resistance in the (doxorubicin-resistant) high P-gp-expressing NCI/ADR-res cell line when compared to the wild type MCF7 counterpart, whereas the anthraquinones, doxorubicin and mitoxantrone were 630- and 1000-fold resistant, respectively. NU:UB 31 was also found to be only 4.8-fold resistant in the P-gp-expressing, doxorubicin-resistant A2780/ADR human ovarian carcinoma cell line, in contrast to doxorubicin (150-fold resistant) when resistance levels were compared to the wild-type A2780 parent cell line. Furthermore, in studies from this laboratory, NU:UB 31 has been found to show 2.7-fold hypersensitivity in a highly P-gp-expressing, mutated Chinese Hamster Ovarian cell line, CHO/ADR-r (14-fold resistant to doxorubicin) when compared to the wild-type CHO- K1 parent (P-gp-expression was measured by flow cytometry as the percentage of cells staining positive with MRK-16 anti-P-gp antibody (21% and 91% for wild-type and resistant variant, respectively) (Gilmour P.S. and Mincher D.J., *unpublished data*). The data may suggest that NU:UB 31 is a poor substrate for the P-gp protein efflux pump and given its hydrophobic cationic properties may facilitate early mechanisms of cell death induction, in contrast to anthracyclines like doxorubicin. Additionally, the hypersensitivity observed with NU:UB 31 may

be correlated to the topoisomerase protein expression in the CHO/ADR cell line. When CHO/ADR was compared with the wild -type it was characterised as having a two-fold decrease in topo II $\alpha$  levels and concomitant increases (2.5-fold and 2-fold, respectively) in topoisomerase II $\beta$  and topoisomerase I proteins. NU:UB 31 has here been shown to inhibit all three topoisomerases (at least *in vitro*) whereas anti-topoisomerase II agents including doxorubicin have been considered largely to target the alpha isoform, that is down-regulated in this and other resistant cell lines.

Camptothecin has been reported to be dependent on the cell cycle for its cytotoxic action. In this study, the MTT IC<sub>50</sub> values at 24h were lower than following 4h exposure in the three cell lines and even more so at the 96h time point. This was also the case for doxorubicin and etoposide. Fewer cells had survived at the 24h time point than at the 4h time point. This may be a reflection that the standard drugs were stable, and did not break down during the course of the MTT assay. The NU:UB compounds had however, at the 4h and 24h time points, similar values in these assays. This suggests that the drug action of the NU:UB compounds took place fairly rapidly, and possibly following this, the NU:UB compound may have been inactivated, broken down. However, previous pharmacokinetic work performed at the Cancer Research Unit at Bradford University assessing the stability of NU:UB 31 gave *in vitro* t<sub>1/2</sub> values of >100h in plasma, 75.1h in tissue culture medium and 25.7h in whole blood, which would indicate that this agent is relatively stable *in vitro*. Additionally, an *in vivo* pharmacokinetic analysis of NU:UB 31 was also performed over an 8h period in MAC15A tumour-bearing mice where

NU:UB 31 was administered i.p. at the maximum tolerated dose (MTD, 100mg/kg). It was demonstrated that NU:UB 31 concentration peaked in plasma after 30 minutes with a  $t_{1/2}$  value of 2.2h. Peak tumour concentrations exceeded the concentration in plasma by approximately 3-fold, peaking at 2h with a  $t_{1/2}$  value of 6h (see Appendix 4). That NU:UB 31 had a fairly long half-life in MAC15A tumours *in vivo* may in part explain the anti-tumour activity seen against these tumours, refractory to several known anti-topoisomerase drugs. Furthermore *in vivo* work in NMRI mice bearing subcutaneous MAC 15A tumours has indeed shown reduced tumour growth following administration of NU:UB 31. Treatment with NU:UB 31 (MTD, 100mg/kg) led to a significant delay in tumour growth ( $P < 0.01$ ) and administration of doses below the MTD also resulted in delayed tumour growth. NU:UB 31, administered to the NMRI mice i.p. at single doses of 67mg/kg and 33mg/kg resulted in a growth delay of 4.3 and 3.2 days respectively. In both cases, treatment resulted in a statistically significant delay in tumour growth ( $p < 0.01$ ) compared to controls. *In vivo* results of comparative studies of NU:UB 31, NU:UB 51, camptothecin, doxorubicin and mitoxantrone can be viewed in Appendix 3.

In addition to the MTT assay, cytotoxicity following NU:UB 31, camptothecin and etoposide treatment was studied with nigrosin exclusion cell counts using HL60 cells. This experiment identified viable and dead cells on the basis of cell membrane permeability of the nigrosin dye. Following 4h exposure, the majority of the cells in all treatments were viable, excluding the blue nigrosin dye. Following 24h and 48h exposures NU:UB 31 (30 $\mu$ M), camptothecin

(0.1 $\mu$ M and 5 $\mu$ M) and etoposide (5 $\mu$ M) all resulted in significantly decreased cell viability as measured with nigrosin exclusion.

Hence, the two cytotoxicity assays used in this study (the MTT assay and the nigrosin exclusion assay) implied that the compounds were cytotoxic *in vitro*. However, the effect appeared to be greater measured by the MTT assay than when measured with nigrosin exclusion cell counts. This may be explained by the fact that the two assays rely on different mechanisms. The MTT assay uses mitochondrial function in distinguishing viable and dead cells, whereas, dead cells are distinguished from viable cells by membrane permeability in the nigrosin exclusion assay. Thus mitochondrial function seemed to be disrupted in cells before the cell membranes became permeable to the nigrosin dye. This may be significant in the light of sub-cellular localisation of NU:UB compound.

In summary, NU:UB compounds were cytotoxic in the cell lines used. NU:UB compounds were, at shorter exposure times, but not at the longer exposure times, more cytotoxic than standard agents. Thus, the NU:UB agents appeared to have a fairly rapid mechanism of action. The IC<sub>50</sub> values of the NU:UB compounds did not differ as much between the time points as the IC<sub>50</sub> values for the standard agents. This may indicate that the NU:UB compounds broke down in cell culture over time, and/or the cells could, following drug uptake, have had mechanisms of excluding (efflux) these agents, and/or repair mechanisms that repaired drug damaged cells and thereby allowed for continued growth. The nigrosin exclusion cell count experiment further

confirmed that NU:UB 31 was cytotoxic. From these investigations it was demonstrated that NU:UB exposure times of 4h and 24h were sufficient to have an impact on cell survival, making these time points suitable for apoptotic studies. Considering the topoisomerase assays conducted earlier and described in the previous chapter (Chapter 3) along with the *in vitro* cytotoxicity studies (Chapter 4 and Appendix 2) and *in vivo* data of NU:UB 31 and NU:UB 51 (Appendix 3), it appears that both these NU:UB agents act via topoisomerases and both agents have been reported to shrink tumours in previous mice studies. NU:UB 51 was however, particularly at the shorter exposure times, the more cytotoxic compound *in vitro*. There might be other targets/mechanisms involved in the way by which these compounds kill cells. That NU:UB 51 was more cytotoxic *in vitro* is likely to be due to OH groups in its anthraquinone chromophore, making this agent more open to free radical formation that could play a part in its cytotoxicity. Although, NU:UB 51 was slightly more potent *in vitro* at the shorter exposure times, NU:UB 31 and NU:UB 51 both had similar cytotoxic potency at longer exposure times, acted via topoisomerases and both shrank tumours *in vivo*. With this in mind, NU:UB 31, rather than NU:UB 51, was chosen as the lead compound, since NU:UB 31 does not contain OH groups and was therefore considered to be less likely to be a source of free radical formation that could potentially increase the probability of non-specific adverse toxic effects *in vivo*.

## **CHAPTER 5**

### **INVESTIGATION OF CELL CYCLE DISTURBANCES FOLLOWING NU:UB TREATMENT**

## 5.1 INVESTIGATION OF CELL CYCLE DISTURBANCES

This part of the research programme investigated whether or not treatment with NU:UB compounds affected cell cycle progression in HL60 cells. The focus was on NU:UB 31, but for comparison, NU:UB 51 as well as classical anti-topoisomerase agents were also used.

It was hoped that studying the cell cycle effects, and the cell cycle phase specificity of anti-cancer agents would help in the understanding of their mechanisms of action. Furthermore, such studies were also hoped to aid in the development of new agents and, in particular, clinical drug regimens, since factors such as simultaneous administration of agents may play a part in resistance, limiting the effectiveness of drugs (Larsen and Skladonowki, 1998). Various anti-topoisomerase agents have been found to affect the cell cycle and/or induce apoptosis in cells, so the reason for arrest in a particular phase of the cell cycle following treatment with anti-cancer drugs may partly be linked to the topoisomerase (I and II) activities in relation to the cell cycle, and how these drugs affect the respective topoisomerase enzymes. Cell cycle arrest can occur in either G1 or G2 phases, but cells may also be inhibited in S-phase. It has been suggested that topoisomerase I is important in all phases of the cell cycle and that topoisomerase II may be required to enter S-phase and to complete G2 phase (Poot *et al.*, 1995).

Two anti-topoisomerase drugs were included in this cell cycle study for comparison, camptothecin and etoposide, since they are reported to act via topoisomerase I, and II respectively. Previously, in Chapter 3 the findings from anti-topoisomerase activity studies of some of the NU:UB compounds were presented and it was found that the NU:UB agents interfered with these enzymes. Therefore if NU:UB agents cause arrest in a particular phase of the cell cycle, similar to the known anti-topoisomerase drugs used for comparison, this may confirm their mechanism of action as anti-topoisomerase I or II inhibitors. This study of cell cycle was facilitated by the use of flow cytometry by measuring emission from the DNA intercalator, propidium iodide. In addition to the cell cycle measurements, analysis of apoptotic cells was also performed. In ethanol fixed and rehydrated apoptotic cells, some of the lower molecular weight DNA fragments may diffuse out, and this lowers the DNA content in apoptotic cells. These cells are quantifiable in a DNA histogram belonging to the so called sub G1 material.

## **5.2 METHODS**

### **5.2.1 Growth Curve Of HL60 Cells**

HL60 cells were seeded in culture flasks at concentrations of  $1 \times 10^4$ ,  $2 \times 10^4$  and  $5 \times 10^4$  cells/ml at day 0. To monitor the growth of this cell line, cells were counted each day over a time course of 8 days. The growth curves were performed in triplicate, and the cells were counted using a haemocytometer.

### **5.2.2 Analysis Of The Cell Cycle Using Flow Cytometry**

One of the most commonly used flow cytometric methods to study how treatment with drugs affects the cell cycle progression, relies on analysis of the DNA distribution of a cell population. DNA content measurements use fluorescent probes with a high degree of specificity for DNA; in this project propidium iodide (PI) was used. The PI probe intercalates into DNA, is excited by the appropriate wavelength, and the fluorescence emission is collected and displayed using flow cytometry. The fluorescence intensity in this method is accepted to be proportional to the amount of bound dye and thereby the fluorescence intensity of the individual cell will be proportional to its DNA content. From each sample, the DNA content of cells was measured and a histogram of the number of cells against DNA content was plotted reflecting the state of the cell cycle. This histogram was further divided into different phases with regard to DNA content (fluorescence). Cells in G1 can be

considered to have a DNA index of 1.0. When the cells start to make new DNA they enter the DNA synthesizing S-phase of the cycle and have a DNA index between 1.0 and 2.0. Cells in the G2/M phase have a DNA content of 2.0. Thereby cells in G2 and M phases of the cell cycle have double the DNA content of those in G1 (and G0), and cells in S phase have DNA content somewhere in between these extremes. Treatment of cells with agents that affect the progression of cells through the cell cycle will result in changes in the DNA distribution, altering the proportion of cells in the individual cell cycle phases.

Various treatments of HL60 cells with NU:UB compounds or standard drugs were performed. HL60 cells were seeded at  $5 \times 10^4$  cells/ml and left to recover overnight. Cells were transferred to universals and pelleted by centrifugation at 500 x g for 5 mins. The cell pellets were resuspended in 10ml drug solution or medium with solvent (control) and incubated at 37°C for 1 or 4h. Following treatment, cells were washed in HBSS, resuspended in fresh medium and left in the incubator to recover for 0h, 4h or 24h. Cells were pelleted at 500 x g for 5 mins, resuspended in 0.1ml PBS and transferred to Eppendorf tubes. Ice cold 70% ethanol (0.9ml), was added and the cells left to fix in the freezer. Cells were harvested by centrifugation at 500 x g for 5 mins, and were rehydrated in 0.4ml PBS. RNase was added, 50µl (1 mg/ml in PBS) and samples were incubated at 37°C for 30 mins. PI, 50µl (0.4mg/ml in water) was added and the samples were left to incubate for another 10 mins in the dark. Cells were recovered at 500 x g for 5 mins, resuspended in 1ml PBS and stored on ice in the dark until analysed.

The DNA content of each cell was analysed using a FACSCalibur flow cytometer (Becton Dickinson Immunocytometry Systems, BDIS) equipped with a 15mW argon-ion air-cooled laser with excitation wavelength 488nm, measuring light scatter and red fluorescence.

### 5.2.2a Treatment Of Results

Cellular DNA content following PI staining was measured and a cell cycle histogram of 10 000 events (cells) was obtained from each sample. Pulse height signals of forward and side light scatter (SSC) were collected for the discrimination of debris. Each fluorescence histogram was analysed with Cellquest software (BDIS) that allowed for estimation of the percentage of cells in G1, S and G2/M phase of the cycle. Each sample was analysed in triplicate (or duplicate), and a mean  $\pm$  SD of the percentage of fluorescence for each cell cycle phase was calculated and plotted in a histogram.

### 5.2.3 Analysis of Apoptosis Using Flow Cytometry

The above method of analysing DNA content of individual PI stained cells using flow cytometry can also be a tool for identifying apoptotic cells in a cell population. In apoptotic cells, the DNA content is thought to be less than in viable cells. Therefore, cells with DNA content below that of G1 cells were considered to be apoptotic and appeared as a sub G1 peak in the cell cycle histograms. In samples with high cell turn over, rapid cell growth or cell kill,

there was however also likely to be a lot of cell debris present in the sub G1 region and information about cell size and granularity was obtained from analysing scattered light as the cells pass through the laser beam.

### 5.2.3a Treatment Of Results

Cells with DNA content below G1 were gated out in each of the above cell cycle histograms, and measured. The sub G1 populations in controls were compared to sub G1 material in treated cells. The result was calculated as the mean value from two or three separate experiments.

## 5.3 RESULTS

### 5.3.1 Growth Curve Of HL60 Cells

Fig. 5.1 shows the growth curves of HL60 cells seeded at  $1 \times 10^4$ ,  $2 \times 10^4$  and  $5 \times 10^4$  cells/ml. Following a brief lag phase, the cells grew exponentially until day 6 for cells seeded at  $5 \times 10^4$  cells/ml, and until day 7 for cell cultures seeded at  $1 \times 10^4$  and  $2 \times 10^4$  cells/ml.

### 5.3.2 Cell Cycle Analysis

The cells were harvested following 1h or 4h treatment, and at 0h, 4h or 24h recovery, fixed in ethanol, stained and measured by flow cytometry.

#### 5.3.2a Cell Cycle Analysis Of HL60 Cells Following 1h Treatment With NU:UB 31 Or Standard Drugs

Cells were treated with NU:UB 31 (and NU:UB 51 1h + 4h), or standard drugs for 1h and recovered for 4h or 24h. Representative cell cycle histograms of these treatments can be seen in Figs. 5.2a-f and Figs. 5.3a-f. Control cells, 1 + 4h and 1 + 24h can be seen in Fig. 5.2a and 5.3a respectively. Both these controls showed sharp major G1 peaks and minor G2/M peaks located at approximately 200 and 400nm, indicating that these control cell populations

were healthy and normal. Treatments with camptothecin and etoposide resulted in cell cycle disturbances. Particularly after 1h treatment followed by 24h recovery, the normal cell cycle distribution was greatly distorted with a build up in S-phase and G2/M phase respectively (Fig. 5.3b, Fig. 5.3c). For NU:UB 31, slight cell cycle disturbances compared to control were observed following 1h treatment with 4h recovery. However, following 24h recovery the cell cycle histograms for these treatments were again normally distributed and hence no permanent cell cycle block appeared to occur once the cells had been washed and left for 24h. The percentages of each cell cycle phase were calculated for each cell cycle distribution histogram. The mean cell cycle phase values from each treatment and time point were plotted in summary histograms. Histograms to summarise the 1h + 4h and the 1h + 24h experiments can be found in Fig. 5.2g and Fig. 5.3g respectively. Following 1h treatment (and 4h recovery) with the anti-topoisomerase I agent, camptothecin (2 $\mu$ M and 5 $\mu$ M) there was an increase, compared to the control, in the number of cells in the G1 phase; the G2/M phase remained the same, but there was a decrease in the S phase population (Fig. 5.2g). When the camptothecin (2 $\mu$ M) treated cells were left to recover for 24h there was a decrease in both G1 and G2/M cells and there seemed to be an accumulation of cells in S phase. Thus camptothecin caused an accumulation of cells in early S phase, which presented as a shift in distribution with a concomitant decrease in G1 and G2 phase cells. Following 1h treatment (and 4h recovery) with the anti-topoisomerase II drug, etoposide (5 $\mu$ M), there was also at first an increased number of G1 phase cells, but over time with 24h recovery this resulted in a G2/M block. NU:UB 31 (20 $\mu$ M, 30 $\mu$ M, 40 $\mu$ M and 50 $\mu$ M) and

NU:UB 51 (0.5 $\mu$ M and 1 $\mu$ M) 1h exposure with 4h recovery showed different histograms compared to the standard drugs, there was a decrease in G1, a slight increase in G2/M and S phases. However, when the cells had been left to recover for 24h, cell cycle distributions were similar in NU:UB 31 treated and untreated control samples (Fig. 5.3g).

### 5.3.2b Cell Cycle Analysis Of HL60 Cells Following 4h Treatment With NU:UB 31

Figs. 5.4a-c show cell cycle histograms representative of the 4h treatments with no recovery, Figs. 5.4d-f represent 4h treatments with 4h recovery, and Figs. 5.4g-h are the 4h treatments followed by 24h recovery. The untreated HL60 controls for these time points did, as expected, appear to have normal and healthy cell cycle distribution with very little material in the sub G1 region (the region in FL2-A below 200nm) (Fig. 5.4a, Fig. 5.4d, Fig. 5.4h). There was a slight decrease in the number of G1 cells, and increase in S phase cells following 4h 30 $\mu$ M NU:UB 31 treatment without recovery (Fig. 5.4b). No apparent changes in the different phases were seen following the 50 $\mu$ M NU:UB 31 treatment at this time point. At this concentration there was rather an increase in the sub G1 material with no cell cycle distribution alterations (Fig. 5.4c). With 4h recovery there was a similar finding; the lower NU:UB 31 concentrations, but not 50 $\mu$ M, gave slight cell cycle distribution changes with what appeared to be a block in the S and G2/M phases (Fig. 5.4e and Fig. 5.4f). At this time point there was also more cell kill, more sub G1 material than in the treatments without recovery. However, when the cells had been

treated with NU:UB 31 at 30 $\mu$ M for 4h and had been allowed to recover for 24h, there was no blockage in the cell cycle and these histograms showed a normal distribution of cells through the cycle (Fig. 5.4h). In addition, at this time point, following 30 $\mu$ M NU:UB 31 treatment, there was only a slight increase in sub G1 material. In contrast, no viable cells were present following 50 $\mu$ M NU:UB 31 treatment for 4h with 24h recovery. Histograms that summarise the mean values of the 4h treatments with 0h, 4h or 24h recovery can be found in Fig. 5.4i.

### **5.3.3 Analysis Of The Sub G1 Population**

For each cell cycle histogram, the cell population (cell material) in the sub G1 region was gated out and measured. Some of this material was likely to be cell debris (late apoptotic and necrotic cells). However, upon analysing light scattering properties of the cells, along with PI in FL2-A, cells with lower (below 200nm) PI staining (less DNA content), but which retained the same degree of side scatter (granularity) were considered to be apoptotic. Cells and cell material with lower PI staining, as well as less granularity, below 200nm were considered to be debris. The levels of debris and apoptotic cells were low in control samples (Fig. 5.2a, Fig. 5.3a, Fig. 5.4a). However, following camptothecin, etoposide and NU:UB 31 treatments the apoptotic population in these samples increased dramatically (Figs. 5.2b-f, Figs. 5.3b-c, Fig. 5.4c, e, f and h). In addition to the increased apoptotic population, the level of debris was also increased in samples treated with camptothecin, etoposide and high (50 $\mu$ M) NU:UB 31 concentration due to the high degree of cell kill induced by

these treatments (Figs. 5.2b-c and f, Figs. 5.3b-c, Fig. 5.4c and f). Figs. 5.5-5.7 summarise the mean values of sub G1 material for each treatment and time point obtained from the cell cycle histograms. Following camptothecin treatment there was a drastic increase in the level of cells located in the sub G1 region following 1h treatment and 4h recovery, and an even higher increase after 24h recovery. Etoposide treatment also induced apoptotic cell death, evident by a massive increase in cell number in the sub G1 region. After 1h NU:UB 31 treatment with 4h recovery there was a slight increase in sub G1 cells compared to control, but not as high as for camptothecin and etoposide. Following 24h recovery, NU:UB 31 treated cells appeared normal with sub G1 levels that were comparable to the control (Fig. 5.5, Fig. 5.6).

For all 4h 20 $\mu$ M and 30 $\mu$ M NU:UB 31 treatments there was an increase in the number of cells in the sub G1 region. However, following 4h recovery the sub G1 levels were higher than following 24h recovery. At the NU:UB 31 50 $\mu$ M concentration there was a massive increase in sub G1 levels after 4h treatment, which after 4h recovery increased to levels comparable to the amount of cell kill induced by standard drugs. Upon examination, the 50 $\mu$ M NU:UB 31 treated cell cultures that had been left to recover for 24h contained no viable cells. The amount of DNA leached out of cells, and hence the position of the apoptotic peak in the sub G1 region of the DNA histogram may depend on the cell type. For some of the HL60 cell histograms presented within this chapter there was a lot of sub G1 material, but not a defined sub G1 peak. Inclusion of a high molarity phosphate-citric acid buffer to the rinsing solution is thought to enhance the extraction of the degraded DNA, improving

resolution with a sharper sub G1 peak following drug treatment (Gong *et al.*, 1994). In addition to the light scattering properties, to confirm that the material in the sub G1 region was indeed apoptotic cells, a sample with high levels of sub G1 material was viewed under the confocal microscope. These cells appeared to be apoptotic and Fig.5.8 shows cells treated with camptothecin at 2 $\mu$ M for 1h with 24h recovery, two pictures were taken of each cell and the picture of PI stained DNA has been fused with the white light picture. This revealed condensed DNA within the apoptotic sub G1 cells.

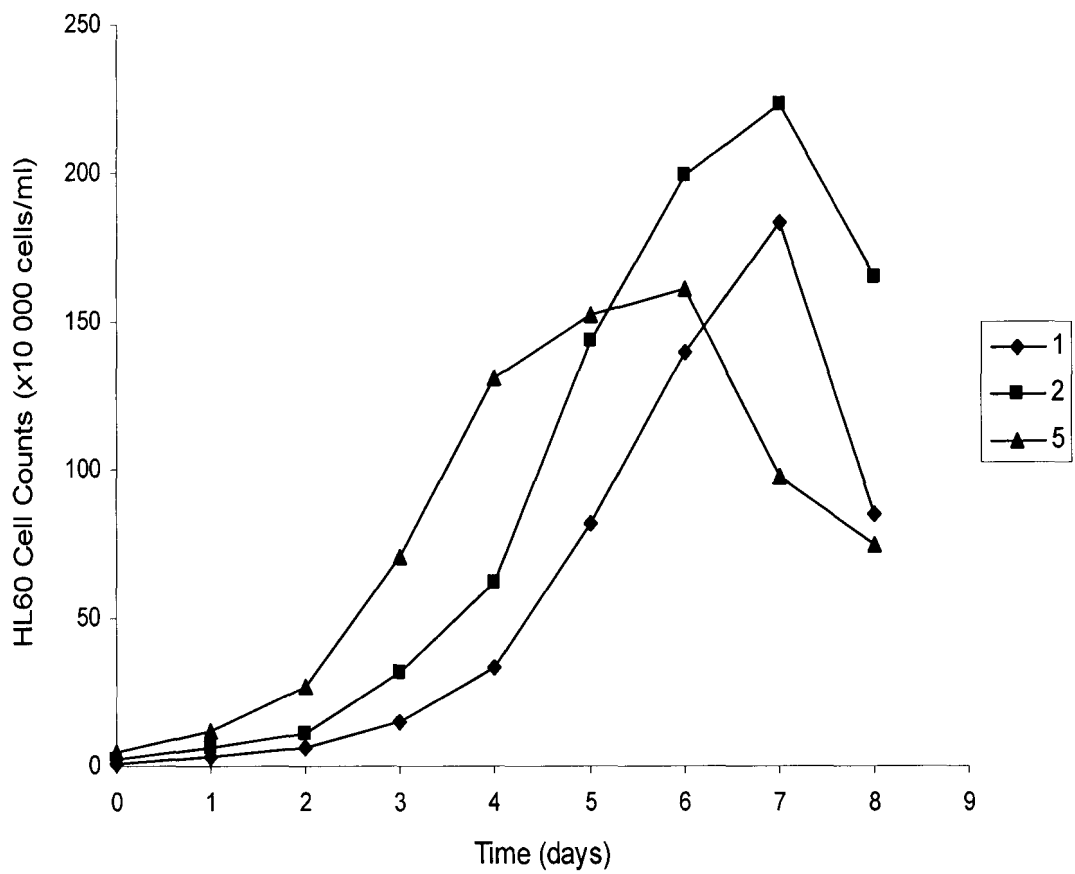


**Fig. 5.1** Growth curve of HL60 cells in culture. Cells were seeded at  $1 \times 10^4$  (1),  $2 \times 10^4$  (2) and  $5 \times 10^4$  (5) cells/ml at day 0. Cells have been counted each day for a time course of 8 days using a haemocytometer.

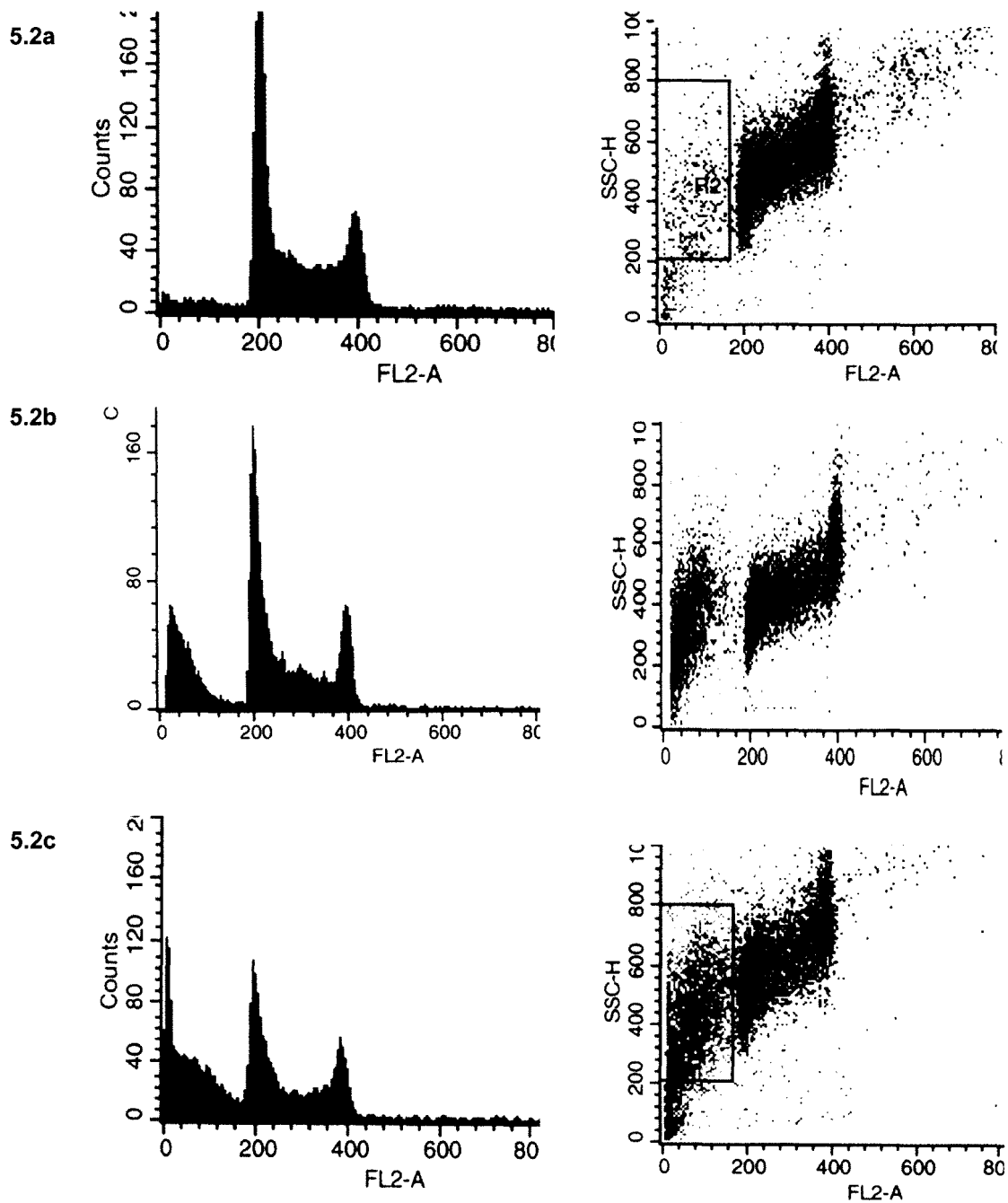


**Fig. 5.2a-c** Representative histograms and respective cytograms of the cell cycle distribution in HL60 cells, measured with flow cytometry. Cells were treated for 1h, were left to recover for 4h, and were then stained in PI. Control (a), camptothecin 2μM (b) and etoposide 5μM (c).

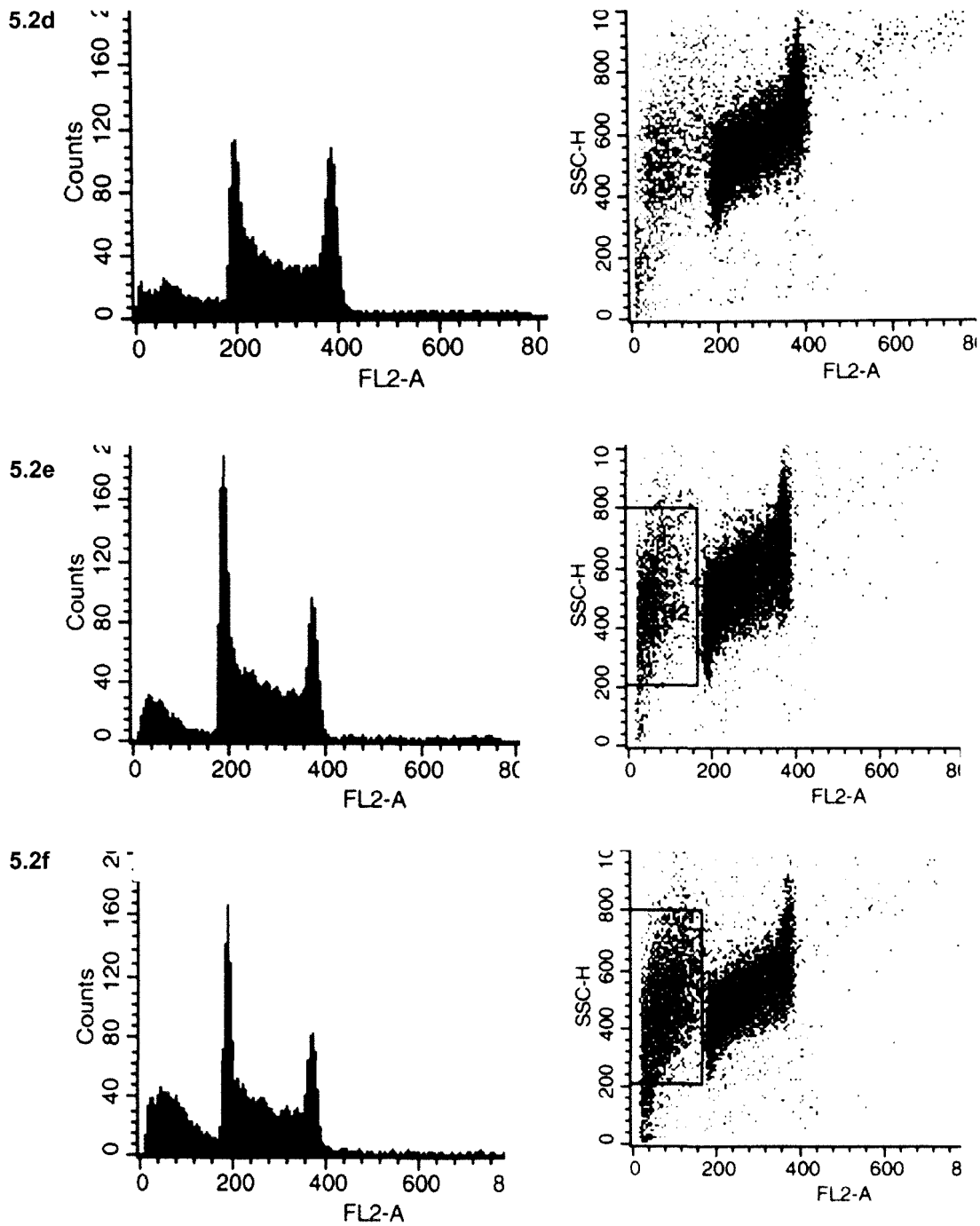


**Fig. 5.2d-f** Representative histograms and respective cytograms of the cell cycle distribution in HL60 cells, measured with flow cytometry. Cells were treated for 1h, were left to recover for 4h, and were then stained in PI. NU:UB 31 30 $\mu$ M (d), NU:UB 31 40 $\mu$ M (e) and NU:UB 31 50 $\mu$ M (f).

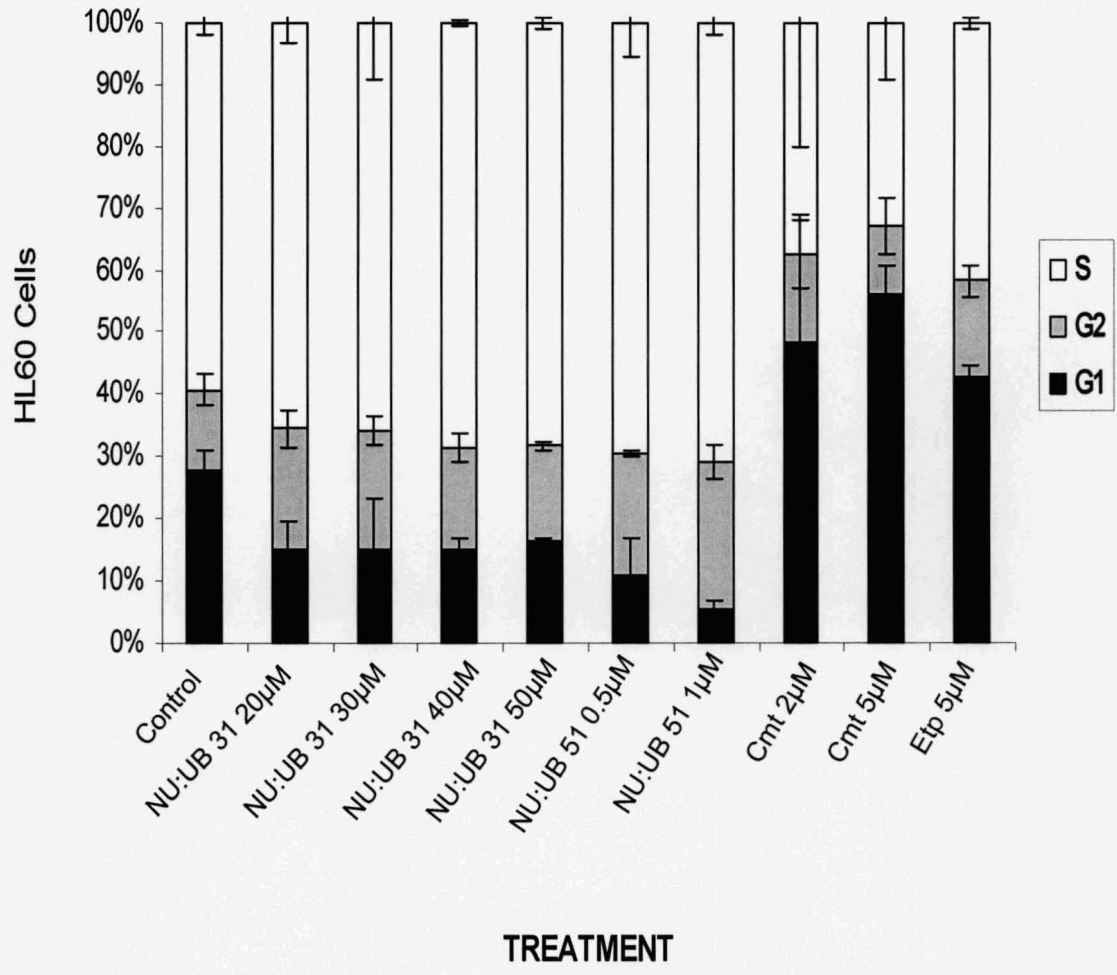
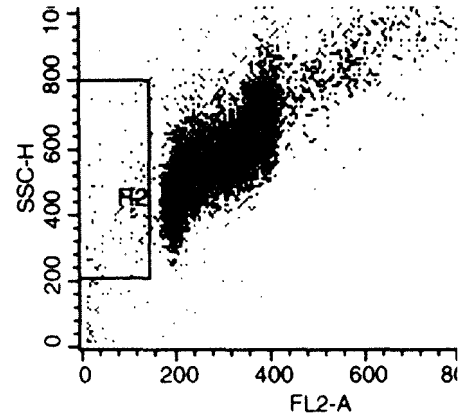
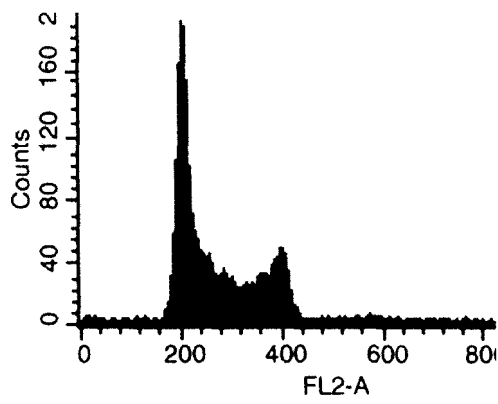
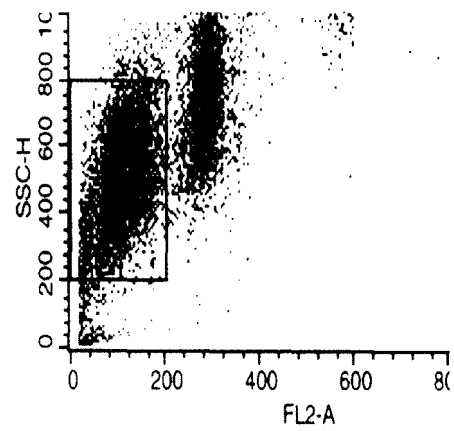
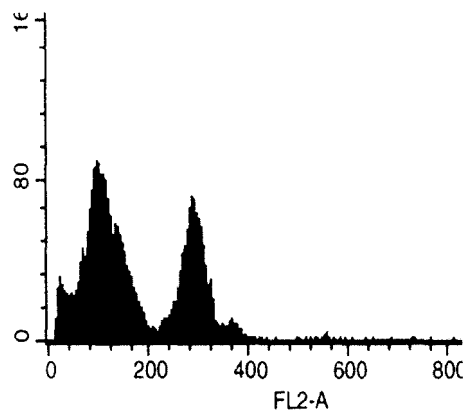


**Fig. 5.2g** Summary histogram of the cell cycle phase distribution in treated and untreated HL60 cells. Cells were treated for 1h, left to recover for 4h and stained in PI. Mean values of each cell cycle phase  $\pm$  SD were calculated.

5.3a



5.3b



5.3c

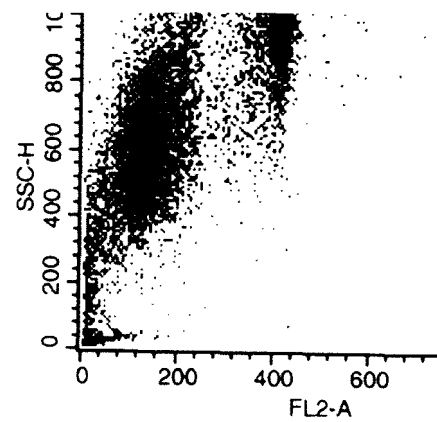
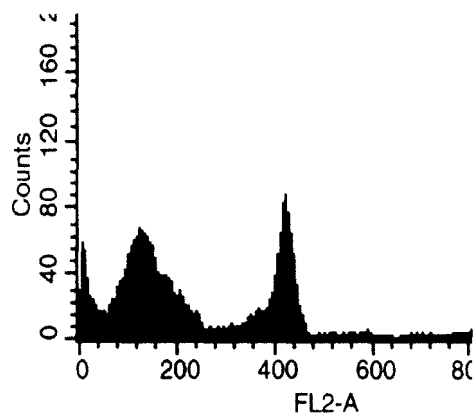


**Fig. 5.3a-c** Representative histograms and respective cytograms of the cell cycle distribution in HL60 cells, measured with flow cytometry. Cells were treated for 1h, were left to recover for 24h, and were then stained in PI. Control (a), camptothecin 2 $\mu$ M (b) and etoposide 5 $\mu$ M (c).

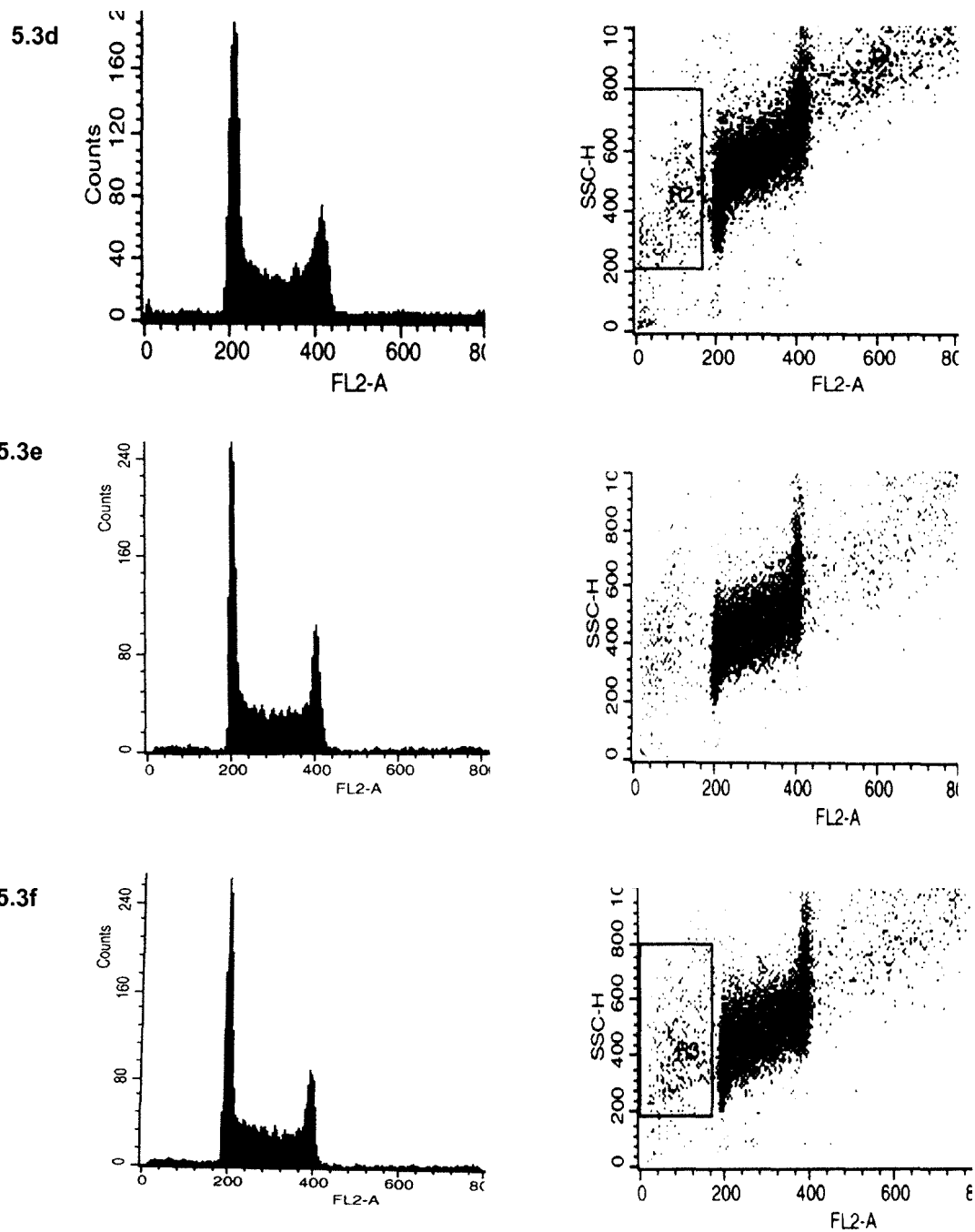


**Fig. 5.3d-f** Representative histograms and respective cytograms of the cell cycle distribution in HL60 cells, measured with flow cytometry. Cells were treated for 1h, were left to recover for 24h, and were then stained in PI. NU:UB 31 30 $\mu$ M (d), NU:UB 31 40 $\mu$ M (e) and NU:UB 31 50 $\mu$ M (f).

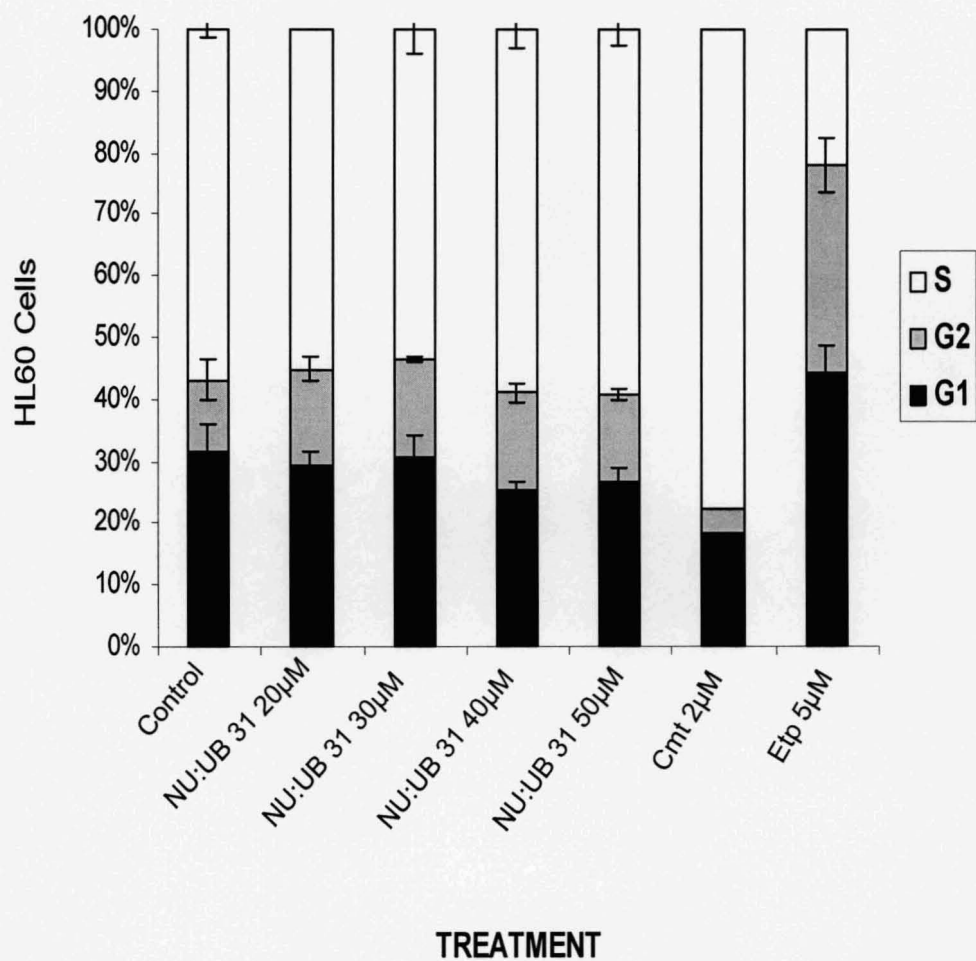


**Fig. 5.3g** Summary histogram of the cell cycle phase distribution in treated and untreated HL60 cells. Cells were treated for 1h, were left to recover for 24h, and were then stained in PI. Mean values of each cell cycle phase  $\pm$  SD were calculated.

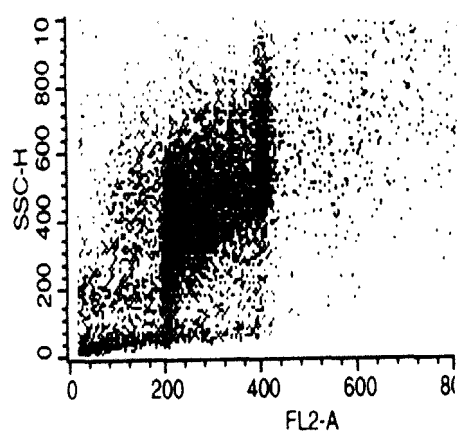
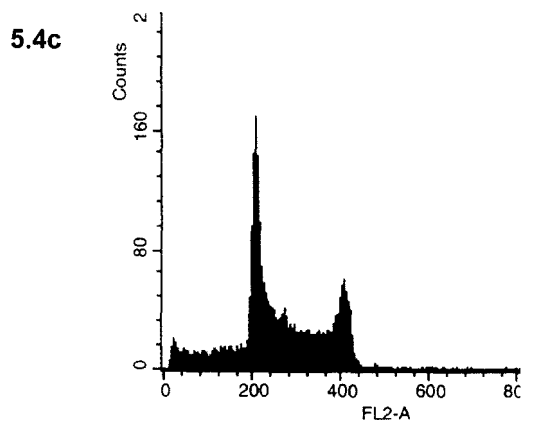
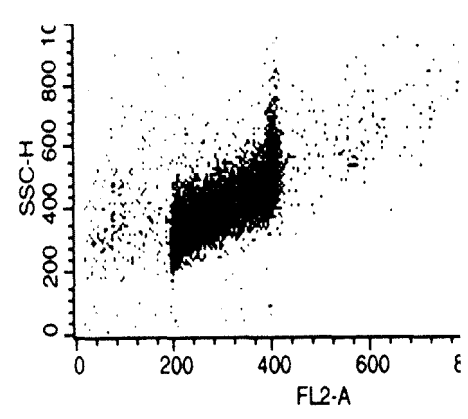
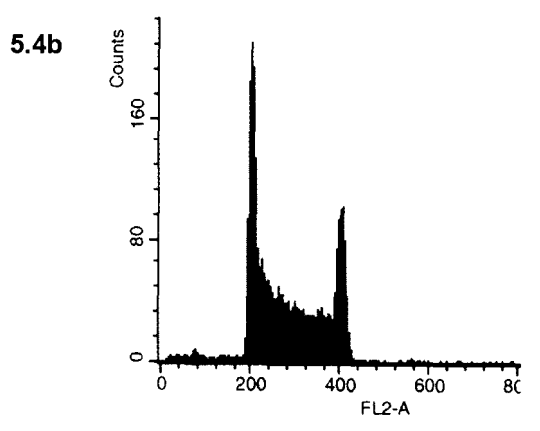
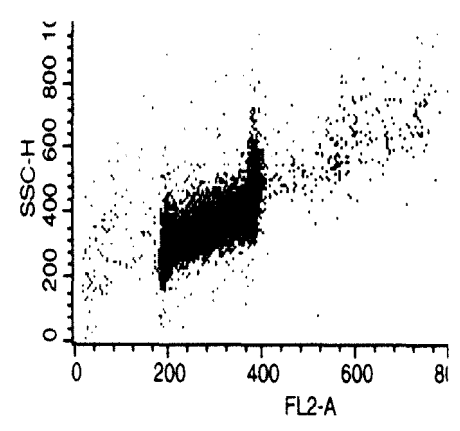
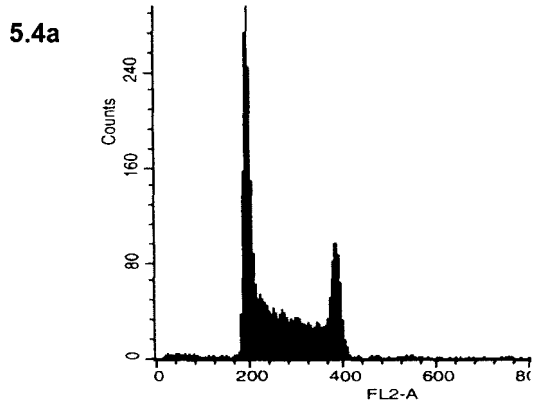


**Fig. 5.4a-c** Representative histograms with respective cytograms of flow cytometry analysis of the cell cycle in HL60 cells. Cells were treated for 4h with no recovery and stained in PI. Control (a), NU:UB 31 30 $\mu$ M (b) and NU:UB 31 50 $\mu$ M (c).

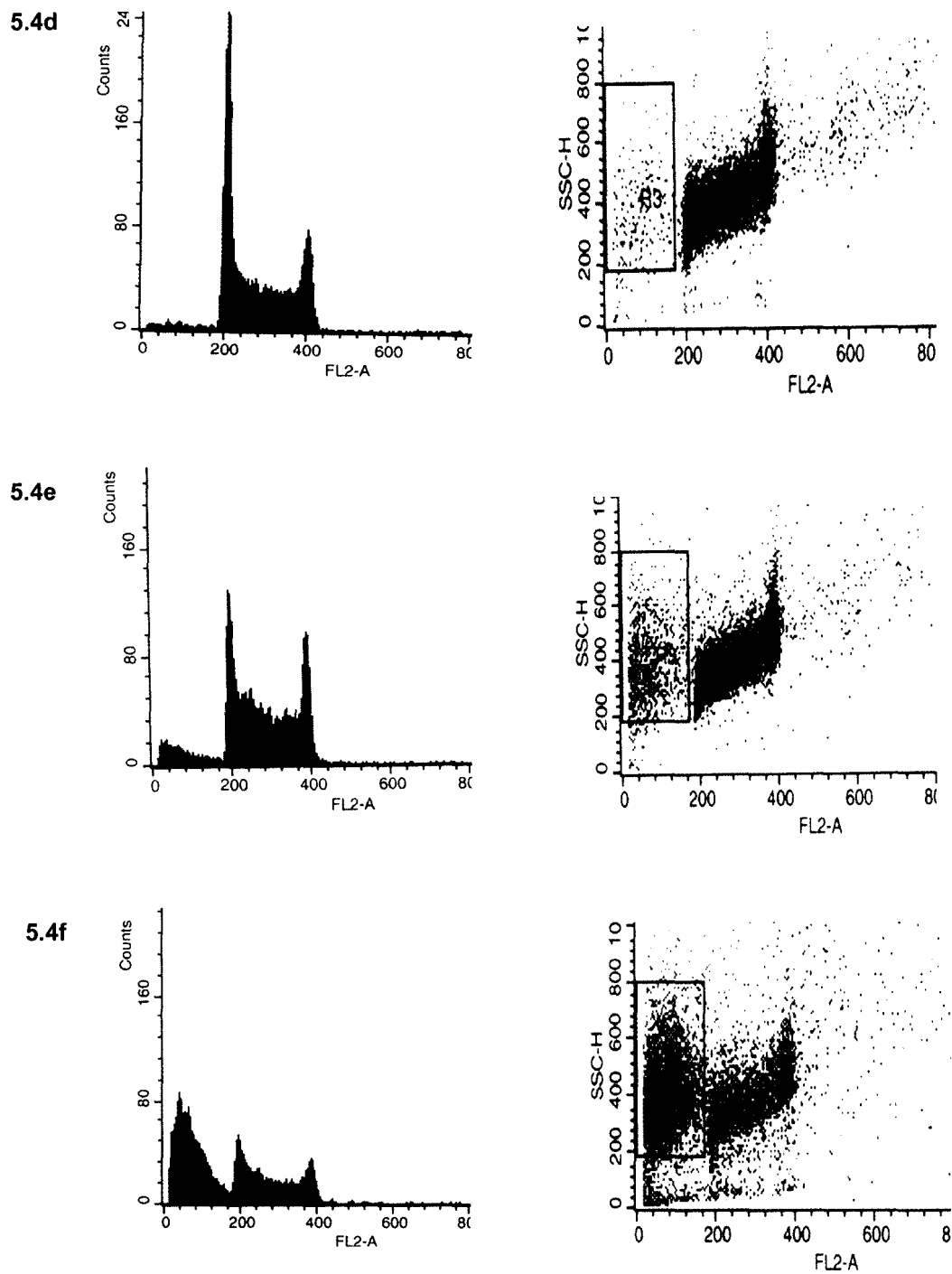


**Fig. 5.4d-f** Representative histograms with respective cytograms of flow cytometry analysis of the cell cycle in HL60 cells. Cells were treated for 4h, left to recover for 4h and were then stained in PI. Control (d), NU:UB 31 30μM (e) and NU:UB 31 50μM (f).

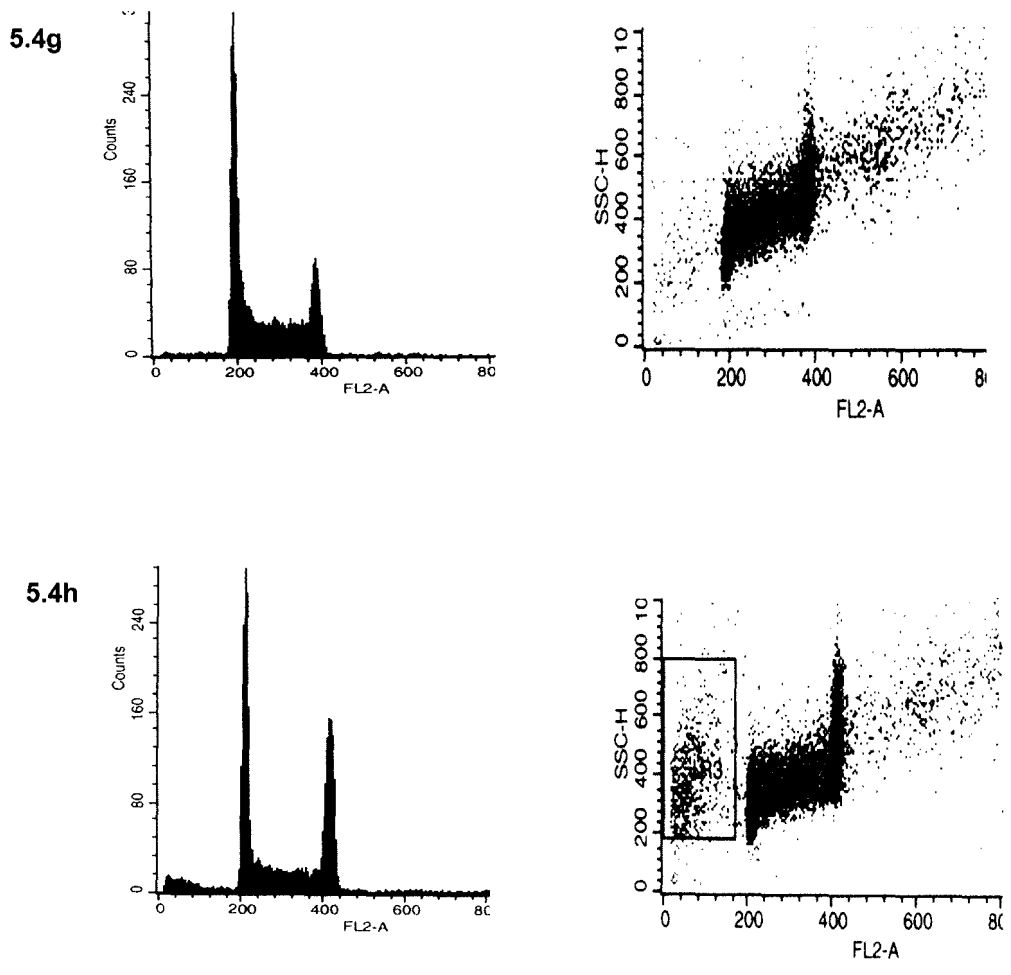


**Fig. 5.4g-h** Representative histograms with respective cytograms of flow cytometry analysis of the cell cycle in HL60 cells. Cells were treated for 4h, left to recover for 24h and were then stained in PI. Control (g), NU:UB 31 30 $\mu$ M (h). Following 24h recovery from 4h NU:UB 31 50 $\mu$ M treatment there were no viable HL60 cells present.

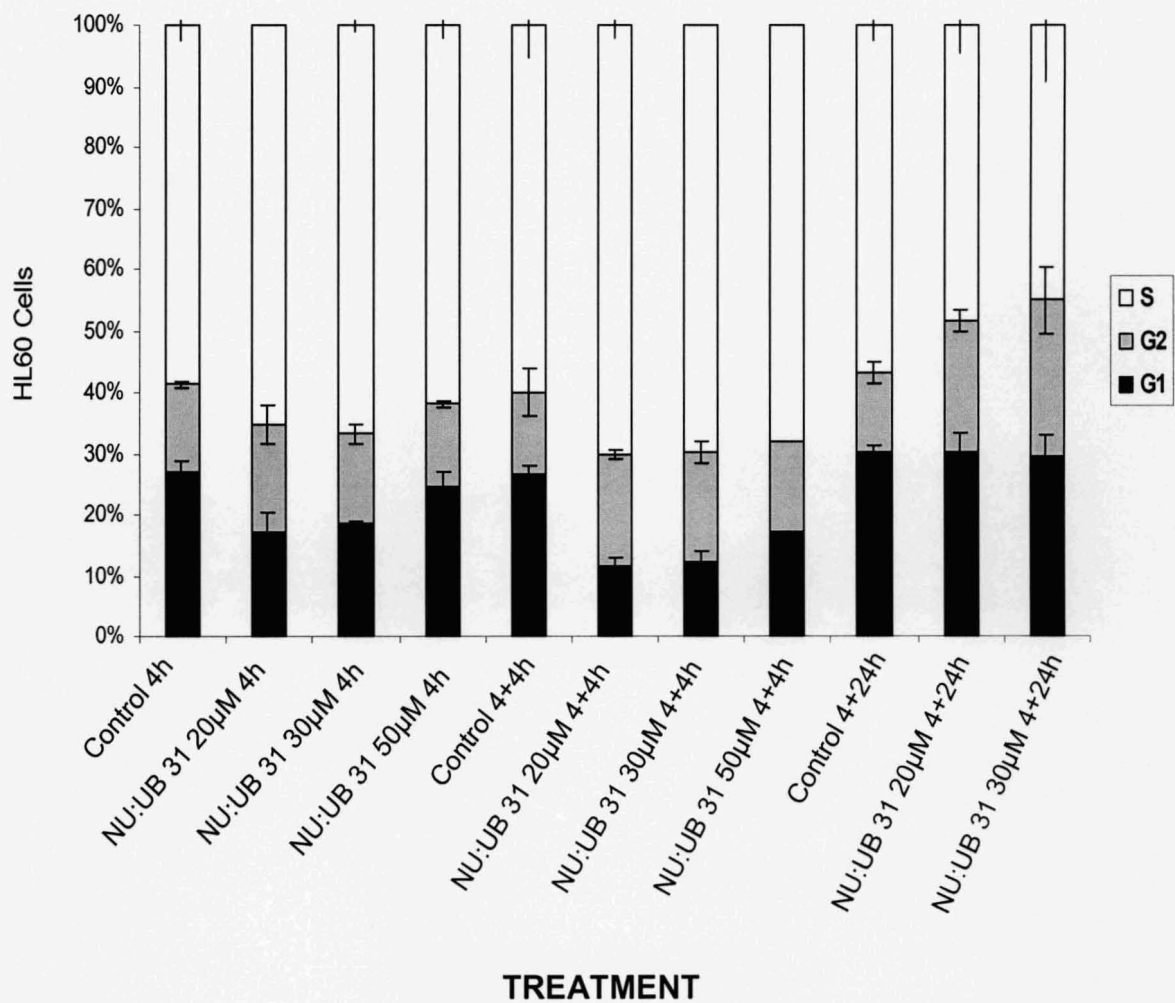


**Fig. 5.4i** Summary of flow cytometry analysis of cell cycle in HL60 cells. Cells were treated for 4h, left to recover for 0, 4 or 24h and stained in PI. Mean values of each cell cycle phase  $\pm$  SD were calculated.

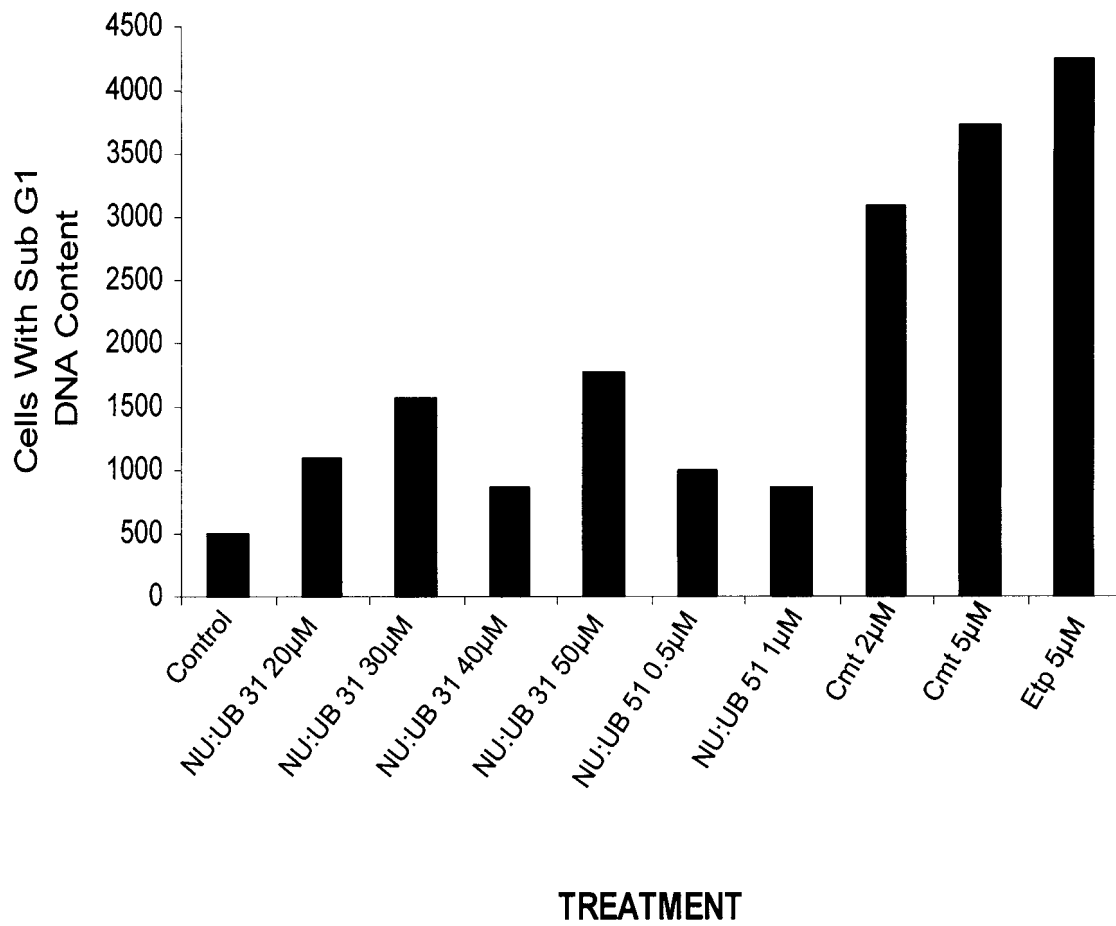


**Fig. 5.5** Summary of flow cytometry analysis of sub G1 material in HL60 cell samples. Cells were treated for 1h, left to recover for 4h and stained in PI. Mean sub G1 values were calculated and plotted.

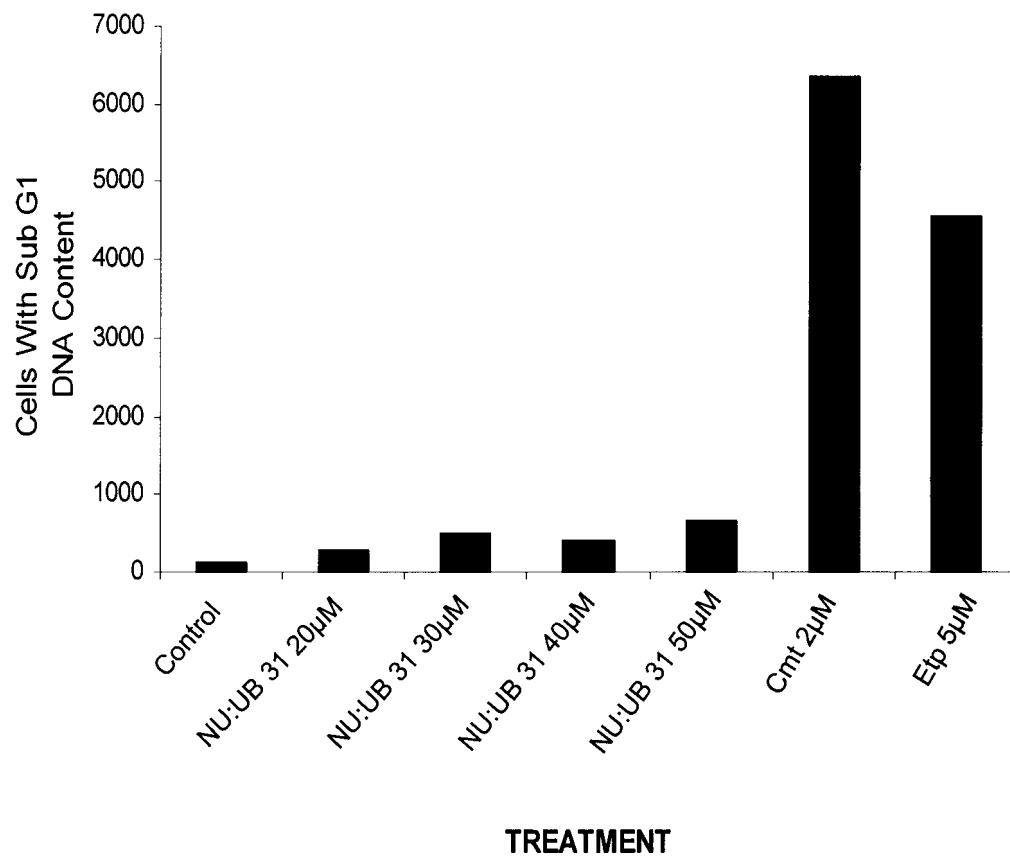


**Fig. 5.6** Summary of flow cytometry analysis of sub G1 material in HL60 cell samples. Cells were treated for 1h, left to recover for 24h and stained in PI. Mean sub G1 values were calculated and plotted.

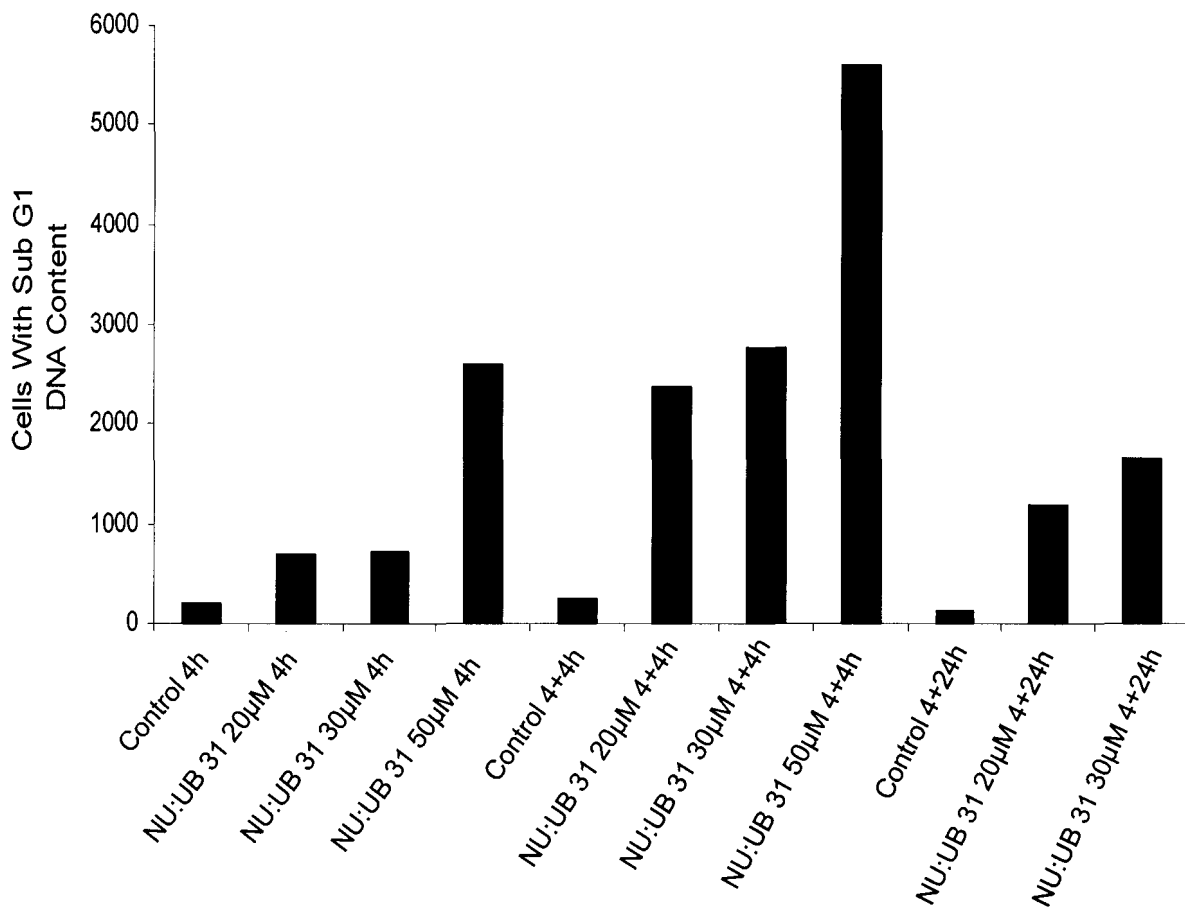


**Fig. 5.7** Summary of flow cytometry analysis of sub G1 material in HL60 cell samples. Cells were treated for 4h, left to recover for 0h, 4h or 24h and stained in PI. Mean sub G1 values were calculated and plotted.

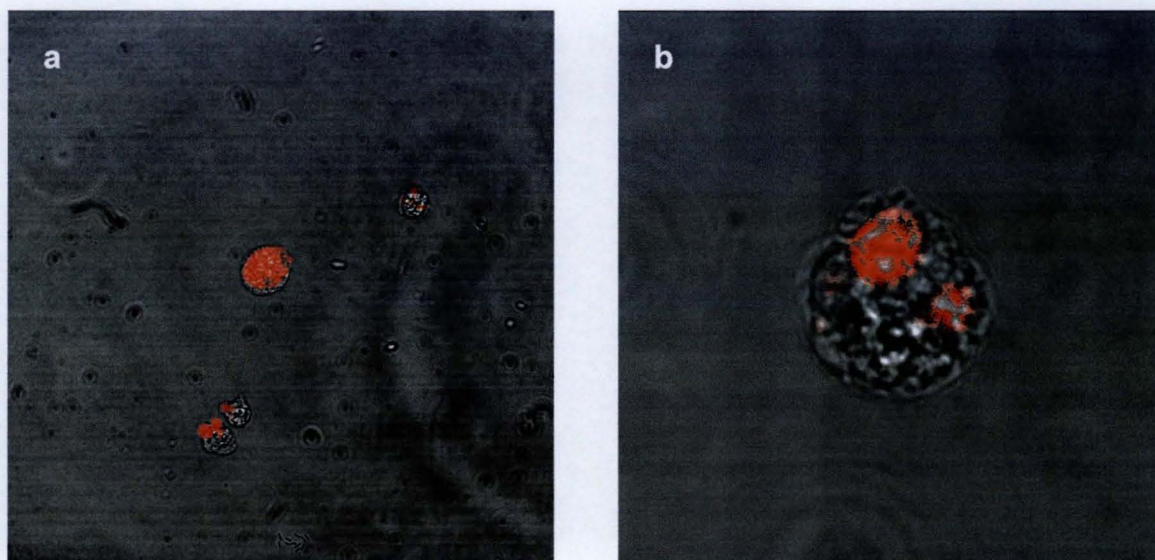


**Fig. 5.8** Representative image of cells from the sub-G1 fraction of HL60 samples treated 1h with 2 $\mu$ M camptothecin and left to recover 24h. White light image merged with fluorescent image to visualise condensed DNA in apoptotic HL60 cells. Cells were viewed at 60x magnification (a) or 60x magnification and zoomed 4 times (b).

## 5.4 DISCUSSION

In order to overcome the resistance problems with current agents, more than one drug is in most cases used to treat a cancer. Drugs used in these combination therapies generally have different cellular targets to avoid development of drug resistant tumour cells. Treatments that synergistically combine both topoisomerase I and topoisomerase II drugs can be used. For example, a study by Kim *et al.* (1992) using human xenografts showed that treatment that increased topoisomerase II levels (in this case pre-treatment with the topoisomerase I drug irinotecan for 24 hours) augmented the activity of topoisomerase II agents. However, combining different types of drugs must be done with care since co-administration of topoisomerase I and II agents may produce antagonism (Kaufman, 1991). In addition, understanding the cell cycle and the possible cell cycle phase specificity of anti-cancer drugs will be helpful in developing clinical protocols. Robles *et al.* (1999) investigated whether anti-cancer drugs were capable of inducing permanent cell cycle arrest in human fibroblasts. This group of researchers used etoposide and camptothecin to induce DNA strand breaks in human fibroblasts. It was found that camptothecin merely transiently arrested the cells, whereas etoposide on the other hand induced a permanent cell cycle arrest in these cells. One reason why a transient versus permanent cell cycle arrest was observed in these cells was suggested to be due to differences in the drug mechanism of inducing DNA breaks. Etoposide directly induces both single strand and double strand DNA breaks. Camptothecin on the other hand first induces

reversible single stranded breaks that have to be converted into irreversible double strand breaks during replication fork movements. The transient arrest following camptothecin treatment observed by Robles and co-workers (1999) could therefore be due to mechanisms repairing the single strand breaks before DNA replication took place.

Chemotherapy drugs may be subdivided into agents that primarily target non-cycling cells or cycling cells, and also according to whether or not they target a particular phase of the cell cycle. Flow cytometry investigations of HL60 cells revealed that different stresses could indeed affect the cells in different phases of the cell cycle. For example, nitrogen mustard primarily affected G<sub>1</sub>-phase cells, S-phase cells were susceptible to camptothecin, whereas G<sub>2</sub>/M phase cells were most sensitive to radiation (Gorczyca *et al.*, 1993). Additionally, etoposide was more potent when added to cells in late S and G<sub>2</sub>/M phases than when added to cells in the G<sub>1</sub> phase (Stacey *et al.*, 2000). Considering that arrest can occur in either the G<sub>1</sub> or the G<sub>2</sub> phase of the cell cycle, and that cells may be inhibited in S-phase, it is feasible to ask, why do some agents mainly arrest cells in G<sub>1</sub> whereas others arrest cells predominantly in G<sub>2</sub> or in S-phase? The S-phase of the cell cycle, during which DNA replication takes place is especially a target of anti-cancer drugs. Studies by Darzynkiewicz *et al.* (1996) have highlighted the cell cycle phase specificity of camptothecin and it is here and elsewhere reported that camptothecin induced cell death in a S-phase specific manner, arresting cells in the S-phase (Gallo *et al.*, 1971; Horowitz and Horowitz, 1973; Malonne and Atassi, 1997). Other studies using human lymphoid cells showed that long-

term camptothecin exposure instead accumulated cells in all compartments of the cell cycle, whereas m-AMSA previously reported to trap topoisomerase II (Liu, 1989) retained cells in the G2 and G0/G1 phases. These findings have been linked to topoisomerase (I and II) activities in relation to the cell cycle. Topoisomerase I being important and expressed at relatively constant levels in all phases of the cell cycle, and topoisomerase II possibly required to enter S-phase and to complete G2 phase. Topoisomerase II $\alpha$  expression levels fluctuate over the course of the cell cycle, its levels increase in S-phase, peak in G2/M phases and then decline as cells approach G1 (Poot *et al.*, 1995).

Most of the cells in an asynchronously growing population will, however, be in the G1 phase in the cell cycle. It may therefore be surprising that the majority of cells are not arrested in G1 accordingly. Although p53 and p21 were up-regulated, cells were not primarily arrested in G1 following doxorubicin treatment. However, in a study by Siu *et al.* (1999) it was found that doxorubicin, in addition to arresting cells in G2, was also capable of inducing G1 arrest in Swiss3T3 cells. The basis of the G1 versus G2 cell cycle arrest following doxorubicin treatment was examined. It was found that the G1 arrest was, in contrast to the G2 arrest, relatively transient, and it was suggested that the cells that initially arrested in G1 might eventually accumulate in the G2 phase over long-term exposure.

Other agents may directly induce apoptosis with little or no cell cycle specificity. NU/ICRF 505 is an example to illustrate this. This compound is an agent, structurally related to the NU:UB series, that in previous studies has

been reported to have a mechanism operating via topoisomerase I (Meikle *et al.*, 1995a; Cummings *et al.*, 1996). In a study by Macpherson *et al.* (1997) the cell cycle effect of NU/ICRF 505 was investigated in Chinese hamster ovary (CHO) cell lines. It was here found that NU/ICRF 505 had little effect on the cell cycle distribution in these cells. Also in these CHO cells, camptothecin treatment was proven not to block cells in G2, and since these cells were capable of arresting in G2 following etoposide treatment, the lack of G2 arrest following NU/ICRF 505 treatment was here considered to be consistent with the cellular response of CHO cells to an anti-topoisomerase I agent.

From the results of cell cycle studies presented within this chapter it seemed that the standard drugs, camptothecin and etoposide induced cell cycle arrests, while camptothecin accumulated the cells in S-phase, etoposide blocked the cells in the G2/M phase. The 1h drug treatments with 4h recovery induced high levels of apoptosis, which were even more evident after 24h recovery. This was in agreement with earlier studies that have reported that death induced by camptothecin is selective to cells in S-phase (Darzynkiewicz *et al.*, 1996), and etoposide arrests cells in G2/M (Sleiman *et al.*, 1998; Stacey *et al.*, 2000). Following NU:UB 31 treatments, there were slight changes in the cell cycle histograms, with decreases in the G1 peak and some cell kill evident, but upon recovery for 24h the cell cycle histograms reverted to normal. Thus, these results suggested that either the cell cycle arrest induced by 1h NU:UB 31 treatment was not sufficient to initiate irreversible changes and cells continued cycling once the drug was removed, or perhaps not all cells were affected by the NU:UB 31 compound. However, in the study of

NU/ICRF 505 in CHO cells mentioned above, the lack of G2 arrest following treatment was considered to be consistent with the cellular response to a topoisomerase I inhibitor (Macpherson *et al.*, 1997). When cells were treated with NU:UB 31 at 20 $\mu$ M or 30 $\mu$ M for 4h more cell kill was seen, but the pattern was similar in that there was no definite cell cycle arrest, the cells that survived the drug impact recovered once drug was removed and the cell cycle profile was looking normal once cells had recovered for 24h. When NU:UB 31 concentration was increased to 50 $\mu$ M, a lot more cells were killed and there was permanent cell damage since after 24h recovery there were no viable cells present in the culture.

Following 1h camptothecin or etoposide treatment the cycle was blocked even when these drugs had been washed off and the cells were left to recover for 4 and 24h. Thus, the DNA damage was permanent and there was a lot of cell kill over time. In contrast, NU:UB 31 seemed to have a more immediate, short term effect. After NU:UB 31 treatment it appeared that once the compound was washed off, NU:UB 31 20 $\mu$ M and 30 $\mu$ M treatments had no long term effect and those cells that did not die fairly quickly would recover. If the concentration was increased to 50 $\mu$ M the damage was made permanent and there was no recovery. Overall, NU:UB 31 did not seem to induce a specific cell phase block in HL60 cells, rather cells might die from all phases of the cycle, and the cells that survived the impact of NU:UB 31 might have been allowed back into cell cycle upon removal of the compound unless the concentration was very high (50 $\mu$ M).

It has been suggested that apoptosis is a premature, abortive mitosis and that apoptosis can be thought of as a cell cycle phenomenon (Meikrantz and Schlegel, 1995). Cell death by mitotic catastrophe is morphologically very similar indeed to apoptosis since one of the most prominent apoptotic morphological feature, chromatin condensation, may also be seen in mitosis (Lazebnik *et al.*, 1993; Rubin *et al.*, 1993). It has further been reported that agents may be capable of inducing both types of cell death, depending on cell type and the cell's position in the cell cycle. This should be taken into consideration when investigating apoptotic cell death. The sub G1 material was here measured for each sample to give an additional indication of the level of apoptosis in drug treated and untreated HL60 cells. There was an increase in sub G1 material compared to control following NU:UB 31 treatments, but after 24h recovery from NU:UB 31 treatment (1h or 4h) the cell cycle appeared normal and there were low levels of sub G1 material in these samples. This might suggest that drug damaged cells that survived the impact of the treatment had recovered and returned back into the cell cycle and thus the drug had no further effect on these cells. A further increased recovery time is, therefore, not likely to kill more cells, but instead allow for continued growth of the cells that survived the impact of the drug. Following 4h 50 $\mu$ M the drug treatment appeared to be high enough to damage all cells in the sample, and thus no recovery was possible with no remaining viable cells following 4h 50 $\mu$ M NU:UB 31 treatment with 24h recovery.

In summary, in contrast to the standard drugs, NU:UB 31 did not appear to cause any specific and permanent arrest of the cell cycle. The cells instead

appeared to die from all phases of the cell cycle following treatment with a high enough dose of NU:UB 31. Following NU:UB 31 and standard anti-topoisomerase inhibitor treatment the cells appeared to become apoptotic, confirmed by flow cytometry investigations of accumulated sub G1 material. The evidence for apoptosis induction by this method was consistent with confocal microscope imaging observations.

## **CHAPTER 6**

### **INVESTIGATION OF APOPTOTIC CELL DEATH**

## 6.1 INVESTIGATION OF APOPTOTIC CELL DEATH

It was established that NU:UB compounds were cytotoxic *in vitro* (data presented in Chapter 4). Furthermore, it was found that there was an increase in the number of cells with a sub G1 DNA content following NU:UB treatment, suggesting that these cells were apoptotic (data presented in Chapter 5). Further in-depth investigations of apoptosis have been presented within this chapter and were obtained by studying the morphological and biochemical changes *in vitro*, in NU:UB treated cells. The focus has been on NU:UB 31, with supporting studies on NU:UB 51 and NU:UB 80; camptothecin and etoposide were also included as positive apoptotic controls.

Viable apoptosis pathways in tumour cells are thought important for chemotherapy to be successful. Many of the morphological and biochemical changes triggered during apoptosis appear to be of a similar nature in different cell types. It is generally believed that apoptotic events at the cellular level include morphological changes such as: reduction in nuclear size, shrinkage of total cell volume, chromatin condensation, increase in cell density, nuclear fragmentation, membrane blebbing and constriction of both the nucleus and the cytoplasm into multiple, small, membrane-bound apoptotic bodies. During the apoptotic response, cellular proteins are thought to be degraded by caspase enzyme activities. Furthermore, DNA is cleaved, degraded by endonucleases, which generates a characteristic ladder on agarose gels (Studzinski 1995; Cohen 1993).

Necrosis is another type of cell death and cell death by necrosis is different from apoptosis in that it is a passive process where the cell swells and ruptures. In necrotic cell death, DNA is also degraded, but not to the same extent as in apoptotic DNA fragmentation. The necrotic DNA products are heterogeneous in size, and therefore do not form discrete bands upon agarose gel electrophoresis. However, although there are differences between these two forms of cell death, there are also similarities that frequently overlap. In addition, these two mentioned types of cell death may not account for all forms of cell death. Conclusive evidence of apoptosis will therefore have to include more than one morphological or biochemical criterion (Studzinski 1995).

It has been demonstrated by Nelson and Kastan (1994) that DNA strand breaks, but not other DNA lesions were capable of inducing p53, and it is thought that p53 serves as a sensor of DNA strand breaks in cells. Although it has been suggested that p53 plays a crucial role in apoptosis as a response to chemotherapeutics, a functional p53-dependent pathway is not the only mechanism for apoptosis to be induced, as p53-independent pathways may play a role. In a study by Shellhaas and Zuckerman (1995), HL60 cells (containing no p53) were used to investigate the capacity of various stimuli in promoting apoptosis. The results of these experiments demonstrated that HL60 offers a well-characterized *in vitro* system for investigating apoptosis in drug treated cells. Earlier studies have also demonstrated that the HL60 cell line showed DNA fragmentation in response to several topoisomerase inhibitors and would thus provide a suitable cell line to use in DNA ladder

assays (Kaufman 1989; Solary *et al.*, 1993). In the apoptotic studies reported within this Chapter, HL60 was the cell line of choice. Studies were performed by treating HL60 cells with camptothecin, etoposide or NU:UB compound for the identification of apoptotic cells. The first aim was to identify apoptotic morphology following NU:UB treatment. In addition to the morphological studies, biochemical changes following NU:UB treatment were also investigated. The second aim in this study was to examine DNA fragmentation as evidence of DNA damage and apoptosis. The third aim was to investigate whether or not NU:UB compounds, in killing cells, activate caspases and for this purpose fluorescein-labelled caspase inhibitors have been used.

## 6.2 METHODS

### 6.2.1 Morphology Studies In HL60 Cells Following Treatment With NU:UB Compounds

HL60 cells were seeded in 24 well plates at  $20 \times 10^4$  cells/ml. Cells were treated with NU:UB compounds, standard drugs or with solvent alone (control) for a selected length of time. Cells in the solvent controls were exposed to the same concentration of solvent as used for the drug treated cells. Following treatment, cells were centrifuged at  $500 \times g$  for 5 mins and were washed twice in PBS. Cytospin (Cytospin3, Shandon) preparations were made up in triplicate with  $1 \times 10^5$  cells per slide. Following cytospin centrifugation at 1000 rpm, 5 mins cells were fixed for 5 mins in methanol and stained using the Diff Quick rapid staining set. The slides were soaked in acid dye for 10-20 secs, and subsequently soaked in basic dye for 10-20 secs. Following staining, the residues were washed off in Sørensen's buffered water. The cells were dehydrated, mounted in DPX and viewed in a light microscope (Axioskop, Zeiss) at 40x magnification.

### 6.2.1a Treatment Of Results

For each treatment, >1000 cells were counted on three different slide preparations. Cells with apoptotic appearance were identified, counted and expressed as a percentage of the total number of counted cells.

### 6.2.2 Additional Experiments

HL60 cells were stained with Hoechst 33342 stain (1/100 dilution of a 100µg/ml stock) to visualise the nuclear morphology. Hoechst 33342 is a cell permeable adenine-thymidine specific fluorescent dye that is widely used to stain DNA for evaluating apoptosis. The HL60 cells were treated as above and were then stained in Hoechst stain for 5 mins. Cells were put onto glass slides and were viewed in a UV fluorescent microscope (Leica DMRB) fitted with a JVC colour video camera (KY-F55B) using AcQuis Bio software to obtain images.

### 6.2.3 DNA Laddering Studies Following Treatment With

#### NU:UB Compounds

The detection of DNA fragments in cells is one of the methods available to identify cells undergoing apoptosis. For this study the ApoTarget Quick Apoptotic DNA ladder detection kit (BioSource) was used. DNA and DNA fragments were extracted from cells and the level of DNA fragmentation visualised by ethidium bromide gel electrophoresis. The time points and

standard drug concentrations chosen were based on the instructions in the DNA ladder kit and the IC<sub>50</sub> values obtained for the NU:UB compounds.

HL60 or Jurkat cells,  $150 \times 10^4$  cells per sample were treated with NU:UB compounds, standard drugs or solvent (control). Cells were transferred to universals and centrifuged at 500g for 5 mins at 4°C. Cell pellets were washed in PBS, transferred to Eppendorf tubes and pelleted by another centrifugation step at 500 x g for 5 mins at 4°C. Supernatants were discarded and the cells resuspended in 20µl TE lysis buffer by careful pipetting. Enzyme A, 5µl was added to each sample and the tubes were gently vortexed and incubated in a 37°C waterbath for 10 mins. Enzyme B, 5µl was added and samples were incubated until the cell lysates were clear (approximately 30 mins). Ammonium acetate, 5µl and ice-cold absolute ethanol, (100µl) was added to each lysate. The samples were vortexed and left in a freezer to precipitate for 15 mins or longer. The samples were centrifuged at 14 000 x g for 10 mins at 4°C to collect the precipitated DNA. The supernatants were discarded and the DNA was washed in 70% ice-cold ethanol and centrifuged at 14 000 x g for 10 mins at 4°C. The ethanol was discarded and the DNA pellets were left to air dry at room temperature. DNA suspension buffer, 30µl was added to each sample to dissolve the DNA. A horizontal mini gel electrophoresis apparatus (HE 33 Hoefer) was used and the samples were loaded onto an agarose gel (1%) containing ethidium bromide (0.5µg/ml) in both gel (1g agarose was boiled in 100ml 1x TBE, and when cooled 5µl ethidium bromide (1mg/ml) was added), and running buffer [250ml 1x TBE with 12.5µl ethidium bromide (1mg/ml)]. The electrophoresis was run at 50V

(5V/cm) for 1.5-2h and the gel was visualized in a UV light and photographed with the SynGene Imager using the GeneSnap and GeneTool software.

#### **6.2.4 Caspase Activation Studies Following Treatment With NU:UB Compounds**

To study general caspase activation, the CaspaTag Fluorescein caspase (VAD) kit (Intergen) was used. Caspase-3 activation was investigated with the CaspaTag caspase-3 (DEVD) activity kit (Intergen). These kits detect active caspases in living cells through the use of a carboxyfluorescein labelled caspase inhibitor, where inhibitor irreversibly binds to active caspases. FAM-VAD-FMK is a derivative of benzyloxycarbonylvalylalanyl aspartic acid fluoromethyl ketone (zVAD-FMK), which is a potent general inhibitor of caspase activity. FAM-DEVD-FMK is a derivative of benzyloxycarbonylaspartylglutamylvalylaspartic acid fluoromethyl ketone (zDEVD-FMK), which is a potent inhibitor of caspase-3. Cells that contained bound inhibitor were analysed with a flow cytometer (FACSCalibur, Becton Dickinson Immunocytometry Systems) equipped with a 15mW argon ion air-cooled laser with excitation wavelength 488nm and with UV fluorescent microscope (Leica DMRB).

Cells were diluted to  $5 \times 10^4$  cells/ml with culture medium and left to recover overnight. The manual provided by Intergen recommended HL60 cells to be treated with 4µg/ml (11.5µM) camptothecin for 4 hours as a positive control for apoptosis. Treatments were carried out at 37°C, 5% CO<sub>2</sub>, for 4 and 24h.

Prior to use, caspase inhibitor solution, 150x was diluted 1:5 in PBS and used as soon as possible. The wash buffer was placed in a 37°C incubator for 30 mins to dissolve precipitated protein and buffer salts. The buffer was then diluted 1:10 in dH<sub>2</sub>O and ready for use. Following drug treatment, cells were pelleted at 400 x g for 5 mins, counted and resuspended at 10<sup>6</sup> cells/ml. Aliquots of 300µl from each treatments were transferred into Eppendorf tubes. FAM-VAD-FMK, 10µl was added to each tube and the samples were then left to incubate in dark for 1h at 37°C under 5% CO<sub>2</sub>. Wash buffer was added to the samples and cells were pelleted by centrifugation at 400x g for 5 mins. After a second wash step, cells were pelleted and finally resuspended in 400µl wash buffer and kept on ice until analysed. If cells could not be analysed immediately, they were fixed by adding 40µl fixative solution to the 400µl cell suspension. Fixed cells could last up to 24h in the dark before analysis. Fluorescein emission intensity was measured on the FL1 channel and log FL1 (X-axis) versus number of cells (Y-axis) was generated into a histogram. On the histogram two cell populations represented by two peaks appeared for caspase positive cell populations. The majority of the caspase negative cells appeared within the first log decade whereas caspase positive cells appeared in a separate peak or as a shoulder of the first peak with increased fluorescence intensity.

For cells that were to be analysed with fluorescence microscopy, the same procedure was followed but after the 1h FAM-VAD-FMK staining, cells were also stained in Hoechst Stain (provided with the kit), adding 1.5µl and incubating for another 5 mins. The same washing procedure was followed but

cells were resuspended in 100µl instead of 400µl to get a higher cell density. One drop of cell suspension was put onto a microscope slide and covered with a coverslip. Cells were observed under UV fluorescence microscope (Leica DMRB) and images were obtained with a fitted JVC colour video camera (KY-F55B).

Caspase-3 activation was investigated with the CaspaTag caspase-3 (DEVD) activity kit, and the protocol for this assay was identical to the above CaspaTag caspase (VAD) activity kit protocol.

#### 6.2.4a Treatment Of Results

Caspase-positive cells appeared in the second log phase on the FL-1, x-axis of the cell histogram, and were expressed as a percentage of the total number of cells analysed. Experiments were performed in duplicate or triplicate, resulting in a mean value of caspase positive cells for every treatment.

## 6.3 RESULTS

### 6.3.1 Morphology Studies In HL60 Cells Following Treatment With NU:UB Compounds, Camptothecin Or Etoposide

For morphology studies, HL60 cells were exposed to solvent (control), NU:UB compounds, camptothecin or etoposide for 8h and 24h. Cells were fixed onto glass slides, stained and viewed in a light microscope at 40x magnification. The standard drugs, camptothecin and etoposide induced high levels of apoptosis in HL60 cells following 8h exposure (Fig. 6.1b; Fig 6.1c; Fig. 6.1j; Fig. 6.2a). The morphology data indicated that HL60 cells also showed apoptotic morphology following NU:UB 31 [Fig. 6.1d (10 $\mu$ M, 8h); Fig. 6.1e (20 $\mu$ M, 8h); Fig. 6.1k (20 $\mu$ M, 24h); Fig. 6.2b] and NU:UB 51 [Fig. 6.1g (5 $\mu$ M, 8h); Fig. 6.1h (10 $\mu$ M, 8h); Fig. 6.1l (1 $\mu$ M, 24h); Fig. 6.1m (5 $\mu$ M, 24h)] treatments. Using Diff Quick staining, apoptotic morphology following NU:UB treatment was evident at the 8h time point, but not to the levels induced by the standard drugs, camptothecin and etoposide. There was in addition to apoptotic morphology also a lot of cells that seemed to have a necrotic (or secondary necrotic) appearance present at the high NU:UB 31, 30 $\mu$ M concentration (Fig.6.1f).

### **6.3.2 Hoechst Staining Of HL60 Cells**

HL60 cells were stained in Hoechst Stain 33342 to visualise nuclei following 4h and 24h treatment with solvent (control), camptothecin or NU:UB compounds (Fig. 6.3). When viewed in a UV fluorescence microscope the nucleus in normal control cells appeared rounded. Treated Hoechst stained HL60 cells seemed to have apoptotic nuclear morphology with apoptotic bodies and intensely stained, condensed and thus smaller nuclei compared to control cells. HL60 cells were exposed to the following treatments: camptothecin [Fig. 6.3b (10 $\mu$ M, 4h); Fig. 6.3f (0.5 $\mu$ M, 24h)], NU:UB 31 [Fig. 6.3c (20 $\mu$ M, 4h); Fig. 6.3g (10 $\mu$ M, 24h)] and NU:UB 51 [Fig. 6.3d (10 $\mu$ M, 4h); Fig. 6.3h (5 $\mu$ M, 24h)], and the highest levels of apoptotic cells were observed following camptothecin treatment.

### **6.3.3 DNA Laddering Studies Following Treatment With NU:UB Compounds Or Camptothecin**

To obtain a positive DNA ladder control, the standard topoisomerase inhibitors camptothecin, and etoposide, both inducers of apoptosis, were investigated in jurkat cells as this cell line was used in the kit protocol. On the basis of these results, camptothecin was chosen as a positive control as this drug clearly induced DNA fragmentation, resulting in a typical apoptotic DNA ladder (Fig. 6.4a). Etoposide did not show as clear laddering as camptothecin, but DNA was damaged followed etoposide treatment (Fig. 6.4b). Although etoposide induced apoptosis (observed morphologically), no DNA ladders

were seen here and longer exposure time, and/or other etoposide concentrations might be required. However, studies do suggest that DNA laddering may not be essential for apoptosis, that apoptosis can take place without the typical DNA fragmentation (Cohen *et al.*, 1992; Ucker *et al.*, 1992; Falcieri *et al.*, 1993; Pandey *et al.*, 1994; Sleiman, 1998).

For this study, HL60 rather than Jurkat cells were used since we had previously found morphological evidence of apoptosis following NU:UB treatment in this cell line. Furthermore, the HL60 cell line is routinely used for investigating apoptosis. HL60 cells were treated with camptothecin to find out whether or not this cell line was suitable for the DNA ladder assay. Following 6h and 24h there was, as expected, no DNA laddering and fragmentation in the solvent control. Treatment with camptothecin revealed substantial DNA fragmentation at the 6h time point, presented as a DNA ladder. Following 24h exposure to camptothecin, DNA appeared as a smear on the gel possibly indicating a 24h exposure time at a 10 $\mu$ M concentration was too long in this cell line. The 6h time point was also sufficient for NU:UB 31 (20 $\mu$ M) to induce DNA damage. At the longer, 24h exposure time, NU:UB 31 at 10 $\mu$ M or 20 $\mu$ M did not result in more laddering (Fig. 6.5). Following NU:UB 51 and NU:UB 80, at 5 $\mu$ M and 15 $\mu$ M respectively there was also DNA laddering, but for the lower concentrations (1 $\mu$ M and 5 $\mu$ M respectively) of these compounds, there was no apparent DNA laddering present (Fig. 6.6).

### **6.3.4 Caspase Activation Studies Following Treatment With NU:UB Compounds Or Camptothecin Using Flow Cytometry**

General caspase activation and caspase-3 activation were studied in HL60 and HCT116 cells by flow cytometry. Two exposure times were chosen (4 and 24h), 4h was the exposure time suggested in the caspase assay protocol using HL60 cells treated with camptothecin. HL60 cells (Fig. 6.7; Fig. 6.8a; Fig. 6.8b) and HCT116 cells (Fig. 6.9a; Fig. 6.9b) were treated with compounds for 4h and 24h, and were then stained with the general caspase inhibitor. These experiments suggested that there was caspase activation following 4h NU:UB 31 at 20 $\mu$ M and NU:UB 51 at 10 $\mu$ M treatment, but not so much at the lower concentrations of these agents. Camptothecin 10 $\mu$ M treatment for 4h only resulted in a slight increase in caspase activation compared to the control (Fig. 6.8a), but following 24h of 0.05 $\mu$ M camptothecin there was a higher increase in caspase activation (Fig. 6.8b). Camptothecin and NU:UB 31 were also assayed in HCT116 cells. At the 4h time point there was no increase in caspase activation following 10 $\mu$ M camptothecin treatment, but at the 24h time point caspase activation was evident. NU:UB 31 at 40 $\mu$ M resulted in caspase activation after 4h, and at the 24h time point 25 $\mu$ M NU:UB 31 showed significant ( $p < 0.05$ ) caspase activation compared to control (Fig. 6.9a; Fig. 6.9b). Thus, NU:UB 31 and NU:UB 51 appeared to activate caspases in HL60 cells as early as 4h. Caspase activation was slightly increased by 4h and was further increased following 24h of camptothecin treatment. In HCT116 cells NU:UB 31 induced caspases at the 4h time point. There was however no caspase activation at 4h following

camptothecin treatment, but following 24h camptothecin treatment, caspase activation was observed.

In addition to investigating general caspase activation, the effector caspase, caspase-3 was studied specifically. The results from this study have been graphed in Fig. 6.10 and show caspase-3 activation following 4h and 24h treatment with camptothecin, NU:UB 31 and NU:UB 51. Following 4h camptothecin treatment there was no increase compared to control. NU:UB 31 at 20 $\mu$ M, on the other hand, showed a slight increase in caspase-3 activation and NU:UB 51 at 15 $\mu$ M showed a significant increase ( $p < 0.01$ ) compared to the control following 4h treatment (Fig. 6.10a). After 24h treatment, 0.5 $\mu$ M camptothecin induced a caspase-3 response, and there was also increased caspase-3 activation compared to control following 24h NU:UB 31 or NU:UB 51 compound treatment (Fig. 6.10b). Thus NU:UB 31 and NU:UB 51 induced caspase-3 in HL60 cells at the 4h time point. There was, however, no caspase-3 activation following 4h camptothecin treatment, but after 24h the response was greatly increased.

### **6.3.5 Caspase Activation Studies Following Treatment With NU:UB Compounds Or Camptothecin Using UV Fluorescence Microscopy**

To confirm caspase and caspase-3 staining observed in the above flow cytometry studies, HL60 cells were also viewed under UV fluorescence microscope. The cells were double stained in Hoechst stain (blue) and the

general caspase, and caspase-3 inhibitors resulted in green fluorescence. Figs. 6.11-6.18 show HL60 cells treated with solvent (control), camptothecin, NU:UB 31 or NU:UB 51. These cells have been stained with Hoechst stain to visualise the nucleus (a), and with the general caspase inhibitor binding to active caspases within the apoptotic cells (b). This series of images revealed that there was caspase activation in cells following camptothecin, NU:UB 31 and NU:UB 51 treatments, many of the cells had condensed nuclei, and apoptotic bodies were also revealed with the blue Hoechst stain.

Caspase-3 stained HL60 cells were captured in Figs. 6.19–6.27. Cells were treated with solvent (control), camptothecin, NU:UB 31 or NU:UB 51. Following staining with Hoechst stain (a), and with caspase-3 inhibitor (b), the cells were viewed under UV fluorescent microscope.

In for example Fig. 6.13b, Fig. 6.17b and Fig. 6.21b the cells were treated with NU:UB 31, which has a bright red intrinsic fluorescence. The bright red colour from NU:UB 31 and from NU:UB 51 was found to strongly interfere with propidium iodide (PI), and thus PI could unfortunately not be used as a measure to separate out the necrotic population from the apoptotic cells in the flow cytometer experiments and this is why we resorted to one colour staining in the flow cytometer studies.

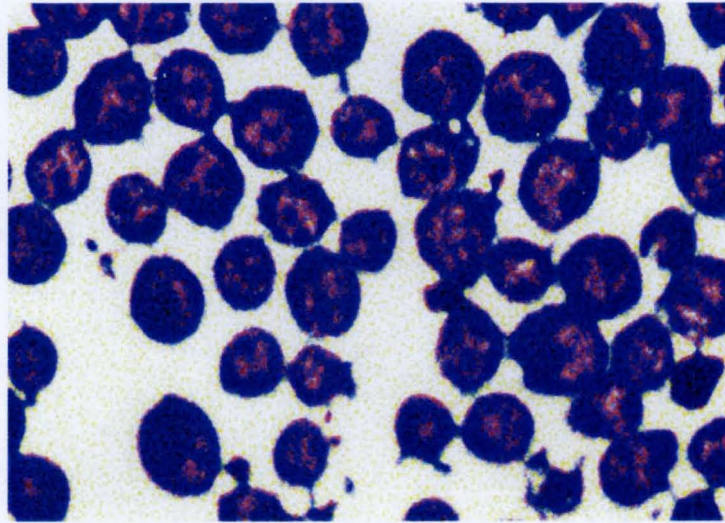


**Fig. 6.1a** Control 8h

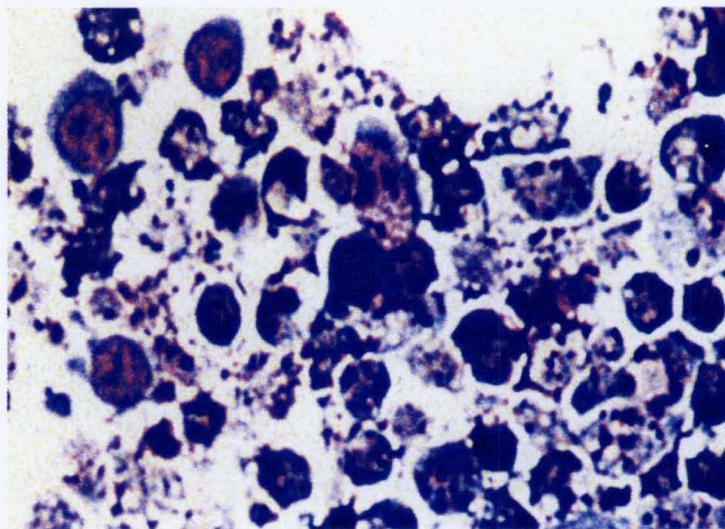


**Fig. 6.1b** Camptothecin 5 $\mu$ M 8h

**Fig. 6.1a-b** HL60 cells treated with solvent (control) or camptothecin (5 $\mu$ M) for 8h. Following treatment, the cells have been visualized by Diff-Quick staining and viewed under light microscope at 40x magnification.

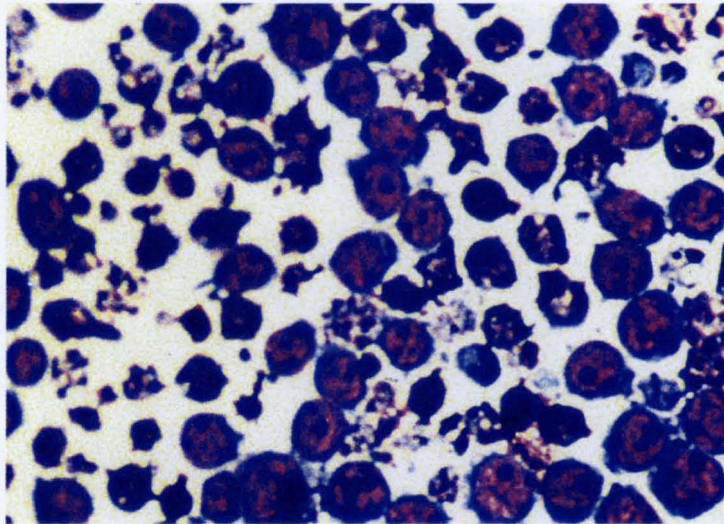


**Fig. 6.1c** Etoposide 5µM 8h

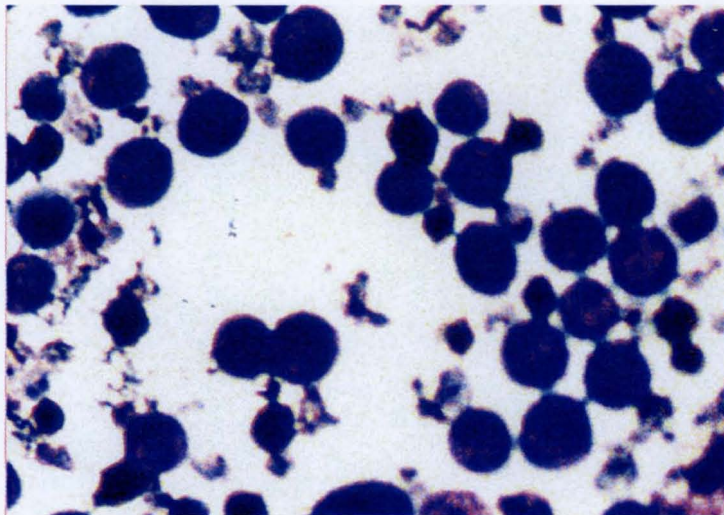


**Fig. 6.1d** NU:UB 31 5µM 8h

**Fig. 6.1c-d** HL60 cells treated with etoposide (5µM) or NU:UB 31 (5µM) for 8h. Following treatment, the cells were visualized by Diff Quick staining and viewed under light microscope at 40x magnification.

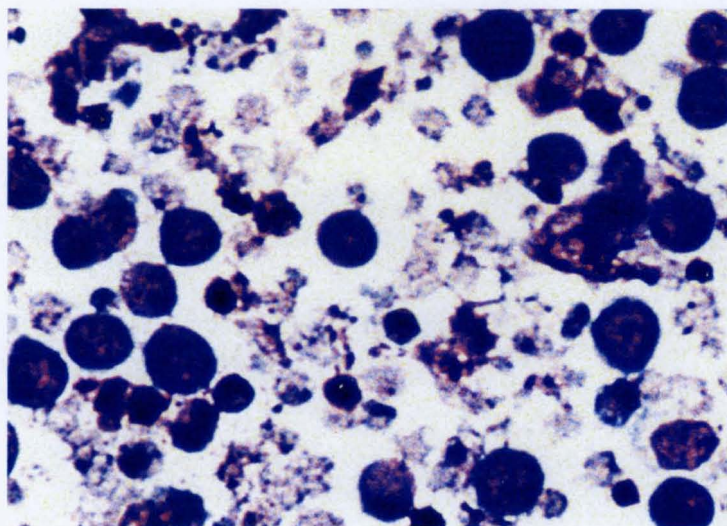


**Fig. 6.1e** NU:UB 31 20 $\mu$ M 8h

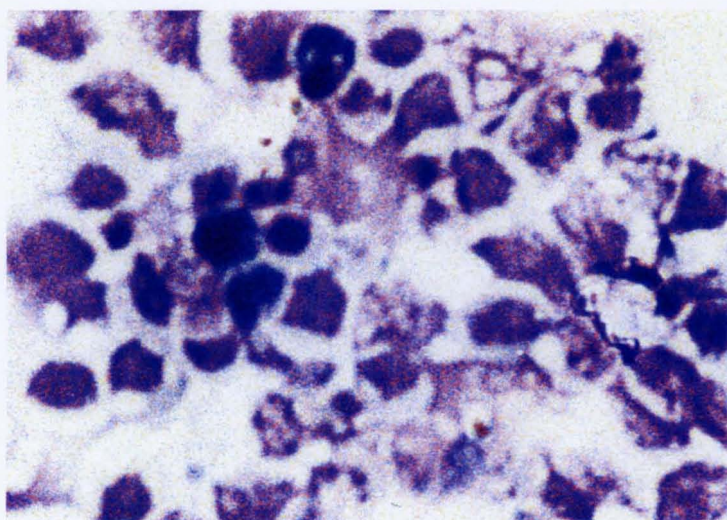


**Fig. 6.1f** NU:UB 31 30 $\mu$ M 8h

**Fig. 6.1e-f** HL60 cells treated with NU:UB 31 (30 $\mu$ M or 20 $\mu$ M) for 8h. HL60 cells have been visualized by Diff Quick staining and viewed under light microscope at 40x magnification.

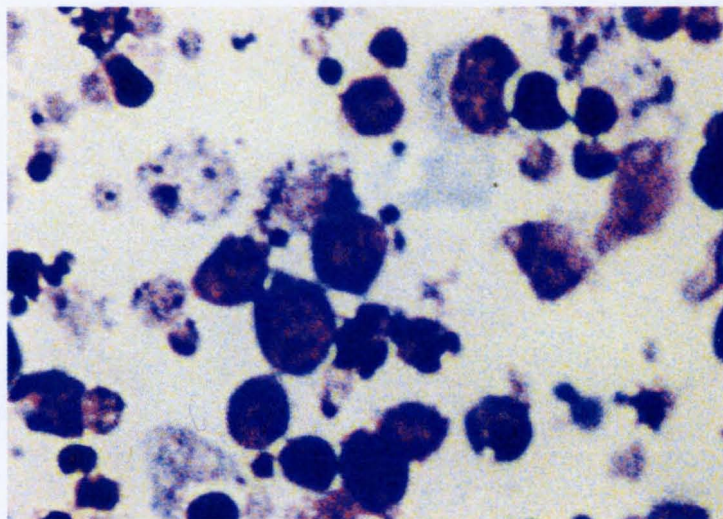


**Fig. 6.1g** NU:UB 51 5 $\mu$ M 8h

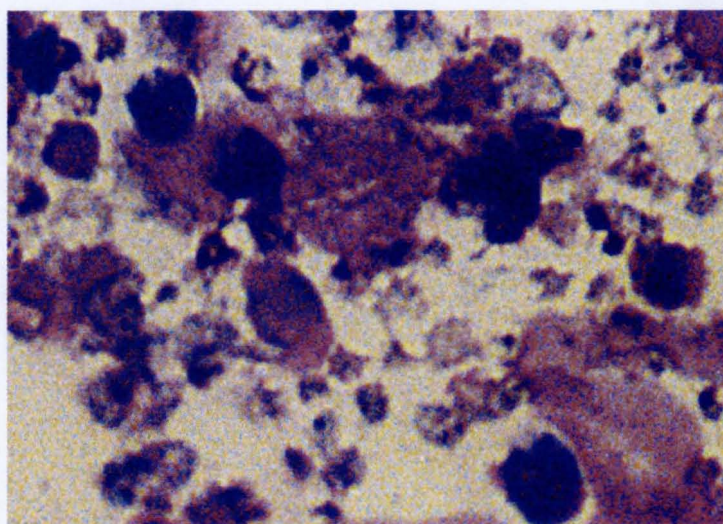


**Fig. 6.1h** NU:UB 51 10 $\mu$ M 8h

**Fig. 6.1g-h** HL60 cells treated with NU:UB 51 (10 $\mu$ M or 5 $\mu$ M) for 8h. Following treatment, the cells were visualized by Diff Quick staining and viewed under light microscope at 40x magnification.

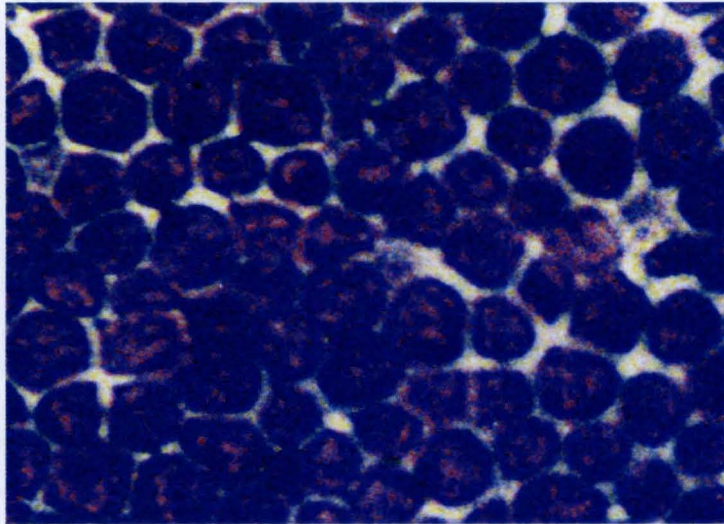


**Fig. 6.1i** Control 24h

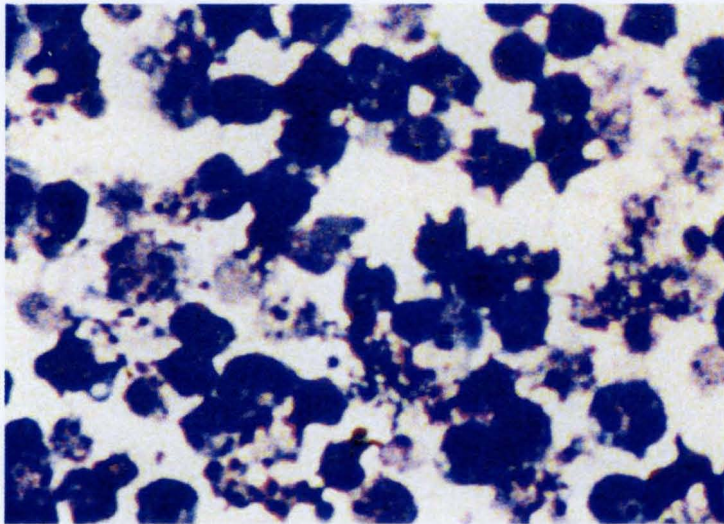


**Fig. 6.1j** Camptothecin 0.5µM 24h

**Fig. 6.1i-j** HL60 cells treated with solvent (control) or camptothecin (0.5µM) for 24h. Following treatment, HL60 cells were visualized by Diff Quick staining and viewed under light microscope at 40x magnification.

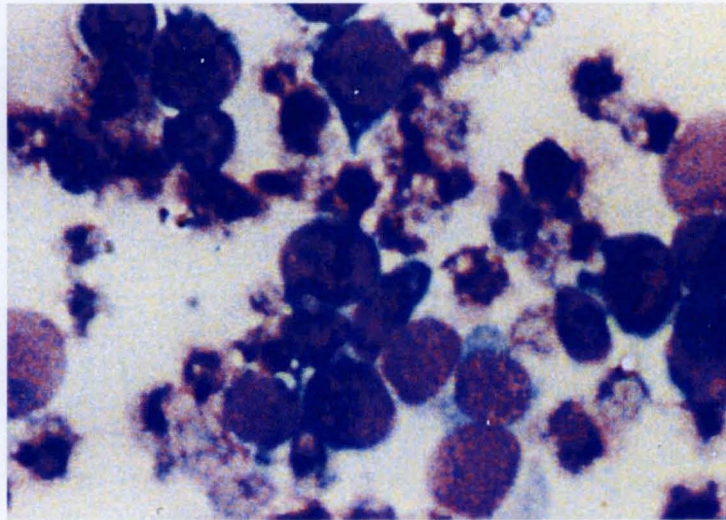


**Fig. 6.1k** NU:UB 31 20 $\mu$ M 24h

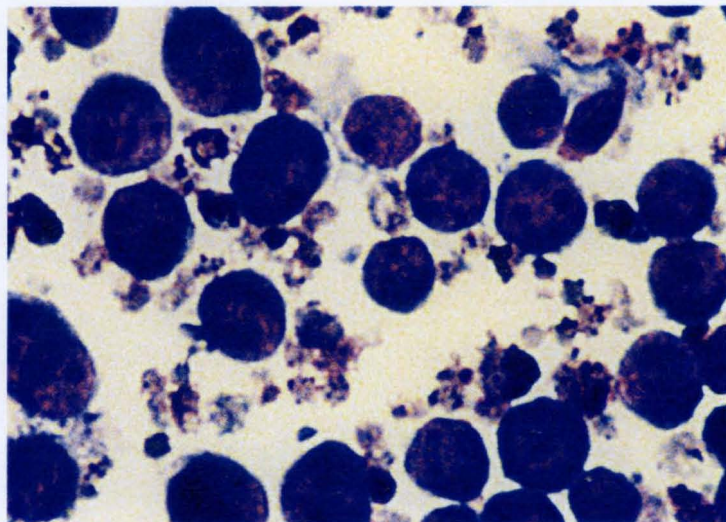


**Fig. 6.1l** NU:UB 51 1 $\mu$ M 24h

**Fig. 6.1k-l** HL60 cells treated with NU:UB 31 (20 $\mu$ M) or NU:UB 51 (1 $\mu$ M) for 24h. Following treatment, the cells were visualized by Diff Quick staining and viewed under light microscope at 40x magnification.

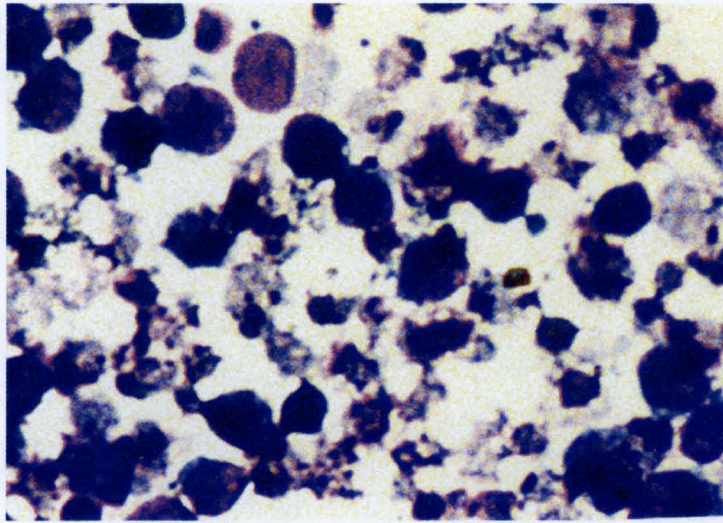


**Fig. 6.1m** NU:UB 51 5µM 24h

**Fig. 6.1m** HL60 cells treated with NU:UB 51 (5µM) for 24h. HL60 cells have been visualized by Diff Quick staining and viewed under light microscope at 40x magnification.

Fig. 6.2 (a)

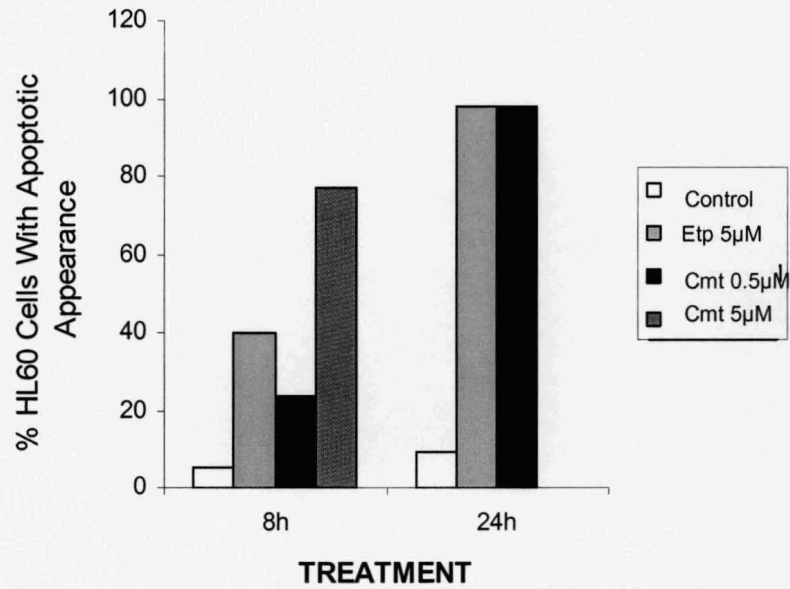


Fig. 6.2 (b)

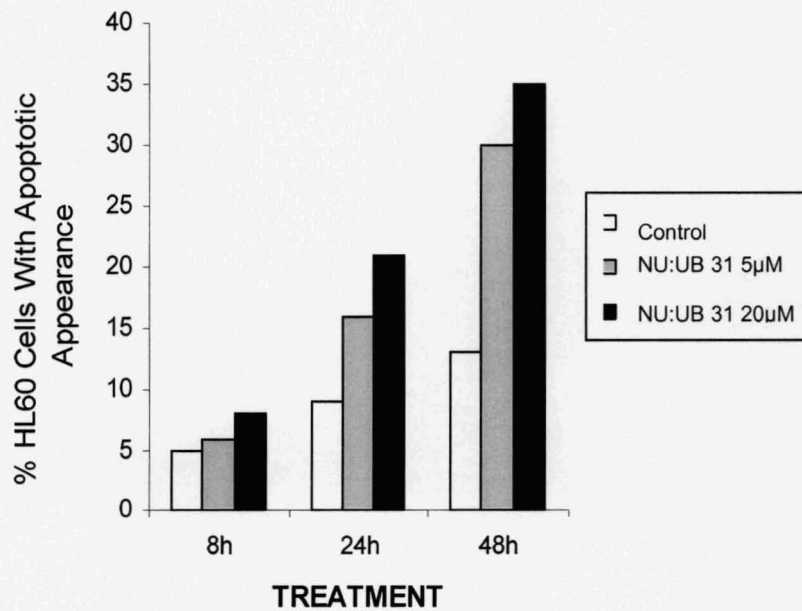
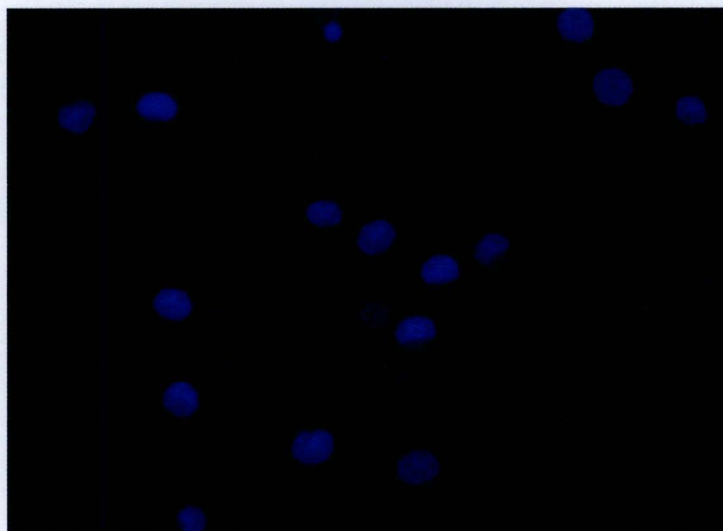
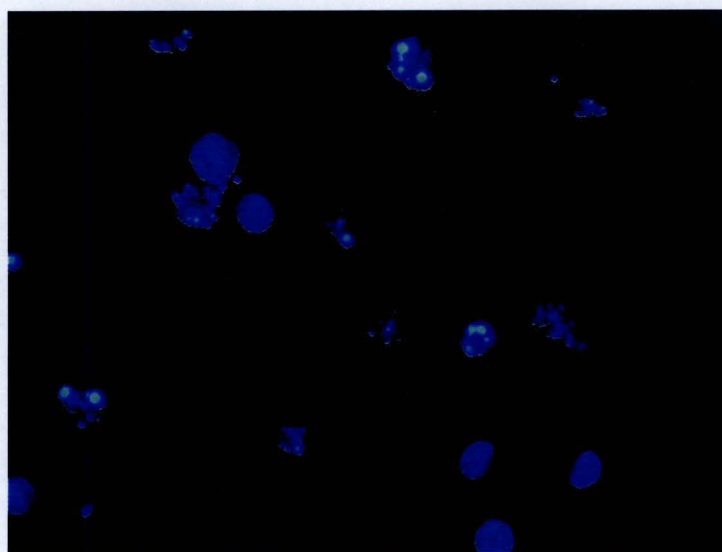


Fig. 6.2 HL60 cells exposed to camptothecin (cmt, 0.5µM or 5µM) or etoposide (etp, 5µM) for 8 and 24h (a). HL60 cells exposed to NU:UB 31 (5µM, 20µM or 30µM) for 8, 24 and 48h (b). Cells were counted and a percentage of cells with apoptotic morphology established for each treatment. Results are the mean percentages of cells counted (>1000) from three slide preparations of one experiment.



**Fig. 6.3a** HL60 control 4h



**Fig. 6.3b** Camptothecin 10 $\mu$ M 4h

**Fig. 6.3a-b** HL60 cells treated with solvent (control) or camptothecin (10 $\mu$ M) for 4h. Following treatment, HL60 cells were stained in Hoechst stain to visualise their nucleus and were then viewed under UV fluorescent microscope at 60x magnification.

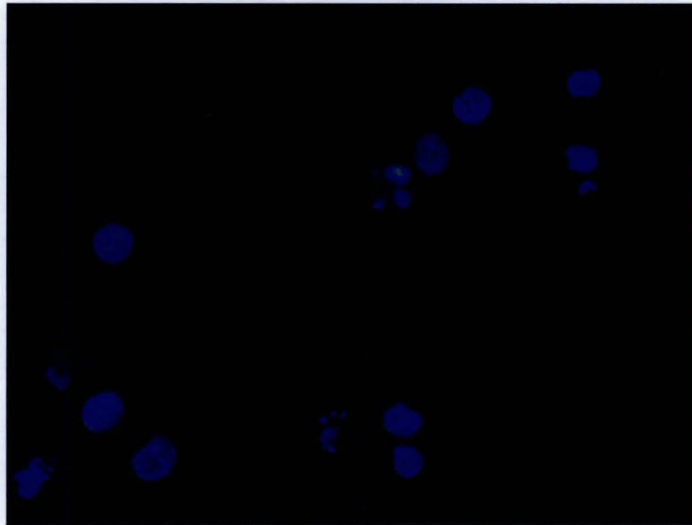


**Fig. 6.3c** NU:UB 31 20µM 4h

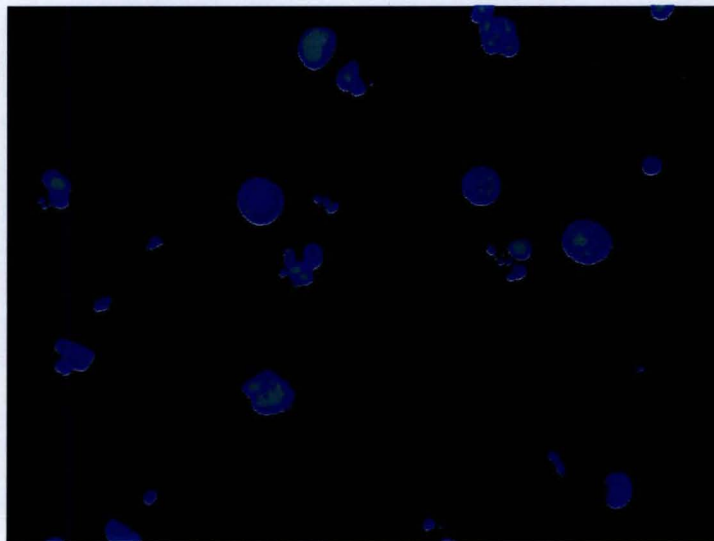


**Fig. 6.3d** NU:UB 51 10µM 4h

**Fig. 6.3c-d** HL60 cells treated with NU:UB 31 (20µM) or NU:UB 51 (10µM) for 4h. Following treatment, HL60 cells were stained in Hoechst stain to visualise their nucleus and were then viewed under UV fluorescent microscope at 60x magnification.

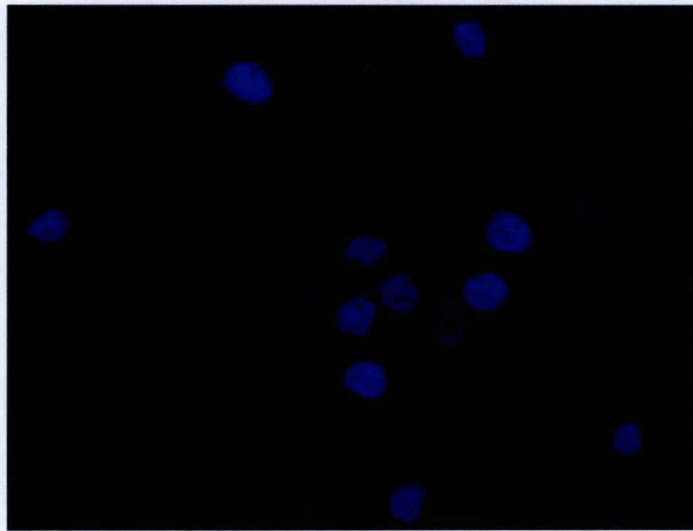


**Fig. 6.3e** Control 24h

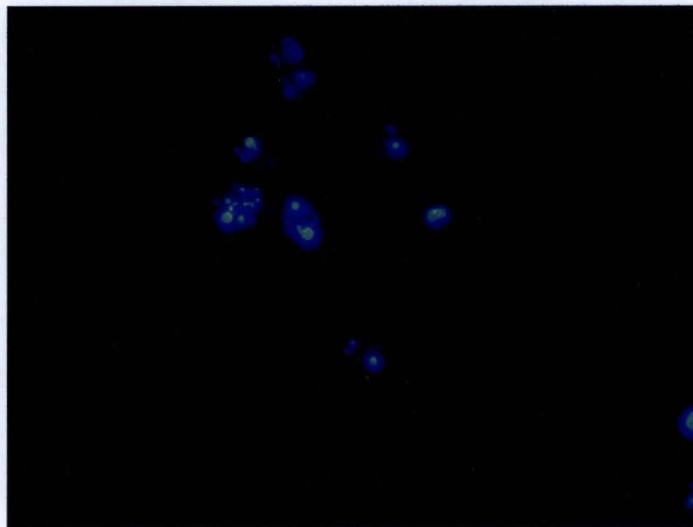


**Fig. 6.3f** Camptothecin 0.5μM 24h

**Fig. 6.3e-f** HL60 cells treated with solvent (control) or camptothecin (0.5μM) for 24h. Following treatment, HL60 cells were stained in Hoechst stain to visualise their nucleus and were then viewed under UV fluorescent microscope at 60x magnification.

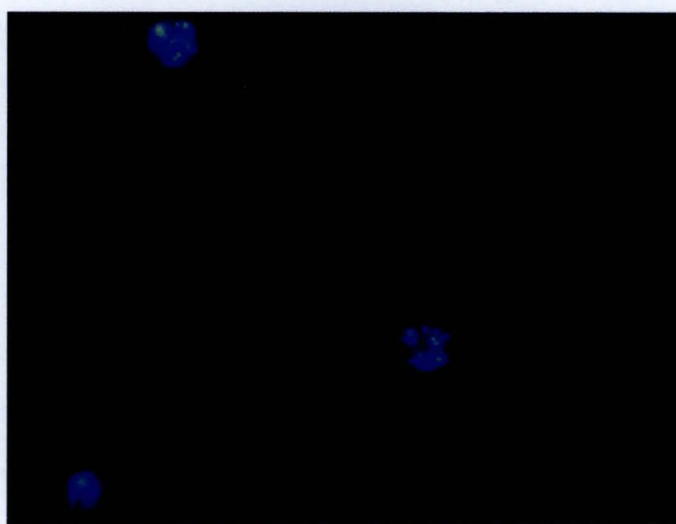


**Fig. 6.3g** NU:UB 31 10 $\mu$ M 24h

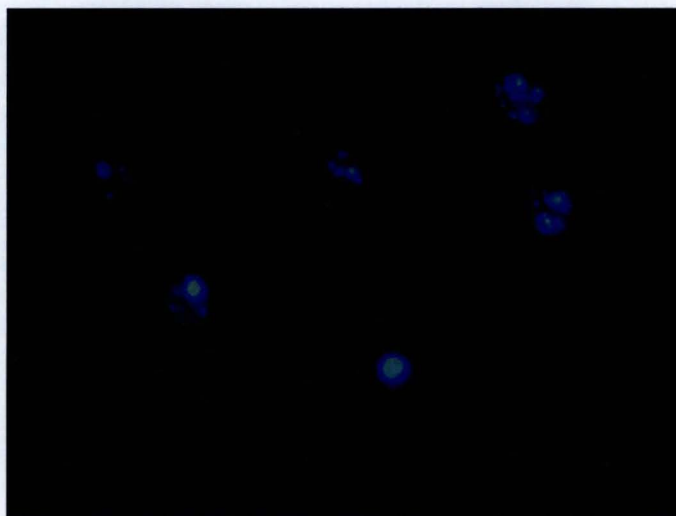


**Fig. 6.3h** NU:UB 51 5 $\mu$ M 24h

**Fig. 6.3g-h** HL60 cells treated with NU:UB 31 (10 $\mu$ M) or NU:UB 51 (5 $\mu$ M) for 24h. Following treatment, HL60 cells were stained in Hoechst stain to visualise their nucleus and were then viewed under UV fluorescent microscope.

**Fig 6.4 (a)**

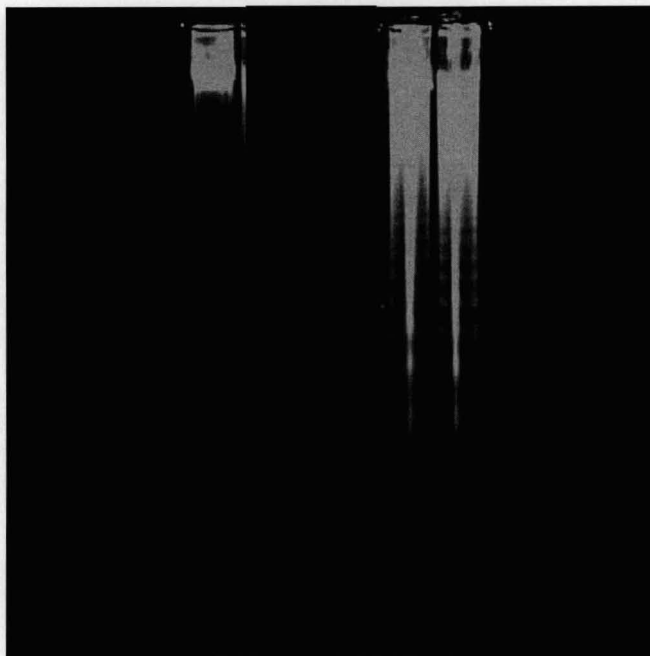


**Fig 6.4 (b)**



**Fig. 6.4** Jurkat cells 6h exposure. Solvent control (lane 1), camptothecin 3µM (lane 2), camptothecin 10µM (lane 3) (a). Jurkat cells 6h exposure. Solvent control (lane 1), camptothecin 10µM (lane 2), etoposide 5µM (lane 3) (b).

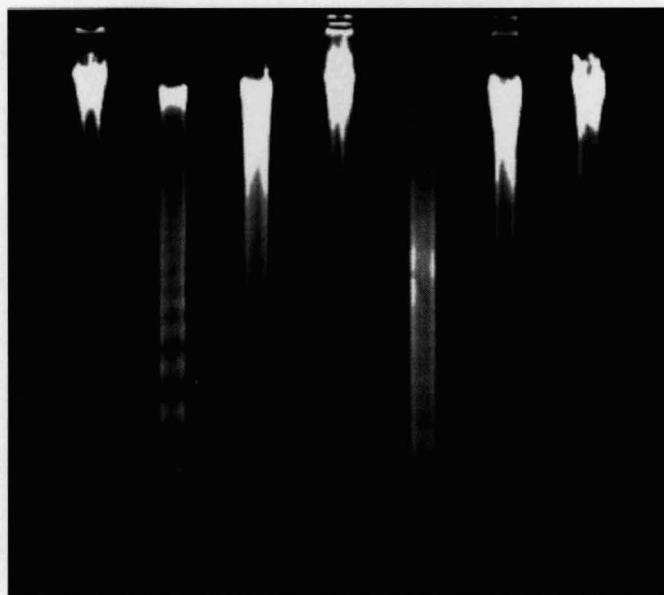


**Fig. 6.5** HL60 cells 6h and 24h exposure. Control 6h (lane 1), camptothecin 10 $\mu$ M 6h (lane 2), NU:UB 31 20 $\mu$ M 6h (lane 3), control 24h (lane 4), camptothecin 10 $\mu$ M 24h (lane 5), NU:UB 31 10 $\mu$ M 24h (lane 6), NU:UB 31 20 $\mu$ M 24h (lane 7).



**Fig. 6.6** HL60 cells 6h exposure. Control (lane 1), camptothecin 10 $\mu$ M (lane 2), NU:UB 31 20 $\mu$ M (lane 3), NU:UB 51 1 $\mu$ M (lane 4), NU:UB 51 5 $\mu$ M (lane 5), NU:UB 80 5 $\mu$ M (lane 6), NU:UB 80 15 $\mu$ M.

**Fig. 6.7a**

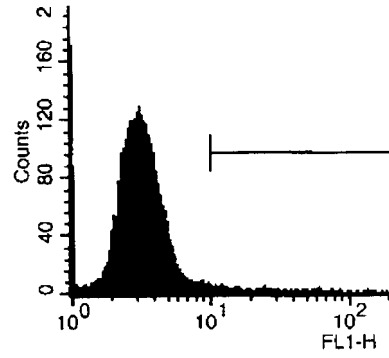
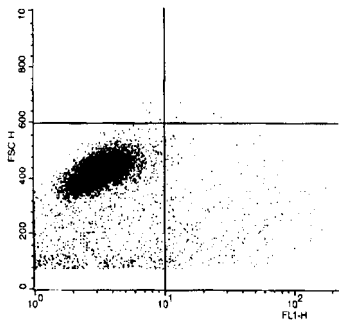


**Fig. 6.7b**

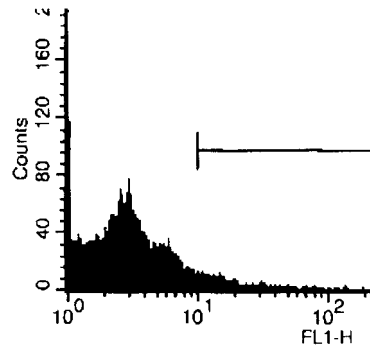
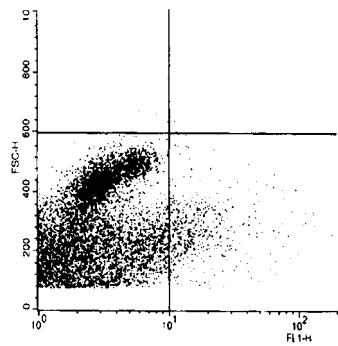


**Fig. 6.7c**

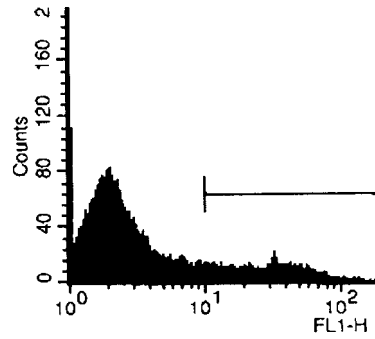
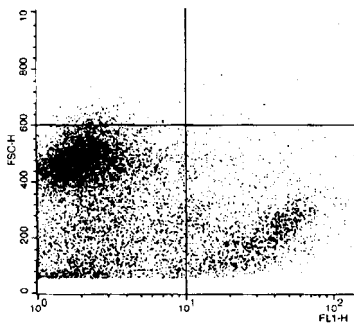


**Fig. 6.7a-c** Flow cytometer cytograms and corresponding histograms of caspase activation in HL60 cells. 4h Control (a), camptothecin 10 $\mu$ M (b) and NU:UB 31 20 $\mu$ M (c).

**Fig. 6.7d**

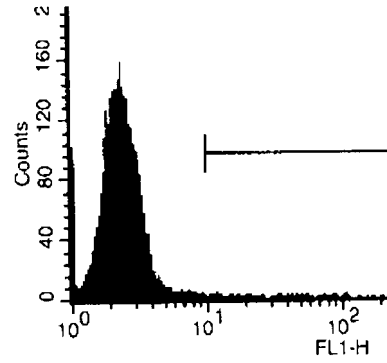
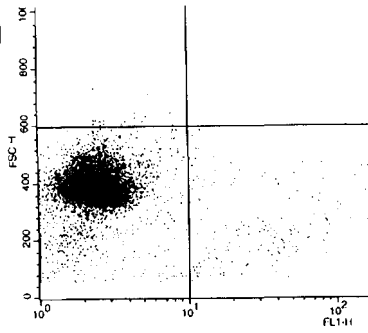


**Fig. 6.7e**

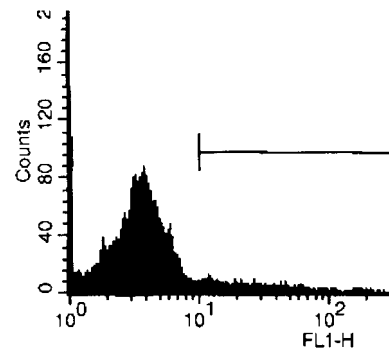
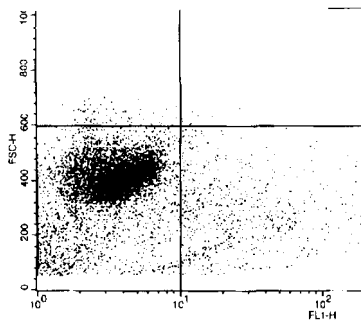


**Fig. 6.7f**

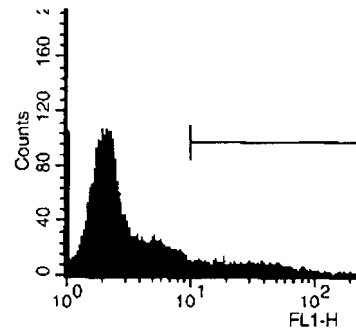
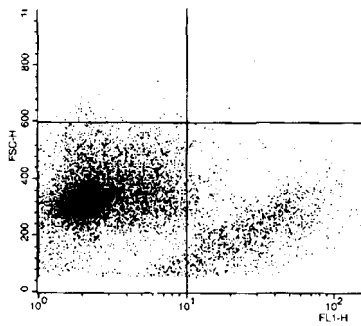


**Fig. 6.7d-f** Flow cytometer cytograms and corresponding histograms of caspase activation in HL60 cells. 24h Control (d), camptothecin 0.05 $\mu$ M (e) or NU:UB 31 10 $\mu$ M (f).

Fig. 6.8 (a)

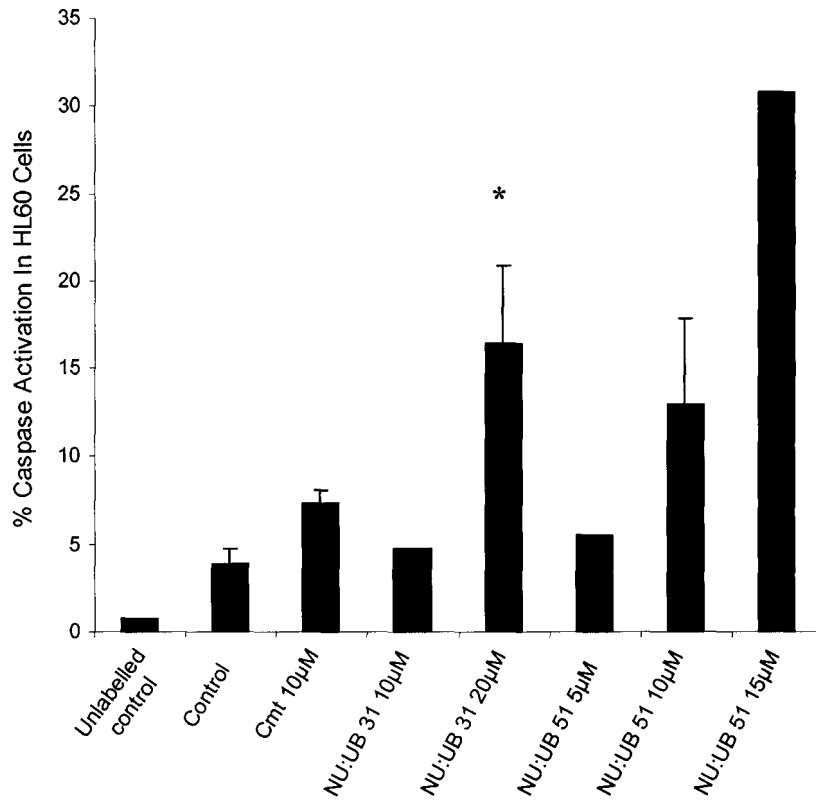


Fig. 6.8 (b)

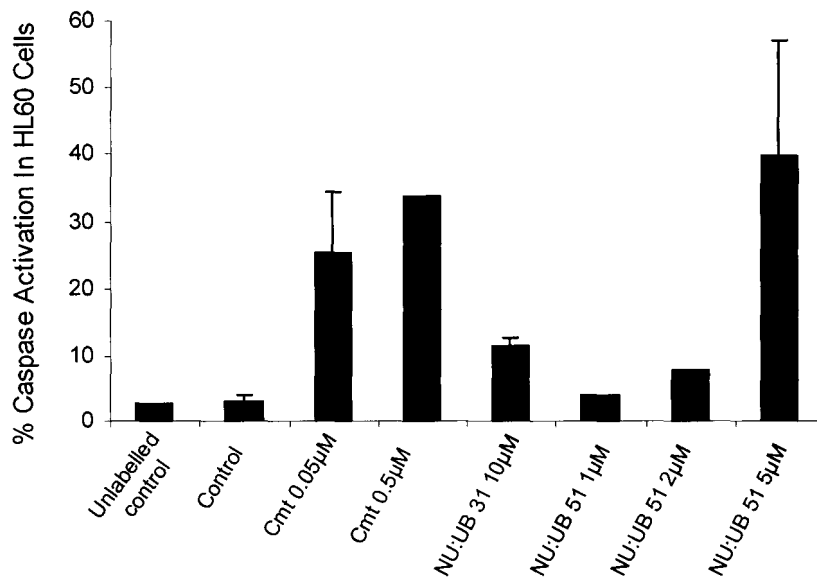
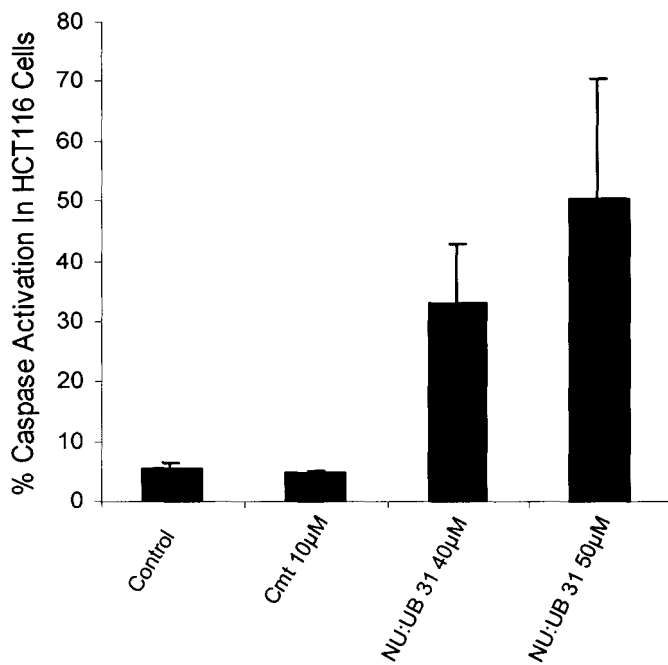
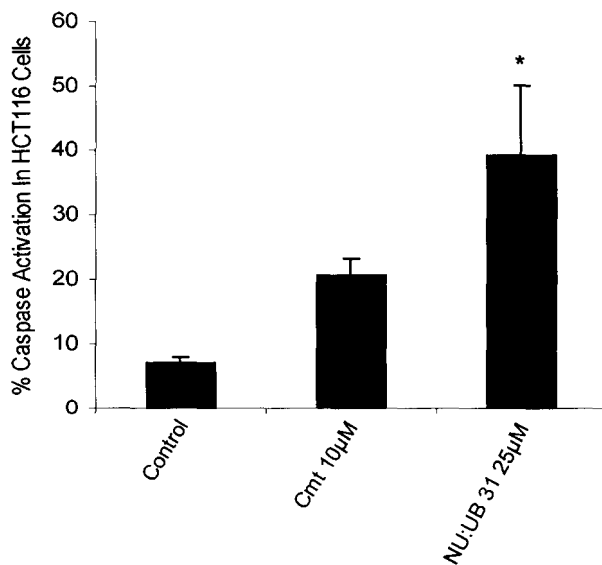


Fig. 6.8a-b General caspase activation expressed as a percentage in HL60 cells. Cells exposed 4h (a) or 24h (b) to solvent (control), camptothecin (cmt), NU:UB 31 or NU:UB 51.

**Fig. 6.9 (a)**



**Fig. 6.9 (b)**



**Fig. 6.9a-b** General caspase activation in HCT116 cells, expressed as a percentage of the total number of cells. Cells exposed 4h (a) and 24h (b) to solvent (control), camptothecin (cmt) or NU:UB 31.

Fig. 6.10 (a)

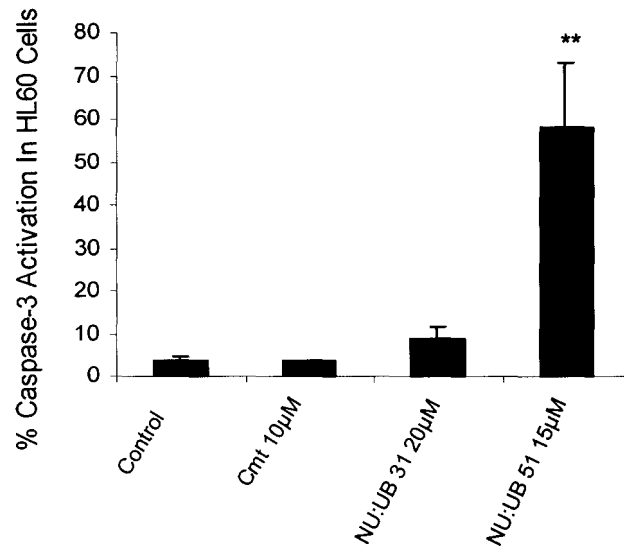


Fig. 6.10 (b)

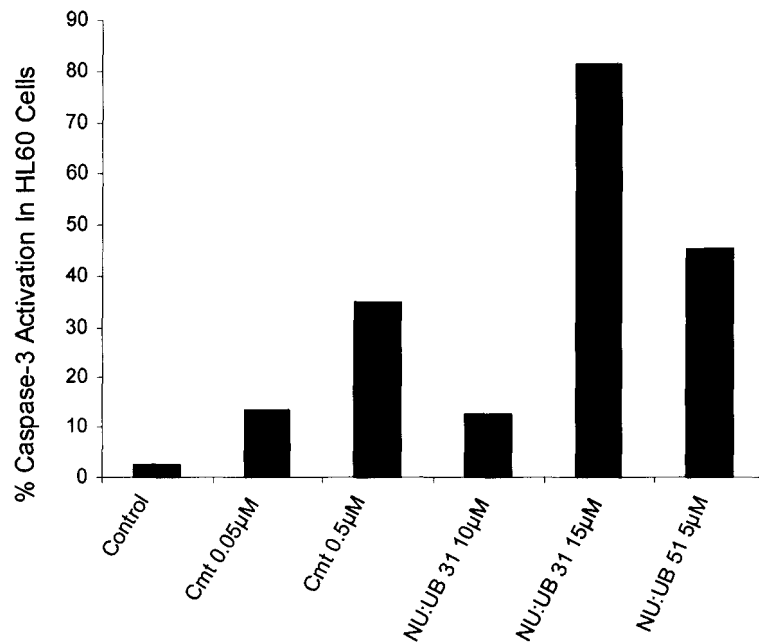
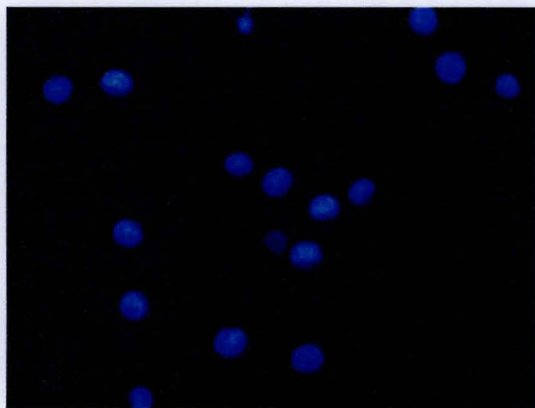
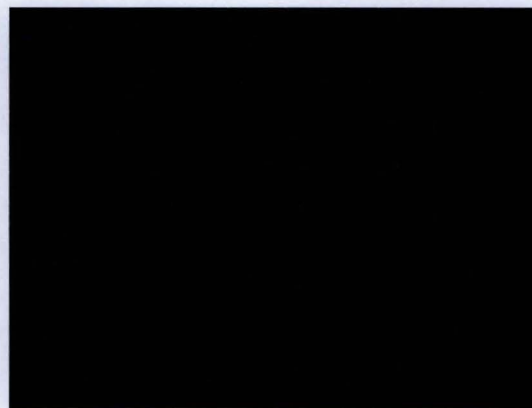


Fig. 6.10a-b Caspase-3 activation in HL60 cells, expressed as a percentage of total cells. Cells exposed 4h (a) and 24h (b) to solvent (control), camptothecin (cmt), NU:UB 31 or NU:UB 51



**Fig. 6.11a** Control 4h, Hoechst stain



**Fig. 6.11b** Control 4h, General caspase stain

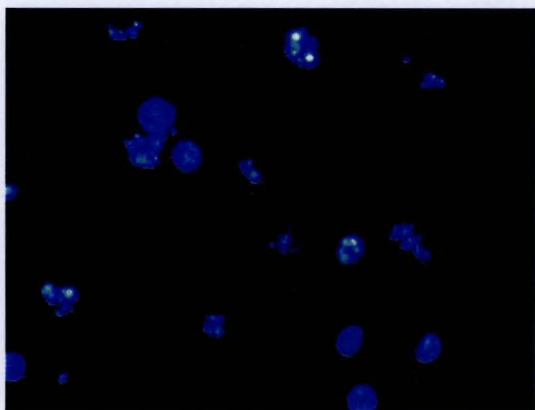


**Fig. 6.12a** Camptothecin 10 $\mu$ M 4h

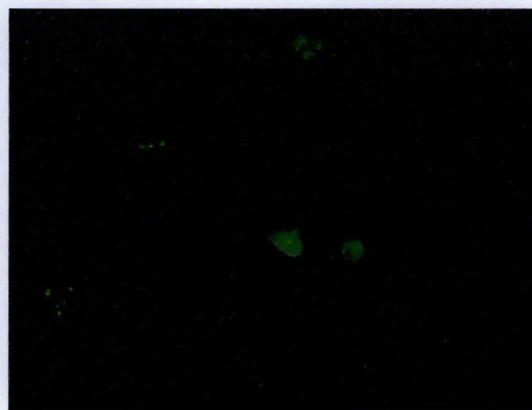


**Fig. 6.12b** Camptothecin 10 $\mu$ M 4h

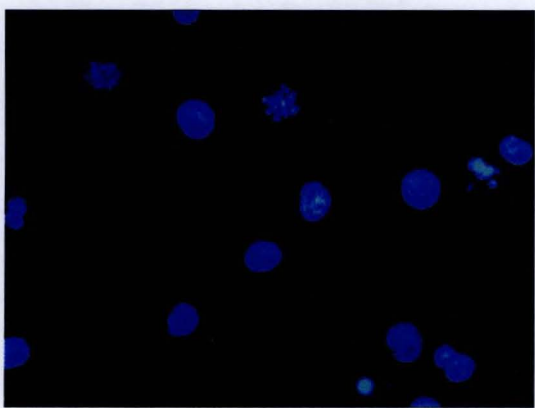


**Fig. 6.13a** NU:UB 31 20 $\mu$ M 4h

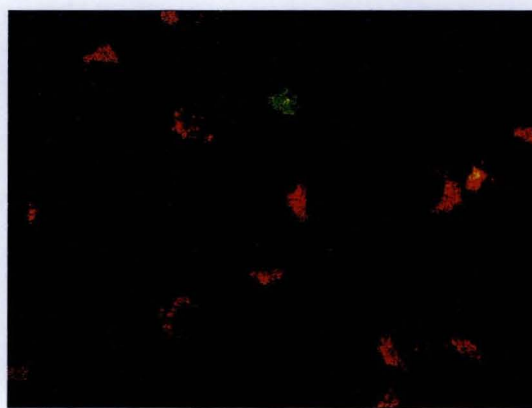


**Fig. 6.13b** NU:UB 31 20 $\mu$ M 4h

**Fig. 6.11–6.13** HL60 cells treated with solvent (control), camptothecin or NU:UB 31 for 4h. Following treatment, cells were stained with Hoechst stain and general caspase inhibitor. The cells were viewed under UV fluorescent microscope at 60x magnification, two pictures were taken of the same field of cells to visualise the blue Hoechst stain (a) and the green caspase stain (b).

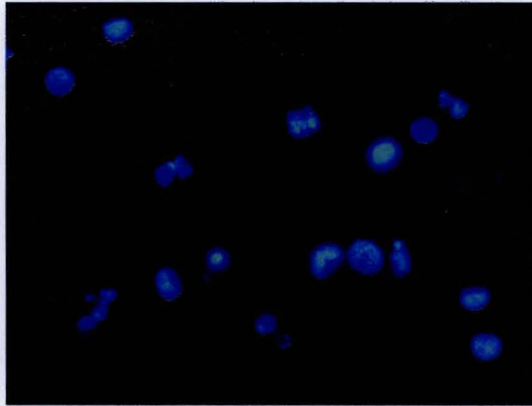


**Fig. 6.14a** NU:UB 51 10 $\mu$ M 4h

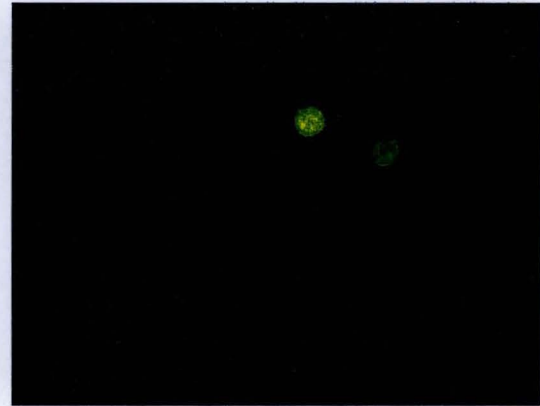


**Fig. 6.14b** NU:UB 51 10 $\mu$ M 4h

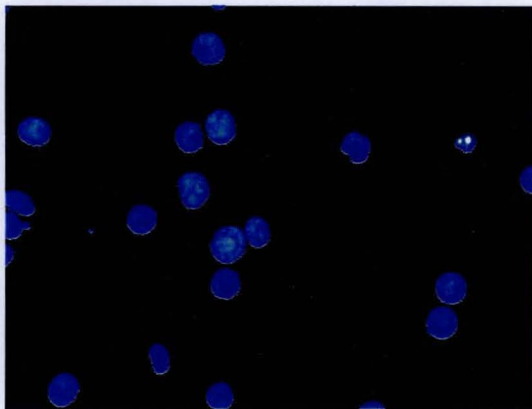


**Fig. 6.15a** Control 24h

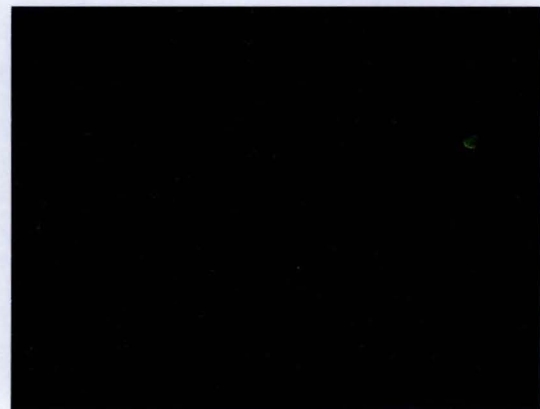


**Fig. 6.15b** Control 24h

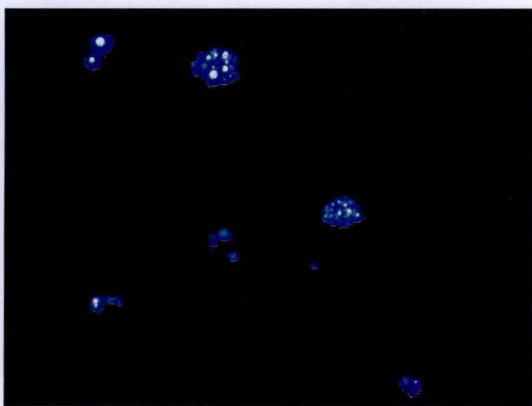


**Fig. 6.16a** Camptothecin 0.5 $\mu$ M 24h

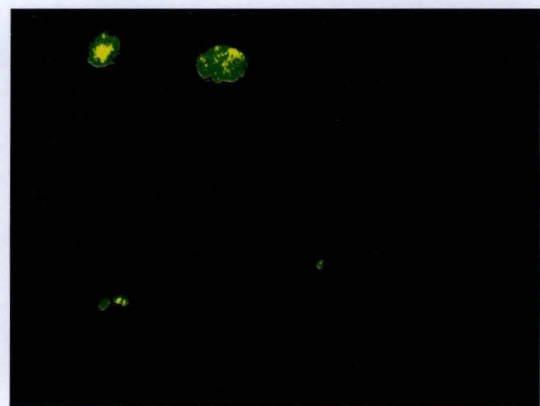


**Fig. 6.16b** Camptothecin 0.5 $\mu$ M 24h

**Fig. 6.14–6.16** HL60 cells treated with solvent (control), camptothecin or NU:UB 51 for 4h and 24h. Following treatment, cells were stained with Hoechst stain and general caspase inhibitor. The cells were viewed under UV fluorescent microscope at 60x magnification, two pictures were taken of the same field of cells to visualise the blue Hoechst stain (a) and the green caspase stain (b).

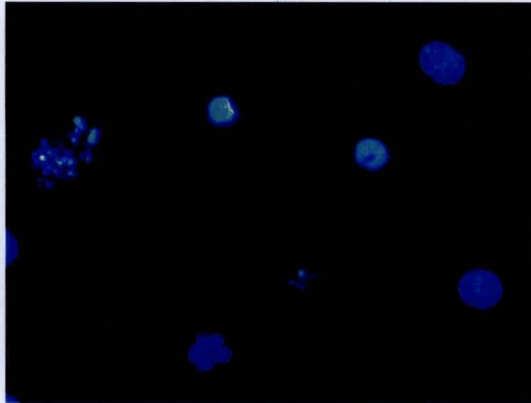


**Fig. 6.17a** NU:UB 31 10 $\mu$ M 24h

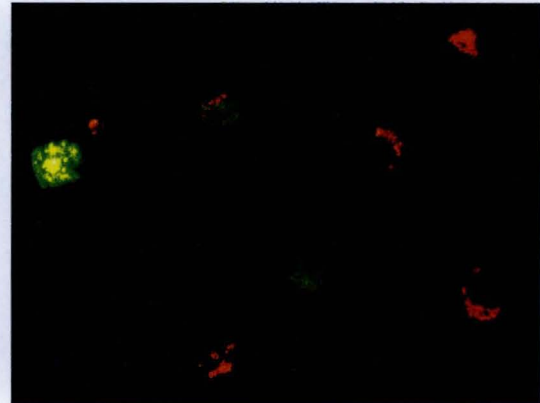


**Fig. 6.17b** NU:UB 31 10 $\mu$ M 24h

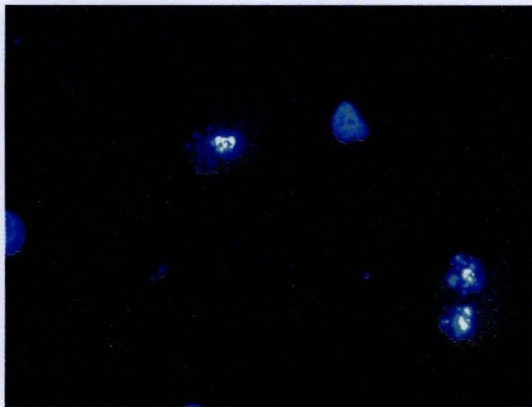


**Fig. 6.18a** NU:UB 51 5 $\mu$ M 24h

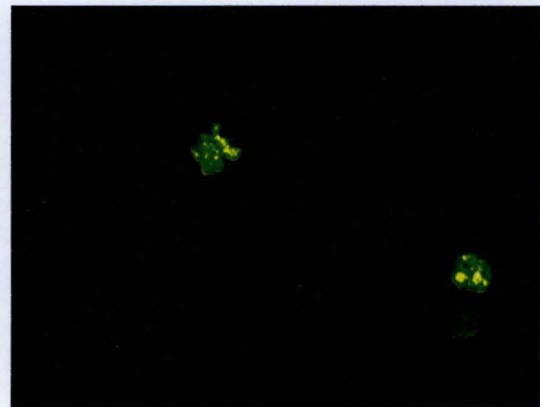


**Fig. 6.18b** NU:UB 51 5 $\mu$ M 24h

**Fig. 6.17–6.18** HL60 cells treated with NU:UB 31 or NU:UB 51 for 24h. Following treatment, cells were stained with Hoechst stain and general caspase inhibitor. The cells were viewed under UV fluorescent microscope at 60x magnification, two pictures were taken of the same field of cells to visualise the blue Hoechst stain (a) and the green caspase stain (b).

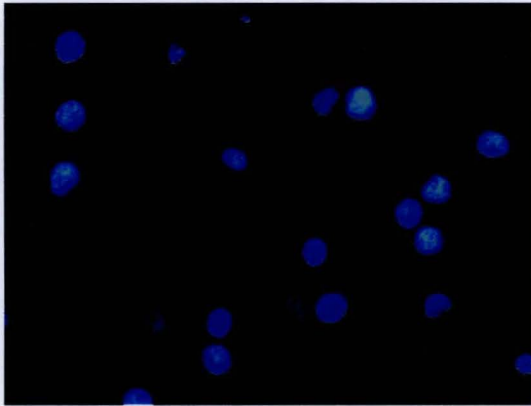


**Fig. 6.19a** Control 4h, Hoechst stain

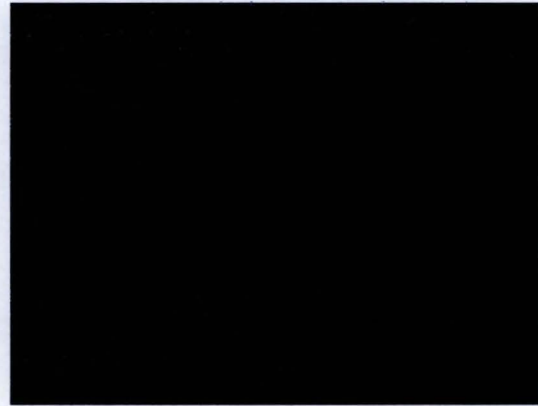


**Fig. 6.19b** Control 4h, Caspase-3 stain

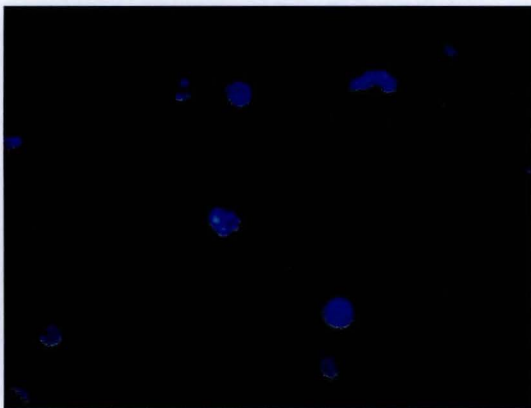


**Fig. 6.20a** Camptothecin 10µM 4h



**Fig. 6.20b** Camptothecin 10µM 4h

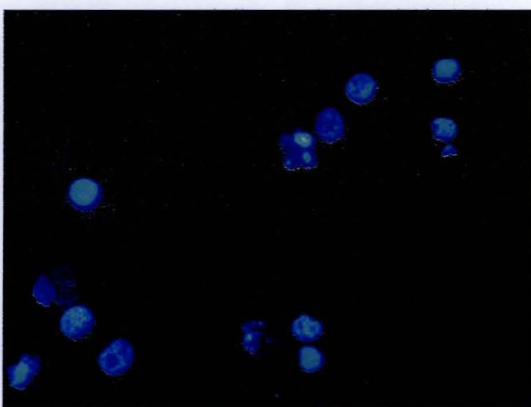


**Fig. 6.21a** NU:UB 31 20µM 4h

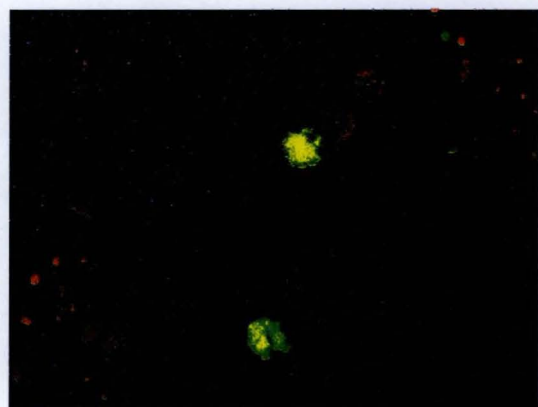


**Fig. 6.21b** NU:UB 31 20µM 4h

**Fig. 6.19–6.21** HL60 cells treated with solvent (control), camptothecin or NU:UB 31 for 4h. Following treatment, cells were stained with Hoechst stain and caspase-3 inhibitor. The cells were viewed under UV fluorescent microscope at 60x magnification, two pictures were taken of the same field of cells to visualise the blue Hoechst stain (a) and the green caspase-3 stain (b).

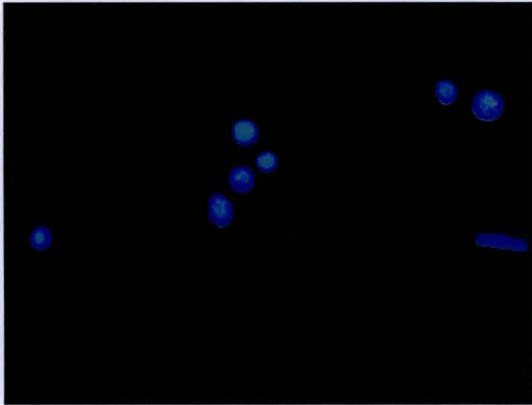


**Fig. 6.22a** NU:UB 51 15 $\mu$ M 4h

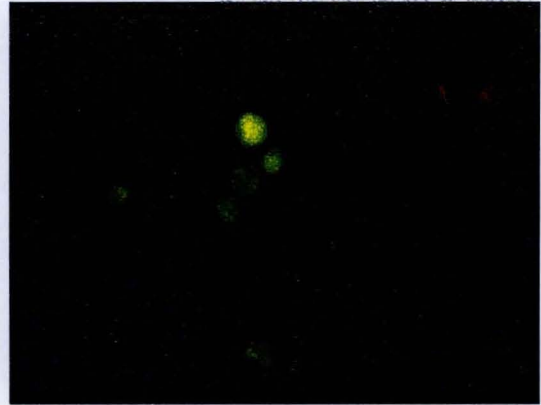


**Fig. 6.22b** NU:UB 51 15 $\mu$ M 4h

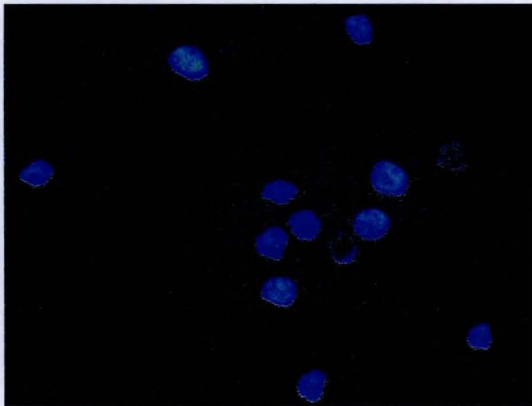


**Fig. 6.23a** Control 24h

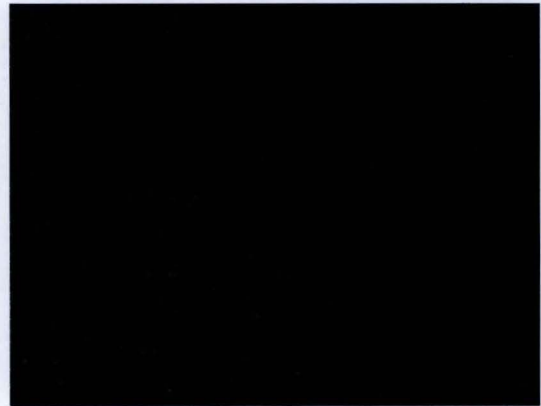


**Fig. 6.23b** Control 24h

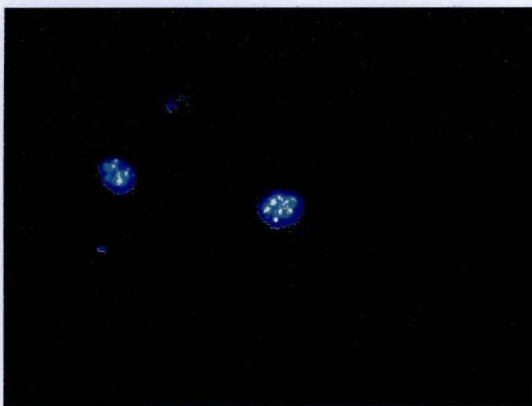


**Fig. 6.24a** Camptothecin 0.05 $\mu$ M 24h

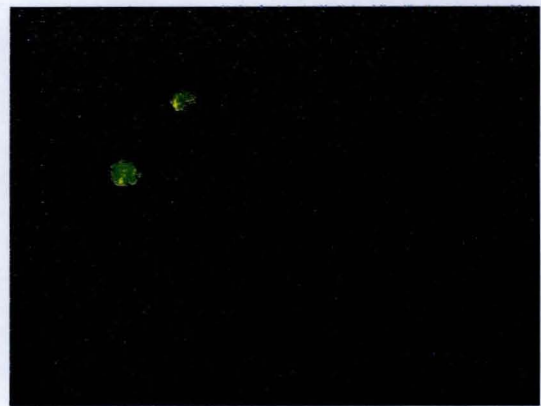


**Fig. 6.24b** Camptothecin 0.05 $\mu$ M 24h

**Fig. 6.22–6.24** HL60 cells treated with solvent (control), camptothecin, NU:UB 51 for 4h and 24h. Following treatment, cells were stained with Hoechst stain and caspase-3 inhibitor. The cells were viewed under UV fluorescent microscope at 60x magnification, two pictures were taken of the same field of cells to visualise the blue Hoechst stain (a) and the green caspase-3 stain (b).

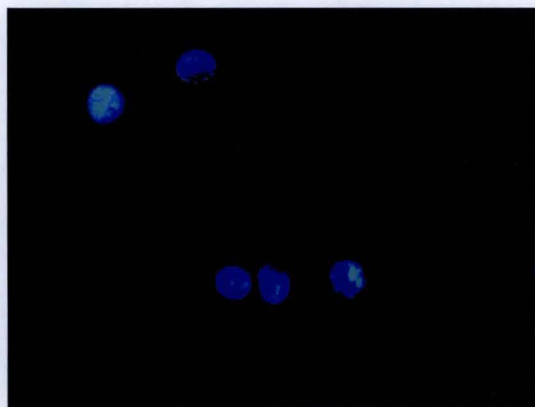


**Fig. 6.25a** NU:UB 31 10 $\mu$ M 24h



**Fig. 6.25b** NU:UB 31 10 $\mu$ M 24h



**Fig. 6.26a** NU:UB 31 15 $\mu$ M 24h



**Fig. 6.26b** NU:UB 31 15 $\mu$ M 24h

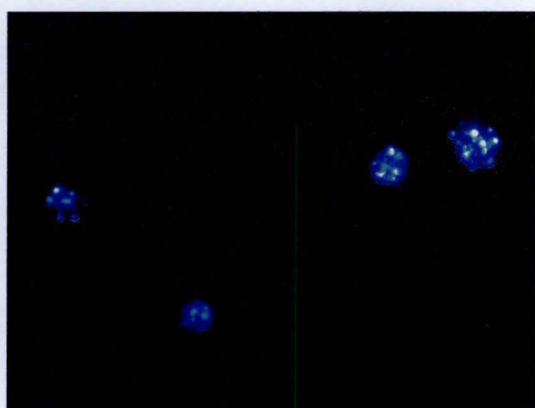


**Fig. 6.27a** NU:UB 51 5 $\mu$ M 24h

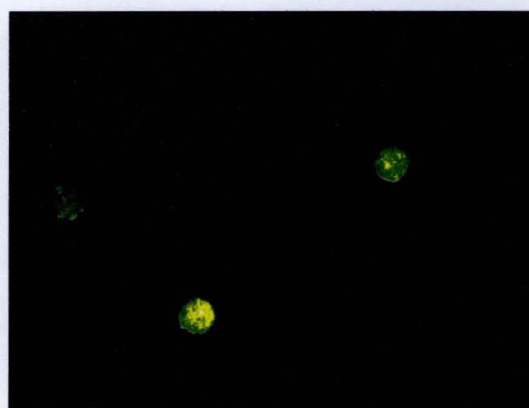


**Fig. 6.27b** NU:UB 51 5 $\mu$ M 24h

**Fig. 6.25–6.27** HL60 cells treated with NU:UB 31 or NU:UB 51 for 24h. Following treatment, cells were stained with Hoechst stain and caspase-3 inhibitor. The cells were viewed in fluorescent microscope, two pictures were taken of the same field of cells to visualise the blue Hoechst stain (a) and the green caspase-3 stain (b).

## 6.4 DISCUSSION

In this part of the research programme, apoptotic studies, including light and UV fluorescent microscopy observations, DNA fragmentation studies and flow cytometry investigations are presented to provide evidence that apoptosis was induced following treatments with NU:UB compounds and classical topoisomerase inhibitors. Etoposide and camptothecin were used as positive apoptotic controls in these studies. Etoposide has in the literature been reported to induce apoptosis in cell lines, including the HL60 cell line (Onishi *et al.*, 1993; Alexandre *et al.*, 2000). The mechanism of cytotoxic action of etoposide and induction of apoptosis, are thought to be related to its interaction with topoisomerase II as this drug has been found to target both topoisomerase II $\alpha$  and topoisomerase II $\beta$  (Willmore *et al.*, 1998). Camptothecin is reported to induce apoptosis in several human cancer cell lines; the exact pathway(s) is not fully understood, but thought to be linked to DNA strand breaks produced by camptothecin through stabilization of the topoisomerase I-DNA cleavable complexes (Covey *et al.*, 1989; Gong *et al.*, 1993; Onishi *et al.*, 1993; Johnson *et al.*, 1997; Alexandre *et al.*, 2000). A previous study with camptothecin showed that changes in cell morphology as well as DNA laddering by camptothecin treatment can be seen as early as 3h in HL60 cells (Gong *et al.*, 1994). Other studies used longer exposure times for investigating apoptotic DNA laddering following camptothecin exposure. For example, Goossens *et al.* (2000) exposed HL60 cells to 1-20 $\mu$ M for 15h, or to 10-50 $\mu$ M for 5h and found that short incubation times at higher drug

concentrations, or longer incubation times with low drug concentrations gave rise to similar results. In agreement with the above mentioned publications, the apoptotic investigations of camptothecin in this study showed DNA fragmentation and morphological changes of HL60 cells. The DNA fragmentation patterns visualized on agarose gels showed that the DNA fragmentations as a result of NU:UB 31, NU:UB 51 and NU:UB 80 treatments appeared similar to DNA fragments extracted from camptothecin-treated HL60 cells. This indicated preferential hydrolysis of DNA at the internucleosomal linker sections. This pattern is characteristic (but not a necessary criterion) for apoptosis.

Observations of cells by microscopy after staining provided evidence of apoptotic morphology. The cell morphology in general appeared similar regardless of treatment by camptothecin, etoposide or NU:UB compounds, both nuclear and cytoplasmic shrinkage were observed. In non-apoptotic HL60 cells, chromatins are generally not well stained, whereas HL60 cells engaged in the apoptotic pathway often present several clumps of condensed chromatin and these features were observed here. In addition to apoptosis there are at least two other types of cell death *in vivo*; necrosis and premature mitosis, also referred to as mitotic catastrophe. These cell deaths are though to be based on different molecular mechanisms and show distinct morphological characteristics, but in spite of this they are often hard to characterise since both biochemical and morphological features may change over time. Further, the mechanism of cell death seems to depend on drug dose, exposure time and cell type as well as expression of certain oncogenes

and tumour suppressor genes. For example, whereas apoptosis can be induced in sensitive cells, more resistant cells may instead die by premature mitosis (mitotic catastrophe) (Larsen and Skladanowski, 1998). Although apoptosis in many ways is similar to premature mitosis with one of the most prominent morphological features of apoptosis, condensation of chromatin, also found in mitosis, there are differences between these types of cell deaths. Similarities and differences between apoptosis and premature mitosis have been outlined by Meikrantz and Schlegel (1995). Thus, the original definition of apoptosis as a form of cell death distinct from necrosis may not be adequate to describe all forms of cell death. In addition, Speranido *et al.* (2000) recently described a form of cell death called 'paraptosis' (para=next to or related to) that they said was morphologically and biochemically distinct from apoptosis. They further suggested that paraptosis in some previous cases may have been assumed to be necrosis due to its morphological features of cytoplasmic vacuolation and mitochondrial swelling and since caspase inhibitors did not appear to have effect. The basis for this alternative form of cell death is yet unknown, but understanding the mechanism behind this may be beneficial in the understanding of the mechanisms of several cancer therapeutics.

Activation of caspases as a strategy in cancer therapy has gained much interest during the past decade, particularly for inducing cell death in tumours and determining the efficacy of chemotherapeutic agents. A reason for failure of current chemotherapeutics in resistant tumours is the possibly of mutations disrupting apoptotic pathways. A strategy to induce apoptosis in cells may be

to design treatments that activate caspases directly. Flow cytometry and UV fluorescent microscopy experiments were performed using general caspase and caspase-3 inhibitors labelled with a green fluorescent probe. These studies indicated that caspases were activated following 4h and 24h NU:UB 31 and NU:UB 51 treatment in HL60 and HCT116 cells. Caspases have been reported to be a marker of apoptotic cell death, so these experiments would thus further imply that cells become apoptotic following NU:UB compound treatment. However, although caspases appeared to be activated following NU:UB treatment it has been reported that apoptosis can take place independently of caspase activation. It was recently suggested by Kawagoe *et al.* (2002) that valproic acid (VPA, a member of the short chain fatty acids) killed cells by both caspase-dependent and caspase-independent apoptosis. Whereas the caspase-dependent pathways were suggested to mediate nuclear apoptotic changes, the caspase-independent pathways mediated PS events (phosphatidylserine exposure) on the cell membrane; the exact mechanism however of the latter caspase-independent apoptotic cell death is still to be determined. With this in mind, caspase-independent pathways may also be triggered by NU:UB compounds resulting in apoptosis.

In summary, we have used several methods to identify apoptotic cells, and found that known anti-topoisomerase drugs and NU:UB compounds induced apoptosis in HL60 and HCT116 cells when assessed by the above assays.

## **CHAPTER 7**

### **PROTEIN STUDIES**

## 7.1 PROTEIN STUDIES

Proteins involved in arresting the cell cycle and in the apoptotic process have been investigated in this research project and the data presented within this chapter. This study included p53 with its down-stream mediators, mdm2 and p21. In addition, the dependency of drug cytotoxicity on p53 status (wild type or mutated p53) in a range of cell lines have been investigated by NCI to give an indication of the importance of this protein for mechanism of action. To confirm the apoptotic caspase-3 activation findings (presented in Chapter 6), procaspase-3 cleavage following NU:UB treatment was investigated.

The information available so far on how certain genes, implicated in tumour formation (oncogenes and/or tumour suppressor genes) have a role in the response to anti-tumour drugs is realised but not clear. For example, the importance of p53 in drug-induced apoptosis is contradictory. Drug research indicates that the DNA damage induced by several chemotherapeutics, including camptothecin, etoposide and doxorubicin can function as a signal to trigger p53-mediated apoptosis, but experiments have also shown that apoptosis can be induced in HL60 cells (which do not contain p53), following treatment with these drugs. Other studies have also reported that apoptosis can take place through p53-independent pathways (Clarke *et al.*, 1993; Lowe *et al.*, 1993a; Lowe *et al.*, 1993b; Liu and Zhang, 1998; Alexandre *et al.*, 2000). Larsen and Skladanowski (1998) gave one explanation to the p53 controversy, suggesting that p53 is a protein involved in several pathways

including apoptosis, DNA repair and in cell cycle regulation. Thus, the interplay between the pathways affecting DNA repair, cell cycle progression and cell death, which again depends on which gene products are expressed in a given cell type, all appear to be important factors for cellular responses and outcome following drug treatment. In healthy cells the p53 tumour suppressor gene function is dampened to allow for normal growth, but it can rapidly be induced upon DNA damage. The cellular responses to p53 activation include both growth arrest and apoptotic cell death. Since p53 is an element of the DNA damage response pathway, this protein was here investigated to get a better understanding of what takes place within cells when treating with experimental (NU:UB) anti-cancer agents.

Tight regulation of p53 is critical for normal cell growth and one mechanism by which p53 is controlled is via mdm2. Mdm2 is a transcriptional target of p53 and enhanced mdm2 expression prevents p53 from acting as a tumour suppressor. Under normal conditions mdm2 binds p53 and shuttles p53 from the nucleus to be degraded in the cytoplasm, maintaining low p53 levels. DNA damage leads to phosphorylation and as a result, stabilisation of the p53 protein and accumulation of p53 in the nucleus (Haupt et al., 1997; Kubbutat *et al.*, 1997; Shieh *et al.*, 1997; Colman *et al.*, 2000). During recovery from DNA damage, maximal mdm2 induction coincides with rapid p53 loss. Thus, mechanisms regulating mdm2-induced degradation of p53 should play a role in controlling the extent and duration of the p53 response. As expected, the cellular effect of inhibitors of the p53-mdm2 interaction is p53 accumulation since these inhibitors should prevent the mdm2 interaction and thereby p53

degradation. P21 provides a link between cell cycle regulation and growth suppression by p53. The p21 gene is thought to be activated directly by p53, and p21 protein induction is suggested to play a part in p53-mediated growth arrest (Evan and Littlewood, 1998). P21 is a reversible cell cycle inhibitor and irreversible G1 or G2 arrest may lead to apoptosis. The exact role(s) of p21 in apoptosis has however been disputed, while p21 has been reported to be up-regulated in p53-mediated apoptosis by some researchers (El-Deiry *et al.*, 1994), this protein was not thought to be required in apoptosis by others (Makri *et al.*, 1998). Cell line variations could again be the reason for these differences.

The p53-mediated apoptotic pathway(s) are thought to converge on caspase activation. However, the mechanism by which p53 activates the caspases, and if these are always required in p53-mediated apoptosis, are still to be deduced. One of the caspases identified, caspase-3, has been implicated in the execution phase of apoptosis and it has been proposed that the p53-mediated cellular destruction in apoptosis could be carried out via activation of caspase-3 (Cregan *et al.*, 1999; Hietanen *et al.*, 2000; Schuler *et al.*, 2000). Caspase-3 activation was earlier investigated by flow cytometry using a fluorescent caspase-3 inhibitor that bound to activated caspase-3 (presented in Chapter 6). In this part of the project procaspase-3 protein cleavage was studied by Western blotting to support (or otherwise) our earlier findings.

## 7.2 METHODS

### 7.2.1 Investigation Of The P53 Protein Content In HCT116, HT29 And HL60 Cells.

Natural p53 protein levels are usually kept low, whereas in mutant cells p53 proteins may be present at much higher concentrations than in cells containing wild type p53. P53 levels were investigated by Western blotting in the three human cell lines that were previously used in our cytotoxicity studies. A mouse monoclonal anti-p53 (DO-1) antibody (Novo Castra), recognising both wild type and mutant p53 was used in these experiments. A high level of p53 in untreated cells would thus suggest that the cell line under investigation contains mutant p53 and low levels would imply wild type p53.

The cells were transferred to a sterile universal and centrifuged at 500 x g for 5 mins at 4°C. The supernatants were discarded and the cell pellets re-suspended in fresh culture medium. Cell counts were performed using a haemocytometer. HL60, HCT116 and HT29 cells were seeded at  $10 \times 10^4$  cells/ml and were left to adhere (HCT116 and HT29). All cell treatments were carried out under cell culturing conditions, 37°C, 5% CO<sub>2</sub>. Cells were treated with doxorubicin (1µM) or with solvent (control) for 24h. Following treatments, cell solutions (HL60), supernatants and trypsinised cells (HCT116 and HT29) were transferred to universals and were centrifuged at 500 x g for 5 mins at 4°C. Cells were lysed with protease inhibitors on ice. Following lysis, the

amount of protein in each sample was determined using the bicinchoninic acid protein assay. Equal amounts of proteins for each sample were separated on an SDS polyacrylamide gel, immunoblotted and stained with the mouse monoclonal anti-p53 (DO-1) antibody. For detailed protocols of these procedures see materials and general methods, Chapter 2.

## **7.2.2 Investigation Of P53 Protein Levels In HCT116 Cells Treated With NU:UB Compounds Or Doxorubicin**

HCT116 cells were seeded at  $10 \times 10^4$  cells/ml and were left to adhere. Cells were treated with NU:UB 31 (20 $\mu$ M), NU:UB 51 (10 $\mu$ M), doxorubicin (0.1 $\mu$ M, 1 $\mu$ M and 10 $\mu$ M), or with solvent (control) over a 24h time course, using 0h, 0.5h, 1h, 2h, 3h, 4h, 6h, 8h and 24h time points. Following treatment, supernatants and trypsinised cells were transferred to universals, pelleted and subsequently lysed with protease inhibitors. Total protein concentration in each sample was determined with the bicinchoninic acid assay. Each sample was separated on an SDS polyacrylamide gel, immunoblotted and stained with mouse monoclonal anti-p53 (DO-1) antibody (for detailed procedures, see materials and general methods, Chapter 2).

### **7.2.2a Treatment of Results**

Experiments were performed in triplicate or more, and each Western blot image was analysed using a digital Syngene imager with the GeneSnap and GeneTool software. The p53 protein band densities of the controls were

aliquoted to 100%, to which the band densities of the treated cells were compared. Mean  $\pm$  SEM was obtained and Tukey's one-way analysis of variance was used to evaluate significant differences between control p53 protein levels and the effects of the various treatments and time points.

### **7.2.3 P53 Protein Immunostaining Of HCT116 Cells Treated With NU:UB Compounds Or Doxorubicin**

Round coverslips (Raymond Lamb) were soaked in 70% ethanol, left to dry and placed in 24 well plates. HCT116 cells were washed and seeded ( $20 \times 10^4$  cells/ml) in the wells. The plates were left in an incubator for the cells to adhere to the coverslips. Once sufficient confluence was reached, the cells were either left untreated (solvent only), or treated with NU:UB 31, NU:UB 51 or doxorubicin. Following treatment, the cells were washed briefly in PBS, fixed, and had their membranes permeabilized by soaking in ice-cold acetone for 10 mins on ice. The acetone was washed off with PBS, and the well plates were put into a humidified chamber to prevent drying out. The immunostaining was performed using a Vectastain ABC mouse IgG kit (Novo Castra) with the components diluted according to manufacturer's recommendations. Cells were blocked in normal serum (1:20 dilution) for 30 mins. Excess serum was removed, and each cover slip was carefully removed from the wells, for them to be stained with primary antibody. This was done by placing a drop of mouse anti-p53 (DO-1) antibody, diluted 1:1000 in PBS, on a sheet of parafilm stretched over a 24 well plate. Each coverslip was placed with the cell side down onto the drop of primary antibody solution and the plates were

left in the humidified chamber for 2h. Following staining, the cover slips were put back into their respective wells and were washed in PBS. The biotinylated secondary antibody (ABC kit) was added (1:10 dilution) and left for 40 mins. Following a PBS wash step, streptavidin-horseradish peroxidase (ABC kit) was added (1:25 dilution) and the plate was left to incubate for 40 mins. Cells were washed in PBS and were then incubated with peroxidase substrate kit DAB (Vector) for 2.5 mins. The cover slips were washed in distilled H<sub>2</sub>O and counterstained in Haematoxylin (1:40 dilution in tap water) for 30 sec. The cover slips were soaked in Scotts tap water for 1 min, and were then removed from their wells and dehydrated. After dehydration the cells were mounted in DPX and were viewed in a light microscope (Zeiss Axioskop) at 40x magnification.

#### **7.2.4 Investigation Of Mdm2 Protein Levels In HCT116 Cells Treated With NU:UB Compounds Or Doxorubicin**

HCT116 cells were seeded ( $10 \times 10^4$  cells/ml) and were left to adhere. Cells were treated with NU:UB 31 (20 $\mu$ M), NU:UB 51 (10 $\mu$ M), doxorubicin (0.1 $\mu$ M, 1 $\mu$ M and 10 $\mu$ M) or with solvent (control) over a 24h time course, using 1h, 2h, 4h, 6h, 8h and 24h time points. Following treatment, supernatants and trypsinised cells were collected and lysed with protease inhibitors, and total protein levels determined with the bicinchoninic acid protein assay. The proteins in each sample were separated on an SDS-polyacrylamide gel, immunoblotted and stained with the mouse monoclonal anti-mdm2 antibody

(Autogen Bioclear) (for detailed procedures, see materials and general methods, Chapter 2).

#### 7.2.4a Treatment Of Results

Experiments were performed in triplicate or more and each Western blot image was analysed in the Syngene imager using the GeneSnap and GeneTool software. The mdm2 protein band densities of the controls were aliquoted to 100%, to which the band densities of the treated cells were compared. Mean  $\pm$  SEM was obtained.

#### **7.2.5 Investigation Of P21 Levels In HCT116 Cells Treated With NU:UB 31 Or Doxorubicin**

HCT116 cells were seeded and left to adhere. Cells were treated with NU:UB 31 (20 $\mu$ M), NU:UB 51 (10 $\mu$ M), doxorubicin or with solvent (control). Following treatment, supernatants and trypsinised cells were transferred to universals, cells were lysed using protease inhibitors, and the total protein levels determined with the bicinchoninic acid assay. The proteins in each sample were separated on an SDS polyacrylamide gel, immunoblotted and stained with the anti-p21 (WAF1) antibody (Oncogene) (for detailed procedures, see materials and general methods, Chapter 2).

### **7.2.6 Investigation Of Procaspase-3 Levels In HL60 And HCT116 Cells Treated With NU:UB Compounds, Doxorubicin Or Camptothecin**

HCT116 and HL60 cells were seeded at  $10 \times 10^4$  cells/ml and were left to recover and adhere (HCT116). HCT116 cells were treated with NU:UB 31 (20 $\mu$ M), NU:UB 51 (10 $\mu$ M), doxorubicin (1 $\mu$ M or 10 $\mu$ M), or with solvent (control). HL60 cells were treated with NU:UB 31 (20 $\mu$ M or 10 $\mu$ M), NU:UB 51 (5 $\mu$ M), camptothecin (0.5 $\mu$ M), or with solvent (control). Following treatment, cell solutions (HL60), supernatants and trypsinised cells (HCT116) were transferred to universals, which were centrifuged at 500 x g for 5 mins at 4°C. Cell pellets were immediately lysed with protease inhibitors. The total protein levels in each sample were detected with the bicinchoninic acid assay. The samples were separated on an SDS polyacrylamide gel and the proteins transferred onto membranes. The immunostaining was performed using the primary mouse monoclonal anti-procaspase-3 antibody (Autogen Bioclear) (for detailed procedures, see materials and general methods, Chapter 2).

## 7.3 RESULTS

### 7.3.1 P53 Protein

#### 7.3.1a P53 Protein Contents In HL60, HCT116 And HT29 Cells

P53 levels were analysed in HL60, HCT116 and HT29 cells following a 24h treatment with doxorubicin (1 $\mu$ M) as this would provide a positive control for p53 induction. Fig. 7.1 shows one of three similar Western blot results. P53 protein levels are normally kept at low levels whereas in mutant cells, p53 may be present at much higher concentrations than in cells with wild type p53. A p53 antibody recognising both wild type and mutant p53 was used in these experiments. A high level of p53 in untreated cells would suggest that the cell line contained mutant p53. HL60 cells were used as a negative control as this cell line has been shown to contain no p53. These results confirmed that there was no p53 protein present in either untreated or treated HL60 cells. In contrast, HCT116 cells had low levels of p53 in untreated cells, and upon doxorubicin treatment there was a great increase in p53 protein levels. The HT29 cell line contained high levels in both untreated and doxorubicin treated cells. This suggested that the HCT116 cell line contained wild type p53, that accumulated in the cells upon DNA damage whereas HT29 contained mutated p53. It was realised from this experiment that the HCT116 would be a suitable cell line to use in studying p53 upregulation.

### 7.3.1b Time Course Of P53 Protein Levels In HCT116 Cells

Western blots of p53 in HCT116 cells showed that NU:UB treatment induced p53 protein upregulation (Fig. 7.2). The data shown in Fig. 7.3a, Fig. 7.3b and Fig. 7.3c represents the p53 protein levels in HCT116 cells as measured by Western blotting over a period of time. P53 levels in the control remained low throughout the 24h exposure time. Doxorubicin was used as a positive control; 24h exposure to doxorubicin resulted in significantly increased p53 levels. NU:UB 31 also to some degree increased p53 levels in HCT116 cells and p53 levels peaked at 2-8h exposure. For NU:UB 51 a similar response was seen. After 24h of NU:UB 31 or NU:UB 51 treatment the p53 protein content had dropped. Thus, for NU:UB 31 and NU:UB 51 it seemed that the highest p53 levels were detected as early as 2-8h. However, these levels were not as progressively increased as with 24h doxorubicin exposure. For doxorubicin, the 24h treatment elicited higher p53 levels than a shorter doxorubicin exposure ( $p < 0.001$ ).

### 7.3.1c Immunostaining Of HCT116 Cells Treated With NU:UB 31, NU:UB 51 Or Doxorubicin

In addition to the Western blotting experiments, p53 immunostainings were performed, and images are presented in Fig 7.4. These images confirmed p53 upregulation in HCT116 cells. Following doxorubicin treatment the cell nuclei were strongly positively stained (brown) compared to the control where there

was no or only low levels of staining (Fig. 7.4a, Fig. 7.4b). NU:UB 31 and NU:UB 51 treated cells were also positively stained (Fig. 7.4c, Fig. 7.4d).

### 7.3.1d Relationship Between Drug Sensitivity And P53 Status In NCI Cell Lines

NU:UB 31, NU:UB 43, NU:UB 80, NU:UB 81 and the standard drug, doxorubicin, have been screened by NCI in a range of wild type p53 versus mutant p53 containing cell lines. GI<sub>50</sub> values for each compound were obtained by NCI (Fig. 7.5). These values were plotted in scattergrams of GI<sub>50</sub> versus p53 status. For each compound two median GI<sub>50</sub> values were provided, one from the p53 wild type cell lines and another from the p53 mutant cell lines. The scattergram of doxorubicin gave an average wild type GI<sub>50</sub> of 0.088 $\mu$ M versus a mutant GI<sub>50</sub> of 0.17 $\mu$ M (Fig. 7.5a). The difference between wild type and mutant GI<sub>50</sub> was thus above 1.9-fold for doxorubicin. The NU:UB compounds were overall less potent than doxorubicin, the average NU:UB GI<sub>50</sub> values were higher in both the wild type and the mutant cell lines (NU:UB 31 wild type 3.98 $\mu$ M versus mutant 5.75 $\mu$ M, Fig. 7.5b; NU:UB 43 wild type 3.08 $\mu$ M versus mutant 4.06 $\mu$ M, Fig. 7.5c; NU:UB 80 wild type 2.65 $\mu$ M versus mutant 3.16 $\mu$ M, Fig. 7.5d; NU:UB 81 wild type 2.37 $\mu$ M versus mutant 3.09 $\mu$ M, Fig. 7.5e). The difference between wild type and mutant median GI<sub>50</sub> values for the NU:UB compounds ranged from 1.2 to 1.4-fold, thus less than for doxorubicin.

## 7.3.2 Mdm2 Protein

### 7.3.2a Time Course Of Mdm2 Protein Levels In HCT116 Cells

Western blot images of mdm2 protein levels in HCT116 cells following NU:UB treatment are given in Fig. 7.6a and Fig. 7.6b. Time course experiments were performed and increased mdm2 levels were evident following 4-8h of NU:UB 31 (Fig. 7.7a) or NU:UB 51 (Fig. 7.7b) treatment. At the 24h time points of NU:UB treatment, mdm2 levels had dropped and were comparable to the mdm2 protein levels in controls. Following doxorubicin treatment there was no increase in mdm2 levels (Fig. 7.7a, Fig. 7.7b).

## 7.3.3 P21 Protein

### 7.3.3a P21 Levels In HCT116 Cells Treated With NU:UB Compound Or Doxorubicin

The HCT116 cell line, which was shown to express wild type p53 in previous studies, was used in these p21 experiments. Doxorubicin was used as a positive control as this drug (at 0.35 $\mu$ M, 14h and 28h) had been shown to cause p21 upregulation in previous research using HCT116 cells (El-Deiry *et al.*, 1994). Contrary to this earlier study, there was in our experiments a high basal level of p21 in HCT116 control cells. There was further no significant

increase in p21 protein levels following doxorubicin or NU:UB 31 (20 $\mu$ M) treatment (Fig. 7.8a).

### 7.3.3b HCT116 Cells Grown In Culture Medium Supplemented With 1%, 5% Or 10% FBS Concentrations

In some cell lines FBS can be involved in inducing proteins. We therefore cultured the HCT116 cells in 1%, 5%, or 10 % FBS supplemented culture medium before drug treatment to investigate whether or not FBS had an effect on p21 levels in these cells. Fig. 7.8b shows a Western blot image of untreated cells, or cells treated with NU:UB 31 or doxorubicin. From these experiments it was shown that FBS did not cause p21 induction, as the levels of p21 were similar in cells grown in 1%, 5%, and 10% FBS supplemented medium.

### 7.3.3c Time Course Of P21 Levels In HCT116 Cells

P53 levels were increased following 3-4h NU:UB treatment in HCT116 cells and decreased after 24h treatment. It may be that p21 levels had peaked prior to the 24h time point. Therefore, p21 protein levels were measured following shorter treatment times. Time course experiments of p21 protein levels were performed and these are represented in Fig 7.8c and Fig. 7.8d. It was discovered that there was no increase in p21 compared to control in this cell line following NU:UB 31 or NU:UB 51 treatment at either of the time points

used. Thus it seemed that NU:UB treatment did not induce p21 in our HCT116 cells.

#### **7.3.4 Procaspase-3 Cleavage In HCT116 And HL60 Cells**

Caspase-3 is synthesised as a 33kDa inactive proenzyme that requires proteolytic activation. Two smaller subunits, derived from this caspase-3 proenzyme have been reported following cleavage activation. These active species have been detected as early as 3h in HL60 cells with etoposide treatment (Martins *et al.*, 1997). Western blotting experiments revealed that high levels of inactive, procaspase-3 were present as a band of approximately 32-34kDa in control cells of both cell lines used. Cleaved procaspase-3 (activated caspase-3) proteins were represented by bands of low molecular weight, below the procaspase-3 bands. There were only low, or no levels of active caspase-3 in the controls for both cell lines used. In HCT116 cells, caspase-3 activation was evident following 24h doxorubicin treatment, but not at the 1h doxorubicin time point. Following NU:UB 31 or NU:UB 51 treatment, cleaved caspase-3 bands appeared at the 8h and 24h time points in HCT116 cells (Fig. 7.9a, Fig.7.9b). While active caspase-3 was not observed in the HL60 controls, NU:UB 31 and NU:UB 51 treatments resulted in a slight increase in the caspase-3 band density at the 4h, 8h and 24h time points. There was however no evident decrease in the level of procaspase-3 band density. In contrast, following 24h camptothecin treatment there was no longer any inactive procaspase-3 present, but instead a high level of active caspase-3 (Fig. 7.9c).



**Fig 7.1** Western blot of p53 contents in untreated HL60, HCT116 and HT29 cells, or following 24h treatment with doxorubicin (1 $\mu$ M). HL60 cells, untreated (lane 1), HL60 cells, doxorubicin treated (lane 2), HCT116 cells, untreated (lane 3), HCT116 cells, doxorubicin treated (lane 4), HT29 cells, untreated (lane 5), HT29 cells, doxorubicin treated (lane 6). Figure is representative of three separate experiments.

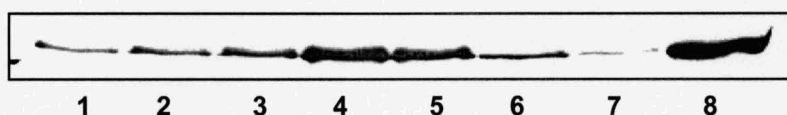


**Fig 7.2a** Time course. Western blot of p53 levels in HCT116 following NU:UB 31 or doxorubicin treatment. Control 1h (lane 1), doxorubicin 10 $\mu$ M 1h (lane 2), NU:UB 31 20 $\mu$ M 1h (lane 3), NU:UB 31 20 $\mu$ M 4h (lane 4), NU:UB 31 20 $\mu$ M 8h (lane 5) NU:UB 31 20 $\mu$ M 24h (lane 6), Control 24h (lane 7), Doxorubicin 1 $\mu$ M 24h (lane 8). Figure is representative of three separate experiments.

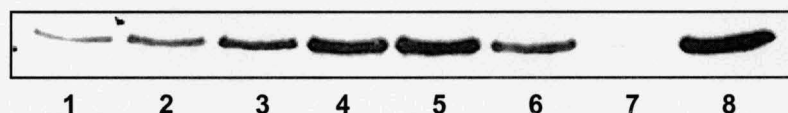


**Fig 7.2b** Time course. Western blot of p53 levels in HCT116 following NU:UB 51 or doxorubicin treatment. Control 1h (lane 1), doxorubicin 10 $\mu$ M 1h (lane 2), NU:UB 51 10 $\mu$ M 1h (lane 3), NU:UB 51 10 $\mu$ M 4h (lane 4), NU:UB 51 10 $\mu$ M 8h (lane 5) NU:UB 51 10 $\mu$ M 24h (lane 6), Control 24h (lane 7), doxorubicin 1 $\mu$ M 24h (lane 8). Figure is representative of three separate experiments.

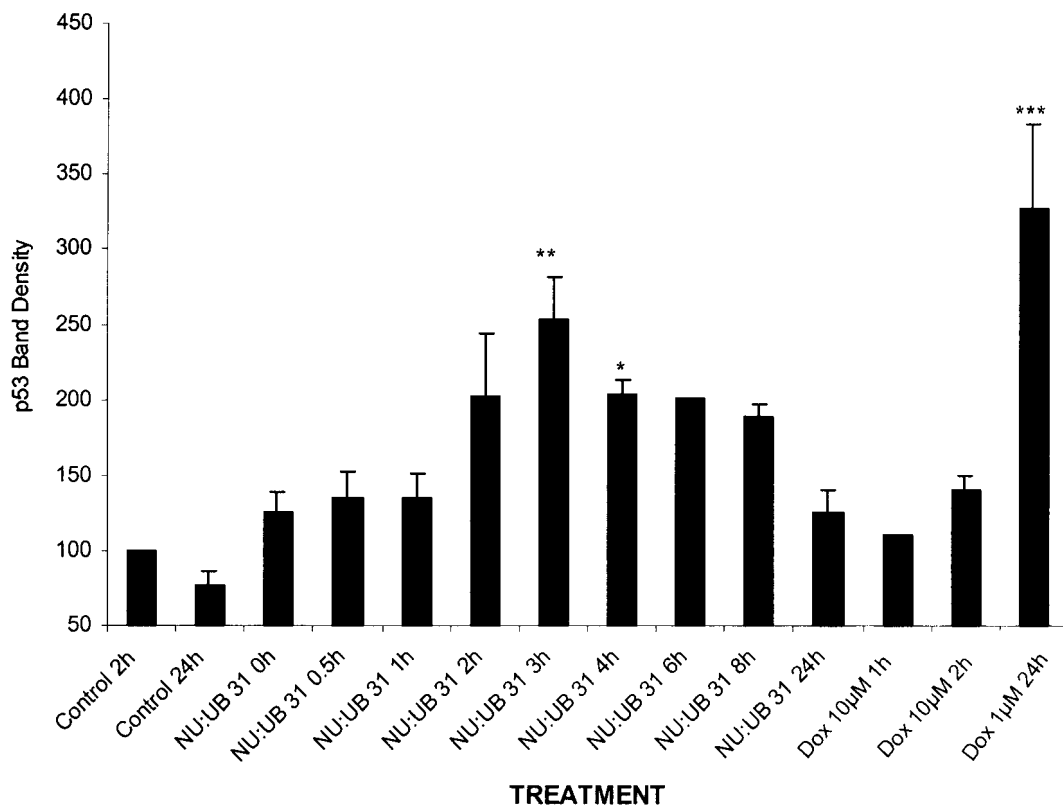


**Fig 7.3a** Time course of p53 levels in HCT116 cells treated with NU:UB 31 (20µM) or doxorubicin (Dox) (10µM 1h and 2h, 1µM 24h). Results are the mean of three or more separate Western blot experiments  $\pm$  SEM (with the exception of doxorubicin 10µM 1h (n=2)). Asterisks denote significant differences from the control (\*  $p < 0.05$ , \*\*  $p < 0.01$ , \*\*\*  $p < 0.001$ ).

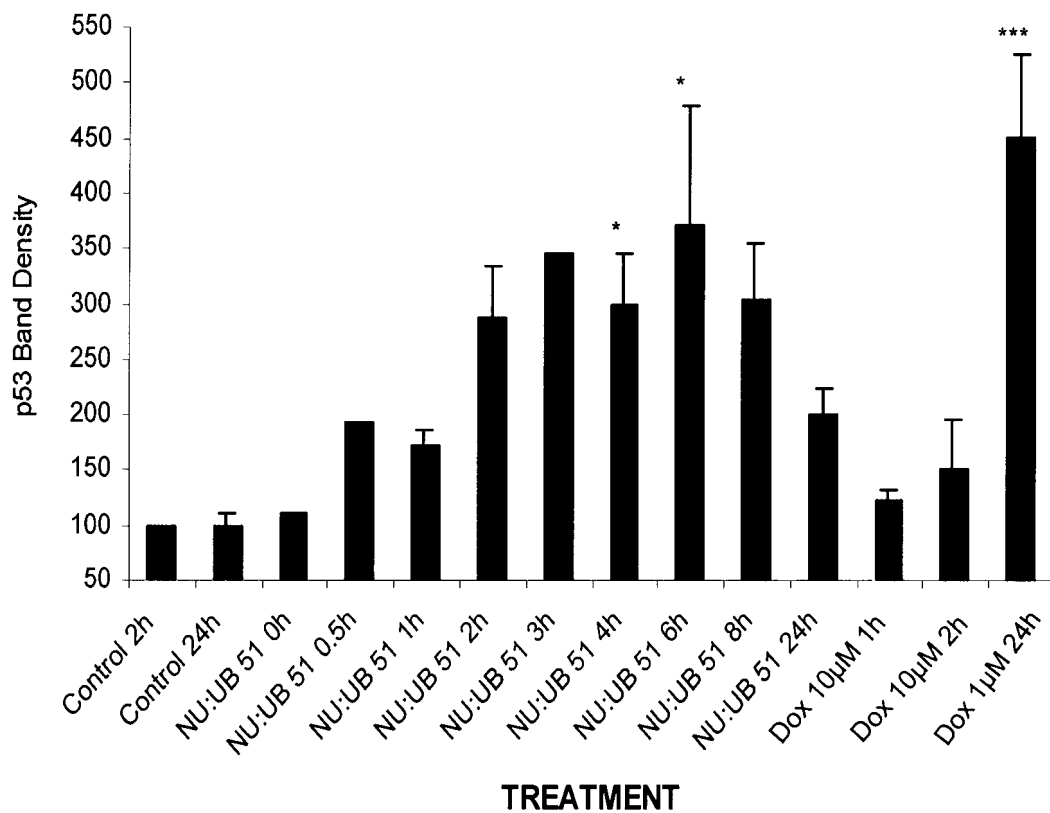


**Fig 7.3b** Time course of p53 levels in HCT116 cells treated with NU:UB 51 (10µM) or doxorubicin (Dox) (10µM 1h and 2h, 1µM 24h). Results are the mean of three or more separate Western blot experiments ± SEM (with the exception of NU:UB 51 0h, 0.5h and 3h (n=2)). Asterisks denote significant differences from the control (\* p<0.05, \*\*\* p<0.001).

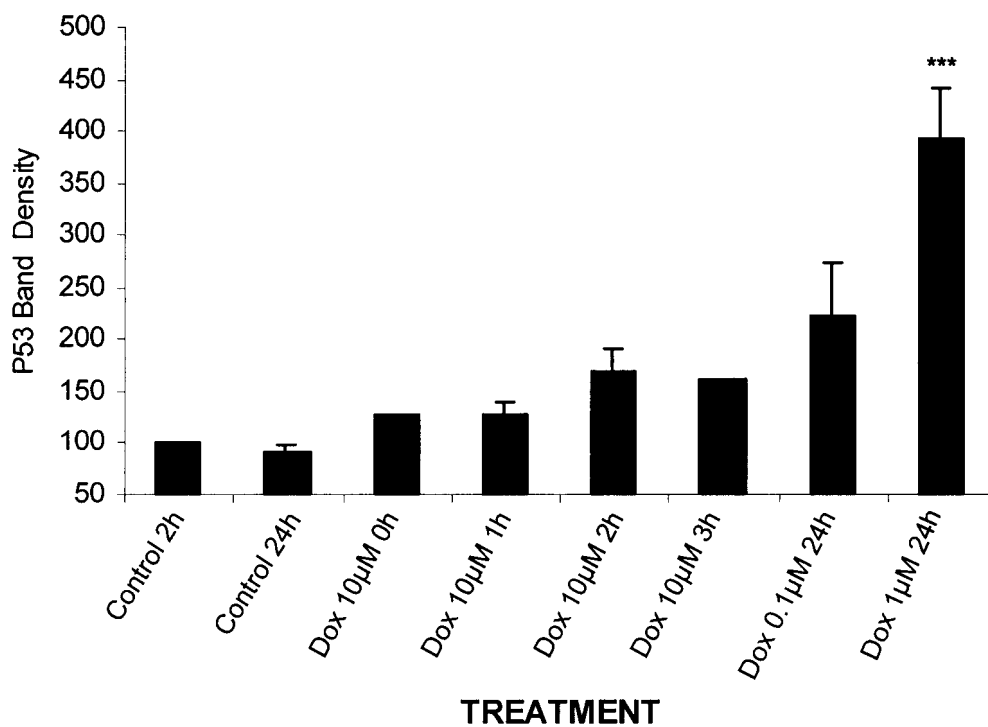


**Fig 7.3c** Time course of p53 levels in HCT116 cells treated with doxorubicin (Dox) (10µM for 0h, 1h, 2h and 3h or, 0.1 and 1µM for 24h). Results are the mean of three or more separate Western blot experiments  $\pm$  SEM (with the exception of 0h and 3h where n=1 and 2 respectively). Asterisks denote significant differences from the control 24h (\*\*\*)  $p < 0.001$ .

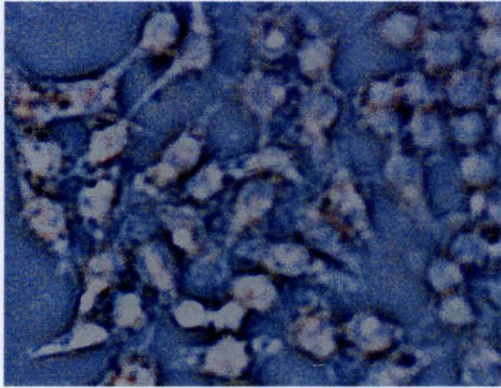


**Fig.7.4a** Control

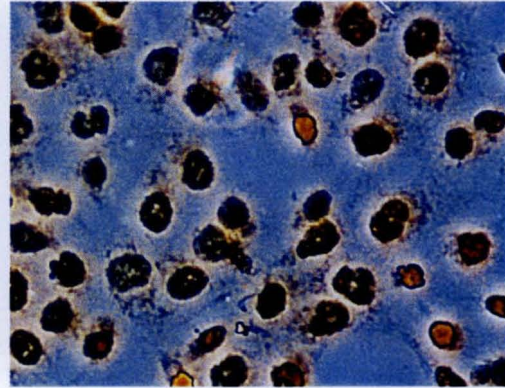


**Fig. 7.4b** Doxorubicin

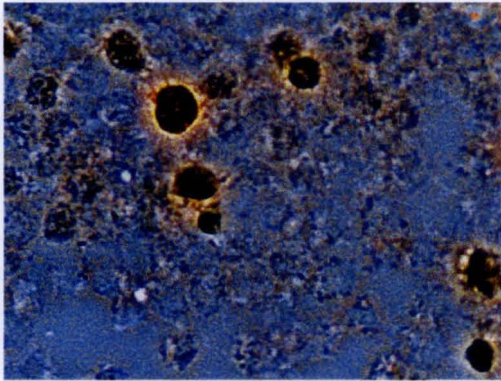


**Fig. 7.4c** NU:UB 31

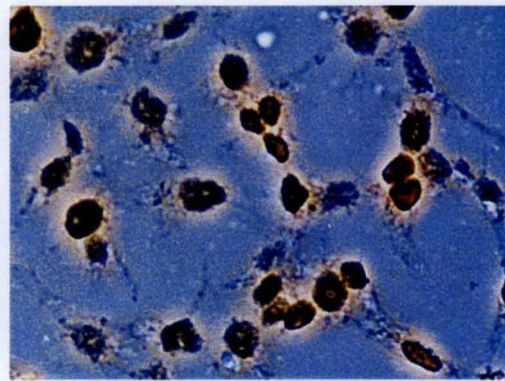


**Fig. 7.4d** NU:UB 51

**Fig. 7.4a-d** P53 immunostaining of HCT116 cells treated for 24h with solvent (control), doxorubicin (1 $\mu$ M), NU:UB 31 (5 $\mu$ M) or NU:UB 51 (5 $\mu$ M). The immunostaining has been performed in duplicate.

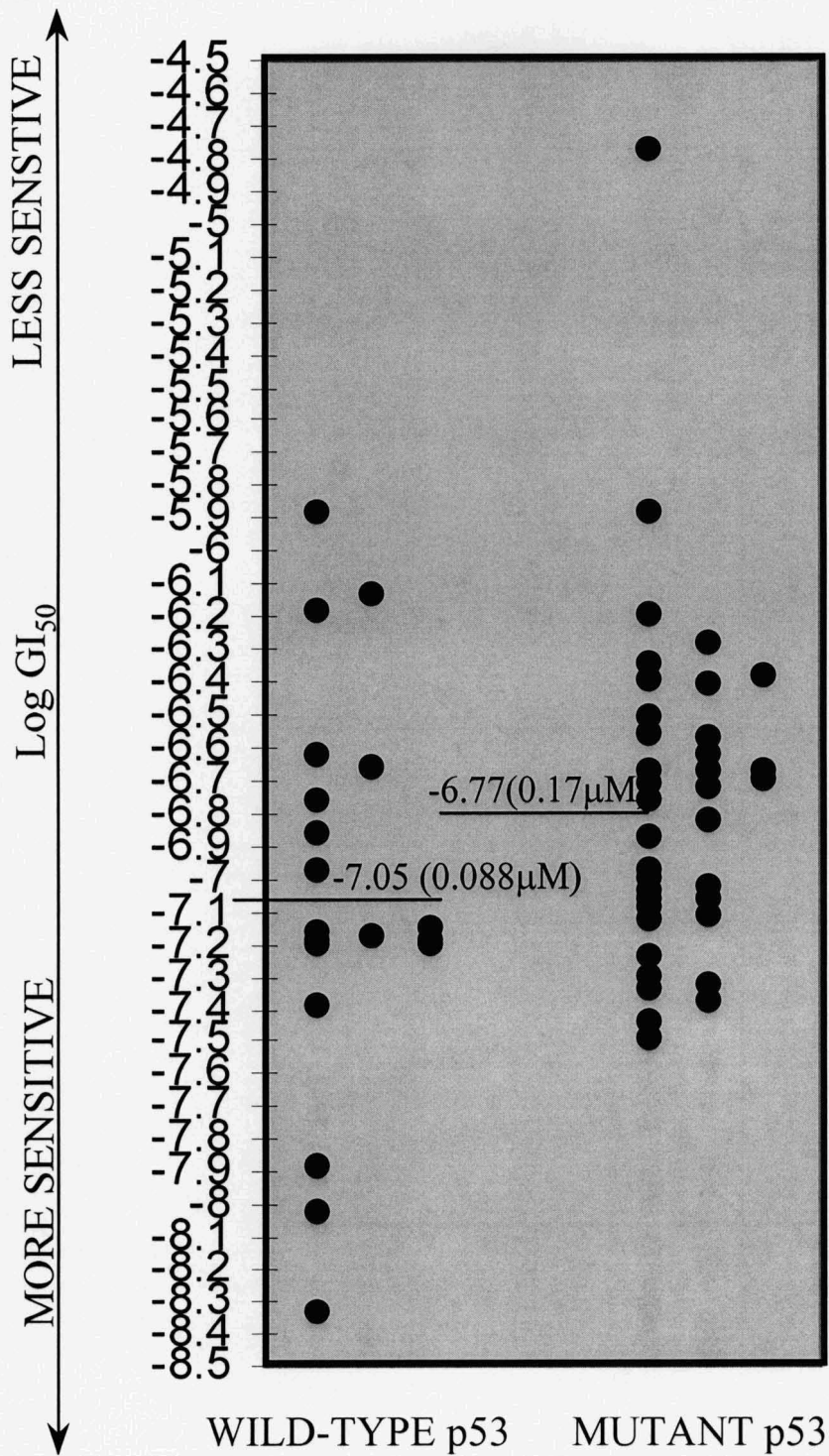


**Fig. 7.5a** Relationship between NCI cell line sensitivity to doxorubicin and expression of wild type or mutated p53

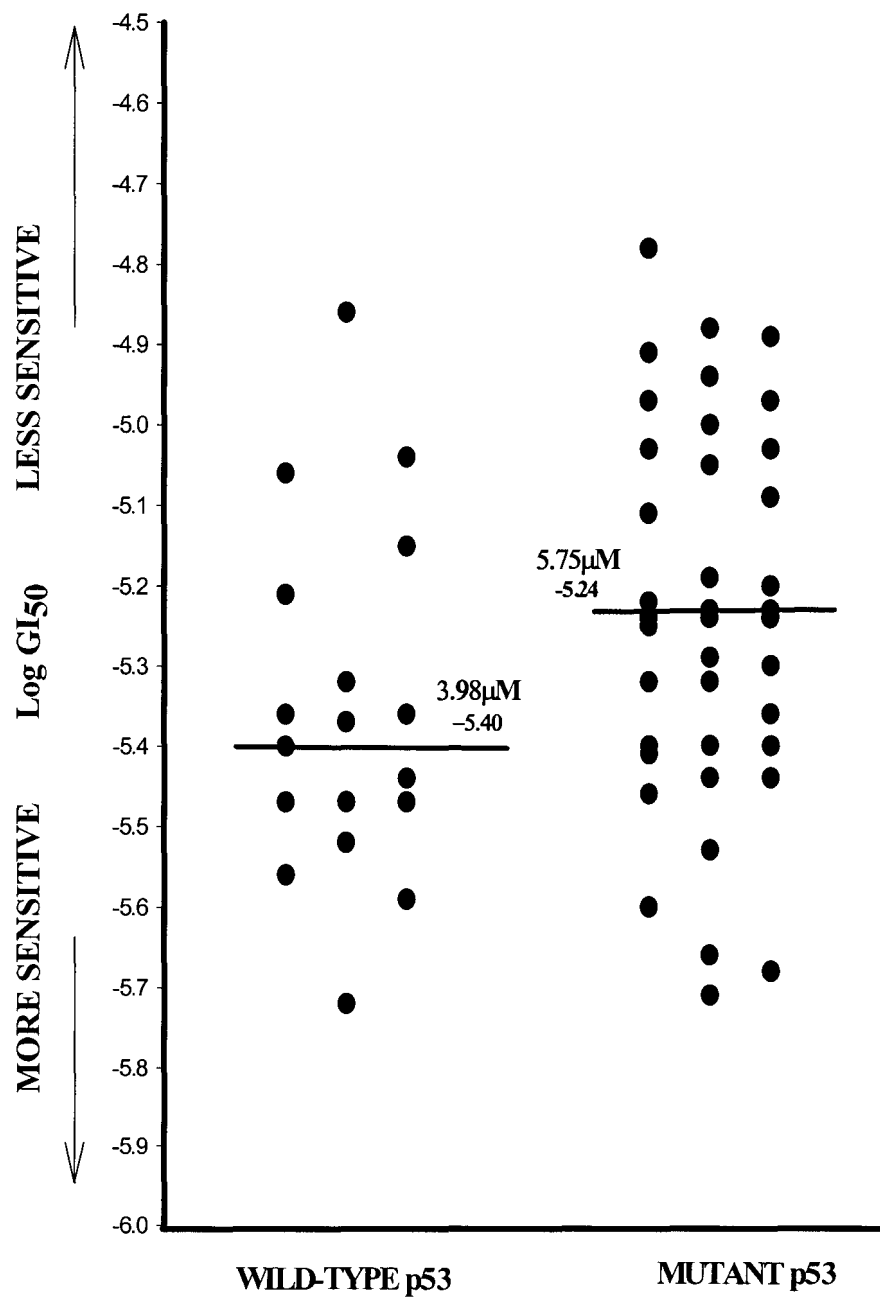


**Fig. 7.5b** Relationship between NCI cell line sensitivity to NU:UB 31 and expression of wild type or mutated p53

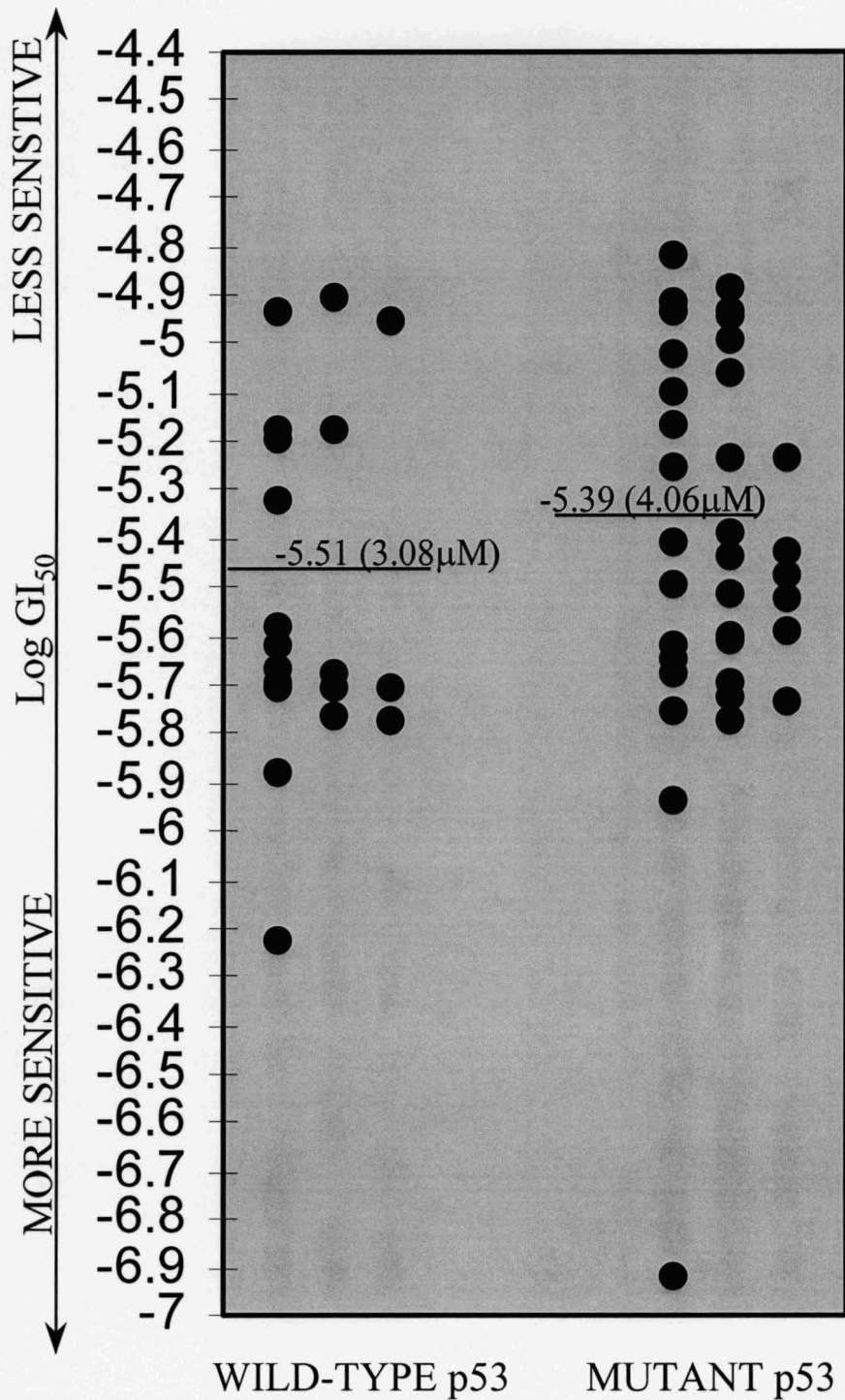
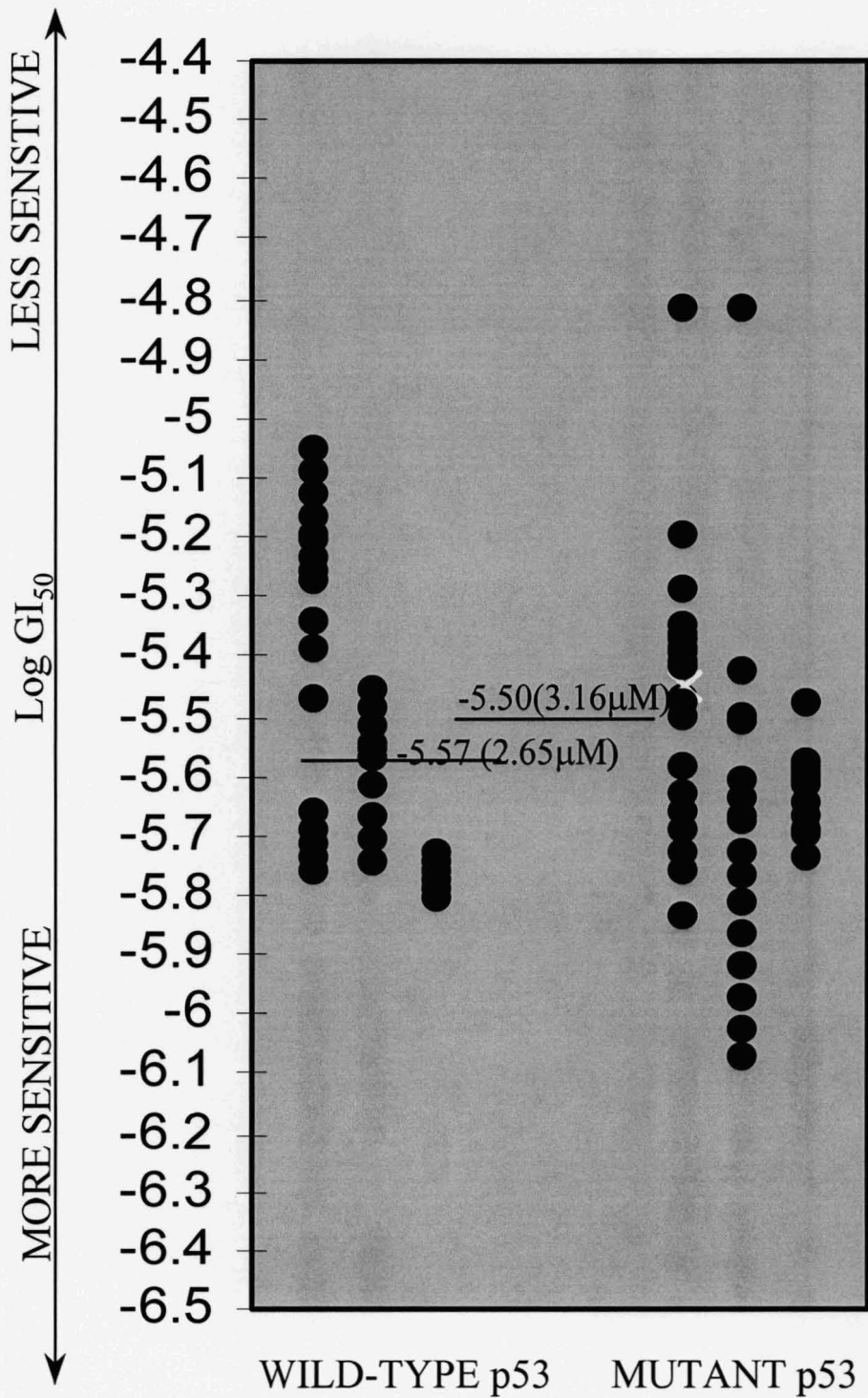
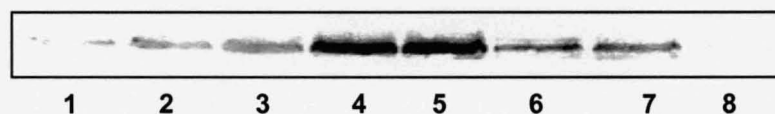


Fig. 7.5c Relationship between NCI cell line sensitivity to NU:UB 43 and expression of wild type or mutated p53



**Fig.7.5d** Relationship between NCI cell line sensitivity to NU:UB 80 and expression of wild type or mutated p53





**Fig 7.6a** Time course. Western blot of mdm2 levels in HCT116 cells following NU:UB 31 or doxorubicin treatment. Control 1h (lane 1), doxorubicin 10µM 1h (lane 2), NU:UB 31 20µM 1h (lane 3), NU:UB 31 20µM 4h (lane 4), NU:UB 31 20µM 8h (lane 5), NU:UB 31 20µM 24h (lane 6), Control 24h (lane 7), doxorubicin 1µM 24h (lane 8). The figure is representative of three separate experiments.

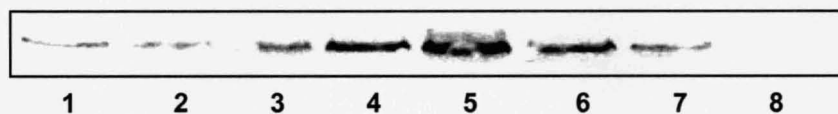


**Fig 7.6b** Time course. Western blot of mdm2 levels in HCT116 cells following NU:UB 51 or doxorubicin treatment. Control 1h (lane 1), doxorubicin 10µM 1h (lane 2), NU:UB 51 10µM 1h (lane 3), NU:UB 51 10µM 4h (lane 4), NU:UB 51 10µM 8h (lane 5), NU:UB 51 10µM 24h (lane 6), Control 24h (lane 7), doxorubicin 1µM 24h (lane 8). The figure is representative of three separate experiments.

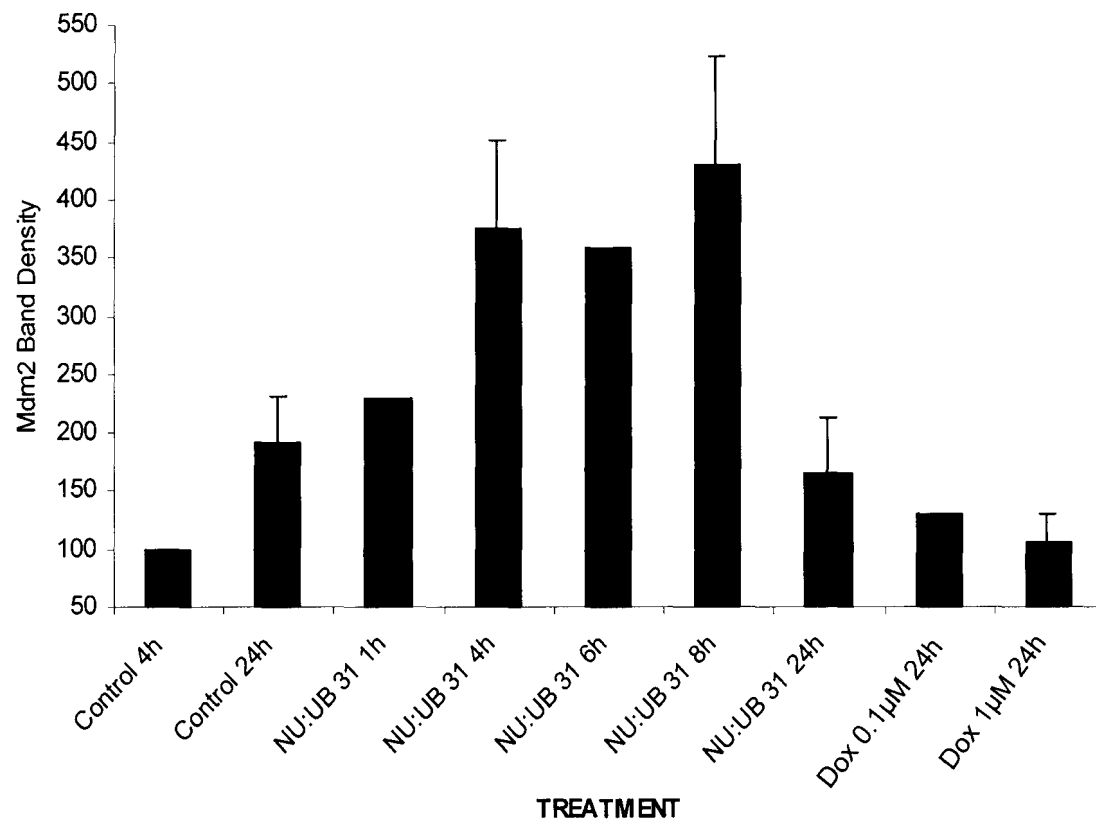


**Fig 7.7a** Time course of mdm2 levels in HCT116 cells treated with NU:UB 31 (20µM) or doxorubicin (Dox) (0.1µM or 1µM for 24h). Results are the mean of three or more separate Western blot experiments ± SEM (with the exception of NU:UB 31 1h and doxorubicin 0.1µM 24h where n=2, and NU:UB 31 6h where n=1).

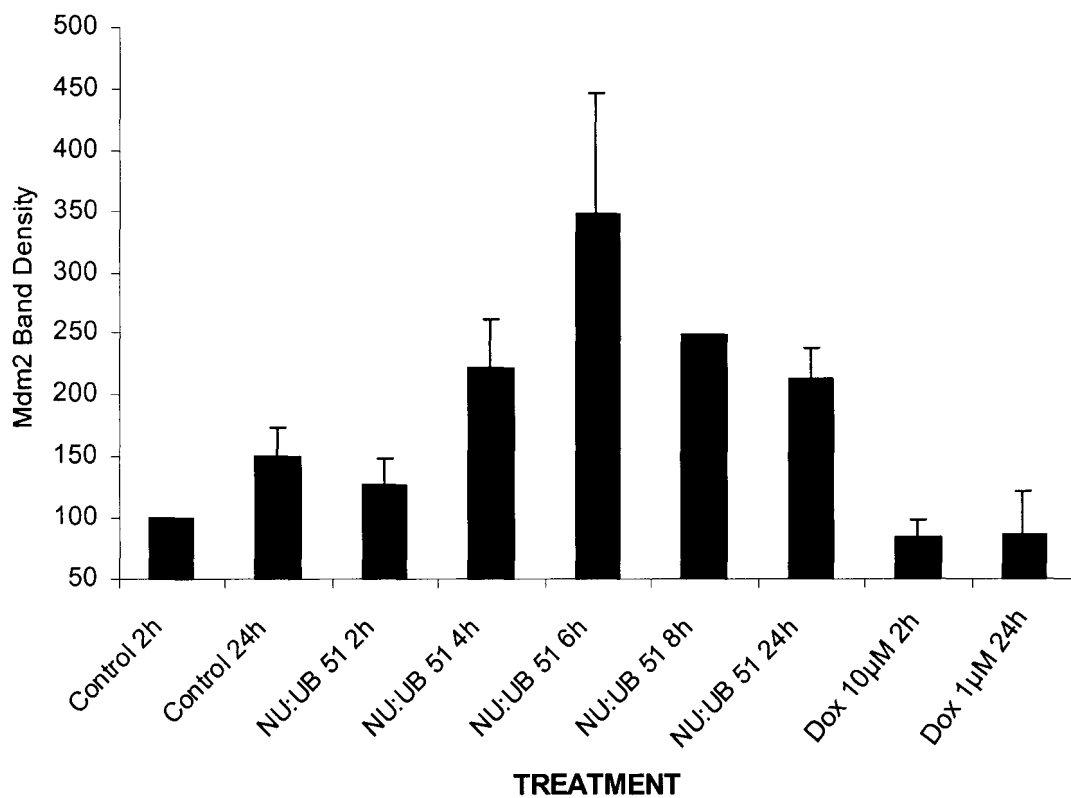


**Fig 7.7b** Time course of mdm2 levels in HCT116 cells treated with NU:UB 51 (10µM) or doxorubicin (Dox) (10µM for 2h, or 1µM for 24h). Results are the mean of three or more separate Western blot experiments  $\pm$  SEM (with the exception of NU:UB 51 8h and doxorubicin 10µM 2h where n=2).

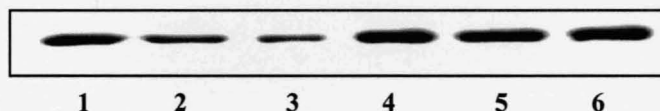


**Fig. 7.8a** 24h exposure. Western blot of p21 levels in HCT116 cells following NU:UB 31 or doxorubicin treatment. Doxorubicin (lane 1), NU:UB 31 20 $\mu$ M (lane 2), Control (lane 3), Doxorubicin 0.35 $\mu$ M (lane 4), NU:UB 31 20 $\mu$ M (lane 5), Control (lane 6). The figure is representative of three separate experiments.

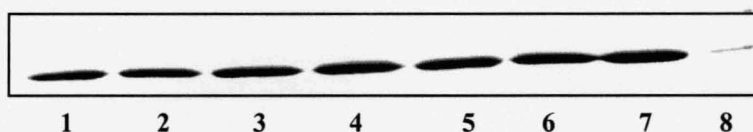


**Fig. 7.8b** 24h exposure. Western blot of p21 levels in HCT116 cells following NU:UB 31 or doxorubicin treatment. Cells grown in 1%, 5% or 10% FBS. Doxorubicin 0.35 $\mu$ M, 5% FBS (lane 1), NU:UB 31 20 $\mu$ M 5% FBS (lane 2), Control 5% FBS (lane 3), Doxorubicin 0.35 $\mu$ M 10% FBS (lane 4), NU:UB 31 20 $\mu$ M 10% FBS (lane 5), Control 10% FBS (lane 6), Control 1% FBS (lane 7), Biotinylated marker (lane 8). The figure is representative of two separate experiments.



**Fig 7.8c** Time course. Western blot of p21 levels in HCT116 cells following NU:UB 31 treatment. Control 4h (lane 1), NU:UB 31 20 $\mu$ M 4h (lane 2), NU:UB 31 20 $\mu$ M 8h (lane 3), NU:UB 31 20 $\mu$ M 12h (lane 4), NU:UB 31 20 $\mu$ M 24h (lane 5), Control 24h (lane 6). The figure is representative of three separate experiments.

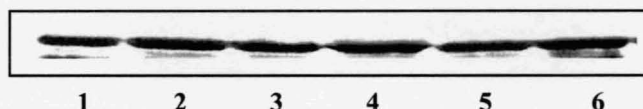


**Fig 7.8d** Time course. Western blot of p21 levels in HCT116 cells following NU:UB 51 treatment. Control 4h (lane 1), NU:UB 51 10 $\mu$ M 4h (lane 2), NU:UB 51 10 $\mu$ M 8h (lane 3), NU:UB 51 10 $\mu$ M 12h (lane 4), NU:UB 51 10 $\mu$ M 24h (lane 5), NU:UB 51 5 $\mu$ M 24h (lane 6). The figure is representative of three separate experiments.

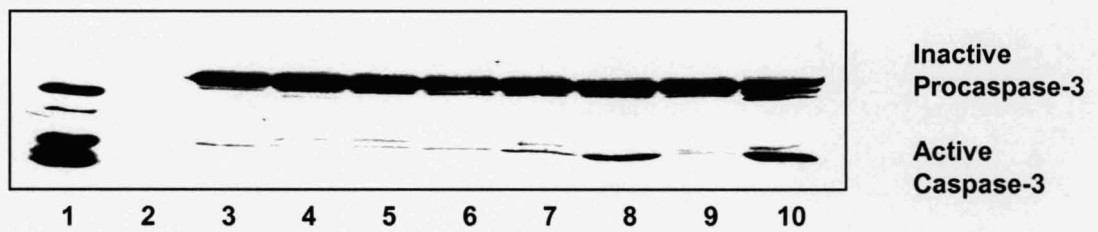


**Fig. 7.9a** Time course. Western blot of procaspase-3 levels in HCT116 following NU:UB 31 or doxorubicin treatment. Biotinylated marker (lane 1), colour marker (lane 2), control 1h (lane 3), doxorubicin 10μM 1h (lane 4), NU:UB 31 20μM 1h (lane 5), NU:UB 31 20μM 4h (lane 6), NU:UB31 20μM 8h (lane 7), NU:UB 31 20μM 24h (lane 8), control 24h (lane 9), doxorubicin 1μM 24h (lane 10). The figure is representative of three separate experiments.

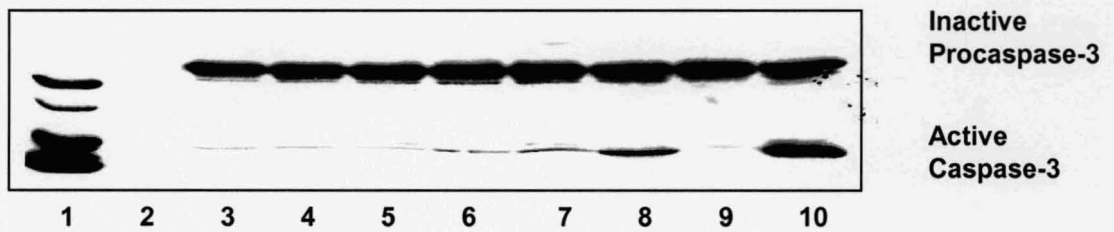


**Fig. 7.9b** Time course. Western blot of procaspase-3 levels in HCT116 following NU:UB 51 or doxorubicin treatment. Biotinylated marker (lane 1), colour marker (lane 2), control 1h (lane 3), doxorubicin 10μM 1h (lane 4), NU:UB 51 10μM 1h (lane 5), NU:UB 51 10μM 4h (lane 6), NU:UB 51 10μM 8h (lane 7), NU:UB 51 10μM 24h (lane 8), control 24h (lane 9), doxorubicin 1μM 24h (lane 10). The figure is representative of three separate experiments.

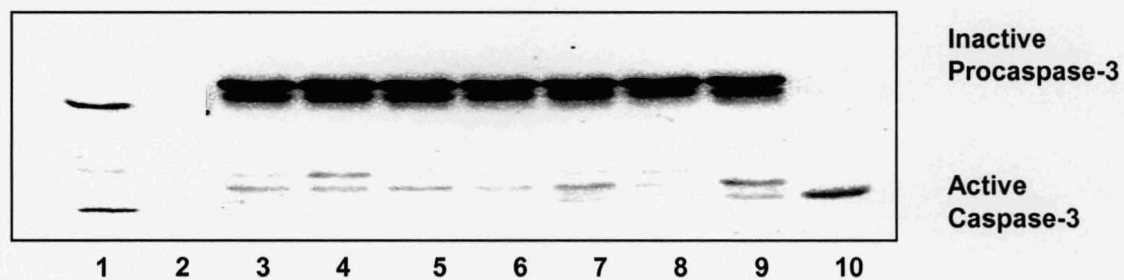


**Fig. 7.9c** Time course. Western blot of procaspase-3 levels in HL60 cells following NU:UB 31, NU:UB 51 or camptothecin treatment. Biotinylated marker (lane 1), colour marker (lane 2), NU:UB 31 20µM 4h (lane 3), NU:UB 31 20µM 8h (lane 4), NU:UB 31 10µM 24h (lane 5), control 24h (lane 6), NU:UB 51 5µM 4h (lane 7), NU:UB 51 5µM 8h (lane 8), NU:UB 51 5µM 24h (lane 9), camptothecin 0.5µM 24h (lane 10). The figure is representative of three separate experiments.

## 7.4 DISCUSSION

Apoptosis and cell cycle arrest have been investigated in cells exposed to NU:UB compounds and these investigations have been presented within this thesis. The morphological and biochemical investigations performed implied that cells exposed to NU:UB agents died by apoptosis (Chapter 6). In this part of the project, apoptotic cell death was further investigated by examining what happens in cells on a protein level when exposed to NU:UB compounds. P53 was one of the proteins studied to determine, whether or not p53 was induced by NU:UB compounds, and if so, how rapidly this induction was detected. For the cancer therapeutic area, the role of p53 in apoptosis is probably more important than its role in arresting the cell cycle. It has been suggested that p53 plays a crucial role in apoptotic cell death in the response to chemotherapeutics, but the p53-dependent pathway is not the only mechanism of apoptosis, since p53-independent pathways may also play meaningful roles. Evidence that apoptosis can be induced in cells regardless of p53 status was obtained in our earlier apoptotic studies where HL60 cells containing no p53 were used. P53 protein levels were studied in HCT116 cells following treatment with NU:UB 31, NU:UB 51 and known topoisomerase inhibitors. In our untreated HCT116 cells there was none, or very low levels of p53 that were increased upon doxorubicin treatment. This indicated that these cells contained wild type p53, which was also in agreement with previous research by O'Connor *et al.* (1997). In contrast, the untreated as well as the

doxorubicin treated HT29 cells had high p53 levels and were therefore thought to contain mutant p53.

Time course Western blot experiments measuring p53 protein levels over 24h were performed. This revealed that p53 protein levels in HCT116 cells exposed to NU:UB 31 or NU:UB 51 increased, compared to controls following 2-8h treatment. After the p53 peak at 2-8h the levels dropped, and were similar to control levels at the 24h time point. Thus, following treatment with NU:UB compound, the p53 concentration increased, reached a maximum, and then decreased. This decrease in p53 concentration could however be a consequence of degradation of the NU:UB compound. To evaluate this possibility in future work, the medium containing the NU:UB agent could be removed and replaced, for example every 4h with medium containing fresh NU:UB compound. By doing this, the p53 levels may not decrease but instead remain high. It may also be feasible that the NU:UB compound was effluxed from cells via resistance mechanisms, and/or repair mechanisms might operate allowing cells to recover from drug damage and thereby decrease the p53 expression. P53 levels following doxorubicin treatment were not increased much following 2h, but reached significantly higher levels after 24h treatment, which was not the case following NU:UB treatment. The highest level of p53 following NU:UB treatment was still lower than the levels induced by 24h doxorubicin exposure. It might be that for NU:UB compounds, the mechanism of action does not only involve the p53 pathway.

The relationship between the cytotoxicity of these compounds *in vitro* and the p53 status of the cell lines used has also been examined by NCI. From screening commonly used clinical anticancer agents in the NCI *in vitro* screen for p53 gene status, it was determined that most of these agents appeared to rely on intact p53 function for optimum potential (Monks *et al.*, 1997; Weinstein *et al.*, 1997). The relationship between cell line sensitivity to the NU:UB compounds (NU:UB 31, NU:UB 43, NU:UB 80 and NU:UB 81) and expression of wild type or mutated p53 was examined in a range of NCI cell lines (p244-248). The topoisomerase inhibitor, doxorubicin was also included in this cell screen. The GI<sub>50</sub> value for each cell line was plotted as a scattergram of drug cytotoxicity versus mutant or wild type p53. From each drug scattergram two median GI<sub>50</sub> values were deduced, a wild type and a mutant median GI<sub>50</sub> and the difference in these values were compared for each drug. The study showed that the standard drug was overall more potent than the NU:UB compounds, with lower GI<sub>50</sub> values. Moreover, doxorubicin sensitivity in wild type cell lines was far greater, compared to mutant cell lines. This was not the case for any of the NU:UB compounds, the sensitivity to the NU:UB compounds being similar in wild type and mutant cell lines, suggesting that these compounds may be able to circumvent p53-reliant cell death pathways.

Current research of different strategies, exploiting the p53 pathway in cancer treatment has recently been summarised by Lane and Lain (2002). The identification of molecules able to restore the function of mutant p53 should be an interesting approach due to the high number of cancers with mutated p53

protein. It was found that several of the mutations of p53 reduce its stability (Bullock *et al.*, 1997), causing it to misfold and mutant p53 lacks the stable conformation required for proper DNA binding (Friedlander *et al.*, 1996b). Bykov *et al.* (2002) hypothesised that reactivation of p53 in tumours with mutant p53 would trigger massive apoptosis, eliminating the tumour cells, and that normal cells expressing low levels of p53 should not be affected. To prevent incorrect p53 folding, Foster *et al.* (1999) identified several small compounds with the following features in common; a hydrophobic part, a linker in-between and a positively charged cationic part that would fit into and stabilise faulty p53. Among these molecules, CP-31398 rescued mutant p53 by stabilizing the active conformation of newly synthesised mutant p53 and as a result, the p53 protein was allowed to regain its tumour suppressive function. In a study by Luu *et al.* (2002) using CP-31398, it was demonstrated that this p53-stabilizing molecule induced apoptosis via bax upregulation, mitochondrial membrane potential alterations and caspase-9 and caspase-3 activation in wild type p53 containing HCT116 cells. In contrast, HCT116 cells devoid of p53 were more or less resistant to CP-31398 induced apoptosis, further supporting the p53-mediated effects of this agent. (It remains to be determined, however, whether or not this agent induces apoptosis in mutant p53 containing cancer cells). Another low molecular weight compound, PRIMA-1 (p53 Reactivation and Induction of Massive Apoptosis), that restored the active p53 conformation, reactivating mutant p53 has also been identified. This compound restored p53-dependent apoptosis in cells containing mutant p53. Growth of cells expressing mutant p53 was inhibited, but there was only a slight effect on cells without mutant p53. Additionally, the

two target genes, p21 and mdm2 were induced exclusively in the presence of mutant p53 but not in HCT116 cells containing wild type p53. However, whereas *in vitro* PRIMA-1 treatment resulted in apoptosis, evidence of growth suppression was seen *in vivo*. Likewise, following *in vivo* CP-31398 administration, induction of p21 was reported. Thus, it may be that growth arrest rather than apoptosis occurs following the *in vivo* administration of these compounds, and it may be more beneficial *in vivo* also to induce pro-apoptotic genes in addition to p21 (Fojo, 2002).

The above research may be of relevance to our study of NU:UB agents, since the NU:UB compounds have a broadly similar structure to some of the molecules identified by Foster *et al.* (1999) in terms of the component parts which may constitute a generalisation pharmacophore. However, whether NU:UB agents act via a similar mechanism, reactivating mutant p53 needs to be further investigated. Our cytotoxic screen of HL60 (p53 null), HCT116 (p53 wild type) and HT29 (p53 mutant) cells did not show striking evidence that the HT29 cells containing mutant p53 were significantly more sensitive to NU:UB 31, 51 nor 80 than the other cells (see Chapter 4). Rather the sensitivity to the NU:UB compounds appeared similar in the wild type and the mutant cell line, which was also reflected in the NCI GI<sub>50</sub> data (see Appendix 2).

Overexpression of mdm2 leads to inhibition of the tumour suppressor activity of p53. Inhibitors of the p53-mdm2 interaction might therefore be attractive agents for the treatment of tumours that overexpress mdm2 but contain functional wild type p53. The aim of a p53-mdm2 inhibitor approach would

thus be to find compounds that could be used as drugs to release wild type p53 from the p53-mdm2 complex. This should then be beneficial for treating certain cancers in which an mdm2 related pathway of p53 inactivation is in operation. The subsequent inhibition of p53 degradation should induce p53 accumulation and possibly cell death by apoptosis. Different groups of researchers have successfully used this approach. For example Chène *et al.* (2000) used an octamer synthetic peptide, referred to as AP peptide in their studies, showing that this small peptide inhibited the p53-mdm2 interaction *in vitro*. When assayed in HCT116 cells this peptide was further found to induce p53 accumulation, as well as accumulation of the two p53 gene products p21 and mdm2. Cells overexpressing mdm2 are good targets for inhibitors of the p53-mdm2 interaction, and the AP peptide was also found to induce apoptosis as measured by caspase-3 activation, in tumour cells that over expressed mdm2. The AP peptide was also compared to the standard agent cisplatin, and the data obtained suggested that AP might activate p53 differently from DNA damaging agents, as measured by p53 phosphorylation on serine 15. Zhao *et al.* (2002) utilized computer aided design to develop a small non-peptidic compound that in tumour cell lines inhibited the p53-mdm2 interaction, activating the p53 pathway which leads to caspase-3 induction and apoptosis. Mdm2 was reported to be induced by p53 (Barak *et al.*, 1993). Since NU:UB compounds induced p53 accumulation, we were interested to see if there was induction of mdm2. By investigating up-regulation of downstream mediators of p53 (mdm2 and p21) we also hoped to confirm the p53 induction observed. As for p53, mdm2 protein levels were investigated in the HCT116 cell line. The data showed that following 4h treatment, mdm2 started

to accumulate, and that maximum accumulation was achieved after 4-8h treatment of HCT116 cells following a single dose of NU:UB compound. These studies suggested that the increased mdm2 levels at 4-8h, were sequential to decreased p53 levels. In future studies it may be of interest to use cells that overexpress mdm2 (and contain wild type p53) to see if p53 and other proteins involved in apoptotic pathways are increased following treatment, since tumours overexpressing mdm2 are good targets for inhibitors of the p53-mdm2 interaction. For doxorubicin there was no significant increase in mdm2 despite high p53 levels after 24h treatment. Thus, it may be that doxorubicin remains active and stable during the course of the experiment and the p53 levels remain high, and the mdm2 levels low. A longer time course may be required to detect mdm2 upregulation following doxorubicin treatment.

Like mdm2, p21 is also a transcriptional target of p53. The major role of p21 is in cell cycle arrest, preventing the progress of a cell through the G1 checkpoint, hence cell growth is inhibited with the over expression of p21 (El-Deiry *et al.*, 1993). It is generally believed that wild type p53 is required for DNA damaging chemotherapeutics to induce p21. The level of p21 protein was investigated in HCT116 cells following drug treatments. In the HCT116 cells used here there were basal levels of p21 present in controls, but in comparison there was no significant increase in p21 levels in HCT116 cells following 24h drug treatment. The reason for this could be that either p21 was induced and cell cycle arrested in all cells, including control cells; or that the drug concentration and/or exposure time were not optimum for this cell line to

see p21 upregulation; or that in contrast these drugs do not work by inducing p21, and arresting the cell cycle in this cell line. Since the p53 upregulation following NU:UB treatments was fairly rapid and brief, shorter exposure times were attempted for our p21 studies. However, no significant p21 induction was seen with these HCT116 cells at any of the time points used, following NU:UB compound treatment. That NU:UB 31 may not act by arresting the cell cycle was also suggested in our earlier cell cycle analysis investigations (Chapter 5), where there was no evidence of a permanent cell cycle block following NU:UB treatment.

P53-responding caspases include caspase-3, and it has been suggested that p53-mediated apoptosis could involve caspase-3. To confirm the findings from our apoptotic caspase-3 study (recorded in Chapter 6) we investigated procaspase-3 cleavage using Western blotting. Using HL60 and HCT116 cells, we found that there were active caspase-3 protein bands present following NU:UB 31 and NU:UB 51 treatments, at 4h and 8h respectively in the two cell lines. Although an increase in caspase-3 protein levels following NU:UB treatment was observed, there was not much of a decrease in the density of the inactive procaspase-3 bands. This has, however, previously been reported by Li *et al.* (1999). This group found that p53 mediated apoptosis involved activation of caspases, but procaspase-3 detected by Western blotting was not cleaved although caspase-3 activity could be detected.

In summary, p53, mdm2 and caspase-3, but not p21 protein levels were increased as measured by Western blotting in HCT116 cells following NU:UB treatment. The level of p53 protein increased early and briefly by NU:UB treatments. The p53 increase was then followed by an increase in the level of mdm2 protein. Following doxorubicin exposure (24h) the p53 levels were higher than at any point throughout the time course of NU:UB compound treatment, and no mdm2 up-regulation was observed. That the p53 induction following NU:UB treatment was brief suggests that the compound might be degraded and/or effluxed from the cells.

## **CHAPTER 8**

### **INTRACELLULAR DRUG ACCUMULATION STUDIES**

## 8.1 INTRACELLULAR DRUG ACCUMULATION STUDIES

Several of the NU:UB compounds have a red colour, and also showed a strong red fluorescence when viewed under the UV fluorescent and the confocal microscopes. This allowed us to directly observe where the NU:UB agents were located in cells following treatment. In this chapter, the results of drug localisation studies have been presented, in an attempt to deduce in which cellular compartment(s) these NU:UB agents accumulate. For this purpose, cells were also stained with Hoechst stain and with fluorescent probes labelling mitochondria and lysosomes. We further intended to study mitochondrial disruptions following NU:UB treatments with the MitoCapture kit, a mitochondrial membrane potential indicator. We have focused on NU:UB 31, but NU:UB 80 and doxorubicin were also used for intracellular drug distribution observations, and betulinic acid was used in mitochondrial disruption investigations.

It was originally thought that mitochondria were not involved in apoptosis since the morphology of these organelles remained intact, and cells lacking mitochondrial DNA can undergo apoptosis. However, mitochondria are these days thought to play an important part in apoptosis and it is now realised that major alterations in mitochondrial membrane functions do take place during the apoptotic process. Drugs can affect the mitochondrial function in many ways. For example, by inhibiting the electron transport chain, or by uncoupling of oxidative phosphorylation, which means that there is no production of ATP

or by oxidative damage to mitochondrial DNA. Opening of mega-channels in the inner mitochondrial membrane (IMM) that lead to swelling and collapse of the mitochondrial transmembrane potential is another feasible mechanism for drug toxicity (Krahenbuhl, 2001). Mitochondrial changes are early events (Metivier *et al.*, 1998; Castedo *et al.*, 2002), likely to take place in cells that still retain normal light scattering characteristics (side/forward scatter) before they have shrunk and formed apoptotic bodies. Hence, preceding the appearance of the characteristic morphologically apoptotic features it has been reported that there are disruptions in the mitochondrial transmembrane potential of the cells, and partial disruption of mitochondria along with release of cytochrome c are thought to be early signs of apoptosis. Thus, mitochondrial disruption may be, although not necessarily, a sign of a drug targeting mitochondria, but could also be an early general indication of apoptosis.

Apoptosis may be induced by different classes of anti-cancer agents by acting on different cellular targets and by activating distinct signalling pathways. If a compound accumulates in cellular mitochondria, targeting components of this organelle, this is likely to cause disruptions in mitochondria. There are compounds that are thought to directly act on the mitochondria, inducing apoptosis and betulinic acid is an example of such an agent and has been included in the present study. Betulinic acid is a triterpene of natural origin isolated from tropical plants. This compound has shown anti-cancer activities but its clinical activity is yet to be established. By directly targeting mitochondria, betulinic acid might be able to bypass the requirement for

upstream signalling, and may therefore still be effective against tumour cells that have a defect in upstream apoptosis pathways and therefore do not respond to classical drugs. Furthermore, growth inhibition following betulinic acid treatment has been reported to be independent of p53 status (Zuco *et al.*, 2002; Fulda *et al.*, 1997; Fulda *et al.*, 1998). In this light, mitochondria may potentially be promising intracellular targets for drug delivery in cases where, for example, the classical topoisomerase inhibitors targeting nuclear enzymes fail to induce a response in cells with defects in their nuclear-originating apoptotic pathway(s). Mitochondria have long been known to contain their own DNA and this has been highlighted as a possible drug target in conjunction with its associated nuclear enzymes that are now known to include a non-nuclear type I topoisomerase (Zhang *et al.*, 2001).

## **8.2 METHODS**

### **8.2.1 NU:UB And Doxorubicin Distribution In HL60 Cells**

Throughout the experiments described in this chapter, HL60 cells were seeded at a density of  $10 \times 10^4$  cells/ml and left to recover overnight before being used.

Cells were left untreated (control) or treated with NU:UB 31 or NU:UB 80 for 0h, 1h, 2h, 4h and 24h. A concentration of  $10\mu\text{M}$  was chosen for NU:UB 31 to give a bright red fluorescence, and to be suitable for the time course. NU:UB 80 was also used at  $10\mu\text{M}$ , and doxorubicin at  $10\mu\text{M}$  and  $1\mu\text{M}$  for 0h and 24h respectively. Following treatments the cells were washed in HBSS, then resuspended in a total volume of  $50\mu\text{l}$  to get a high cell density. Each sample was then put onto glass slides and viewed using the confocal microscope (Nikon Eclipse TE 2000-U) at 60x oil immersion.

### **8.2.2 Localisation Of The Nucleus In HL60 Cells Treated With NU:UB 31 Or Doxorubicin**

To localise the nucleus, the cells were stained with Hoechst 33342 Stain. Cells were treated with NU:UB 31 ( $10\mu\text{M}$ ) or doxorubicin ( $10\mu\text{M}$ ) for 1h. Drugs were washed off and cells were stained in Hoechst stain ( $100\mu\text{g/ml}$  stock

diluted 1/100) for 5 mins and were then viewed under the confocal microscope at 60x oil immersion.

### **8.2.3 MitoTracker Green And Hoechst Staining Of NU:UB 31**

#### **Treated HL60 Cells**

We set out here to investigate if NU:UB 31 enters mitochondria. The mitochondria in HL60 cells were labelled with MitoTracker green FM (Molecular Probes). MitoTracker probes exist in several colours and green was chosen to be able to distinguish this green colour from the red NU:UB fluorescence. Cells were probed with MitoTracker according to manufacturers instructions. Briefly, MitoTracker green was dissolved in DMSO to a stock of 1mM. For the MitoTracker green probe a concentration range was suggested of 20-200nM and an incubation time of 15-45 mins. We chose an incubation time of 30 mins, made a series of dilutions of the MitoTracker probe and found that 50nM was sufficient to visualise the mitochondria in HL60 cells. Treated (NU:UB 31, 1h at 10 $\mu$ M) and untreated cells (solvent) were washed in pre-warmed HBSS, pelleted by centrifugation 500 x g, 5 mins and resuspended in fresh pre-warmed 37 $^{\circ}$ C HBSS (or medium) containing the MitoTracker at 50nM. Cells were incubated for 30 mins in the dark at 37 $^{\circ}$ C. To visualise the nucleus, cells were centrifuged 500 x g, 5 mins and resuspended in Hoechst stain (100 $\mu$ g/ml stock diluted 1/100) for an additional 5 mins. There was no wash step included in this protocol since the MitoTracker probe only becomes fluorescent once accumulated in the lipid environment of mitochondria and there is therefore no problem with background fluorescence. Following

Hoechst staining, cells were pelleted and resuspended in 50µl of pre-warmed HBSS. The green MitoTracker was not suitable for fixing so the cells were viewed immediately in the confocal microscope (Ex 490 nm, Em 516 nm).

#### **8.2.4 Investigation Of Mitochondrial Disruption In HL60 Cells With A MitoCapture Kit Using Flow Cytometry**

Mitochondrial function can be measured with JC-1, a lipophilic cationic fluorescent probe that was used in the MitoCapture assay. When JC-1 is in its monomeric form it emits green fluorescence. On the contrary, at a high mitochondria transmembrane potential that can be achieved in functioning mitochondria, JC-1 forms multimers (J-aggregates), which upon excitation emits red/orange fluorescence. Upon mitochondrial disruption there is a resulting decrease in red J-aggregate fluorescence and this decrease is likely mirrored by an increase in green JC-1 monomers (Cossarizza *et al.*, 1993; Bradbury *et al.*, 2000). Betulinic acid is an agent that is thought to target the mitochondria directly and thereby induce apoptosis. We sought to investigate whether or not NU:UB 31 directly targets mitochondria, disrupting the mitochondrial membrane potential as a possible mechanism of inducing cell kill. For this purpose a mitochondrial membrane potential indicator, a MitoCapture kit was used (BioVision). Since we wanted to study if NU:UB 31 had an immediate effect on mitochondria, short exposure times were used. A recent study of mitochondrial disruption in osteosarcoma cells using JC-1 reported that there was a loss in mitochondrial transmembrane potential after 1h treatment with staurosporine (1µM), and further that this loss was over the

same time course as caspase-3 activation (Jiang *et al.*, 1999). We had previously seen caspase-3 activation following 4h treatments, and therefore a 4h exposure time was used in this MitoCapture study, as well as a shorter exposure time of 1h. Thus, cells were left untreated (solvent), treated for 1h, or treated for 4h with NU:UB 31 or betulinic acid. NU:UB 31 was used at 20 $\mu$ M, 30 $\mu$ M or 40 $\mu$ M, based on previous IC<sub>50</sub> results for the HL60 cell line. Betulinic acid was included for comparison in these experiments and was used at 20 $\mu$ M (10 $\mu$ g/ml) or 40 $\mu$ M (20 $\mu$ g/ml). For the MitoCapture assay the manufacturers instructions were followed. Briefly, untreated (solvent), NU:UB 31 and betulinic acid treated HL60 cells (1 x 10<sup>6</sup> cells per sample) were washed and resuspended in 1ml fresh MitoCapture containing pre-warmed incubation buffer (provided with the kit, 1 $\mu$ l MitoCapture/ml buffer). The samples were allowed to incubate with the MitoCapture stain in the dark for 1h at 37°C. Following staining the cells were washed in the provided MitoCapture wash buffer, resuspended in pre-warmed incubation buffer and immediately analysed in flow cytometry. The MitoCapture stain is red or green depending on its localisation. In normal, viable cells the MitoCapture stain enters, remains in mitochondria and shows red fluorescence. Upon mitochondrial disruption the stain enters cytoplasm and fluoresces green. It was anticipated that if NU:UB 31 caused mitochondrial disruptions, an increase in green fluorescence and a decrease in the red fluorescent signal would be observed. Green monomer versus red aggregate fluorescence was measured on the FL1 (Ex 488nm, Em 530nm) and FL2 (Ex 488nm, Em 590nm) channels respectively.

## **8.2.5 LysoTracker Green And Hoechst Staining Of NU:UB 31**

### **Treated HL60 Cells**

We sought to investigate if NU:UB 31 accumulated in lysosomes using LysoTracker green DND-26 (Molecular Probes) to visualise these acidic organelles. Weak bases are thought to selectively accumulate in cellular compartments with low internal pH e.g. lysosomes. LysoTracker green consists of a fluorophore linked to a weak base that can freely penetrate cell membranes and concentrate and thereby labelling the acidic organelles in living cells. LysoTracker green was used according to manufacturers instructions. Briefly, the LysoTracker was provided in vials of 1mM in DMSO and was further diluted to in pre-warmed culture medium. A 45 mins incubation time was chosen, a series of LysoTracker dilutions was made and 50nM was found sufficient in this assay. Untreated (solvent) and treated (NU:UB 31 1h at 10  $\mu$ M) HL60 cells were washed in pre-warmed HBSS, resuspended in 1ml pre-warmed HBSS containing 50nM LysoTracker green and incubated for 45 mins in the dark at 37°C. Cells were resuspended in Hoechst stain (100 $\mu$ g/ml stock diluted 1/100) for 5 mins. Following centrifugation, 500 x g, 5 mins, each sample was resuspended in 50 $\mu$ l pre-warmed HBSS and was then viewed in the confocal microscope (Abs 504nm, Em 511nm).

## **8.3 RESULTS**

### **8.3.1 Time Course Of NU:UB 31, NU:UB 80 Or Doxorubicin Treated HL60 Cells**

Confocal microscope images over a time course ranging from 0 to 24h of drug accumulation (NU:UB 31 and NU:UB 80) are given in Fig. 8.1 and Fig. 8.2. This study indicated that the NU:UB compounds, which have a bright red colour (white in Fig. 8.1 and Fig. 8.2), seem to enter the cellular cytosol immediately following treatment. NU:UB localisation looked similar at all time points, but these NU:UB agents did not seem to enter all areas of the cells (a black space in cells was observed). Cells treated with doxorubicin show that this drug is also readily taken up, but its localisation patterns differ from that of NU:UB agents (Fig. 8.3). Considering that NU:UB 31 accumulation appeared to remain the same throughout the time course, we chose a 1h exposure time in further localisation experiments.

### **8.3.2 Hoechst Staining Of NU:UB 31 Treated HL60 Cells To Visualise The Nucleus**

To identify drug localisation in relation to the nucleus in NU:UB 31 treated cells Hoechst 33342 stain was used. Fig 8.4 shows that the black space with no red NU:UB 31 fluorescence present is the nucleus of the cell. Thus, there

was no fluorescence from NU:UB 31 in this area of the cell, the red fluorescence was instead seen in the cytosol. This appeared to be the case throughout the 24h exposure time. Doxorubicin did however appear to reach, and accumulate in the nucleus instantly and remained here at the 24h time point (Fig. 8.3).

### **8.3.3 MitoTracker And Hoechst Staining Of NU:UB 31 Treated Cells**

Next we sought to identify organelles in the cytosol in which NU:UB 31 accumulated. The mitochondria were the first organelles to be studied, NU:UB compounds were synthesised to intercalate and groove bind into DNA, interacting with DNA topoisomerases, and mitochondria contain their own DNA (and are thought to have topoisomerase activity). To visualise mitochondria in the cells, MitoTracker green was used. Fig. 8.5 shows green mitochondria in untreated HL60 cells, the nucleus was stained blue with Hoechst stain. In Fig. 8.6 NU:UB 31 treated HL60 cells were observed. NU:UB 31 was bright red (a), the blue Hoechst stain located the nucleus (b) and the green MitoTracker revealed the localisation of mitochondria (c). Fig. 8.6d is a merged picture of the three above and from this as well as the zoomed image in Fig. 8.7, it seems that the main concentration of NU:UB 31 did not accumulate in the mitochondria. However, this does not exclude the possibility that NU:UB 31 reached the mitochondria, as there seems to be lower levels of NU:UB 31 within these organelles and throughout the cytosol.

### **8.3.4 Investigation Of Mitochondrial Disruption In HL60 Cells With A MitoCapture Kit**

An attempt to investigate if NU:UB 31 targets mitochondria directly was made using the MitoCapture kit. Betulinic acid was used as a positive control in these experiments as this agent is has been found to work primarily on mitochondria in its mechanism of action. Untreated and treated cells were stained in MitoCapture stain and analysed by flow cytometer. Untreated cells stained both green and red and therefore in treated cells with damaged mitochondria, a drop in the red signal and increase in green signal would be expected as the stain would remain as monomers in the cytosol rather than aggregating in mitochondria. In cells treated for 1h, there was no change compared to respective control following NU:UB 31 nor betulinic acid treatments (Fig. 8.8, Fig. 8.9a, Fig. 8.9b). The lack of mitochondrial damage could have been due to too short an exposure time, however following 40 $\mu$ M NU:UB 31 treatment there appeared to be cells killed, with a lot of material with low green and low red fluorescence (Fig. 8.8d). Treating the cells for 4h with betulinic acid 40 $\mu$ M resulted in a drop in red fluorescence compared to control, indicating that these cells have damaged mitochondria, however the green remained the same (Fig. 8.9c, Fig. 8.9d). Following 4h NU:UB 31 exposure (20 $\mu$ M and 30 $\mu$ M) there was rather an increase in red fluorescence compared to control (Fig. 8.10). It might be that NU:UB 31 did not affect mitochondria. However, since NU:UB 31 has a bright red fluorescence, it is likely that NU:UB 31 interfered with the red MitoCapture colour which would explain the increase in red fluorescence compared to control. This red

interference presented problems, but it was thought that there would be an increase in green fluorescence as an indication of mitochondrial membrane disruptions. This was, however, not the case in this assay, even following treatment with betulinic acid. Without a change in green signal it was not possible to use this stain to investigate possible mitochondrial membrane disruptions caused by NU:UB 31. In summary, betulinic acid showed a drop in red signal (but no change in green) and could therefore be used as a positive control of mitochondrial disruption. NU:UB 31 was however, red like the MitoCapture stain, and this assay was therefore not suitable for NU:UB 31 (or other red compounds). Any conclusions whether NU:UB 31 targets mitochondria or not could not be drawn using the MitoCapture assay.

### **8.3.5 LysoTracker And Hoechst Staining Of NU:UB 31 Treated HL60 Cells**

The green LysoTracker stain reveals the localisation of lysosomes in HL60 cells. Lysosomes in untreated HL60 cells are seen in Fig. 8.11. Cells were treated for 1h with 10 $\mu$ M NU:UB 31 in Fig. 8.12 and Fig. 8.13. From this study it seemed that the main localisation of NU:UB 31 coincided with the green LysoTracker stain within the cells, and thus it appeared that the drug accumulated in acidic compartments in cells, which mainly were lysosomes. Although a lot of the drug seemed to be taken up by lysosomes, NU:UB 31 may also reach other organelles within the cell.

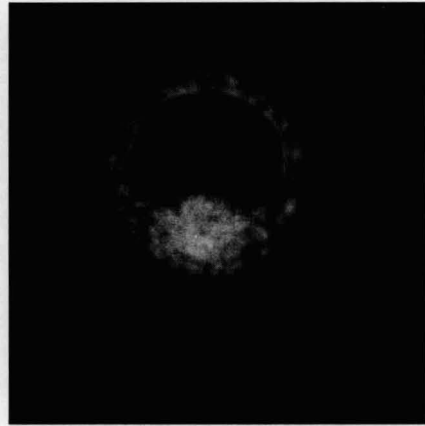
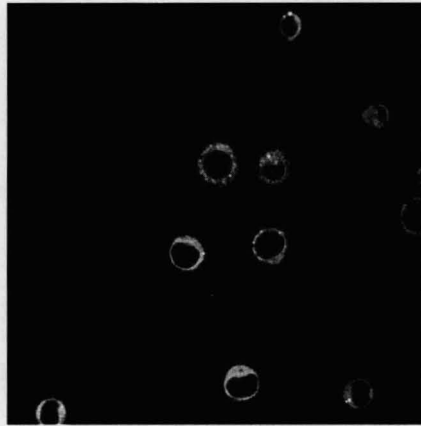


**Fig. 8.1a** NU:UB 31 10 $\mu$ M, viewed immediately

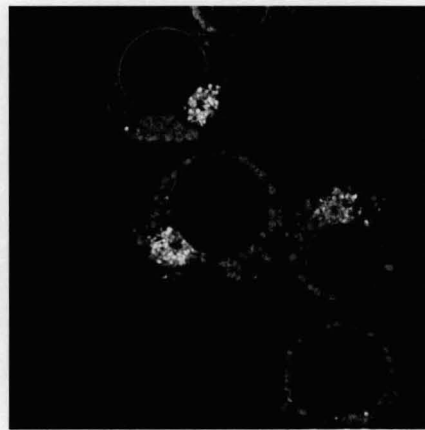
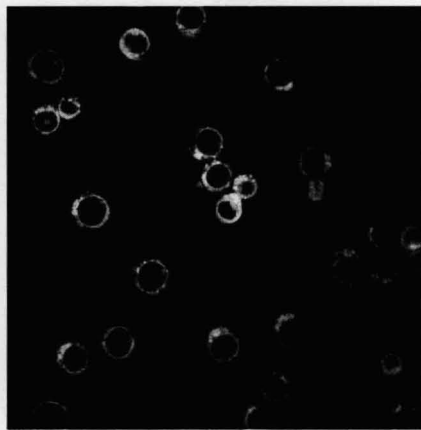


**Fig. 8.1b** NU:UB 31 10 $\mu$ M 1h

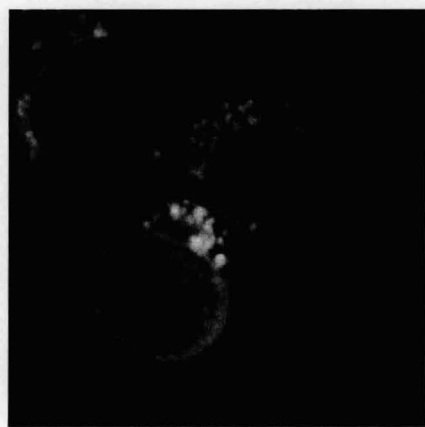
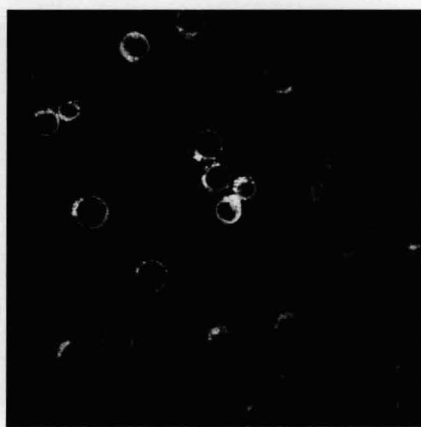


**Fig. 8.1c** NU:UB 31 10 $\mu$ M 2h

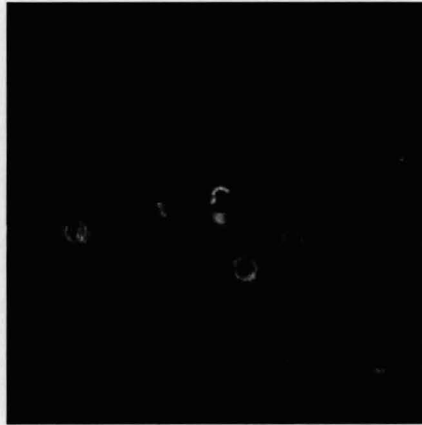


**Fig. 8.1d** NU:UB 31 10 $\mu$ M 4h

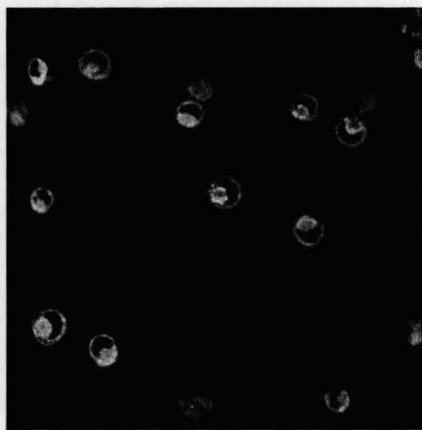
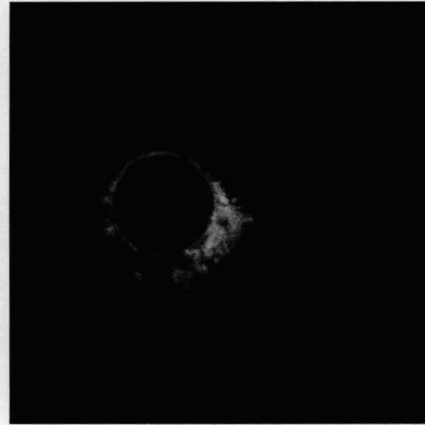


**Fig. 8.1e** NU:UB 31 10 $\mu$ M 24h

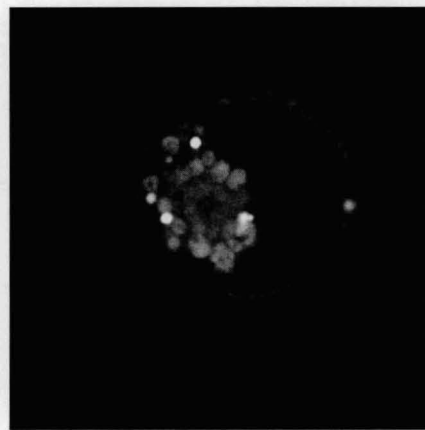


**Fig. 8.1a-e** Time course of HL60 cells treated with NU:UB 31 for 0h (a), 1h (b), 2h (c), 4h (d) and 24h (e) and viewed under confocal microscope with 60x magnification, or 60x magnification and zoomed 4 times. White represents the red NU:UB 31 fluorescence.

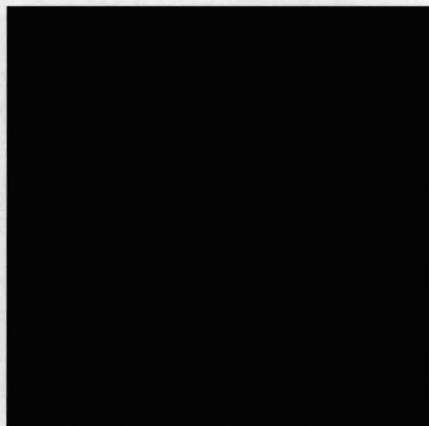


**Fig. 8.2a** Control

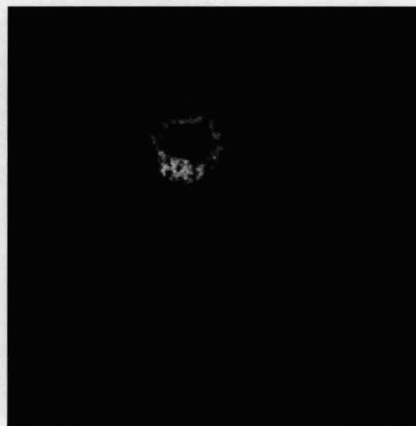


**Fig. 8.2b** NU:UB 80 10µM,  
viewed immediately



**Fig. 8.2c** NU:UB 80 10µM 1h

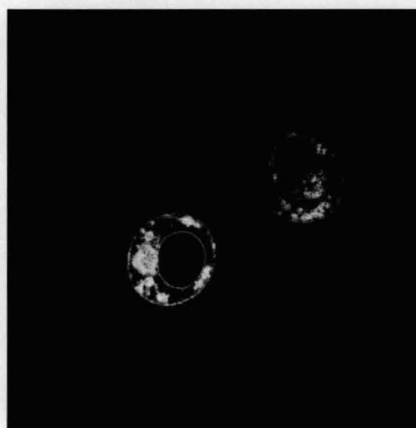


**Fig. 8.2d** NU:UB 80 10µM 2h

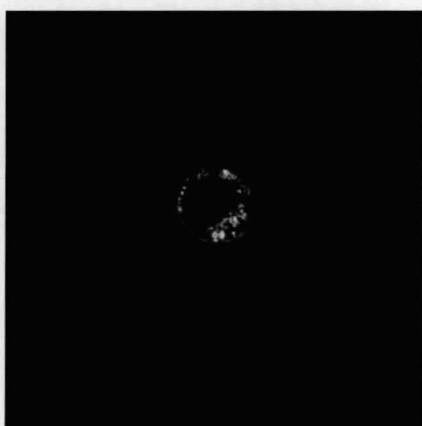


**Fig. 8.2e** NU:UB 80 10µM 4h

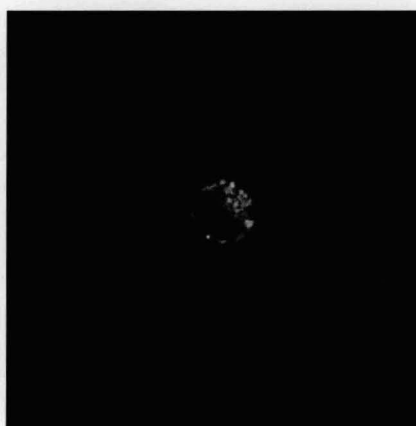


**Fig. 8.2f** NU:UB 80 10µM 24h

**Fig. 8.2a-f** Time course of HL60 cells treated with NU:UB 80 for 0h (a), 1h (b), 2h (c), 4h (d) and 24h (e) and viewed under confocal microscope with 60x magnification. White represents the red NU:UB 80 fluorescence.

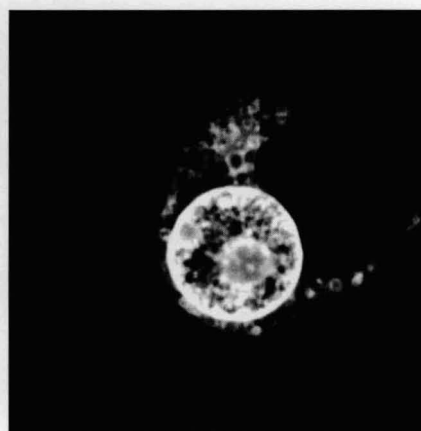


**Fig. 8.3a** Doxorubicin 10 $\mu$ M, viewed immediately

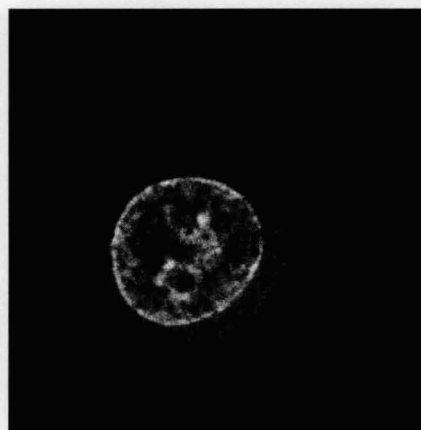
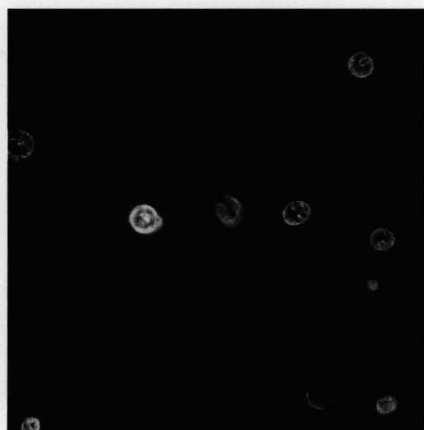


**Fig. 8.3b** Doxorubicin 10 $\mu$ M 24h

**Fig. 8.3a-b** Time course of HL60 cells treated with Doxorubicin for 0h (a) as well as 24h (b) and viewed under confocal microscope at 60x magnification, or at 60x magnification with 4 times zoom. White represents the red doxorubicin fluorescence.

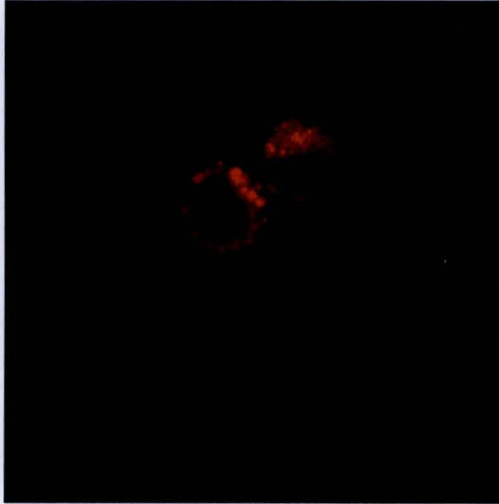


**Fig. 8.4a** NU:UB 31 10 $\mu$ M 1h



**Fig. 8.4b** Hoechst stain in NU:UB 31 treated cells

**Fig. 8.4a-b** NU:UB 31 (10 $\mu$ M, 1h) treated HL60 cells viewed under confocal microscope. The same HL60 cells, where red (a) shows NU:UB 31 localisation, and blue Hoechst stain visualises the nucleus (b) in these cells. NU:UB 31 was not found in the blue, Hoechst stained nucleus. These cells were viewed under confocal microscope at 60x magnification.

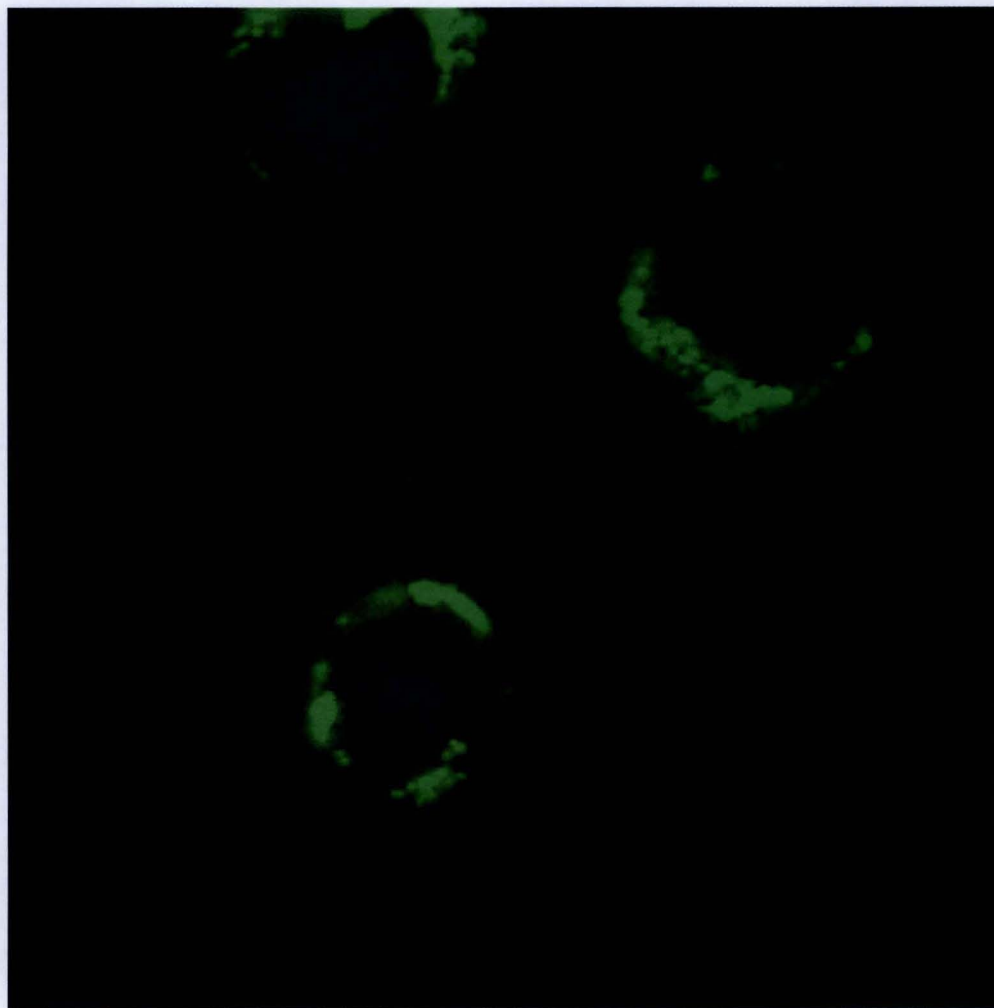


**Fig. 8.5** Confocal microscope picture of untreated HL60 cells. Hoechst stained nucleus (blue) and MitoTracker green stained mitochondria (green). 60x magnification, zoomed 4 times

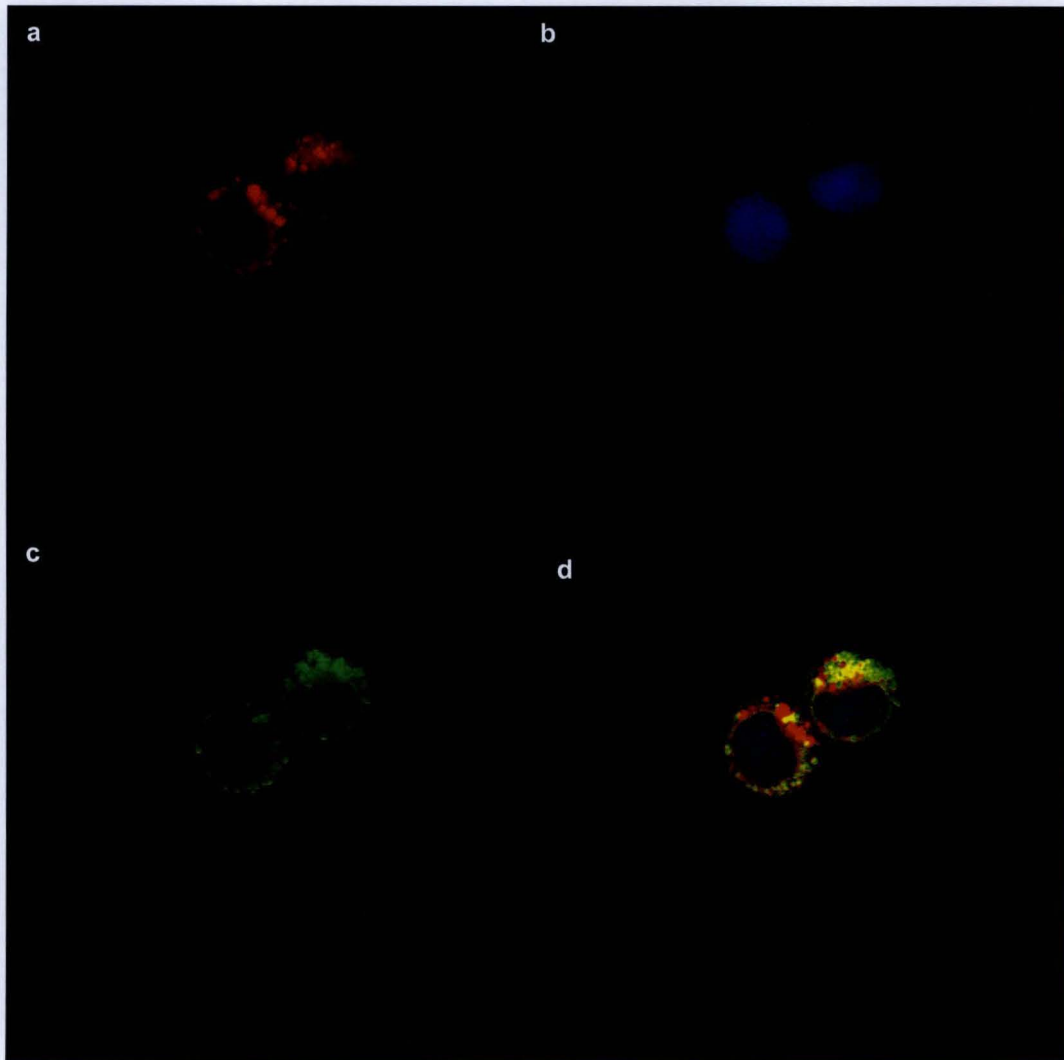


**Fig. 8.6a-d** Confocal microscope pictures of 1h NU:UB 31 (10 $\mu$ M) treated HL60 cells. NU:UB 31 localisation (a), Hoechst stained nucleus (b), MitoTracker green (c) and merged picture of the three above (d). 60x magnification.

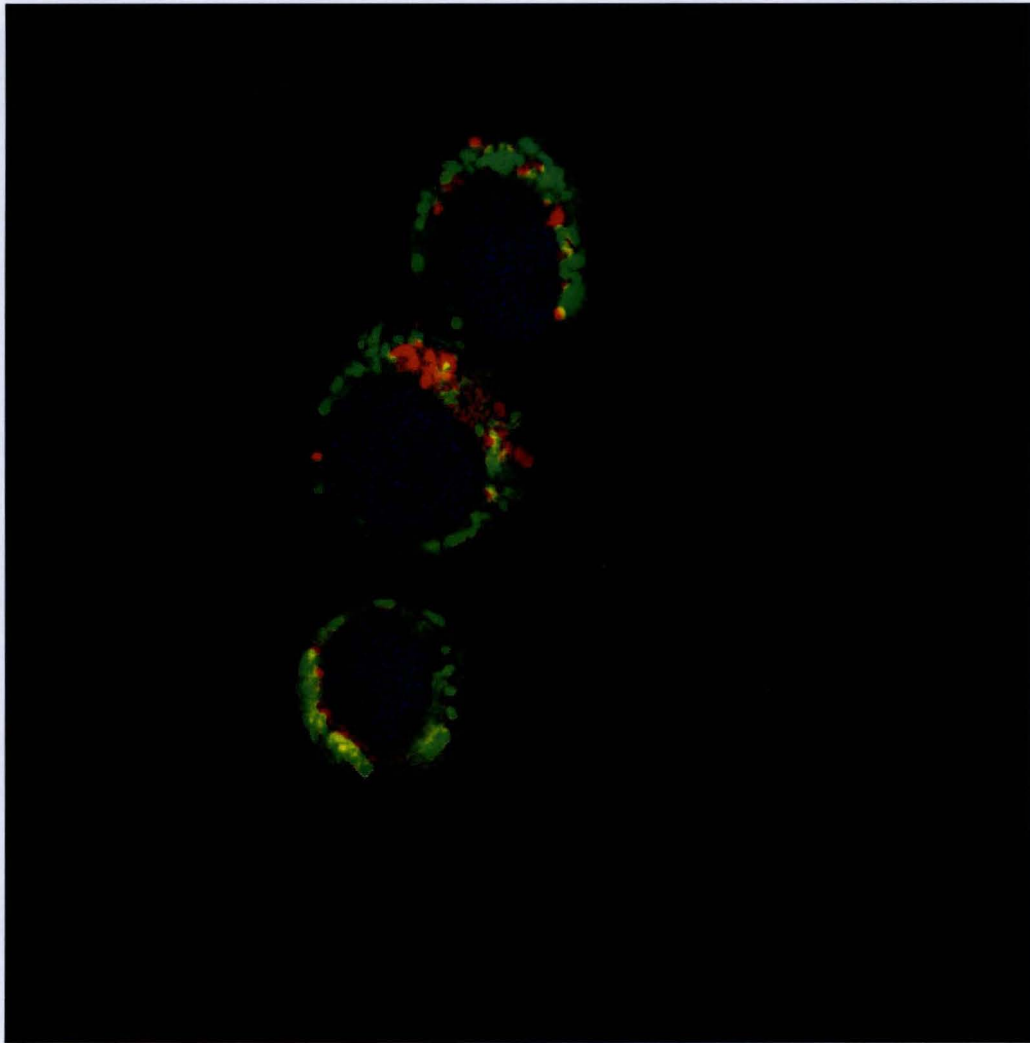


**Fig. 8.7** Confocal microscope picture of NU:UB 31 (10 $\mu$ M, 1h) treated HL60 cells. NU:UB 31 localisation (red), Hoechst stained nucleus (blue) and MitoTracker green stained mitochondria (green). 60x magnification, zoomed 4 times

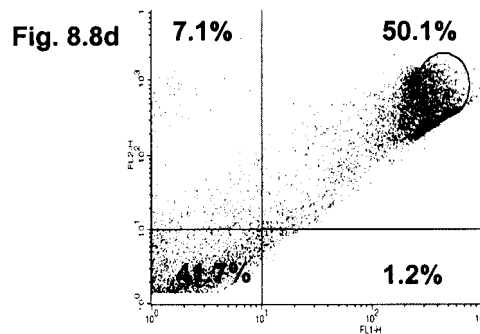
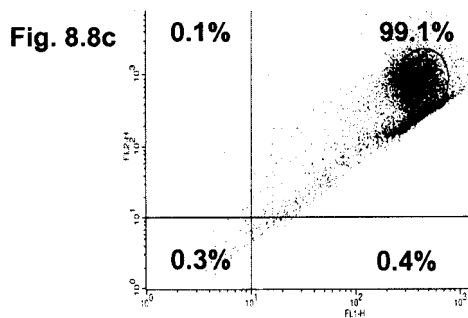
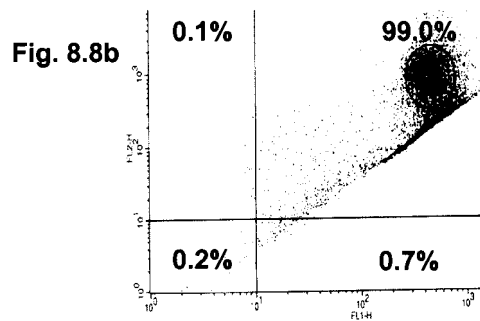
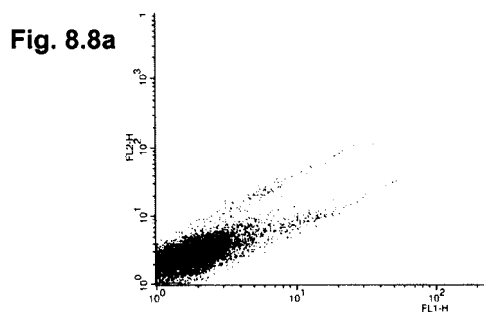


**Fig. 8.8a-d** Flow cytometer cytograms of MitoCapture stained HL60 cells. Unstained cells (a), Stained control cells 1h (b), NU:UB 31 20µM 1h (c), NU:UB 31 40µM 1h (d). Treatments were carried out for 1h, cells were washed and left to recover for 4h.

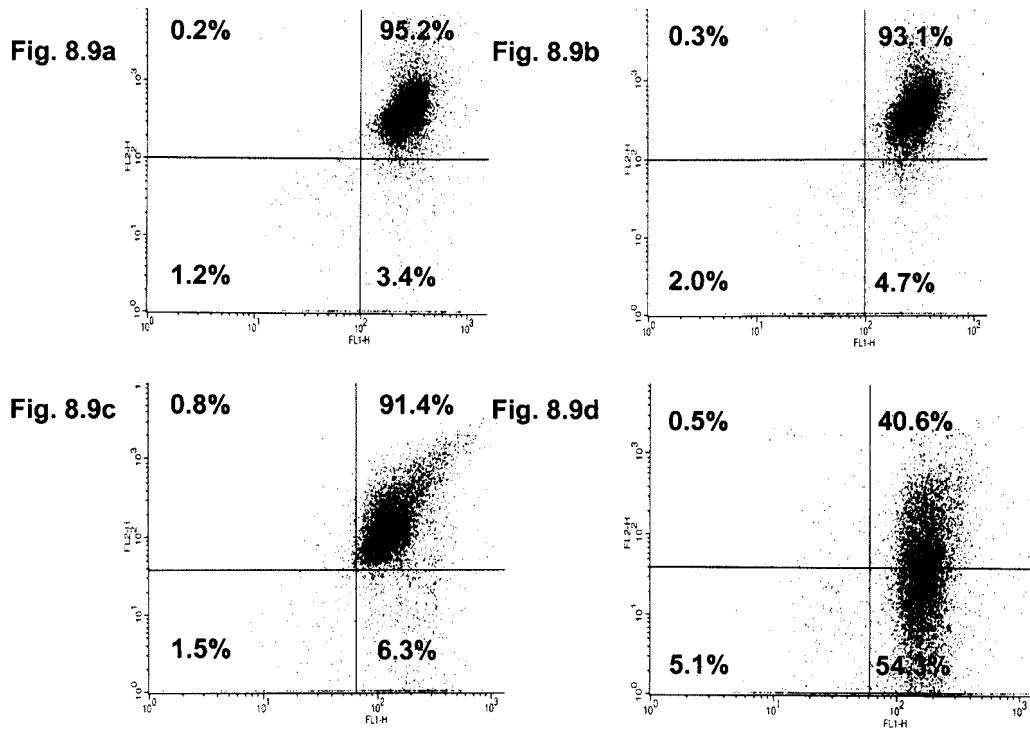


**Fig. 8.9a-d** Flow cytometer cytograms of MitoCapture stained HL60 cells. MitoCapture stained control cells 1h (a), betulinic acid 40 $\mu$ M 1h (b), Stained control cells 4h (c), betulinic acid 40 $\mu$ M 4h (d).

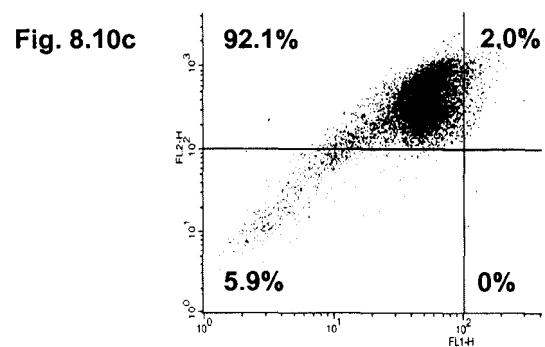
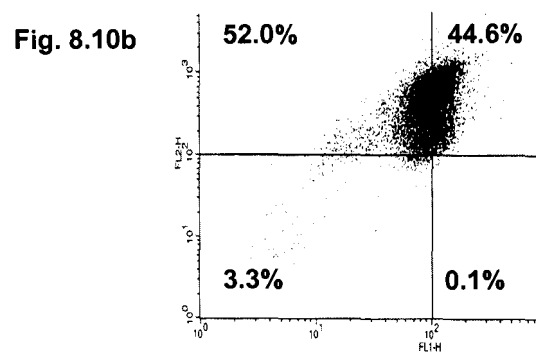
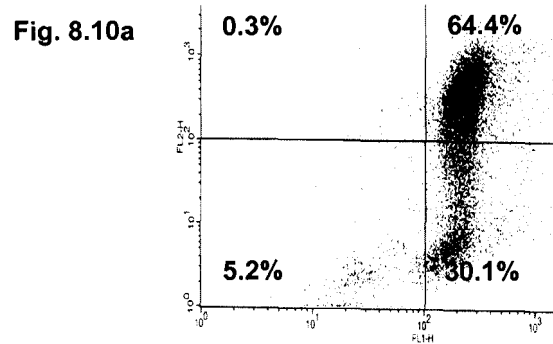


**Fig. 8.10a-c** Flow cytometer cytograms of MitoCapture stained HL60 cells. MitoCapture stained control cells 4h (a), NU:UB 31 20µM 4h (b), NU:UB 31 30µM 4h (c).

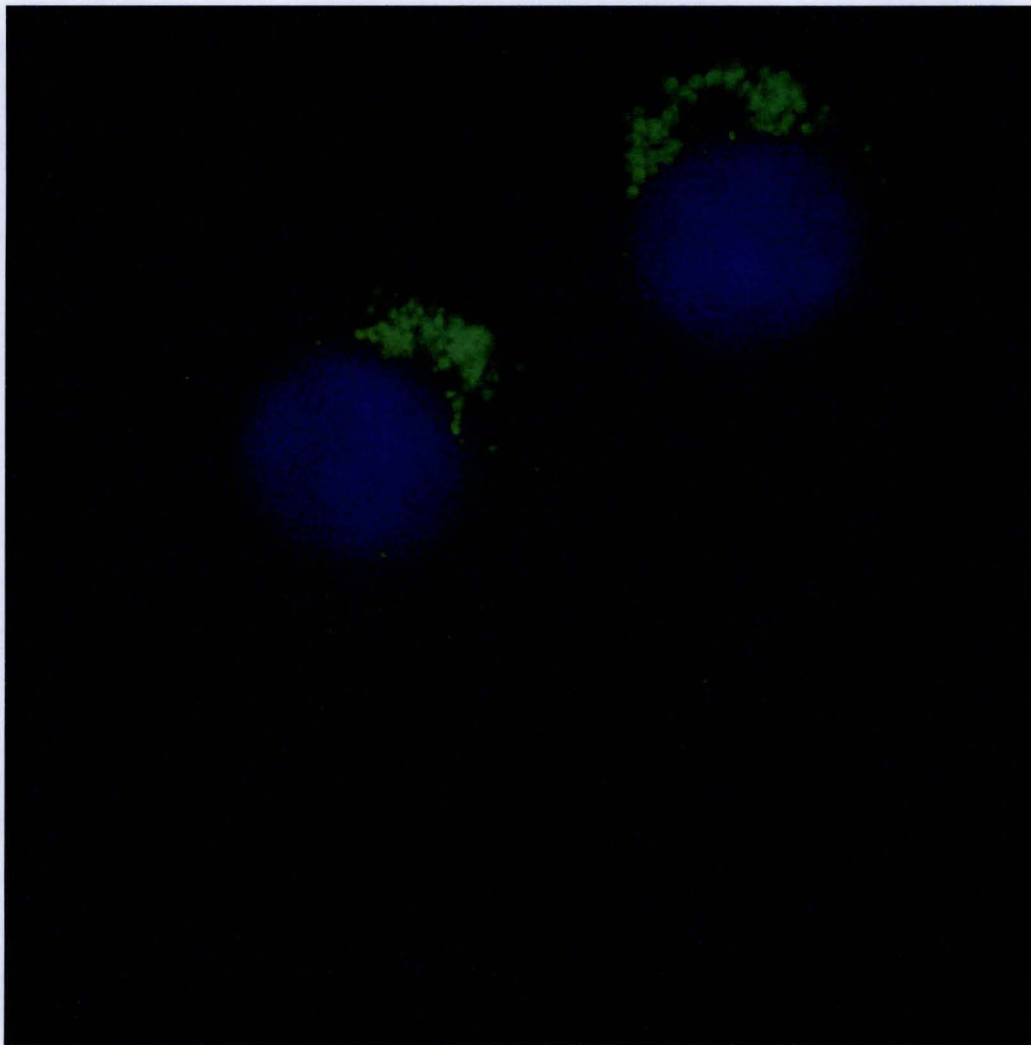


**Fig. 8.11** Confocal microscope picture of untreated HL60 cells. Hoechst stained nucleus (blue) and LysoTracker green stained lysosomes (green). 60x magnification, zoomed 4 times.

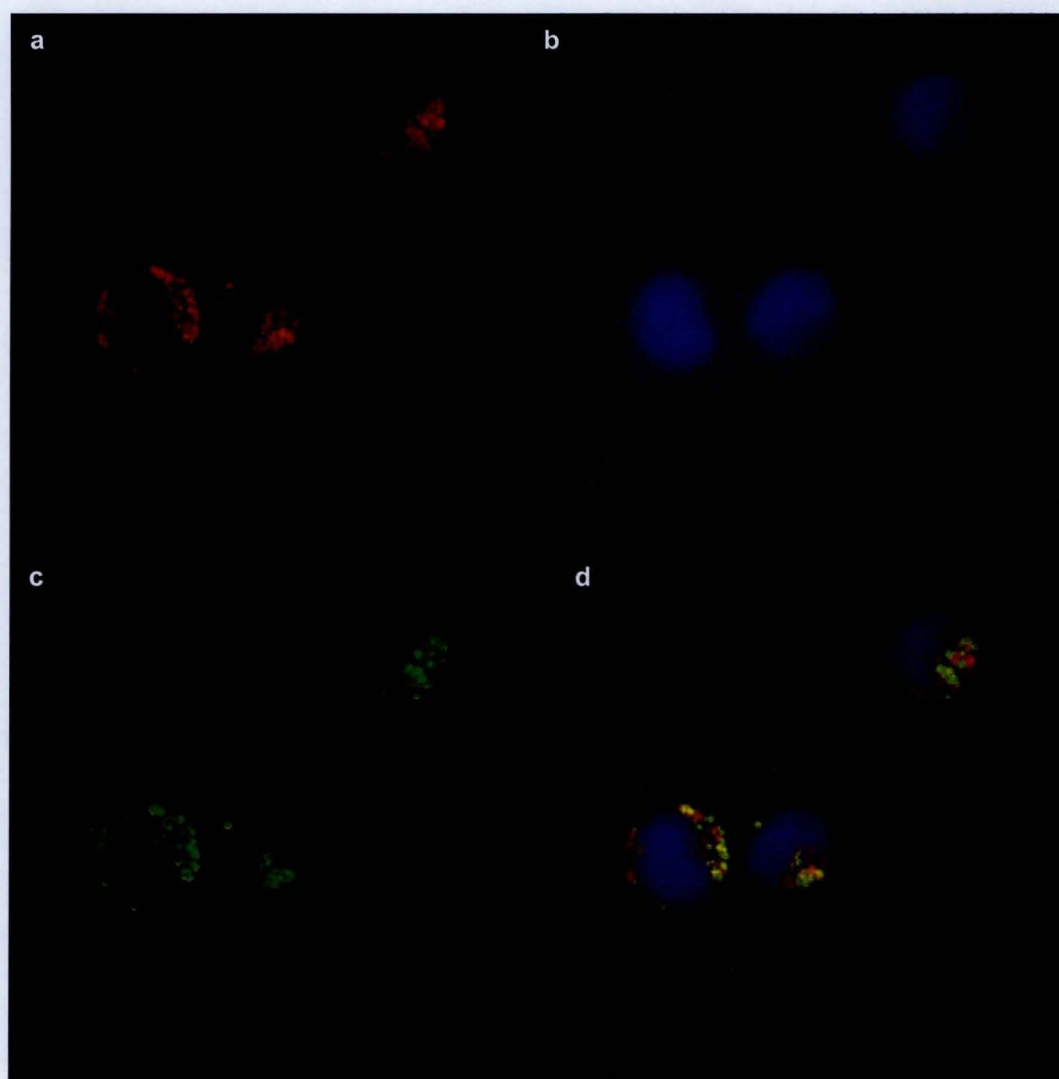


**Fig. 8.12a-d** Confocal microscope pictures of 1h NU:UB 31 (10 $\mu$ M) treated HL60 cells. NU:UB 31 localisation (a), Hoechst stained nucleus (b), LysoTracker green (c) and merged picture of the three above (d). 60x magnification.

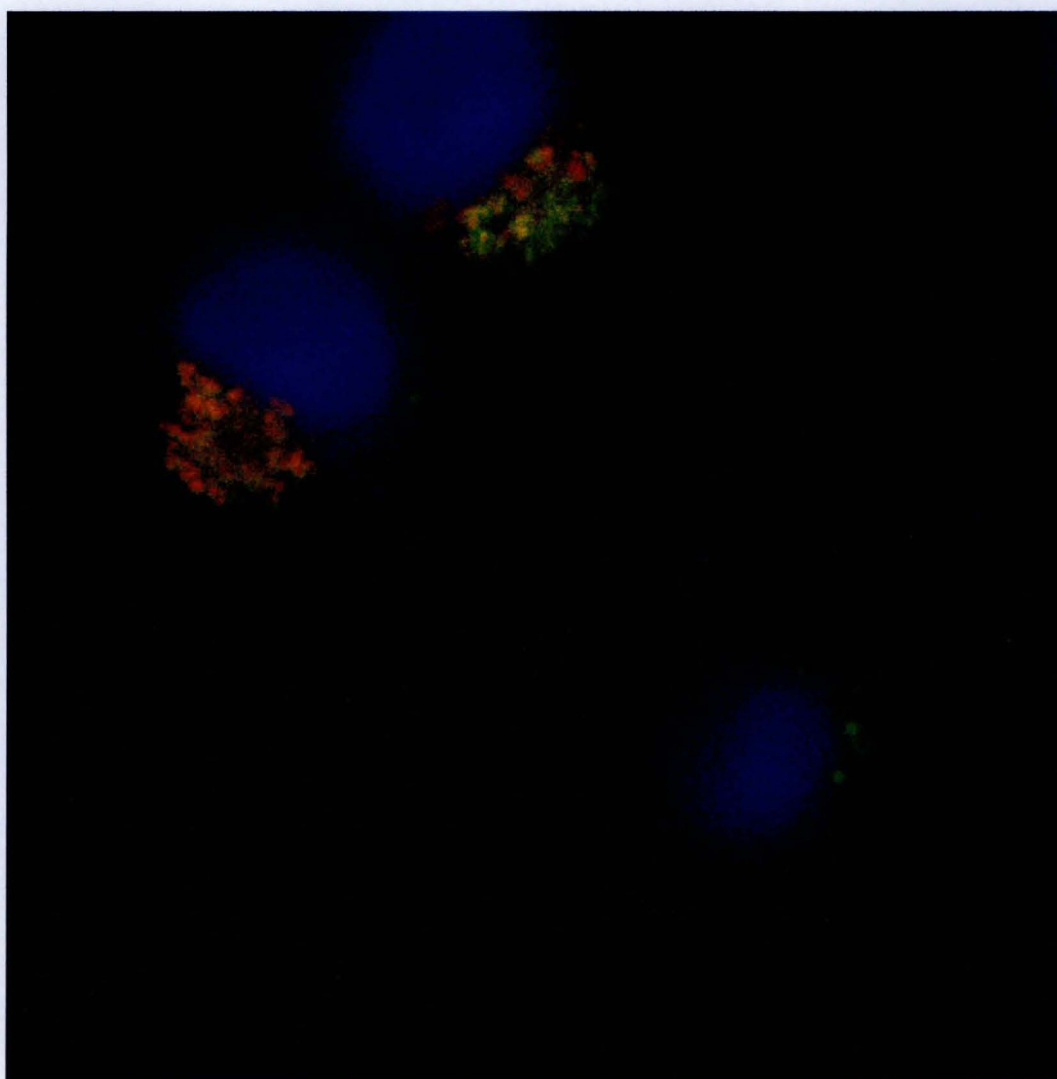


**Fig. 8.13** Confocal microscope picture of NU:UB 31 (10 $\mu$ M, 1h) treated HL60 cells. NU:UB 31 localisation (red), Hoechst stained nucleus (blue) and LysoTracker green stained lysosomes (green). 60x magnification, zoomed 4 times.

## 8.4 DISCUSSION

The confocal microscope observations and images presented in this chapter revealed intracellular sites where NU:UB (NU:UB 31 and NU:UB 80) and doxorubicin fluorescence was seen. All agents were rapidly taken up into cells. When comparing the fluorescence patterns of doxorubicin and NU:UB compounds, these differed, but the fluorescence from each agent appeared to remain the same at the various time points. Whereas the main fluorescence from doxorubicin was found in the nucleus, confirmed with Hoechst stain, the NU:UB agent fluorescence was not seen in this location. Rather, for the two NU:UB compounds, the fluorescence was observed in the cytoplasm, with the brightest fluorescence found in small circular compartments within the cytoplasm. The NU:UB agents had however been synthesised to interact with their proposed targets, nuclear DNA and DNA topoisomerases. No red fluorescence was confirmed with Hoechst stain to be within the nucleus. Thus, in contrast to doxorubicin, the NU:UB agents did not appear to reach the nucleus, the localisation of their intended topoisomerase targets. This would imply that these do not target nuclear DNA and nuclear topoisomerases, and their mechanism of action would then not be what it was designed to be. Other explanations for the lack of fluorescence in the nuclear region include: Firstly, when NU:UB 31 (or NU:UB 80) reaches acidic vesicles and organelles such as lysosomes, the compound is broken down. The bright red fluorescence would then originate from this degraded species rather than from the intact NU:UB 31 (or NU:UB 80). Intact NU:UB 31 would then not fluoresce

within the cell, and may thus be located in the nuclear region where no red fluorescence was observed. Secondly, a more feasible phenomenon, that was observed by others is quenching. NU:UB 31 could reach the nucleus as well as other sites within the cell. However, upon reaching and intercalating DNA its conformation would then change so that it no longer fluoresces. Tkaczyk-Gobis *et al.* (2001) studied anticancer agents (BP1, BP2 and BP3) from the benzoperimidine family, a family supporting a flat conjugated ring system that is likely intercalated between the base pairs of DNA. Upon adding these fluorescent compounds to whole cells, cell nuclei or to naked DNA there was a decrease in the fluorescence, and this quenching of the fluorescence signal was here thought here to be due to the drug-DNA interaction. Like these drugs, the NU:UB compounds, also consist of rings and therefore a similar quenching mechanism may take place when NU:UB compounds interact with DNA. However, doxorubicin is also made up of a ring system that is known to intercalate DNA, yet the doxorubicin fluorescence was readily observed. It is likely that doxorubicin accumulated in the nucleus at very high concentrations, so that although quenching may occur, this did not prevent the detection of doxorubicin fluorescence in the nucleus. Hence, NU:UB agents may not accumulate in the nucleus at high concentrations, but low concentrations of NU:UB compound with quenched fluorescence may still reach and affect its nuclear target(s). However, in an earlier study by Lampidis *et al.* (1997) the quenching phenomenon of a series of anthracyclines was disputed. Cell nuclei were isolated and treated with different anthracycline analogues (exhibiting different lipophilic, charge and drug localisation properties), following treatment the drugs were extracted and assayed by HPLC. The

results were compared to microscopic observations of the anthracycline analogues and suggested that nuclear/DNA quenching did not alter the microscopic observations of nuclear/cytoplasmic localisation. Thus, in contrast to the finding by Tkaczyk-Gobis *et al.* (2001), the lack of drug fluorescence in nucleus in the study by Lampidis *et al.* (1997) did not appear to be due to DNA quenching but rather to an absence of drug in the nuclear compartment. Furthermore, it was also suggested that positive charge, along with degree of lipophilicity, influenced whether or not the anthracyclines were recognised by P-gp, and anthracycline analogues that localised in the cytoplasm rather than in the nuclear region of the cell were able to overcome MDR. Although absolute intracellular localisation to the nucleus or cytoplasm was not likely to occur with any of the anthracyclines they tested, a general pattern was suggested by Lampidis *et al.* (1997), that, with decreased affinity for binding DNA, anthracyclines shift in their primary localisation from nuclear to mitochondrial to diffuse cytoplasmic localisation. Thus, as lipophilicity increased and nuclear DNA binding properties of the studied anthracycline analogues decreased, the analogues seemed to distribute in mitochondria suggesting that mitochondria may pose as an anthracycline target, although this was not the case for doxorubicin, showing no mitochondrial localisation.

Further sub-cellular localisation studies suggested that the main NU:UB 31 fluorescence was contained within the cytoplasmic lysosomes, and possibly other acidic vesicles and organelles such as endosomes. Although the main fluorescence was thought to be within acidic organelles, this does not mean that NU:UB 31 does not at all reach other cytosolic compartments such as

mitochondria. Apart from the very bright red (possibly high concentrations of NU:UB 31) sites, NU:UB 31 seemed to be present at somewhat lower concentration throughout the cytosol. It may be that these levels at which NU:UB 31 is present throughout the cytosol are sufficient to have effect on other cytosolic targets. Possibly, the high intensity of NU:UB 31 that is seen, in what appear to be lysosomes is a mechanism used by the cells to exclude the NU:UB compound. Since many drugs target nuclear DNA and/or nuclear enzymes, distribution of drug into cytoplasmic organelles and vesicles may decrease the toxicity of a drug as a result of less drug-target interactions. Altered drug sequestration is often seen in resistant cells and from such studies different patterns of drug distribution in sensitive and MDR cells have been revealed (Hindenburgh *et al.* 1989). MDR cells are thought to express certain proteins acting as efflux pumps. P-gp is an example of such a protein associated with resistance. The increased expression of P-gp in the plasma membrane is the most consistent change detected in MDR cells, correlating with decreases in intracellular drug accumulation and increased drug resistance (Larsen *et al.*, 2000). While some of the transporters associated with resistance are capable of transporting drugs from the plasma membrane, others can transport drugs from the cytoplasm into vesicles, eventually resulting in drug exclusion (efflux). In a study by Hindenburgh *et al.* (1989), sensitive cells showed daunorubicin drug distribution into both the nucleus and the cytoplasm, whereas in resistant cells the drug had a cytoplasmic, dotted distribution, in what was possibly vesicles moving towards the plasma membrane. Thus, it may, in part be transporter proteins related to MDR that alter drug distribution and bring the intracellular drug concentration down.

However, if the drug concentrations were increased to levels that exceed the capacity of this transporter system, the intracellular drug concentrations may become toxic to cells. Additionally, in the case of altered drug distribution of weak lipophilic base topoisomerase inhibitors (including agents for the anthracyclines and anthracenediones e.g. daunorubicin, doxorubicin and mitoxantrone) a mechanism has been proposed (Larsen *et al.*, 2000). As long as a substantial fraction of these agents stay uncharged, as they are at normal intracellular pH (7.2-7.6), they can freely penetrate the membranes of cytoplasmic organelles. Once inside, for example, the acidic lysosomes (pH 4.8-5.2), these weak bases are thought to be converted into charged molecules that cannot escape. As a result, these drugs will be retained within the organelle, can therefore not reach their nuclear target(s) and will instead be excluded from the cell.

Although it is generally believed that cytotoxicity from anthracycline anti-cancer drugs such as doxorubicin is linked to interactions with nuclear DNA and topoisomerase II, the exact mechanism for inducing cell death and apoptosis is yet to be completely understood. Serafino *et al.* (1999) suggested that anthracycline mediated apoptosis was induced by interactions with both nuclear as well as cytoplasmic components. In this project we investigated NU:UB 31 accumulation in relation to mitochondria. Although NU:UB 31 to some degree was found throughout the cytoplasm it was more likely lysosomes, rather than the mitochondria that supported the main fluorescence from NU:UB 31. Mitochondria do however also contain their own DNA and topoisomerases. Recent publications have supported the idea that for

mitochondrial DNA metabolism such as replication, repair and transcription there is a requirement for mitochondrial topoisomerases. Mitochondrial topoisomerase I is further thought to be homologous to nuclear topoisomerase I so perhaps it is not surprising therefore that mitochondrial topoisomerase I was reported to be sensitive to camptothecin. However, whether or not mitochondrial topoisomerase I is a target for camptothecin, contributing to its cytotoxicity is still to be revealed (Zhang *et al.*, 2001; Wang *et al.*, 2002). Since mitochondria contain DNA and topoisomerases, it may be feasible that like nuclear effects, fluorescence quenching may take place within these organelles upon NU:UB 31 interaction. The faint red NU:UB 31 fluorescence in mitochondria may thus be due to fluorescence quenching rather than this compound not being present at high levels in the mitochondria. Therefore, despite there being no red fluorescence observed within nuclear DNA and faint fluorescence observed through out the cytosol including the mitochondria, neither the nucleus nor mitochondria can be fully excluded from being possible NU:UB agent targets. In a study by Bigioni *et al.* (2001) doxorubicin was compared to its disaccharide analogue (MEN 10755) in the context of cellular drug uptake, localisation and induction of DNA damage and apoptosis. It was found that higher concentrations of doxorubicin accumulated within the nucleus than its analogue. In spite of this, the disaccharide analogue induced more topoisomerase-mediated DNA damage than that produced by doxorubicin. This damage was possibly achieved through fewer but more long-lasting interactions with topoisomerase II (increased stabilisation of the cleavable complex). Furthermore, the doxorubicin analogue MEN 10755 appeared to accumulate in the cytoplasmic

compartment of the cell. Based on this, and the fact that this analogue was more effective than doxorubicin in inducing Bcl-2 phosphorylation mitochondria were suggested as an additional target of the MEN 10755 doxorubicin analogue. Strikingly, correlations of NU:UB agents with topoisomerase inhibitors as well as pyrimidine biosynthetic enzyme inhibitors in the NCI database have been made. NU:UB 31, 43, 80 and 81 were used as seeds to produce the LC<sub>50</sub> comparison table that can be found in appendix 5. In this table, Pearson correlation coefficients above 0.6 are considered to be statistically relevant. For the NU:UB agents there are coefficients above 0.6 making correlations between NU:UB agents and topoisomerase inhibitors and also between NU:UB agents and inhibitors of pyrimidine biosynthesis. Interestingly, pyrimidine synthesis take place in mitochondria (Baldwin *et al.*, 2002) and agents that interfere with this pathway should thus target components and enzymes participating in the mitochondrial pyrimidine biosynthesis pathway. An agent that regularly appears in correlation with NU:UB compounds is brequinar. Brequinar inhibits the pyrimidine biosynthesis pathway at the dihydroorotate dehydrogenase step (step 4 in pyrimidine biosynthesis) (McLean *et al.*, 2001). Thus, the cytotoxicities of NU:UB agents may partly be attributed to a common pathway to brequinar or to other mitochondria-targeted drugs, involving inhibition of dihydroorotate dehydrogenase or other enzymes involved in biosynthetic pathways taking place within the mitochondria. A deeper investigation of these possibilities is thus merited.

Several groups have used etoposide to investigate what effect(s) this topoisomerase drug has on mitochondria. The formation of free radicals, the release of cytochrome c, condensed mitochondria, reduced mitochondrial transmembrane potential, and the release of apoptogenic proteins have been identified following etoposide treatment (Kagan *et al.*, 1994; Chen *et al.*, 2000; Zhuang *et al.*, 1998; Meng *et al.*, 2000). It was also suggested by Custodio *et al.* (2001) that etoposide may induce mitochondrial permeability transition releasing mitochondrial apoptogenic factors, and their study showed the effects of etoposide on mitochondrial permeability transition *in vitro*. The authors concluded that the drug effects, as well as the side effects in normal cells *in vivo*, could be explained by etoposide induced mitochondrial permeability transition, mediating apoptotic cell death and/or ATP depletion. The mitochondrial transmembrane potential was investigated by Facompre' *et al.* (2000) using flow cytometry with cationic fluorescent probes. The relationship between the HL60 cell cycle effects of etoposide and mitochondrial transmembrane potential variations were studied here. This group found that an arrest in the G2/M phase of the cells was associated with an increase in the potential of mitochondrial membranes at low etoposide concentrations (0.5 $\mu$ M, 24h treatment). Following this there was a subsequent decrease of mitochondrial transmembrane potential and the appearance of a sub G1 peak indicative of apoptosis. Complete collapse of mitochondrial transmembrane potential and extensive apoptosis was, on the other hand, triggered by higher etoposide concentrations ( $\geq 1\mu$ M, 24h treatment). In a study by Robertson *et al.* (2000), it was also stated that the concentration of etoposide appeared to decide which apoptotic pathway(s) was induced. High

concentrations appeared to induce cytochrome c release by mitochondrial pathways, and low concentrations via nuclear pathways. Thus, the topoisomerase II inhibitor etoposide appears to induce apoptosis by pathways that vary depending on concentration. However, this may or may not be the case for all topoisomerase inhibitors and Facompre *et al.* (2000) also suggested that topoisomerase II drugs may differ from topoisomerase I agents in their effect on mitochondria. With regard to NU:UB 31 it may be that this compound, like etoposide, has different nuclear/mitochondria effects depending on concentration.

Mitochondrial disruption investigations were performed in our studies using a MitoCapture kit and betulinic acid was used as a positive control as this agent has been reported to directly target mitochondria. Unfortunately the MitoCapture assay proved to be unsuitable for use when treating cells with NU:UB 31 due to problems with overlapping fluorescence spectra. In addition to directly targeting mitochondria, betulinic acid has also been found to have a similar potency in wild type as it has in mutant p53-containing cell lines. This was, however, not the case for doxorubicin, which is more cytotoxic in wild type p53-containing cell lines. In a cell line screen containing both p53 types, doxorubicin exerted its anti-proliferative activity in a large range of concentrations whereas betulinic acid showed activity in a very narrow range of doses. These observations were suggested to reflect the wild type p53-dependent cytotoxicity of doxorubicin and the p53-independent cytotoxicity of betulinic acid (Zuco *et al.*, 2002). Although p53-dependent apoptotic pathways have a role in response to DNA damage, it is not certain that wild type p53

function is required for anthracyclines to induce apoptosis. The disaccharide doxorubicin analogue MEN 10755 was more effective in the treatment of p53-mutant tumours than doxorubicin, which would suggest that the analogue had an increased ability to induce p53-independent apoptosis (Perego *et al.*, 2001). The NU:UB agents showed a relatively narrow IC<sub>50</sub> range when screened in the NCI 60 cell line screen (Appendix 1). Also, in the NCI p53 screen, the cytotoxicity of the NU:UB compounds tested were similar in wild type and mutant cell lines (reported in Chapter 7). From this it may be suggested that an intact p53 pathway may not be essential for the NU:UB agents, but that p53-independent pathways could also be important for NU:UB cytotoxicity. In addition to the fairly narrow IC<sub>50</sub> range of the NU:UB agents, the MTT assay results showed that the assayed NU:UB agents also had a very rapid effect, exerting cytotoxicity within short, 4h exposure times. Could this rapid effect be due to a direct action on mitochondria, considering that the MTT assay relies on functional mitochondria as a measure of cytotoxicity? For betulinic acid the mitochondria are the main targets, for NU:UB 31 these organelles may be implied, but no conclusions can so far be made to confirm or deny this idea. A suitable experimental model to study whether or not NU:UB agents affect mitochondria (interacting with mitochondrial DNA, or requiring proper function of these organelles to exert cytotoxicity), could be to use cells that lack mitochondrial DNA. The NU:UB cytotoxicity in these cells could then be compared to that in their parental, wild type counterparts. Cells devoid of mitochondrial DNA are referred to as p<sup>0</sup>, these cannot perform electron transport or oxidative phosphorylation. In a study by Hu *et al.*, (2000) the cytotoxicities of rhodamine 123 and doxorubicin

were investigated in a human osteosarcoma p<sup>0</sup> cell line and in its wild type counterpart. It was found that doxorubicin had similar IC<sub>50</sub> values in these cell lines, whereas rhodamine 123 had a much higher IC<sub>50</sub> value in the p<sup>0</sup> cell line, containing no mitochondrial DNA. Further, less rhodamine 123 was accumulated in the p<sup>0</sup> cells compared to wild type, whereas both cell types accumulated similar amounts of doxorubicin. The results thus showed that doxorubicin did not appear to target mitochondria. Rhodamine 123 did however seem to rely on normal functioning mitochondria and maintenance of normal mitochondrial membrane potential may play an important role in the intracellular accumulation and subsequent cytotoxicity of this compound. These p<sup>0</sup> cell line results were in agreement with previous findings that rhodamine 123 localises in the mitochondria (Chen *et al.*, 1982), while doxorubicin is found mainly in the nucleus (Lampidis *et al.*, 1997). With regard to doxorubicin, the study by Hu *et al.* (2000) further implied that doxorubicin has a non-mitochondrial dependent mechanism of action. This suggestion however argues against previous findings that doxorubicin in addition to utilising nuclear DNA, also uses the mitochondrial electron transport system to form cytotoxic superoxides and free radicals.

In summary, NU:UB 31 (and possibly other NU:UB compounds) may reach its nuclear target(s), acting as an anti-topoisomerase inhibitor, but it is also feasible that cytosolic organelles are important for its cytotoxic actions, such as mitochondria, considering these organelles contain mitochondrial DNA and topoisomerases. The recent NCI comparison correlations of LC<sub>50</sub> values further suggest that NU:UB agents as well as acting as nuclear

topoisomerase inhibitors, may have additional mechanisms of action. Considering the frequency of correlation with agents acting on enzymes participating in the pyrimidine biosynthesis pathway such as dihydroorotate dehydrogenase, mitochondrial enzymes or functions may be additional targets of the NU:UB agents. Further investigations are warranted to deduce whether or not NU:UB agents interact with mitochondrial components as part of their mechanism of action. In our studies, NU:UB 31 also seemed to accumulate within the lysosomes and possibly other acidic vesicles and this could be due to its weak base properties and possibly be a mechanism for the cell to efflux the NU:UB 31 agent. Anti-topoisomerase agents with concomitant anti-metabolite activity may represent a novel dual mechanism of cytotoxic action; further work to elucidate whether or not these dual properties are vested in the NU:UB series are warranted.

## **CHAPTER 9**

### **SUMMARY DISCUSSION**

## 9.0 SUMMARY DISCUSSION

The discovery that topoisomerases were the targets for many of the most potent anti-cancer drugs led to a great interest in these enzymes and in the synthesis of more of these types of drugs. The current clinically useful anti-cancer agents doxorubicin, mitoxantrone and etoposide are examples of such drugs acting via the type II topoisomerase enzyme. More recently the topoisomerase I targeting camptothecin derivatives irinotecan and topotecan have also been introduced into the clinic. However, most of the current anti-topoisomerase drugs were, from the beginning, not specifically designed to target topoisomerases, this has been a later discovery. Furthermore, it has now been realised that these drugs are not clean topoisomerase inhibitors, but that many, in addition to their anti-topoisomerase activities, also have other activities that are unrelated to these enzymes and that in many cases can result in dose-limiting side effects when administered to patients (Cummings *et al.* 1991; Cummings and Smyth, 1993).

In addition to the non-specific toxicities induced by many currently used therapeutics, there is also a severe problem with drug resistance that limits the uses of today's anti-cancer drugs. Many topoisomerase inhibitors are prone to so-called altered topoisomerase (atypical) drug resistance. This type of resistance is modulated by alterations in the expression levels of topoisomerase enzyme (type I or II). Studies have indicated that cells responsive to topoisomerase I-targeted drugs have elevated levels of

topoisomerase I, require active DNA replication, and may need a functional apoptotic pathway (Coleman, 2001). One of the mechanisms associated with resistance to topoisomerase I inhibitors has been reported to be decreased activity of the topoisomerase I enzyme (Uemura, 1984; Goto, 1985). Furthermore, it is known that when cells lose topoisomerase I activity, topoisomerase II instead takes care of the roles of topoisomerase I in cells (Brill, 1987). This increased importance of topoisomerase II can then make topoisomerase I-negative cells more sensitive to topoisomerase II inhibitors (Nitiss, 1994b; Byl, 1999). Thus, it may be possible to actively exploit the cellular imbalance of topoisomerase I and topoisomerase II enzymes as a rationale in chemotherapy regimens. Sequential chemotherapy targeting of topoisomerase enzymes, modulating topoisomerase II expression levels by topoisomerase I inhibitors might be more effective than using a topoisomerase II inhibitor alone (Kim, 1999).

Another approach to defeat resistance due to altered topoisomerase function, may be to invest in both topoisomerase I and topoisomerase II targeting properties within the same molecule. Compounds that may be truly classified as dual (or mixed) topoisomerase I and topoisomerase II inhibitors are currently few in number. The anthracycline aclarubicin, the acridine DACA (Fig. 9.1) and the indenoquinone TAS-103 (Fig. 9.2) are examples of recently identified drugs in clinical trials that are thought to exhibit dual topoisomerase inhibitory properties, although some controversy still exists over the relative contributions of anti-topoisomerase I versus anti-topoisomerase II action. Studies using cell free, purified enzyme cleavable complex formation assays,

revealed that DACA and TAS-103 seemed to poison both topoisomerase I and topoisomerase II. Despite this, in a study using the recently developed TARDIS assay (trapped in agarose DNA immunostaining), these agents showed a preference for topoisomerase II $\alpha$  in whole cells. For topoisomerase I, TAS-103 only induced low levels of drug-stabilised cleavable complexes, and DACA did not appear to form cleavable complexes with topoisomerase I. However, although whole cell and cell free systems appeared to show different results, whole cell assays in comparison with the purified enzyme assays, are more complex systems, so although both DACA and TAS-103 showed the preference for topoisomerase II $\alpha$  in whole cells by TARDIS assay, the formation of low levels of topoisomerase I and II $\beta$  cleavable complexes may ultimately play a role in their *in vivo* mechanisms of cytotoxicity (Padgett *et al.*, 2000). Similar to the NU:UB compounds, both TAS-103 and DACA are cationic side chain-substituted polycyclic systems that are thought to owe their cytotoxicity to interactions with DNA. However, whereas studies of the acridine DACA suggested that its rings intercalate DNA, and its aminoalkyl carboxamide chain was located in the minor groove of DNA (Pastawa *et al.*, 1998), TAS-103 showed a different binding mode, binding mainly to the surface of DNA (outside binding), and only minor binding via intercalation (Ishida and Asao, 2002).

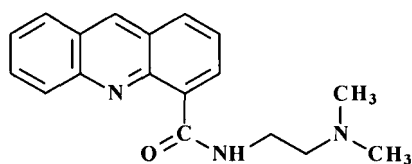


**Fig. 9.1** Chemical structure of DACA

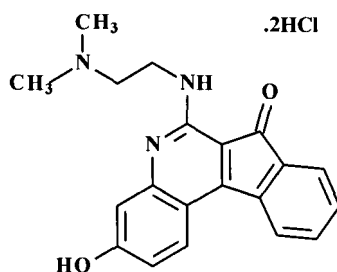


**Fig.9.2** Chemical structure of TAS-103

A feature observed with DACA is that while this agent at low concentrations acts to poison topoisomerases, at higher concentrations it mainly acts as a catalytic inhibitor. So at high concentrations the drug binding may obstruct topoisomerase binding sites on DNA, suppressing cleavable complex formation and poisoning. Similar findings have also been uncovered with some of the NU:UB compounds, where these appear to inhibit their own cleavage reaction when used at high concentrations (self-inhibition), for example, evident in the gel electrophoresis results of NU:UB 31 induced stimulation of topoisomerase I-mediated DNA cleavage (Fig.3.5). In addition to concentration-dependent effects that appeared to be able to affect the balance between enzyme poisoning and enzyme inhibition, small changes in the DACA structure also seemed to alter this balance as well as the bias towards topoisomerase I and topoisomerase II interaction (Bridewell *et al.*, 1999). Since the NU:UB agents, containing an anthraquinone ring system and cationic aminoalkyl side-chains, have structural similarities to the two agents above (TAS-103 and DACA), what has been learnt in studying TAS-103 and DACA could therefore provide useful information in relation to the investigations of anti-topoisomerase I and anti-topoisomerase II activity of the

NU:UB agents. Strikingly, anthraquinone-based amino acid substituted drugs (NU/ICRF 600, 601 and 602), investigated by Meikle *et al.* (1995b) were also shown to be dual inhibitors of the catalytic activity of topoisomerase I and topoisomerase II, notably, however, these compounds contained C-terminally free and uncharged side-chains with consequently reduced DNA-binding capacity. In a study of DACA by Finlay *et al.* (1993) the sensitivity of this compound in drug resistant cell lines was compared to other topoisomerase-directed drugs, including amsacrine, etoposide and doxorubicin. It was shown that DACA was different from the other topoisomerase-directed drugs, overcoming atypical multidrug resistance in a series of Jurkat leukaemia cell lines. Furthermore, DACA was also said to exhibit reduced susceptibility to P-gp mediated multidrug resistance mechanisms. This lack of DACA susceptibility to P-gp mediated multidrug resistance was further thought to be related to the lipophilic character of the DACA structure, allowing for rapid uptake by tumour cells exceeding the rate of P-gp mediated drug efflux. In this study, DACA proved to be unique in comparison to the included clinical topoisomerase II drugs in its ability to overcome two different multidrug resistance mechanisms. Hence, in common with most classes of chemotherapeutics, drugs that target a single topoisomerase (either type I or II) protein are, in addition to atypical resistance, also at risk of MDR (e.g. P-gp and MRP transporter-mediated resistance), where certain transporter molecules are capable of excluding the drug (or several drugs) from resistant cells. For a drug to be effective it is therefore beneficial if this agent is not a substrate of MDR related transporters. In the study by Finlay *et al.* (1993) DACA proved to be capable of circumventing P-gp mediated multidrug

resistance. This was supported and extended in a more recent study of DACA by Davey *et al.* (1997), where DACA, in addition to avoiding P-gp mediated MDR mechanisms, was also effective against MRP-mediated MDR. The focus of the present study, NU:UB 31, has like DACA been shown to circumvent atypical and P-gp mediated MDR. NU:UB 31 was demonstrated to be active and non-cross resistant to doxorubicin in (resistant) cell lines with elevated expression of the P-gp MDR gene product (Chapter 4).

For any cytotoxic agent to be clinically useful, its administration ultimately has to lead to tumour cell kill, ideally with tumour cell selectivity. The NU:UB compounds have been screened in the NCI panel of 60 human cancer cell lines, including sub-panels of melanomas, breast cancer, lung cancer, colon and ovary cancers using the sulforhodamine B cytotoxicity assay with 48h endpoints. From this *in vitro* screen it was demonstrated that these agents proved to be cytotoxic at this time point in a range of different cell lines. Strikingly, some of the NU:UB compounds, for example NU:UB 31, 43, 80 and 81, showed selectivity for the colon and melanoma (including metastatic melanoma) sub-panels of the NCI 60 cell line *in vitro* drug screen (see Appendix 2). It is possible that this activity is related to the NU:UB compounds' ability to induce both topoisomerase I and topoisomerase II induced DNA lesions that trigger apoptosis in the sensitive cell lines of these sub-panels. Furthermore, MTT cytotoxicity assays performed within this project using leukaemia and colon cell lines revealed that the NU:UB agents tested had IC<sub>50</sub> values in the low  $\mu$ M range even at exposure times that were shorter than 48h. For the comparator anti-topoisomerase inhibitors, the IC<sub>50</sub>

values were not as low at the shorter exposure times as those recorded for the NU:UB conjugates, but were indeed lower than for the NU:UB agents at longer exposure times. This fairly rapid effect may be as a result of increased cellular uptake of the NU:UB compounds due to their cationic lipophilic character, and possibly related to diminished capacity to serve as a substrate for P-gp efflux pumps in common with N,N-dialkylaminoanthracyclines (Lampidis *et al.*, 1997).

It should be recognised that the relationship between cell cycle and response to topoisomerase inhibitors is important and that topoisomerase I and topoisomerase II $\alpha$  targeted drugs require active cell proliferation. The ability of the NU:UB conjugates to target topoisomerase II $\beta$ , in addition to topoisomerase I and topoisomerase II $\alpha$  may explain their activity against solid tumours that tend to develop large G0/G1 cell populations. Thus, NU:UB conjugates offer the prospect of efficacy against tumours with large proportions of both cycling and non-cycling cell populations. Although both solid tumours and many normal tissues would be expected to have large G0/G1 populations, solid tumour cells are more likely to have defects in cell cycle checkpoints that prevent replication in the presence of DNA damage caused by drug stabilised topoisomerase II $\beta$ -DNA cleavable complexes (Mincher D. J., *personal communications*). A topoisomerase II $\beta$ -targeting quinoxaline XK469 was recently reported for which topoisomerase I and II $\alpha$  were not significant contributors to cytotoxicity and which killed large numbers of non-cycling cells in solid tumour models (Gao *et al.*, 1999). Cell cycle analyses were performed to deduce whether or not NU:UB 31 had an effect

on the cell cycle progression, and if so, whether or not this was similar to the cell cycle effect induced by the known anti-topoisomerase I or II inhibitors used for comparison. Results demonstrated that whereas the known anti-topoisomerase drugs caused a cell cycle block, NU:UB 31 did not appear to have such effects. Although the cells were killed, being found in the sub G1 region of the cell cycle histogram (indicative of apoptotic cell death), they seemed to be killed without cell cycle phase specificity. Thus, this further highlighted that more than one type of topoisomerase enzyme may be targeted, and/or that there could be mechanisms other than purely anti-topoisomerase interactions involved following treatment with the NU:UB compounds.

Anti-topoisomerase action is likely to induce DNA damage due to the DNA cleaving nature of these enzymes. DNA damage is known to induce the tumour suppressor protein p53 and this is likely to result in cell cycle arrest and repair of the damaged DNA or in apoptotic cell death. Several anti-topoisomerase inhibitors induce apoptotic cell kill and do so via induction of p53. Doxorubicin is an example of an agent that was used in this project as a positive control for the induction of p53-mediated apoptosis. Following NU:UB treatment of human leukemia (HL60) cells, apoptotic cell death was confirmed with morphological as well as various biochemical assays. Furthermore, p53 was rapidly induced in human colon carcinoma (HCT116) cells by NU:UB treatment, although this induction was fairly brief and not as significant as the maximum induction produced by doxorubicin. Down stream mediators of p53 were also investigated to confirm activation of the p53 induction pathway.

Mdm2 levels, but not p21 levels were increased in HCT116 cells after treatments with NU:UB compounds. The lack of p21 induction could possibly be related to the lack of cell cycle block following NU:UB treatment. It may be that since NU:UB compounds appeared to have a rapid mechanism of action, apoptosis was perhaps induced via p53-dependent, as well as p53-independent pathways and such pathways could also play a part in the NU:UB-induced cell kill mechanism considering p53 was briefly induced but no excessive p53 levels were maintained following NU:UB treatment. To support this, the NCI drug screen is not purely a cytotoxicity screen, but it can also be used as a tool to search for p53-independent candidate drugs. This drug screen has previously shown remarkably good correlation between functional p53 status and sensitivity of many of the DNA damaging drugs currently used in the clinic (Makin and Hickman, 2000). Results from the NCI p53-wild type/mutant drug screen included within this study revealed that while the standard drugs doxorubicin and mitoxantrone were more potent in wild type p53 containing cells, the NU:UB compounds had overall similar (equipotent) values in the p53 wild type and p53 mutant cell lines. Thus, this further supported the possibility that the NU:UB compounds had a p53-independent component in their cell kill mechanism (along with, or in place of a p53-dependent mechanism).

In another aspect of intracellular drug action, mitochondria have now been identified as sub-cellular targets for clinically used anthracyclines. Data is being accumulated to suggest that anthracyclines, in addition to targeting nuclear DNA and nuclear enzymes, may also interact with mitochondria

interfering with the functions of these organelles as part of their toxicity (Jung and Reszka, 2001). Many of the conventional anti-cancer agents including doxorubicin and etoposide have, however, no direct effect on mitochondria, but may instead elicit mitochondrial membrane permeabilisation in an indirect fashion by inducing endogeneous effectors that are involved in the control of apoptosis. A recurrent problem when using these types of classical drugs is, however, that the endogeneous apoptosis-induction pathways often are compromised by alterations such as mutations of p53. One strategy to circumvent this, and enforce cell death may be to trigger downstream events of the common apoptotic pathway. In contrast to the conventional drugs, an increasing number of experimental anti-cancer agents are thought to have a direct effect on mitochondria. These types of agents may then induce apoptosis when conventional drugs do not work due to disruptions in endogeneous apoptosis induction pathways such as those involving p53 and caspases (Constantini, 2000). These drugs were, however, not originally designed to act on mitochondrial targets. Instead as these drugs were developed and as more information on mechanisms became available, their effects on mitochondria were revealed (Howell *et al.*, 2003). Betulinic acid is an example of a novel (natural product) experimental agent with anti-tumour activity. Fulda *et al.* (1998) have shown that betulinic acid induces apoptosis via direct mitochondrial alterations in intact cells and cell free systems. When added to isolated mitochondria, betulinic acid directly induced loss of mitochondrial transmembrane potential in a way not affected by caspase inhibitors. Thus, betulinic acid may induce cell death in cells with compromised endogeneous apoptosis-induction pathways by triggering p53-

independent apoptosis and thereby permeabilise mitochondrial membranes in a caspase-independent fashion (Constantini *et al.*, 2000). F16 is another example of an agent that is thought to directly target mitochondria. F16 is a small lipophilic cationic molecule that, due to its fluorescent properties, allows for cellular localisation studies to be carried out. Mitochondrial hyperpolarisation is a shared feature of many tumour cell lines and lipophilic cations are found to accumulate in the mitochondria driven by the electrochemical gradient. Several types of cancer cells have been described to accumulate cationic agents to a higher level than normal cells (Fantin *et al.*, 2002). Accumulation studies of F16 have revealed that this molecule accumulated in cells with a high mitochondrial membrane potential, providing some degree of cancer cell selectivity. Fantin *et al.* (2002) reported that F16 induced mitochondrial damage, which resulted in swelling, failure to synthesise ATP, and release of cytochrome c, but no specific mitochondrial target of F16 has so far been identified.

Like F16, NU:UB 31 is also a small cationic lipophilic molecule. In this study, fluorescent NU:UB 31 and stained mitochondria were observed under the confocal microscope using a MitoTracker probe. NU:UB 31 appeared to be present within these organelles (as well as the lysosomes, investigated with LysoTracker). What outcome this had for cell survival and whether or not NU:UB 31 had a direct or indirect effect on mitochondria is, however, at this stage impossible to confirm. In addition, the Compare pattern of the LC<sub>50</sub> data from the NCI drug screen allowed more detailed information on mechanisms of drug action to be hypothesised. Each compound pattern from this drug

screen could be considered as a molecular fingerprint and these patterns are being used in conjunction with molecular structural features of the tested agents to give insight into potential target molecules and modulators (Weinstein *et al.*, 1997). Similarity in pattern often indicates similarity in mechanism of action, mode of resistance, and molecular structure. By using the NU:UB compounds as seeds in such a Compare study it was noted that, in addition to significant similarities to topoisomerase inhibitors, NU:UB agents also had significant similarities to several drugs thought to interact with the components of mitochondria and thus with mitochondrial function (see Appendix 5). This suggests that both nuclear DNA-related enzymes, as well as mitochondrial enzymes may play a part in the ultimate cytotoxic effect that NU:UB compounds have *in vitro*.

This study has thus identified topoisomerases and mitochondria, in part, as potential targets for NU:UB agents *in vitro*. Further investigations will, however, be needed to determine whether or not there are other NU:UB interactions involved that contribute to the cytotoxicity of these compounds. Studies are also required, if indeed mitochondria are involved, to establish what is the mitochondrial target enzyme(s), pathway(s) or mitochondrial function(s) that is being disrupted by the NU:UB agents. Moreover, once the NU:UB mechanism(s) of action has been fully realised *in vitro*, it should be established if this is a valid explanation for the anti-tumour activity observed *in vivo*.

## CONCLUSIONS AND SUGGESTIONS FOR FURTHER WORK

The NU:UB compounds were initially synthesised and developed with the objective of exerting cytotoxicity by selectively inhibiting topoisomerase enzymes and by limiting other non-specific interactions that may result in unwanted side effects. This research project aimed to investigate the cell kill properties of selected NU:UB compounds (focusing on NU:UB 31) in an *in vitro* setting, specifically to prove or disprove the working hypothesis that NU:UB compounds have anti-topoisomerase properties that, in part, contribute to their mechanism of cytotoxic action *in vitro*.

The anti-topoisomerase activity of NU:UB 31 was investigated and it was revealed that this compound had anti-topoisomerase activity *in vitro* when using both whole cell systems and purified recombinant enzyme. NU:UB 31 inhibited topoisomerase I and II mediated DNA relaxation in cell free systems. Topoisomerase I mediated DNA relaxation was partially inhibited by NU:UB 31 at 10 $\mu$ M. Partial topoisomerase II $\alpha$  and II $\beta$  inhibition was achieved by NU:UB 31 concentrations of 10 $\mu$ M and 15 $\mu$ M, with complete inhibition at 25 $\mu$ M and 20 $\mu$ M, respectively. Notably, NU:UB 31 (optimum concentration 5 $\mu$ M) stimulated topoisomerase I-mediated cleavage of supercoiled DNA in a manner comparable to the topoisomerase I poison camptothecin. NU:UB 31 also induced drug-stabilised topoisomerase I and II ( $\alpha$  and  $\beta$ ) cleavable complex formation in intact cells, as well as in purified enzyme assays. Topoisomerase I-DNA cleavable complexes were stabilised in whole cells by

100 $\mu$ M NU:UB 31. Cleavable complex formation with topoisomerase II $\alpha$  and topoisomerase II $\beta$  in intact cells, was achieved by NU:UB 31 at concentrations of 300 $\mu$ M and 200 $\mu$ M respectively. Thus, from these experiments it was found that the NU:UB mechanism of action, at least in part, was topoisomerase mediated. Furthermore, NU:UB 31 seemed to exhibit a dual action on both topoisomerase I and II that could prove to be beneficial for circumvention of altered topoisomerase resistance mechanisms.

The cell survival assays showed that NU:UB compounds were cytotoxic in the low micro-molar range as early as 4h in the HL60, HCT116 and HT29 cell lines. NU:UB 31 had 4h IC<sub>50</sub> values in the order of 27.5 $\mu$ M, 30.0 $\mu$ M and 33.5 $\mu$ M and 96h IC<sub>50</sub> values of 3.1 $\mu$ M, 2.8 $\mu$ M and 4.2 $\mu$ M in HL60, HCT116 and HT29 cells respectively. Morphological and biochemical experiments showed that NU:UB treatment induced apoptosis. In the caspase activation studies, 4h NU:UB 31 treatment at 20 $\mu$ M resulted in approximately 15% caspase positive cells in the (p53 negative) HL60 cell line and 40 $\mu$ M NU:UB 31 resulted in approximately 30% caspase positive HCT116 cells (p53 positive). DNA fragmentation was evident (gel electrophoretic detection of DNA laddering) in HL60 cells following 6h NU:UB 31 (at 20 $\mu$ M) treatment. Furthermore over 20% of HL60 cells showed apoptotic morphology following 8h NU:UB 31 (at 20 $\mu$ M) treatment. Current chemotherapeutics generally induce DNA damage and p53-mediated apoptosis. Whereas clinically used topoisomerase inhibitors are deemed to require a functional p53 pathway, from the observations made in this study, together with supporting data from NCI where NU:UB agents had comparable GI<sub>50</sub> values in p53 wild type and

p53 mutated cell lines, it was suggested that apoptosis induced by NU:UB compounds may partly have a p53-independent component. Moreover, observations made in this project of the sub-cellular localisation of NU:UB 31, and with Compare data from NCI, suggested that mitochondria may provide an additional target for these agents. In summary, this NU:UB study has provided further information on the mechanism of cell death induced by NU:UB conjugates, information that hopefully will be of benefit in the future development of novel NU:UB agents as potential anti-cancer drugs.

For future work with the NU:UB agents, it may be beneficial to extend the study of NU:UB compound cellular localisation patterns to include more cell types to further investigate whether or not the lack of nuclear NU:UB 31 fluorescence in HL60 cells was due to absence of NU:UB 31 in the nucleus, or due to a fluorescence quenching phenomenon. NU:UB 31 could be added directly to cell nuclei, or to naked DNA and its fluorescence could be monitored to see whether it decreased as NU:UB 31 interacted with DNA (observed with other DNA-intercalating drugs). Targeting mitochondria may be favourable since it has been realised that mitochondria are central to several of the apoptotic pathways, as they contain various apoptotic mediators. Thus, mitochondrial-targeting properties may prove to be beneficial in killing cells with defective mechanisms of inducible apoptotic pathway(s). Therefore, a thorough investigation of the possible mitochondrial component contribution to the NU:UB mechanism of action is warranted. To study whether or not NU:UB agents, as well as interacting with nuclear DNA and topoisomerases, also interact with mitochondrial DNA and topoisomerases,

assays using mitochondrial extracts may be suitable given the presence of topoisomerase I, type II $\beta$  topoisomerase and topoisomerase III $\alpha$  enzymes in mitochondria, independent of the nuclear enzymes that may shuttle between nucleus and the mitochondria (Zhang *et al.*, 2001; Wang *et al.*, 2002; Low *et al.*, 2003). Furthermore, cytotoxic investigations, comparing IC<sub>50</sub> values obtained using normal cells and cells devoid of functional mitochondria could be performed. Progressing from the use of cell lines resistant to topoisomerase I or II inhibitors for cytotoxic investigations of NU:UB agents, use could be made of yeast systems transfected with mutated topoisomerase enzyme, rendering the cells insensitive to the specific enzyme which should then allow an assessment of the relative contributions of type I versus type II interactions to cell-kill (Woo *et al.*, 2001; Nitiss and Nitiss, 2001). Mutated topoisomerase I, for example, confers drug resistance to the camptothecin poisons. These yeast cell survival assays could thus be used as a mechanism-based screen for a panel of NU:UB agents. Equally, cancer cell lines bearing mutated topoisomerase enzymes could be used to probe the cytotoxic properties of compounds for dependency on catalytically functional topoisomerases.

## REFERENCES

- Adolphs K.W., Cheng S.M., Paulson J.R. and Laemmli U.K. (1977) Isolation of a protein scaffold from mitotic HeLa cell chromosomes. *Proc. Natl. Acad. Sci. USA* **74**: 4937-4941
- Agarwal M.L., Taylor W.R., Chernov M.V., Chernova O.B. and Stark G.R. (1998) The p53 network, minireview. *J. Biol. Chem.* **273**: 1-4
- Alberts B., Bray D., Johnson A., Lewis J., Roberts K. and Walter P. (1998) Energy generation in mitochondria and chloroplasts. In: *Essential Cell Biology*. pp407-446. Garland, New York
- Albor A., Kaku S. and Kulez-Martin M. (1998) Wild-type and mutant forms of p53 activate human topoisomerase I, a possible mechanism for gain of function in mutants. *Cancer Res.* **58**: 2091-2094
- Alexandre S., Rast C., Nguyen G. and Vasseur P. (2000) Detection of apoptosis induced by topoisomerase inhibitors and serum deprivation in syrian hamster embryo cells. *Exp. Cell Res.* **255**: 30-39
- Allen J.A. and Coombs M.M. (1980) Covalent binding of polycyclic aromatic compounds to mitochondrial and nuclear DNA. *Nature.* **287**: 244-245
- Alnemri E.S., Livingston D.J., Nicholson D.W., Salvesen G., Thornberry N.A., Wong W.W. and Yuan J. (1996) Human ICE/CED-3 protease nomenclature. *Cell.* **87**: 171
- Ames B.N., Shigenaga M.K. and Hagen T.M. (1993) Oxidants, antioxidants and the degenerative diseases of aging. *Proc. Natl. Acad. Sci. USA.* **90**: 7915-7922
- Andreyev A. and Fiskum G. (1999) Calcium induced release of mitochondrial cytochrome c by different mechanisms selective for brain versus liver. *Cell Death Differ.* **6**: 825-832
- Anselmi C., Ettore A., Andreassi M., Centini M., Neri P. and Di Stefano A. (2002) In vitro induction of apoptosis vs. necrosis by widely used preservatives: 2-phenoxyethanol, a mixture of isothiazolinones, imidazolidinyl urea and 1,2-pentanediol. *Biochem. Pharmacol.* **63**: 437-453
- Attardi L.D., Lowe S.W., Brugarolas J. and Jacks T. (1996) Transcriptional activation by p53, but not induction of the p21 gene, is essential for oncogene-mediated apoptosis. *EMBO J.* **15**: 3693-3701

Austin C.A., Marsh K.L., Wasserman R.A., Willmore E., Sayer P.J. and Wang J.C. (1995) Expression, domain structure and enzymatic properties of an active recombinant human DNA topoisomerase II $\beta$ . *J. Biol. Chem.* **270**: 15739-15746

Bailly C., Pommery N., Houissin R. and Henichart J.P. (1989) Design, synthesis, DNA binding, and biological activity of a series of DNA minor groove-binding intercalating drugs. *J. Pharm Sci.* **78**: 910-917

Baldwin J., Farajallah A.M., Malmquist N.A., Rathod P.K. and Phillips M.A. (2002) Malarial dihydroorotate dehydrogenase. *J. Biol. Sciences.* **277**: 41827-41834

Barak Y., Juven T., Haffner R. and Oren M. (1993) Mdm2 expression is induced by wild type p53 activity. *EMBO J.* **12**: 461-468

Bargonetti J., Friedman P.N., Kern S.E., Vogelstein B. and Prives C. (1991) Wild-type but not mutant p53 immunopurified proteins bind to sequences adjacent to the SV40 origin of replication. *Cell.* **65**: 1083-1091

Becker W.M., Reece J.B. and Poenie M.F. (1996) In: *The world of the cell*. 3<sup>rd</sup> edition. pp453-494. The Benjamin/Cummings Publishing Company

Berezney R. and Coffey D.S. (1974) Identification of a nuclear protein matrix. *Biochem. Biophys. Res. Commun.* **60**: 1410-1417

Berger J.M. (1998) Structure of DNA topoisomerases. *Biochim. Biophys. Acta.* **1400**: 3-18

Bigioni M., Salvatore C., Bullo A., Bellarosa D., Lafrate E., Animati F., Capranico G., Goso C., Maggi C.A., Pratesi G., Zunino F. and Manzini S. (2001) A comparative study of cellular and molecular pharmacology of doxorubicin and MEN 10755, a disaccharide analogue. *Biochem. Pharmacol.* **62**: 63-70

Bischoff J.R., Kirn D.H., Williams A., Heise C., Horn S., Muna M., Ng L., Nye J.A., Sampson-Johannes A., Fattaey A. and McCormick F. (1996) An adenovirus mutant that replicates selectively in p53-deficient human tumour cells. *Science.* **274**: 373-376

Blandino G., Levine A.J. and Oren M. (1999) Mutant p53 gain of function: differential effects of different p53 mutants on resistance of cultured cells to chemotherapy. *Oncogene.* **18**: 477-485

Boege F., Kjeldsen E., Gieseler F., Alsner J. and Biersack H. (1993) A drug resistant variant of topoisomerase II $\alpha$  in human HL60 cells exhibits alterations in catalytic pH optimum, DNA binding and subnuclear distribution. *Eur. J. Biochem.* **218**: 575-584

- Boege F., Straub T., Kehr A., Boesenberg C., Christiansen K., Andersen A., Jakob F. and Köhrle J. (1996) Selected Novel Flavones inhibit the DNA binding or the DNA religation step of eukaryotic topoisomerase I. *J. Biol. Chem.* **271**: 2262-2270
- Bottger A., Bottger V., Sparks A., Liu W.L., Howard S.F. and Lane D.P. (1997) Design of synthetic mdm2-binding mini protein that activates the p53 response in vivo. *Curr. Biol.* **7**: 860-869
- Bradbury D.A., Simmons T.D., Slater K.J. and Crouch S.P.M. (2000) Measurement of the ADP:ATP ratio in human leukaemic cell lines can be used as an indicator of cell viability, necrosis and apoptosis. *J. Immunol. Methods.* **240**: 79-92
- Bridewell D.J.A., Finlay G.J. and Baguley B.C. (1999) Mechanism of cytotoxicity of N-[2-(dimethylamino)ethyl]acridine-4-carboxamide and of its 7-chloro derivative: the roles of topoisomerase I and II. *Cancer Chemother. Pharmacol.* **43**: 302-308
- Brill S.J., DiNardo S., Voelkel-Meiman K. and Sternglanz R. (1987) DNA topoisomerase activity is required as a swivel for DNA replication and for ribosomal RNA transcription. *Natl. Cancer Inst. Monogr.* **4**: 11-15
- Bullock A.N., Henckel J., DeDecker B.S., Johnson C.M., Nikolova P.V., Proctor M.R., Lane D.P. and Fersht A.R. (1997) Thermodynamic stability of wild-type and mutant p53 core domain. *Proc. Natl. Acad. Sci. USA.* **94**: 14338-14342
- Bykov V.J.N., Issaeva N., Shilov A., Hultcrantz M., Pugacheva E., Chumakov P., Bergman J., Wiman K.G. and Selivanova G. (2002) Restoration of the tumour suppressor function to mutant p53 by a low-molecular-weight compound. *Nature Medicine.* **8**: 282-288
- Byl J.A.W., Fortune J.M. Burden D.A. Nitiss J.L. Utsugi T. Yamada Y. and Osheroff N. (1999) DNA topoisomerases as targets for the anticancer drug TAZ-102: primary cellular target and DNA cleavage enhancement. *Biochemistry.* **38**: 15573-15579
- Cain K., Bratton S.B. and Cohen G.M. (2002) The Apaf-1 apoptosome: a large caspase activating complex. *Biochimie.* **84**: 203-214
- Campbell N.A. (1993) In: *Biology*. pp235-237, pp384-386. The Benjamin / Cummings Publishing Company. Inc.
- Cano-Abad M.F., Villarroya M., Garcia A.G., Gabilan N.H. and Lopez M.G. (2001) Calcium entry through L-type calcium channels causes mitochondrial disruption and chromatin cell death. *J. Biol. Chem.* **276**: 39695-39704

- Capranico G., Binaschi M., Borgnetto M.E., Zunino F. and Palumbo M. (1997) A protein-mediated mechanism for the DNA sequence-specific action of topoisomerase II poisons. *Trends Pharmacol. Sci.* **18**: 323-329
- Capranico G. and Binaschi M. (1998) DNA sequence selectivity of topoisomerases and topoisomerase poisons. *Biochim. Biophys. Acta.* **1400**: 185-194
- Castedo M., Ferri K., Roumier T., Metivier D., Zamzami N. and Kroemer G. (2002) Quantitation of mitochondrial alterations associated with apoptosis. *J. Immunol. Methods.* **265**: 39-47
- Cayrol C., Knibiehler M. and Ducommun B. (1998) P21 binding to PCNA causes G1 and G2 cell cycle arrest in p53-deficient cells. *Oncogene.* **16**: 311-320
- Chang J.Y., Dethlefsen L.A., Barley L.R., Zhou B.S. and Cheng Y.C. (1992) Characterisation of camptothecin resistant Chinese hamster lung cells. *Biochem. Pharmacol.* **43**: 2443-2452
- Chen A.Y. and Liu L.F. (1994) DNA topoisomerases: essential enzymes and lethal targets. *Annu. Rev. Pharmacol. Toxicol.* **34**: 191-218
- Chen J., Marechal V. and Levine A.J. (1993) Mapping of the p53 and mdm2 interaction domains. *Mol. Cell Biol.* **13**: 4107-4114
- Chen L.B., Summerhayes I.C., Johnson L.V., Walsh M.L., Bernal S.D. and Lampidis T.J. (1982) Probing mitochondria in living cells with rhodamine 123. *Cold Spring Harb. Symp. Quant. Biol.* **46**: (Pt 1) 141-155
- Chen Q., Gong B. and Almasan A. (2000) Distinct stages of cytochrome c release from mitochondria: evidence for feedback amplification loop linking caspase activation to mitochondrial dysfunction in genotoxic stress induced apoptosis. *Cell Death and Differ.* **7**: 227-233
- Chen X., Ko L.J., Jayaraman L., Prives C. (1996) P53 levels, functional domains and DNA damage determine the extent of the apoptotic response of tumour cells. *Genes Dev.* **10**: 2438-2451
- Chène P., Fuchs J., Bohn J., Garcia-Echeverria C., Furet P. and Fabbro D. (2000) A small synthetic peptide, which inhibits the p53-hdm2 interaction, stimulates the p53 pathway in tumour cell lines. *J. Mol. Biol.* **299**: 245-253
- Cheng C.C. and Zee-Cheng R.K.Y. (1983) The design, synthesis and development of a new class of potent antineoplastic anthraquinones. *Prog. Med. Chem.* **20**: 83-118
- Chetty R. (2002) Cyclin E and p27: their putative role as prognostic markers. *Curr. Diagnostic Pathol.* **8**: 289-296

Cho Y., Gorina S., Jeffrey P.D. and Pavletich N.P. (1994) Crystal structure of p53 tumour suppressor–DNA complex: understanding tumourigenic mutations. *Science*. **265**: 346-355

Christensen M.O., Barthelmes H.U., Feineis S., Knudsen B.R., Andersen A. H., Boege F. and Meilke C. (2002) Changes in mobility account for camptothecin-induced subnuclear relocation of topoisomerase I. *J. Biol. Chem.* **277**: 15661-15665

Cima I. and Brunner T. (2003) T cell apoptosis: about killers and victims, *Biologist*. **50**: 11-115

Clarke A.R., Purdie C.A., Harrison D.J., Morris R.G., Bird C.C., Hooper M.L. and Wyllie A.H. (1993) Thymocyte apoptosis induced by p53 dependent and independent pathways. *Nature*. **362**: 849-852

Cohen G.M., Sun X.M., Snowden R.T., Dinsdale D., Skilleter D.N. (1992) Key morphological features of apoptosis may occur in the absence of internucleosomal DNA fragmentation. *Biochem. J.* **286**: 331-334

Cohen J.J. (1993) Apoptosis. *Immunology Today*. **126**: 126-130

Cole S.P.C., Bhardwaj G., Gerlach J.H., Mackie J.E., Grant C.E., Almquist K.C., Steward A.J., Kurz E.U., Duncan A.M.V. and Deeley R.G. (1992) Overexpression of a transporter gene in a multidrug resistant human lung cancer cell line. *Science*. **258**: 1650-1654

Colman M.S., Afshari C.A. and Barrett J.C. (2000) Regulation of p53 stability and activity in response to genotoxic stresses. *Mutation Res.* **462**: 179-188

Coleman L.W., Bronstein I.B. and Holden J.A. (2001) Immunohistochemical staining for DNA topoisomerase I, topoisomerase II-alpha and p53 in gastric carcinomas. *Anticancer Research*. **21**: 1167-1172

Constantini P., Jacotot E., Decaundin D. and Kroemer G. (2000) Mitochondrion as a novel target of anticancer chemotherapy. *J. Natl. Cancer Inst.* **92**: 1042-1053

Cossarizza A., Baccarani-Contri M., Kalashnikova G. and Franceschi C. (1993) A new method for the cytofluorimetric analysis of mitochondrial membrane potential using the J-aggregate forming lipophilic cation 5,5', 6,6'-tetrachloro-1,1', 3, 3'-tetraethylbenzimidazolcarbocyanine iodine (JC-1). *Biochem. Biophys. Res. Comm.* **197**: 40-45

Covey J.M., Jaxel C., Kohn K.W. and Pommier Y. (1989) Protein-linked DNA strand breaks induced in mammalian cells by camptothecin an inhibitor of topoisomerase I. *Cancer Res.* **49**: 5016-5022

- Cowell I.G., Orookov A.L., Cutts S.A., Padget K., Bell M., Milner J. and Austin C.A. (2000) Human topoisomerase II $\alpha$  and II $\beta$  interact with the C-terminal region of p53. *Exp. Cell Res.* **255**: 86-94
- Cregan S.P., MacLaurin J.G., Craig C.G., Robertson G.S., Nicholson D.W., Park D.S. and Slack R.S. (1999) Bax-dependent caspase-3 activation is a key determinant in p53-induced apoptosis in neurons. *J. Neurosci.* **19**: 7860-7869
- Cummings J., Anderson L. and Willmott N. *et al.* (1991) The molecular pharmacology of doxorubicin in vivo. *Eur. J. Cancer.* **22**: 532-535
- Cummings J., Macpherson J.S., Meikle I. and Smyth J.F. (1996) Development of anthracenyl-amino acid conjugates as topoisomerase I and II inhibitors that circumvent drug resistance. *Biochem. Pharmacol.* **52**: 979-990
- Cummings J. and Smyth J.F. (1993) DNA topoisomerase I and II as targets for rational design of new anticancer drugs. *Annals of Oncology* **4**: 533-543
- Custodio J.B.A., Cardoso C.M.P., Madeira V.M.C. and Almeida L.M. (2001) Mitochondrial permeability transition induced by the anticancer drug etoposide. *Toxicology in vitro.* **15**: 265-270
- Darzynkiewicz Z., Bruno S., Del Bino G. and Traganos F. (1996) The cell cycle effects of camptothecin. *Annals New York Academy of Sciences.* **803**: 93-100
- Daugas E., Nochy D., Ravagnan L., Loeffler M., Susin S.A., Zamzami N. and Kroemer G. (2000) Apoptosis-inducing factor (AIF): a ubiquitous mitochondrial oxidoreductase involved in apoptosis. *FEBS Lett.* **476**: 118-123
- Daujat S., Neel H., Piette J. (2001) MDM2: life without p53. *Trends in Genetics.* **17**: 459-464
- Davey R.A., Su G.M., Hargrave R. M., Harvie R. M., Baguley B. C. and Davey M.W. (1997) The potential of N-[2-(dimethylamino)ethyl]acridine-4-carboxamide to circumvent three multidrug-resistance phenotypes in vitro. *Cancer Chemother. Pharmacol.* **39**: 424-430
- Denizot F. and Lang R. (1986) Rapid colorimetric assay for cell growth and survival-Modifications to the tetrazolium dye procedure giving improved sensitivity and reliability. *J. Immunol. Methods.* **89**: 271-277
- Desagher S., Osensand A., Nichols A., Eskes R., Montessuit S., Lauper S., Maundrell K., Antonsson B. and Martinous J.C. (1999) Bid-induced conformational change of Bax is responsible for mitochondrial cytochrome c release during apoptosis, *J. Cell. Biol.* **144**: 891-901
- Di Leonardo A., Linke S.P., Clarkin K. and Wahl G.M. (1994) DNA damage triggers a prolonged p53-dependent G1 arrest and long-term induction of Cip1 in normal human fibroblasts. *Genes Dev.* **8**: 2540-2551

Dive C. and Hickman J.A. (1991) Drug target interactions: only the first step in the commitment to a programmed cell death. *Br. J. Cancer*. **64**: 192-196

Donehower L.A., Harvey M., Slagle B., McArthur M., Montgomery C., Butel J. and Bradley A. (1992) Mice deficient for p53 are developmentally normal but susceptible to spontaneous tumours. *Nature*. **356**: 215-221

Drake F.H., Hofmann G.A., Bartus H.F., Mattern M.R., Crooke S.T. and Mirabelli C.K. (1989) Biochemical and pharmacological properties of p170 and p180 forms of topoisomerase II. *Biochemistry*. **28**: 8154-8160

Drake F.H., Zimmerman J. P., McCabe F.L., Bartus H.F., Per S.R., Sullivan D.M., Ross W.E., Mattern M.R., Johnson R. K., Crooke S.T. and Mirabelli C.K. (1987) Purification of topoisomerase II from amsacrine-resistant P388 leukemia cells. Evidence for two forms of the enzyme. *J. Biol. Chem*. **262**: 16739-16747

Driggers W.J., Grishko V.I., Ledoux S.P. and Wilson G.L. (1996) Defective repair of oxidative damage in the mitochondrial DNA of a xeroderma pigmentosum group A cell line. *Cancer Res*. **56**: 1262-1266

Du C., Fang M., Li Y., Li L. and Wang X. (2000) Smac, a mitochondrial protein that promotes cytochrome c-dependent caspase activation by eliminating IAP inhibition. *Cell*. **102**: 33-42

El-Deiry W.S., Harper J.W., O'Connor P.M., Velculescu V.E., Canman C.E., Jackman J., Pietenpol J.A., Burrell M., Hill D.E., Wang Y., Wiman K.G., Mercer W.E., Kastan M.B., Kohn K.W., Elledge S.J., Kinzler K.W. and Vogelstein B. (1994) WAF1/CIP1 is induced in p53-mediated G1 arrest and apoptosis. *Cancer Res*. **54**: 1169-1174

El-Deiry W.S., Tokino T., Velculescu V.E., Levy D.B., Parsons R., Trent J.M., Lin D., Mercer W.E., Kinzler K.W. and Vogelstein B. (1993) WAF1, a potential mediator of p53 tumour suppression. *Cell*. **75**: 817-825

Evan G. and Littlewood T. (1998) A matter of life and cell death. *Science*. **281**: 1317-1321

Facompre M., Watez N., Kluza J., Lansiaux A. and Bailly C. (2000) Relationship between cell cycle changes and variations of the mitochondrial membrane potential induced by etoposide. *Mol. Cell Biol. Res. Comm*. **4**: 37-42

Falcieri E., Martelli A.M., Bareggi R., Cataldi A. and Cocco L. (1993) The protein kinase inhibitor staurosporine induces morphological changes typical of apoptosis in MOLT-4 cells without concomitant DNA fragmentation. *Biochem. Biophys Res Commun*. **193**: 19-25

- Fakharzadeh S.S., Trusko S.P. and George D.L. (1991) Tumorigenic potential associated with enhanced expression of a gene that is amplified in a mouse tumor cell line. *EMBO J.* **10**: 1565-1569
- Fantin V.R., Berardi M.J., Scorrano L., Korsmeyer S.J. and Leder P. (2002) A novel mitochondriotoxic small molecule that selectively inhibits tumor cell growth. *Cancer Cell.* **2**: 29-42
- Feller N., Broxterman H.J., Wahrer D.C. and Pinedo H.M. (1995) ATP-dependent efflux of calcein by the multidrug resistance protein (MRP): no inhibition by intracellular glutathione depletion. *FEBS Lett.* **368**: 385-388
- Finlay G. J., Marshall E., Matthews J. H. L., Paull K. D. and Baguley B. C. (1993) In vitro assessment of N-[2-(dimethylamino)ethyl]acridine-4-carboxamide, a DNA-intercalating antitumour drug with reduced sensitivity to multidrug resistance. *Cancer Chemother. Pharmacol.* **31**: 401-406
- Fischer B., Coelho D., Dufour P., Bergerat J.P., Denis J.M., Gueulette J. and Bischoff P. (2003) Caspase 8-mediated cleavage of the pro-apoptotic BCL-2 family member BID in p53-dependent apoptosis. *Biochem. Biophys. Res. Comm.* **306**: 516-522
- Fleischmann G., Pflugfelder G., Steiner E.K., Javaherian K., Howard G.C., Wang J.C. and Elgin S.C.R. (1984) Drosophila DNA topoisomerase I is associated with transcriptionally active regions of the genome. *Proc. Natl. Acad. Sci. USA.* **81**: 6958-6962
- Flens M.J., Zaman G.J., van der Valk P., Izquierdo M.A., Schroeijers A.B., Scheffer G.L., van der Groep P., de Haas M., Meijer C.J. and Scheper R.J. (1996) Tissue distribution of the multidrug resistance protein. *Am. J. Pathol.* **148**: 1237-1247
- Fojo T. (2002) P53 as a therapeutic target: unresolved issues on the road to cancer therapy targeting mutant p53, Mini reviews. *Drug resistance updates.* **5**: 209-216
- Foster B.A., Coffey H.A., Morin M.J., Rastinejad F. (1999) Pharmacological rescue of mutant p53 conformation and function. *Science.* **286**: 2507-2510
- Friedlander P., Haupt Y., Prives C. and Oren M. (1996a) A mutant p53 that discriminate between p53-responsive genes cannot induce apoptosis. *Mol Cell Biol.* **16**: 4961-4971
- Friedlander P., Legros Y., Soussi T. and Prives C. (1996b) Regulation of mutant p53 temperature-sensitive DNA binding. *J. Biol. Chem.* **271**: 25468-25478
- Froelich-Ammon S.J. and Osheroff N. (1995) Minireview Topoisomerase poisons: Harnessing the dark side of enzyme mechanism. *J. Biol. Chem.* **270**: 21429-21432

Fuchs E.J., McKenna K.A. and Bedi A. (1997) P53-dependent DNA damage-induced apoptosis requires Fas/APO-1-independent activation of CPP32beta. *Cancer Res.* **57**: 2550-2554

Fulda S., Friesen C., Los M., Scaffidi C., Mier W., Benedict M., Nunez G., Krammer P.H., Peter M.E. and Debatin K.M. (1997) Betulinic acid triggers CD95 (Apo-1/Fas)-and p53-independent apoptosis via activation of caspases in neuroectodermal tumors. *Cancer Res.* **57**: 4956-4964

Fulda S., Scaffidi C., Susin S.A., Krammer P.H., Kroemer G., Peter M.E. and Debatin K.M. (1998) Activation of mitochondria and release of mitochondrial apoptogenic factors by betulinic acid. *J. Biol. Chem.* **273**: 33942-33948

Gallo R.C.J., Whang-Peng J. and Adamson R.H. (1971) Studies on the antitumour activity, mechanism of action, and cell cycle effects of camptothecin. *J. Natl. Cancer Inst.* **46**: 789-795

Gao H., Huang K.C., Yamasaki E. F., Chan K. K., Chohan L., Snapka R. M., (1999). XK469, a selective topoisomerase II $\beta$  poison. *PNAS.* **96**: 12168-12173.

Gellert M. (1981) DNA topoisomerases. *Ann. Rev. Biochem.* **50**: 879-910

Gobert C., Bracco L., Rossi F., Oliver M., Tazi J., Lavelle F., Larsen A.K. and Riou J.F. (1996) Modulation of topoisomerase I activity by p53. *Biochemistry.* **35**: 5778-5786

Gomez-Manzano C., Fueyo J., Kyritsis A.P., Steck P.A., Roth J.A., McDonnell T.J., Steck Klevin V.A. and Yung W.K.A (1996) Adenovirus mediated transfer of p53 gene produces rapid and generalised death of human glioma cells via apoptosis. *Cancer Res.* **56**: 694-699

Gong J., Li X. and Darzynkiewicz Z. (1993) Different patterns of apoptosis of HL60 cells induced by cycloheximide and camptothecin. *J. Cell Physiol.* **157**: 263-270

Gong J., Traganos F. and Darzynkiewicz Z. (1994) A selective procedure for DNA extraction from apoptotic cells applicable for gel electrophoresis and flow cytometry. *Analytical Biochem.* **218**: 314-319

Goossens J.F., Henichart J.P., Dassonneville L., Facompre M. and Bailly C. (2000) Relationship between intracellular acidification and camptothecin induced apoptosis in leukaemic cells. *Eur. J. Pharm. Sciences.* **10**: 125-131

Gorczyca W., Gong J., Ardelt B., Traganos F. and Darzynkiewicz Z. (1993) The cell cycle related differences in susceptibility of HL-60 cells to apoptosis induced by various antitumour agents. *Cancer Res.* **53**: 3186-3192

Goto T. and Wang J.C. (1985) Cloning of yeast TOP1, the gene encoding DNA topoisomerase I, and construction of mutants defective in both DNA topoisomerase I and DNA topoisomerase II. *Proc. Natl. Acad. Sci. USA.* **82**: 7178-7182

Goyal L. (2001) Cell death inhibition keeping caspases in check. *Cell.* **104**: 805-808

Gros P., Neriah Y.B., Croop J.M. and Houseman D.E. (1986) Isolation and expression of complementary DNA that confers multidrug resistance. *Nature.* **323**: 728-731

Halevy O., Michalovitz D. and Oren M. (1990) Different tumour-derived p53 mutants exhibit distinct biological activities. *Science.* **250**: 113-116

Hall P.A. (1998) P53: The challenge of linking basic science and patient management. *The Oncologist.* **3**: 218-224

Hall P.A., Meek D. and Hall D.P. (1996) p53-integrating the complexity. *J. Pathol.* **180**: 1-5

Hande K.R. (1998), Gene structure and expression, Clinical applications of anticancer drugs targeted to topoisomerase II. *Biochim. Biophys. Acta* **1400**: 173-184

Hannun Y.A. (1997) Apoptosis and the dilemma of cancer chemotherapy. *Blood.* **89**: 1845-1853

Harada K. and Ogden G.R. (2000) An overview of the cell cycle arrest protein, p21<sup>WAF1</sup>. *Oral oncology* **36**: 3-7

Harker W.G., Slade D.L., Parr R.L. Feldhoff P.W., Sullivan D.M. and Holguin M.H. (1995) Alterations in the topoisomerase II alpha gene, messenger RNA and subcellular protein distribution as well as reduced expression of the DNA topoisomerase II beta enzyme in a mitoxantrone-resistant HL-60 human leukaemia cell. *Cancer Res.* **55**: 1707-1716

Harper J.W., Adami G.R., Wei N., Keyomarsi K. and Elledge S.J. (1993) The p21 Cdk-interacting protein cip1 is a potent inhibitor of cyclin-dependent kinases. *Cell.* **75**: 805-816

Haupt Y., Maya R., Kazaz A. and Oren M. (1997) Mdm2 promotes the rapid degradation of p53. *Nature.* **387**: 296-299

Heck M.M.S., Hittleman W.N. and Eranshaw W.C. (1988) Differential expression of DNA topoisomerase I and II during the eukaryotic cell cycle. *Proc. Natl. Acad. Sci. USA.* **85**: 1086-1090

Hermeking H. and Eick D. (1995) Mediation of c-myc-induced apoptosis by p53. *Science.* **265**: 2091-2093

Hertzberg R.P., Busby R.W., Caranfa M.J., Holden K.G., Johnson R.K., Hecht S.M. and Kingsbury W.D. (1990) Irreversible trapping of the DNA-topoisomerase I covalent complex, Affinity labelling of the camptothecin binding site. *J. Biol. Chem.* **265**: 19287-19295

Hietanen S., Lain S., Kravz E., Blattner C. and Lane D.P. (2000) Activation of p53 in cervical carcinoma cells by small molecules. *Proc. Natl. Acad. Sci. USA.* **97**: 8501-8506

Hindenburgh A.A., Gervasoni J.E. Jr, Krishna S., Steward V.J., Rosado M., Lutzky J., Bhalla K., Baker M.A. and Taub R.N. (1989) Intracellular distribution and pharmacokinetics of daunorubicin in anthracycline sensitive and resistant HL-60 cells. *Cancer Res.* **49**: 4607-4614

Hitt M., Addison C.L. and Graham F.L. (1997) Human adenovirus vectors for gene transfer into mammalian cells. *Adv. Pharmacol.* **40**: 137-205

Hollstein M., Sidransky D., Vogelstein B. and Harris C.C. (1991) P53 mutations in human cancers. *Science.* **253**: 49-53

Horowitz S.B. and Horowitz M. (1973) Effects of camptothecin on the breakage and repair of DNA during the cell cycle. *Cancer Res.* **33**: 2834-2836

Howell N., Taylor S.W., Fahy E., Murphy A. and Ghos S.S. (2003) Restoring energy in a power crisis: mitochondrial targets for drug development. *Targets.* **2**: 208-216

Hu Y.P., Moraes C.T., Savaraj N., Priebe W., Lampidis T.J. (2000) p<sup>0</sup> tumor cells: a model for studying whether mitochondria are targets for rhodamine 123, doxorubicin and other drugs. *Biochem. Pharmacol.* **60**: 1897-1905

Hunter T. (1993) Braking the cycle. *Cell.* **75**: 839-841

Hurley L.H. (2002) in 'DNA and its associated processes as targets for cancer therapy'. *Macmillan Magazines Ltd.* **2**: 188-200

Hwang J. And Hwong C-L. (1991) Cellular regulation of mammalian DNA topoisomerases. *Adv. Pharmacol.* **29A**: 167-188

Ishida K. and Asao T. (2002) Self-association and unique DNA binding properties of the anti-cancer agent TAS-103, a dual inhibitor of topoisomerase I and II. *Biochimica et Biophysica Acta.* **1587**: 155-163

Jiang S., Cai J., Wallace D.C. and Jones D.P. (1999) Cytochrome c-mediated apoptosis in cells lacking mitochondrial DNA. *J. Biol. Chem.* **274**: 29905-29911

Johnson N., Tony T.C. and Parkin J.M. (1997) Camptothecin causes cell cycle perturbations within T-lymphoblastoid cell followed by dose dependent induction of apoptosis. *Leukemia Res.* **21**: 961-972

Joza N., Susin S.A., Daugas E., Stanford W.L., Cho S.K., Li C.Y., Sasaki T., Elia A.J., Cheng H.Y., Ravagnan L., Ferri K.F., Zamzami N., Wakeham A., Hakem R., Yoshida H., Kong Y.Y., Mak T.W., Zuniga-Pflucker J.C., Kroemer G. and Penninger J.M. (2001) Essential role of the mitochondrial apoptosis-inducing factor in programmed cell death. *Nature.* **410**: 549-554

Juan C.C., Hwang J., Liu A.A., Whang-Peng J., Knutsen T., Huebner K., Croce C.M., Zhang H., Wang J.C. and Liu L.F. (1988) Human DNA topoisomerase I is encoded by a single copy gene that maps to chromosome region 20q12-13.2. *Proc. Natl. Acad. Sci. USA.* **85**: 8910-8913

Jung K. and Reszka R. (2001) Mitochondria as subcellular targets for clinically useful anthracyclines. *Adv. Drug Delivery reviews.* **49**: 87-105

Kagan V.E., Yalowich J.C., Day B.W., Goldman R., Gantchev T.G. and Stoyanovsky D.A. (1994) Ascorbate is the primary reductant of the phenoxy radical of etoposide in the presence of thiols both in cell homogenates and in model systems. *Biochemistry.* **33**: 9651-9660

Kastan M.B., Zhan Q., El-Deiry W.S., Carrier F., Jacks T., Walsh W.V., Plunkett B.S., Vogelstein B. and Fornace Jr A.J. (1992) A mammalian cell cycle checkpoint pathway utilising p53 and GADD45 is defective in ataxia-telangiectasia. *Cell.* **71**: 587-597

Kaufman S.H. (1991) Antagonism between camptothecin and topoisomerase II-directed chemotherapeutic agents in a human leukemia cell line. *Cancer Res.* **51**: 1129-1136

Kaufmann S.H. (1989) Induction of endonucleolytic DNA cleavage in human acute myelogenous leukaemia cells by etoposide, camptothecin, and other cytotoxic anticancer drugs: a cautionary note. *Cancer Res.* **49**: 5870-5878

Kaufmann S.H. and Earnshaw W.C. (2000) Induction of apoptosis in chemotherapy. *Exp. Cell Res.* **256**: 42-49

Kaufmann S.H. and Svingen P.A. (1999) Immunoblot analysis and band depletion assays. In: *Methods in molecular biology.* Vol 94, part I. *DNA topoisomerase protocols, DNA topology and enzymes.* pp 253-268. Edited by. Bjornsti M.A. and Osheroff N. Human press Inc. Totowa. New Jersey

Kawagoe R., Kawagoe H. and Sano K. (2002) Valproic acid induces apoptosis in human leukaemia cells by stimulating both caspase-dependent and -independent apoptotic signalling pathways. *Leukemia Res.* **26**: 495-502

Keller W. (1975) Determination of the number of superhelical turns in simian virus 40 DNA by gel electrophoresis. *Proc. Natl. Acad. Sci. USA.* **72**: 4876-4880

Kern S. E., Kinzler K.W., Bruskin A., Jarosz D., Friedman P., Prives C. and Vogelstein B (1991) Identification of p53 as a sequence-specific DNA-binding protein. *Science.* **252**: 1708-1711

Kerr J.F.R., Winterford C.M. and Harmon B.V. (1994) Apoptosis, its significance in Cancer and Cancer Therapy. *Cancer.* **73**: 2013-2026

Kerr J.F.R., Wyllie A.H. and Currie A.R. (1972) Apoptosis: a basic biological phenomenon with wide-ranging implications in tissue kinetics. *Br. J. Cancer.* **26**: 239-257

Kim R., Ohi H., Inoue H. and Toge T. (1999) Expression and relationship between topoisomerase I and II alpha genes in tumour and normal tissues in esophagael, gastric and colon cancers. *Anticancer Res.* **19**: 5393-5398

Kim R., Hirabayashi N., Nishiyama M., Jinushi K., Toge T. and Okada K. (1992) Experimental studies on biochemical modulation targeting topoisomerase I and II in human tumour xenografts in nude mice. *Int. J. Cancer* **50**: 760-766

Kohn K.W. and Pommier Y. (2000) Molecular and Biological determinants of the cytotoxic actions of camptothecins. *Annals of the New York Academy of Sciences.* **922**: 11-26

Krahenbuhl S. (2001) Mitochondria: important target for drug toxicity? *J. Hepatology.* **34**: 334-336

Kubbutat M.H., Jones S.N. and Vousden K.H. (1997) Regulation of p53 stability by mdm2. *Nature.* **387**: 299-303

Lampidis T.J. Kolonias D. Podona T. Israel M. Safa A. R. Lothstein L. Savaraj N. Tapiero H. and Priebe W. (1997) Circumvention of P-GP MDR as a function of anthracycline lipophilicity and charge. *Biochemistry.* **36**: 2679-2685

Lane D.P. (1992) P53, guardian of the genome. *Nature.* **358**: 15-16

Lane D.P. and Benchimol S. (1990) p53 oncogene or anti oncogene. *Genes and Dev.* **4**: 1-8

Lane D.P. and Crawford L.V. (1979) T antigen is bound to a host protein in SV40-transformed cells. *Nature.* **278**: 261-263

Lane D.P. and Lain S. (2002) Therapeutic exploitation of the p53 pathway. *Trends in Molecular Medicine.* **8**: S38-42

Lansiaux A., Facompre M., Wattez N., Hildebrand M.P., Bal C., Demarquay D., Lavergne O., Bigg D.C. and Bailly C. (2001) Apoptosis induced by the homocamptothecin anticancer drug BN80915 in HL-60 cells. *Mol. Pharmacol.* **3**: 450-461

Larsen A.K., Escargueil A.E. and Skladanowski A. (2000) Resistance mechanisms associated with altered intracellular distribution of anticancer agents. *Pharmacol. Therapeutics.* **85**: 217-229

Larsen A.K. and Skladanowski A. (1998) Cellular resistance to topoisomerase-targeted drugs: from drug uptake to cell death. *Biochim. Biophys. Acta.* **1400**: 257-274

Lazebnik Y.A., Cole S., Cooke C.A., Nelson W.G. and Earnshaw W.C. (1993) Nuclear events of apoptosis in vitro in cell free mitotic extracts: a model system for analysis of the active phase of apoptosis. *J. Cell Biol.* **123**: 7-22

Lee C.C.R. and Fukushima S. (1998) Alterations in cyclin D1, p53 and the cell cycle related elements: Implications for distinct genetic pathways of urinary bladder carcinogens. *Urologic Oncol.* **4**: 58-72

Legrand O., Simonin G., Beauchamp-Nicoud A., Zittoun R. and Marie J.P. (1999) Simultaneous activity of MRP1 and Pgp is correlated with in vitro resistance to daunorubicin and with in vivo resistance in adult acute myeloid leukaemia. *Blood.* **94**: 1046-1056

Leist M. and Nicotera P. (1998) Apoptosis, excitotoxicity, and neuropathology. *Exp. Cell. Res.* **239**: 183-201

Leist M. and Nicotera P. (1997) The shape of cell death. *Biochem. Biophys. Res. Commun.* **236**: 1-9

Levine A.J. (1997) P53 the cellular gatekeeper for growth and division. *Cell.* **88**: 323-331

Li P.F., Dietz R. and von Harsdorf R. (1999) P53 regulates mitochondrial membrane potential through reactive oxygen species and induces cytochrome c independent apoptosis blocked by Bcl-2. *EMBO J.* **18**: 6027-6036.

Liang Y., Yan C. and Schor N.F. (2001) Apoptosis in the absence of caspase3. *Oncogene.* **20**: 6570-6578

Lindsley J.E. and Wang J.C. (1991) Proteolysis patterns of epitopically labelled yeast DNA topoisomerase II suggests an allosteric transition in the enzyme induced by ATP binding. *Proc. Natl. Acad. Sci. USA.* **88**: 10485-10489

Linzer D.L. and Levine A.J. (1979) Characterisation of a 54K Dalton cellular SV40 tumour antigen present in SV40 transformed cells and uninfected embryonal carcinoma cells. *Cell.* **17**: 43-52

- Liu L.F. (1989) DNA topoisomerase poisons as antitumor drugs. *Annu. Rev. Biochem.* **58**: 351-375
- Liu T., Raetz E., Moos P.J., Perkins S.L., Bruggers C.S., Smith E. and Carroll W.L. (2002) Diversity of the apoptotic response to chemotherapy in childhood leukaemia. *Leukemia*. **16**: 223-232
- Liu T.J., Zhang W.W., Taylor D.L., Roth J.A., Goepfert H. and Clayman G.L. (1994) Growth suppression of human head and neck cancer cells by introduction of a wild type p53 gene via a recombinant adenovirus. *Cancer Res.* **54**: 3662-3667
- Liu W. and Zhang R. (1998) Upregulation of p21<sup>WAF1/CIP1</sup> in human breast cancer cell lines MCF-7 and MDA-MB-468 undergoing apoptosis induced by natural product anticancer drugs 10-hydroxycamptothecin and camptothecin through p53-dependent and independent pathways. *Int. J. Oncol.* **12**: 793-804
- Low R.L., Orton S. and Friedman D.B. (2003) A truncated form of DNA topoisomerase II $\beta$  associates with the mtDNA genome in mammalian mitochondria. *Eur. J. Biochem.* **270**: 4173-4186
- Lowe S.W., Ruley H.E., Jacks T. and Houseman D.E., (1993a) P53 dependent apoptosis modulates the cytotoxicity of anticancer agents. *Cell* **74**: 957-967
- Lowe S.W., Schmitt E.M., Smith S.W., Osborne B.A. and Jacks T. (1993b) P53 is required for radiation-induced apoptosis in mouse thymocytes. *Nature*. **362**: 847-849
- Luo X., Budihardjo I., Zou H., Slaughter C. and Wang X.D. (1998) Bid, a Bcl2 interacting protein, mediates cytochrome c release from mitochondria in response to activation of cell surface death receptors. *Cell*. **94**: 481-490
- Luu Y., Bush J., Cheung Jr K.J. and Li G. (2002) The p53 stabilizing compound CP-31398 induces apoptosis by activating the intrinsic bax/mitochondrial/caspase-9 pathway. *Exp. Cell Res.* **276**: 214-222
- Macpherson J.S., Cummings J., Meikle I., Miller E.P. and Smyth J.F. (1997) Cell cycle effects of the novel topoisomerase I inhibitor NU/ICRF 505 in a panel of Chinese hamster ovary cell lines. *Eur. J. Cancer*. **33**: 280-283
- Madelaine I., Prost S., Naudin A., Riou G., Lavelle F. and Riou J.F. (1993) Sequential modifications of topoisomerase I activity in a camptothecin-resistant cell line established by progressive adaptation. *Biochem. Pharmacol.* **45**: 339-348
- Majno G. and Joris I. (1995) Apoptosis, oncosis and necrosis: an overview of cell death. *Am. J. Pathol.* **46**: 3-15

Makin G. and Hickman J.A. (2000) Apoptosis and cancer chemotherapy. *Cell Tissue Res.* **301**: 143-152

Makri D., Schulz W.A., Grimm M.O., Clasen S., Bojar H. and Schmitz-Drager B.J. (1998) WAF1/p21 regulates proliferation, but does not mediate p53-dependent apoptosis in urothelial carcinoma cell lines. *Int. J. Oncol.* **12**: 621-628

Malonne H. and Atassi G. (1997) Review paper: DNA topoisomerase targeting drugs: mechanisms of action and perspectives, *Anti-Cancer Drugs.* **8**: 811-822

Marsh K.L., Willmore E., Tinelli S., Cornarotti M., Meczes E.L., Capranico G., Fisher L.M. and Austin C.A. (1996) Amsacrine-promoted DNA cleavage site determinants for the two human DNA topoisomerase isoforms  $\alpha$  and  $\beta$ . *Anticancer Research.* **16**: 1603-1610

Martins L.M., Mesner P.W., Kottke T.J., Basi G.S., Sinha S., Tung J.S., Svingen P.A., Madden B.J., Takahashi A., McCormick D.J., Earnshaw W.C. and Kaufmann S.H. (1997) Comparison of caspase activation and subcellular localisation in HL-60 and K562 cells undergoing etoposide-induced apoptosis. *Blood.* **90**: 4283-4296

McConnaughie A.W. and Jenkins T.C. (1996) Novel acridine-triazines as prototype combilexins: synthesis, DNA bonding and biological activity. *J Med. Chem.* **38**: 3488-3501

McLean J.E., Neidhardt E.A., Grossman T.H. and Hedstrom L. (2001) Multiple inhibitor analysis of the brequinar and leflunomide binding sites on human dihydroorotate dehydrogenase. *Biochemistry.* **40**: 2194-2200

McLeod H.L., Douglas F., Oates M., Symonds R.P., Prakash D., van der Zee G.J., Kaye S.B., Brown R. and Keith W.N. (1994) Topoisomerase I and II activity in human breast, cervix, lung and colon cancer. *Int. J. Cancer.* **59**: 607-611

Meikle I., Cummings J., Macpherson J.S., Hadfield J.A. and Smyth J.F. (1995a) Biochemistry of topoisomerase I and II inhibition by anthracenyl-amino acid conjugates. *Biochem. Pharmacol.* **49**: 1747-1757

Meikle I., Cummings J., Macpherson J.S. and Smyth J.F. (1995b) Identification of anthracenyl-dipeptide conjugates as novel topoisomerase I and II inhibitors and their evaluation as potential cancer drugs. *Anti-cancer Drug Design.* **10**: 515-527

Meikrantz W. and Schlegel R. (1995) Apoptosis and the cell cycle. *J. Cell. Biochem.* **58**: 160-174

- Meng X.W., Fraser M.J., Feller J.M. and Ziegler J.B. (2000) Caspase-3-dependent and caspase-3-independent pathways leading to chromatin DNA fragmentation in HL-60 cells. *Apoptosis*. **5**: 61-67
- Metivier D., Dallaporta B., Zamzami N., Larochette N., Susin S.A., Marzo I. and Kroemer G. (1998) Cytofluorometric detection of mitochondrial alterations in early CD95/Fas/APO-1-triggered apoptosis of Jurkat T lymphoma cells. Comparison of seven mitochondrion-specific fluorochromes. *Immunology Letters*. **61**: 157-163
- Miyashita T. and Reed J.C. (1995) Tumor suppressor p53 is a direct transcriptional activator of the human bax gene. *Cell*. **80**: 293-299
- Monks A., Scudiero D.A., Johnson G.S., Paull K.D. and Sausville E.A. (1997) Mini-review. The NCI anti-cancer drug screen: a smart screen to identify effectors of novel targets. *Anti-Cancer Drug Design*. **12**: 533-541
- Morgan M.A. and Rubin S.C. (1998) Long-term complications of chemotherapy. *Oncology Update*. **5**: 65-68
- Mosmann T. (1983) Rapid colorimetric assay for cellular growth and survival: application to proliferation and cytotoxicity assays. *J. Immunological Methods* **65**: 55-62
- Murphy M.P., Smith R.A.J. (2000) Drug delivery to mitochondria: the key to mitochondrial medicine. *Advanced drug delivery reviews*. **41**: 235-250
- Murren J.R., Beidler D.R. and Cheng Y.C. (1996) Camptothecin resistance related to drug-induced down regulation of topoisomerase I and steps occurring after the formation of protein-linked DNA breaks. *Annals New York Academy of Sciences*. **803**: 74-92
- Neidle S. (2002) Principles of Small Molecule-DNA Recognition. In '*Nucleic Acid Structure and Recognition*'. pp88-138. Oxford University Press
- Nakano K. and Vousden K.H. (2001) PUMA, a novel proapoptotic gene, is induced by p53. *Mol. Cell*. **7**: 683-694
- Nelson E.M., Tewey K.M. and Liu L.F. (1984) Mechanism of antitumour drugs. Poisoning of mammalian DNA topoisomerase II on DNA by an antitumour drug m-AMSA. *Proc. Natl. Acad. Sci. USA*. **81**: 1361-1365
- Nelson W.G. and Kastan M.B. (1994) DNA strand breaks: the DNA template alterations that trigger p53-dependent DNA damage response pathways. *Mol. Cell Biol*. **14**: 1815-1823
- Newmeyer D.D. and Ferguson-Miller S. (2003) Mitochondria: Releasing power for life and unleashing the mechineries of death. *Cell*. **112**: 481-490

Nitiss J.L. (1994a) Roles of DNA topoisomerases in chromosomal replication and segregation. *Adv. Pharmacol.* **29**: 103-134

Nitiss J.L. (1994b) Yeast as a genetic model system for studying topoisomerase inhibitors. *Adv. Pharmacol.* **29B**: 201-226

Nitiss J.L. (1998) Investigating the biological functions of DNA topoisomerases in eukaryotic cells. *Biochim. Biophys. Acta.* **1400**: 63-81

Nitiss J.L., Liu Y.X., Harbury P., Jannatipour M., Wasserman R. and Wang J.C. (1992) Amsacrine and etoposide hypersensitivity in yeast cells overexpressing DNA topoisomerase II. *Cancer Res.* **52**: 4467-4472

Nitiss J.L. and Nitiss K.C. (2001) Yeast system for demonstrating the targets of anti-topoisomerase II agents. In *Methods in Molecular Biology*. Vol 95, part II. DNA topoisomerase protocols, enzymology and drugs. pp315-327. Edited by Osheroff N. and Bjornsti M.A. Humana Press Inc. Totowa New Jersey

Noda A., Ning Y., Venable S.F., Pereira-Smith O.M. and Smith J.R. (1994) Cloning of senescent cell-derived inhibitors of DNA synthesis using an expression screen. *Exp. Cell Res.* **211**: 90-98

Oberley T.D. and Oberley L.W. (1997) Antioxidant enzyme levels in cancer. *Histol. Histopathol.* **12**: 525-535

O'Connor P.M., Jackman J., Bae I., Myers T.G., Fan S., Mutoh M., Scudiero D.A., Monks A., Sausville E.A., Weinstein J.N., Friend S., Fornace Jr A.J. and Kohn K.W. (1997) Characterisation of the p53 tumour suppressor pathway in cell lines of the National Cancer Institute anticancer drug screen and correlations with the growth-inhibitory potency of 123 anticancer agents. *Cancer Res.* **57**: 4285-4300

Oda E., Ohki R., Murasawa H., Nemoto J., Shibue T., Yamashita T., Tokino T., Taniguchi T. and Tanaka N. (2000) Noxa, a BH3-only member of the Bcl-2 family and candidate mediator of p53 induced apoptosis. *Science.* **288**: 1053-1058

Oliner J.D., Kinzler K.W., Meltzer P.S., George D.L. and Vogelstein B. (1992) Amplification of a gene encoding a p53-associated protein in human sarcomas. *Nature.* **358**: 80-83

Onishi Y., Azuma Y., Sato Y., Mizuno Y., Tadakuma T. and Kizaki H. (1993) Topoisomerase inhibitors induce apoptosis in thymocytes. *Biochim. Biophys. Acta.* **1175**: 147-154

Ormerod M.G. (2000) Flowcytometry, 3<sup>rd</sup> edition, p84, Oxford University Press.

- Padgett K., Stewart A., Charlton P., Tilby M.J. and Austin C.A. (2000) An investigation into the formation of N-[2-(dimethylamino)ethyl]acridine-4-carboxamide (DACA) and 6-[2-(dimethylamino)ethylamino]-3-hydroxy-7H-indeno[2,1-C]quinolin-7-onedihydrochloride (TAS-103) stabilised DNA topoisomerase I and II cleavable complexes in human leukaemia cells. *Biochem. Pharmacol.* **60**: 817-821
- Pandey S., Walker P.R. and Sikorska M. (1994) Separate pools of endonuclease activity are responsible for internucleosomal and higher molecular mass DNA fragmentation during apoptosis. *Biochem. Cell Biol.* **72**: 625-629
- Parone P.A., James D. and Martinou J.C. (2002) Mitochondria: regulating the inevitable. *Biochimie.* **84**: 105-111
- Pastawa E., Ciesielska E., Piestrzeniewicz M.K., Denny W.A., Gniazdowski M. and Szmigiero L. (1998) Cytotoxic and DNA-damaging-4-carboxamide (DACA) and its analogues. *Biochem. Pharmacol.* **56**: 351-359
- Perego P., Corna E., De Cesare M., Gatti L., Polizzi D., Pratesi G., Supino R. and Zunino F. (2001) Role of apoptosis and apoptosis-related genes in cellular response and antitumor efficacy of anthracyclines. *Curr. Med. Chem.* **8**: 31-37
- Pervaiz S., Hirpara J.L. and Clément M.V. (1998) Caspase proteases mediate apoptosis induced by anticancer agent preactivated MC540 in human tumor cell lines. *Cancer Letters.* **128**: 11-22
- Picksley S.M. and Lane D.P. (1993) The p53 mdm2 autoregulatory feedback loop: a paradigm for the regulation of growth control by p53? *BioEssays.* **15**: 689-690
- Pines J. (1994) P21 inhibits cyclin shock. *Nature.* **369**: 520-521
- Polyak K., Xia Y., Zweier J.L., Kinzler K.W. and Vogelstein B. (1997) A model for p53-induced apoptosis. *Nature.* **389**: 300-305
- Pommier Y., Kerrigan D., Hartman K.D., Glazer R.I. (1990) Phosphorylation of mammalian DNA topoisomerase I and activation by protein kinase C. *J. Biol. Chem.* **265**: 9418-9422
- Pommier Y., Pourquier P., Urasaki Y., Wu J. and Laco G.S. (1999) Topoisomerase I inhibitors: selectivity and cellular resistance. *Drug Resistance Updates.* **2**: 307-318
- Poot M., Hiller K.H., Heimpel S. and Hoehn H. (1995) Distinct patterns of cell cycle disturbance elicited by compounds interfering with DNA topoisomerase I and II activity. *Exp. Cell Res.* **218**: 326-330

- Postow L., Peter B.J. and Cozzarelli N.R. (1999) Knot what we thought before: the twisted story of replication. *BioEssays*. **21**: 805-808
- Preston T.J., Abadi A., Wilson L. and Singh G. (2001) Mitochondrial contributions to cancer cell physiology: potential for drug development. *Advanced Drug Delivery Reviews*. **49**: 45-61
- Pruschy M., Rocha S., Zaugg K., Tenzer A., Hess C., Fisher D.E., Glanzmann C. and Bodis S. (2001) Key targets for the execution of radiation-induced tumor cell apoptosis: the role of p53 and caspases. *Int. J. Radiation Oncol. Biol. Phys.* **49**: 561-567
- Rigberg D.A., Blinman T.A., Kim F.S., Cole M.A. and McFadden D.W. (1999) Antisense blockade of p21/WAF1 decreases radiation-induced G2 arrest in esophageal squamous cell carcinoma. *J. Surgical Res.* **81**: 6-10
- Robertson J.D., Gogvadze V., Zhivotovsky B. and Orrenius S. (2000) Distinct pathways for stimulation of cytochrome c release by etoposide. *J. Biol. Chem.* **275**: 32438-32443
- Robles S.J., Buehler P.W., Negrusz A. and Adami G.R. (1999) Permanent cell cycle arrest in asynchronously proliferating normal human fibroblasts treated with doxorubicin or etoposide but not camptothecin. *Biochem. Pharmacol.* **58**: 675-685
- Roca J. and Wang J.C. (1992) The capture of a DNA double helix by an ATP-dependent protein clamp: a key step in DNA transport by type II DNA topoisomerases. *Cell*. **71**: 833-840
- Rowan S., Ludwig R.L., Haupt Y., Bates S., Lu X., Oren M. and Vousden K.H. (1996) Specific loss of apoptotic but not cell-cycle arrest function in a human tumour derived p53 mutant. *EMBO J.* **15**: 827-838
- Rubin L.L., Philpott K.L. and Brooks S.F. (1993) The cell cycle and cell death. *Curr. Biol.* **3**: 391-394
- Ryan K.M. and Vousden K.H. (1998) Characterization of structural p53 mutants which show selective defects in apoptosis but not cell cycle arrest. *Mol. Cell Biol.* **18**: 3692-3698
- Salvesen G.S. and Dixit V.M. (1997) Caspases: Intracellular signalling by proteolysis. *Cell*. **91**: 443-446
- Schuler M., Bossy-Wetzel E., Goldstein J.C., Fitzgerald P. and Green D.R. (2000) P53 induces apoptosis by caspase activation through mitochondrial cytochrome c release. *J. Biol. Chem.* **275**: 7337-7342
- Schwartzmann R.A. and Cidlowski J.A. (1993) Apoptosis, the biochemistry and molecular biology of programmed cell death. *Endocrine Reviews*. **14**: 133-151

Serafino A., Sinibaldi-Vallebona P., Pierimarchi P., Bernard P., Guadiano G., Massa C., Rasi G. and Ranagnan G. (1999) Induction of apoptosis in neoplastic cells by anthracycline antitumour drugs: nuclear and cytoplasmic triggering?. *Anticancer Res.* **19**: 1909-1918

Serrano M., Hannon G.J. and Beach D. (1993) A new regulatory motif in cell-cycle control causing specific inhibition of cyclin D/CDK4. *Nature.* **366**: 704-707

Shellhaas J.L. and Zuckerman S.H. (1995) In vitro detection of apoptotic stimuli by use of the HL60 myeloid cell line. *Clinical and Diagnostic Laboratory Immunology.* **2**: 598-603

Sherr C.J. (1993) Mammalian G1 cyclins. *Cell.* **73**: 1059-1065

Shigenaga M.K., Hagen T.M. and Ames B.N. (1994) Oxidative damage and mitochondrial decay in aging. *Proc. Natl. Acad. Sci. USA.* **91**: 10771-10778

Shieh S.Y., Ikeda M., Taya Y. and Prives C. (1997) DNA damage induced phosphorylation of p53 alleviates inhibition by MDM2. *Cell.* **91**: 325-334

Shimamura A. and Fisher D.E. (1996) Minireview, P53 in life and death. *Clin. Cancer Res.* **2**: 435-440

Singh G, Maniccia-Bozzo E, Evidence for lack of mitochondrial DNA repair following cis-dichlorodiamine platinum treatment, *Cancer Chemother. Pharmacol.* **26**, 1990, 97-100

Siu W.Y., Yam C.H. and Poon R.Y.C. (1999) G1 versus G2 cell cycle arrest after adriamycin-induced damage in mouse Swiss3T3 cells. *FEBS Letters.* **461**: 299-305

Slater T.F., Swayer B. and Strauli U. (1963) Studies on succinate-tetrazolium reductase systems III. Points of coupling of four different tetrazolium salts. *Biochim. Biophys. Acta.* **77**: 383-393

Slee E.A., Adrian C. and Martin S.J. (1996) Serial killers: ordering caspase activation events in apoptosis. *Cell Death Differ.* **6**: 1067-1074

Sleiman R.J., Catchpoole D.R. and Stewart B.W. (1998) Drug-induced death of leukaemic cells after G2/M arrest: higher order DNA fragmentation as an indicator of mechanism. *Br. J. Cancer.* **77**: 40-50

Smith M.L., Chen I.T., Zhan Q., Bae I., Chen C.Y., Gilmer T., Kastan M.B., O'Connor P.M. and Fornace A.J. (1994) Interaction of the p53 regulated protein GADD45 with proliferating cell nuclear antigen. *Science.* **266**: 1376-1380

- Smith P.K., Krohn R.I., Hermanson G.T., Mallia A.K., Gartner F.H., Provenzano M.D., Fujimoto E.K., Goetze N.M., Olson B.J. and Klenk D.C. (1985) Measurement of protein using bichromic acid. *Anal Biochem.* **150**: 76-85
- Solary E., Bertrand R., Kohn K.W. and Pommier Y. (1993) Differential induction of apoptosis in undifferentiated and differentiated HL60 cells by DNA topoisomerase I and II inhibitors. *Blood.* **81**: 1359-1368
- Sorensen M., Sehested M., Christensen I.J. and Jensen P.B. (1997) Poster presentation: Characterization of high and low level resistance to topoisomerase I poisons in small cell lung cancer cells resistant to camptothecin and topotecan. *Lung Cancer.* **18**: 33
- Speranido S., de Belle I. and Bredesen D.E. (2000) An alternative, nonapoptotic form of programmed cell death. *PNAS.* **97**: 14376-14381
- Squir M.K.T., Sehnert A.J. and Cohen J.J. (1995) Apoptosis in leukocytes, *J. Leukocyte Biol.* **57**: 2-10
- Stacey D.W., Hitomi M. and Chen G. (2000) Influence of cell cycle and oncogene activity upon topoisomerase II $\alpha$  expression and drug toxicity. *Mol. Cell. Biol.* **20**: 9127-9137
- Steinman R.A., Hoffman B., Iro A., Guillouf C., Liebermann D.A. and El-Houseini M.E. (1994) Induction of p21 (WAF1/CIP1) during differentiation. *Oncogene.* **9**: 3389-3396
- Stewart L., Redinbo M.R., Qiu X., Hol W.G.J. and Champoux J.J. (1998) A model for the mechanism of human topoisomerase I. *Science.* **279**: 1534-1540
- Studzinski G.P. (1995) *Cell growth and apoptosis, a practical approach.* 1<sup>st</sup> edition. pp119-142. Oxford University Press.
- Sun X.M., McFarlane M., Zhuang J., Wolf B.B., Green D.R. and Cohen G.M. (1999) Distinct caspase cascades are initiated in receptor-mediated and chemical-induced apoptosis. *J. Biol. Chem.* **274**: 5053-5060
- Takimoto C.H. and Thomas R. (2000) The clinical development of 9-aminocamptothecin. *Annals of the New York Academy of Sciences.* **922**: 224-236
- Tan K.B., Dorman T.E., Falls K.M. Chung T.D.Y., Mirabelli C.K., Crooke S.T. and Mao J. (1992) Topoisomerase II alpha and topoisomerase II beta genes: Characterisation and mapping to human chromosome 17 and 3 respectively. *Cancer Res.* **52**: 231-234
- Tannock I.F. and Hill R.P. (1998) Cell proliferation and cell death. *The basic science of oncology.* 3rd edition. pp134-139

Tewey K.M., Chen G.L., Nelson E.M. and Liu L.F. (1984a) Intercalative antitumour drugs interfere with the breakage-reunion of mammalian DNA topoisomerase II. *J. Biol. Chem.* **259**: 9182-9187

Tewey K.M., Rowe T.C., Yang L., Halligan B.C. and Liu L.F. (1984b) Adriamycin-induced DNA damage mediated by mammalian DNA topoisomerase II. *Science*. **266**: 466-468

Thibodeau G.A. and Patton K.T. (1992) *The Human Body in Health and Disease*. pp86-90, p562. Mosby Year Book

Thornberry N.A. and Lazebnik Y. (1998) Caspases: Enemies within, *Science*. **281**: 1312-1316

Tkaczyk-Gobis K., Tarasiuk J., Seksek O., Stefanska B., Borowski E. and Garnier-Suillerot A. (2001) Transport of new non-cross-resistant antitumour compounds of the benzoperimidine family in multidrug resistant cells. *Eur. J. Pharmacol.* **413**: 131-141

Tortora G.J. and Grabowski S.R. (2000) *Principles of Anatomy and Physiology*. 9th edition. pp91-98. John Wiley & Sons Inc.

Turner S.D., Wijnhoven S.W.P., Tinwell H., Lashford L.S., Rafferty J.A., Ashby J., Vrieling H. and Fairbairn L.J. (2001) Assays to predict the genotoxicity of the chromosomal mutagen etoposide-focussing on the best assay. *Mutation Res.* **493**: 139-147

Ucker D.S., Obermiller P.S., Eckhart W., Apgar J.R., Berger N.A. and Meyers J. (1992) Genome digestion is a dispensable consequence of physiological cell death mediated by cytotoxic T lymphocytes. *Mol. Cell. Biol.* **12**: 3060-3069

Ueda K., Cardarelli C., Gottesman M.M. and Pastan I. (1987) Expression of a full-length cDNA for the human MDR1 gene confers resistance to colchicin and vinblastine. *Proc. Natl. Acad. Sci. USA.* **84**: 3004-3008

Uemura T. and Yanagida M. (1984) Isolation of type I and II DNA topoisomerase mutants from fission yeast: single and double mutants show different phenotypes in cell growth and chromatin organisation. *EMBO J.* **3**: 1737-1744

Valkov N.I., Gump J.L., Engel R. and Sullivan D.M. (2000) cell density-dependent VP-16 sensitivity of leukaemic cells is accompanied by the translocation of topoisomerase II $\alpha$  from the nucleus to the cytoplasm. *Br. J. Haematology.* **108**: 331-345

Verhagen A.M., Ekert P.G., Pakusch M., Silke J., Connolly L.M., Reid G.E., Moritz R.L., Simpson R.J. and Vaux D.L. (2000) Identification of DIABLO, a mammalian protein that promotes apoptosis by binding to and antagonizing IAP proteins. *Cell.* **102**: 43-53

- Vistica D.T., Skehan P., Scudiero D., Monks A., Pittman A. and Boyd M.R. (1991) Tetrazolium-based assays for cellular viability: a critical examination of selected parameters affecting formazan production. *Cancer Res.* **51**: 2515-2520
- Vogelstein B. and Kinzler K.W. (2001) Achilles' heel of cancer. *Nature.* **412**: 865-866
- Vogelstein B. and Kinzler K.W. (1992) P53 function and dysfunction, minireview. *Cell.* **70**: 523-526
- Vousden K.H. (2000) P53: Death star. *Cell.* **103**: 691-694
- Vousden K.H. (2002) Activation of the p53 tumor suppressor protein. *Biochim. Biophys. Acta* **1602**: 47-59
- Wagner A.J., Kokontis J.M. and Hay N. (1994) Myc-mediated apoptosis requires wild type p53 in a manner independent of cell cycle arrest and the ability of p53 to induce p21waf1/cip1. *Genes Dev.* **8**: 2817-2830
- Waldman T., Lengauer C., Kinzler K.W. and Vogelstein B. (1996) Uncoupling of S phase and mitosis induced by anticancer agents in cells lacking p21. *Nature.* **381**: 713-716
- Wallace D.C. (1999) Mitochondrial diseases in man and mouse. *Science* **283**: 1488-1493
- Wang J.C. (1971) Interaction between DNA and an Escherichia coli protein  $\omega$ . *J. Mol. Biol.* **55**: 523-533
- Wang J.C. (1991) DNA topoisomerases: why so many? *J. Biol. Sci.* **266**: 6659-6662
- Wang J.C. (1994) DNA topoisomerases as targets of therapeutics, an overview. *Adv. Pharmacol.* **29A**: 1-19
- Wang J.C. (1996) DNA topoisomerases. *Annu. Rev. Biochem.* **65**: 635-692
- Wang J.C. and Liu L.F. (1979) DNA topoisomerases. Enzymes that catalyse the concerted breaking and rejoining of DNA bonds. *Molecular Genetics*. pp65-88. ed Taylor J.H. New York Academic.
- Wang Y., Lyu Y.L. and Wang J.C. (2002) Dual localisation of human DNA topoisomerase III $\alpha$  to mitochondria and nucleus. *Proc. Natl. Acad. Sci. USA.* **99**: 12114-12119
- Waterhouse N.J., Ricci J.E. and Green D.R. (2002) And all of a sudden its over: mitochondrial outer-membrane permeabilization in apoptosis. *Biochimie.* **84**: 113-121

Weinstein J.N., Myers T.G., O'Connor P.M., Friend S.H., Fornace Jr A.J., Kohn K.W., Fojo T., Bates S.E., Rubinstein L.V., Anderson N.L., Buolamwini J.K., van Osdol W.W., Monks A.P., Scudiero D.A., Sausville E.A., Zaharevitz D.W., Bunow B., Viswanadhan V.N., Johnson G.S., Wittes R.E. and Paull K.D. (1997) An information-intensive approach to the molecular pharmacology of cancer. *Science*. **275**: 343-349

Willis A.C. and Chen X. (2002) The promise and obstacle of p53 as a cancer therapeutic agent. *Curr. Mol. Med.* **2**: 329-345

Willmore E., Frank A.J., Padgett K., Tilby M.J. and Austin C.A. (1998) Etoposide targets topoisomerase II $\alpha$  and II $\beta$  in leukemic cells: Isoform-specific cleavable complexes visualized and quantified in situ by a novel immunofluorescence technique. *Mol. Pharmacol.* **53**: 78-85

Woessner R.D., Mattern M.R., Mirabelli C.K., Johnson R.K. and Drake F.H. (1991) Proliferation and cell cycle-dependence differences in expression of the 170 kilodalton and 180 kilodalton forms of topoisomerase II in NIH-3T3 cells. *Cell Growth Diff.* **209**: 209-214

Woo M.H., Vance S.R. and Brnnski M.A. (2001) Studying DNA topoisomerase I-targeted drugs in the yeast. In *Methods in Molecular Biology*. Vol 95, part II. DNA topoisomerase protocols, enzymology and drugs. pp303-313. Edited by Osheroff N. and Bjornski M.A. Humana Press Inc. Totowa New Jersey

Wyllie A.H. (1980) Glucocorticoid-induced thymocyte apoptosis is associated with endogenous endonuclease activation. *Nature*. **284**: 555-556

Wyllie A.H., Kerr J.F.R. and Currie A.R. (1980) Cell death: the significance of apoptosis. *Int. Rev. Cytol.* **68**: 251-306

Xiong Y., Zhang H. and Beach D. (1992) D type cyclins associate with multiple protein kinases and the DNA replication and repair factor PCNA. *Cell*. **71**: 505-514

Yakes F.M. and Vanhouten B. (1997) Mitochondrial DNA damage is more extensive and persists longer than nuclear DNA damage in human cells following oxidative stress. *Proc. Natl. Acad. Sci. USA*. **94**: 514-519

Yonish-Rouach E., Resnitsky D., Lotem J., Sachs K., Kim-Chi A. and Oren M. (1991) Wild type p53 induces apoptosis of myeloid leukemic cells that is inhibited by interleukin-6. *Nature*. **352**: 345-347

Yuwen H., Hsia C.C., Nakashima Y., Evangelista A. and Tabor E. (1997) Binding of wild-type p53 by topoisomerase II and overexpression of topoisomerase II in human hepatocellular carcinoma. *Biochem. Biophys. Res. Comm.* **234**: 194-197

Zhang H., Barcelo J.M., Lee B., Kohlhagen G., Zimonjic D.B., Popescu N.C. and Pommier Y. (2001) Human mitochondrial topoisomerase I, *Proc. Natl. Acad. Sci. USA*. **98**: 10608-10613

Zhang H., Xiong Y. and Beach D. (1993) Proliferating cell nuclear antigen and p21 are components of multiple cell cycle kinase complexes. *Mol. Biol Cell*. **4**: 897-906

Zhao J., Wang M., Chen J., Luo A., Wang X., Wu M., Yin D. and Liu Z. (2002) The initial evaluation of non-peptidic small-molecule HDM2 inhibitors based on p53-HDM2 complex structure. *Cancer Letters*. **183**: 69-77

Zhu X.F., Liu Z.C., Xie B.F., Li Z.M., Feng G.K., Xie H.H., Wu S.J., Yang R.Z., Wei X.Y. and Zeng Y.X. (2002) Involvement of caspase-3 activation in squamocin-induced apoptosis in leukaemia cell line HL-60. *Life Sciences*. **70**: 1259-1269

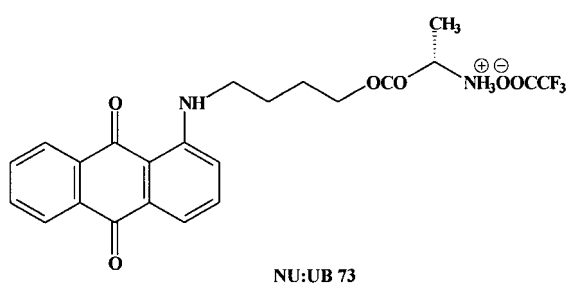
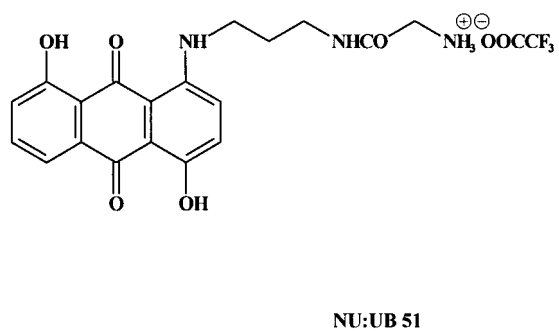
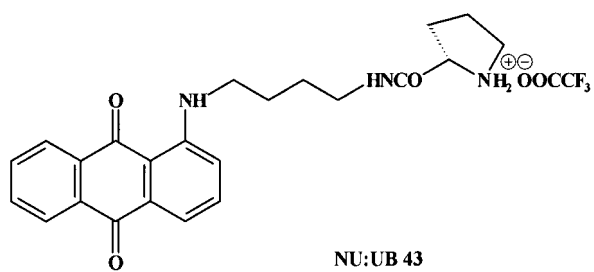
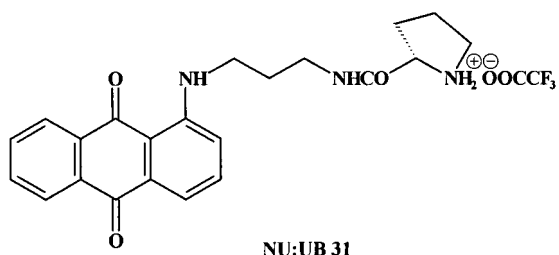
Zhuang J., Dinsdale D. and Cohen G.M. (1998) Apoptosis in human monocytic THP1 cells results in the release of cytochrome c from mitochondria prior to their ultracondensation, formation of outer membrane discontinuities and reduction in inner membrane potential. *Cell Death Differ*. **5**: 953-962

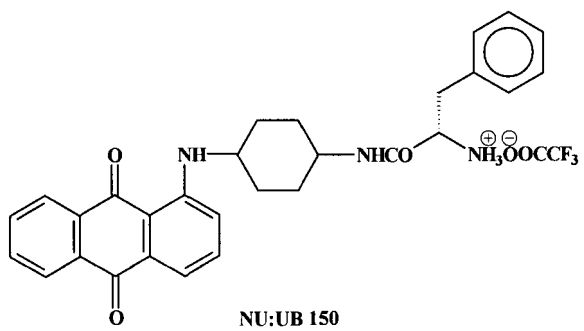
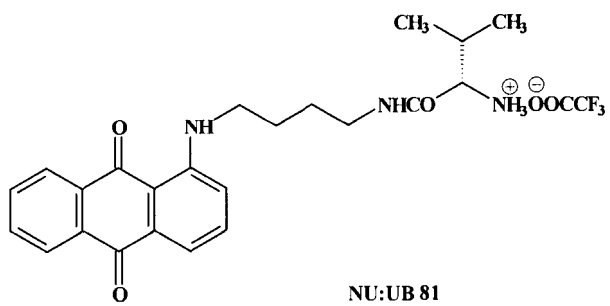
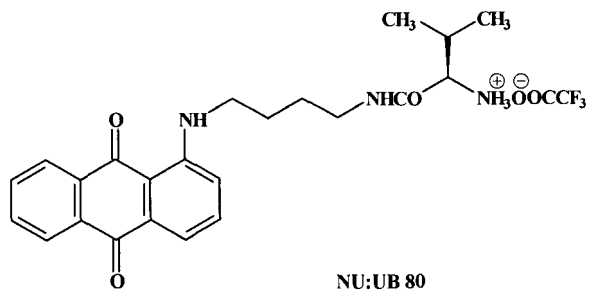
Zini N., Martelli A.M., Sabatelli P. et al, The 180-kDa isoform of topoisomerase II is localised in the nucleolus and belongs to the structural elements of the nucleolar remnant (1992) *Exp. Cell. Res*. **200**: 460-466

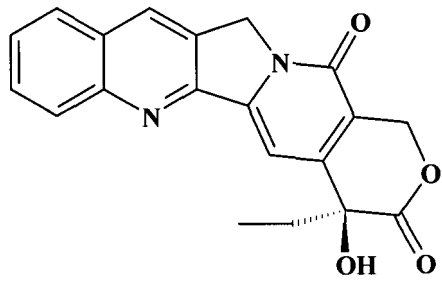
Zuco V., Supino R., Righetti S.C., Cleris L., Marchesi E., Gambacorti-Passerini C. and Formelli F. (2002) Selective cytotoxicity of betulinic acid on tumour cell lines, but not on normal cells. *Cancer Letters*. **175**: 17-25

Zunino F. and Capranico G. (1990) DNA topoisomerase II as the primary target of anti-tumor anthracyclines. *Anti-Cancer Drug Design*. **5**: 307-317

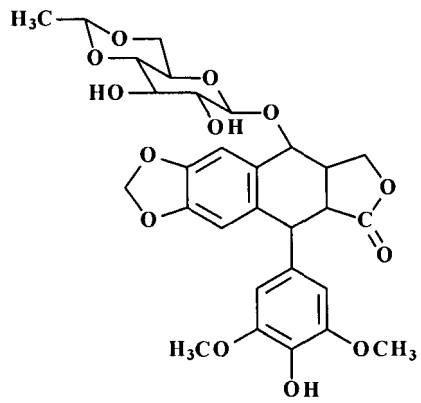
## **APPENDIX 1**



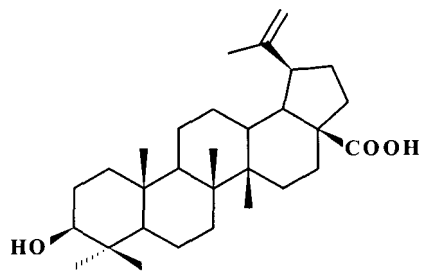




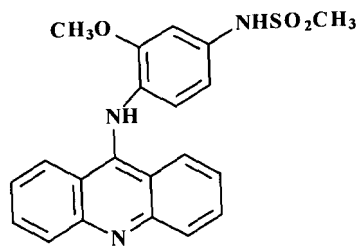
CAMPTOTHECIN



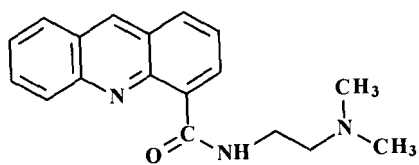
ETOPOSIDE



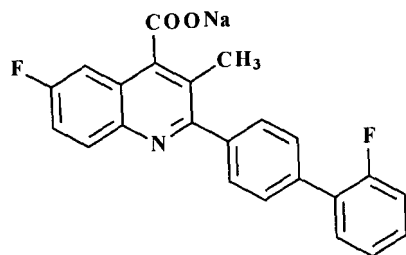
BETULINIC ACID



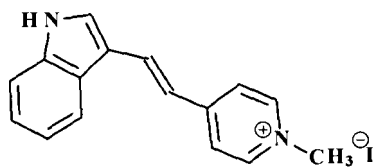
m-AMSA



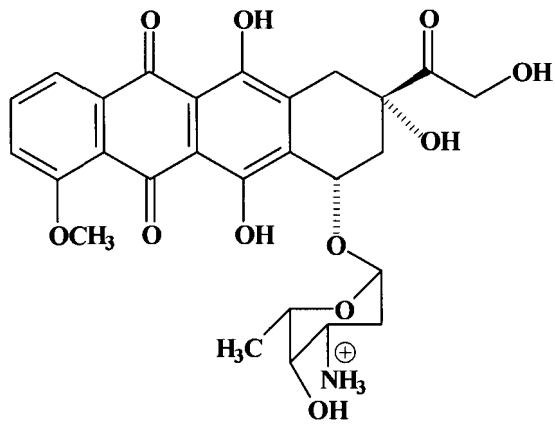
DACA



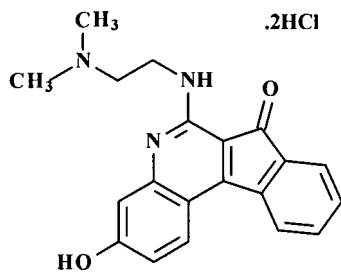
BREQUINAR



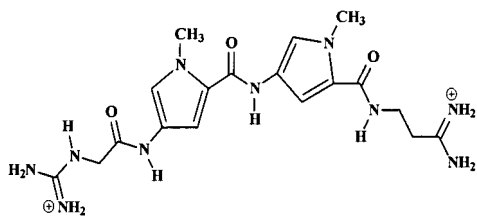
F16



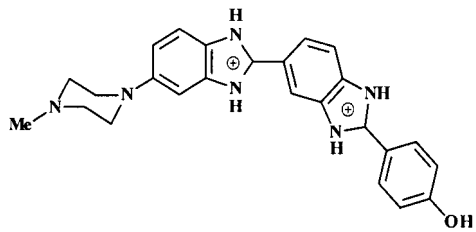
DOXORUBICIN



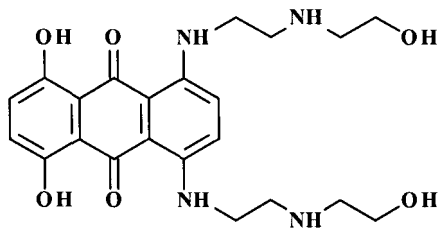
TAS-103



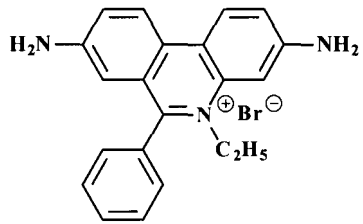
NETROPSIN



HOECHST 33258



MITOXANTRONE

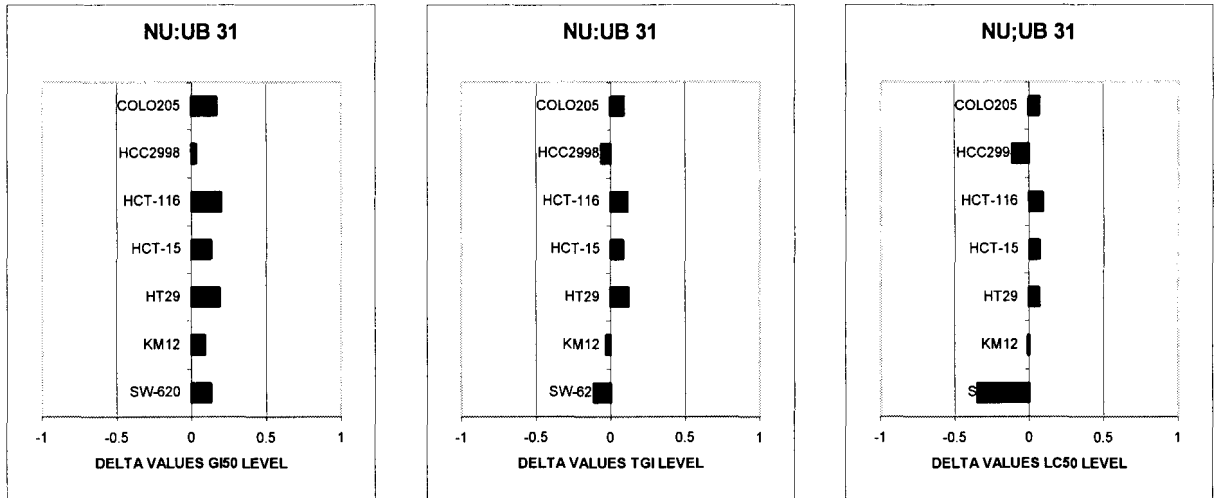


ETHIDIUM BROMIDE

## **APPENDIX 2**

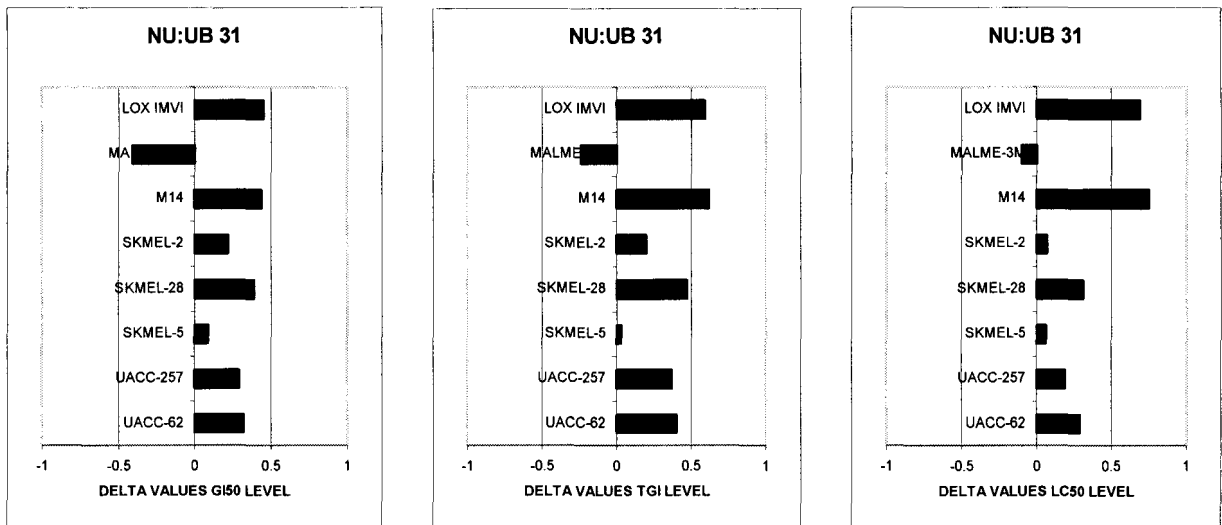
**NCI *in vitro* screen of tumour-specific cell line sensitivity to NU:UB 31**

COMPARISON OF DELTA VALUES FOR THE NCI COLON CANCER SUB-PANEL (plotted in log mean graph format)



**Appendix 2. graph 1.** Cytotoxicity of NU:UB 31 in the NCI colon cancer sub-panel.

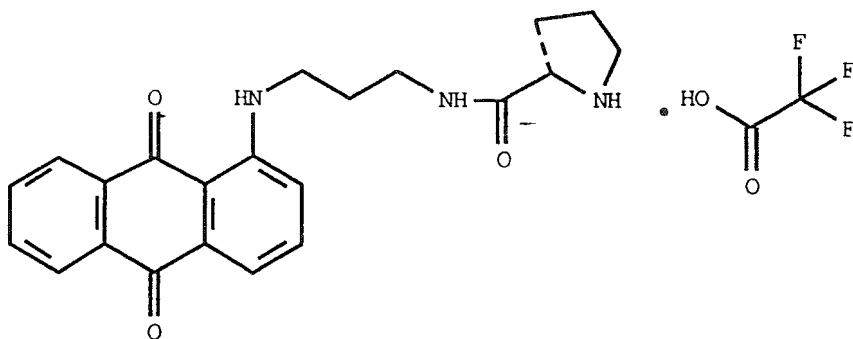
COMPARISON OF DELTA VALUES FOR THE NCI MELANOMA SUB-PANEL (plotted in log mean graph format)



**Appendix 2. graph 2.** Cytotoxicity of NU:UB 31 in the NCI melanoma sub-panel.

NU:UB 31 (and close analogues) shows exceptional broad spectrum activity against both colon and melanoma (including metastatic melanoma) not seen with comparator clinical agents.

NSC D- 709766



DRUG SYNTHESIS AND CHEMISTRY BRANCH, DTP, DCTD, NCI  
NSC NUMBER LIST

Dr. R. C. Harrison  
Pharmaceuticals Division  
British Technology Group  
101 Newington Causeway  
London SE1 6BU  
United Kingdom

Transmittal Letter or Collection Date: 01/26/99  
Supplier Compound ID: NU:UB 31  
NSC Number: D709766-S  
Molecular Formula: C<sub>22</sub>H<sub>23</sub>N<sub>3</sub>O<sub>3</sub>.C<sub>2</sub>HF<sub>3</sub>O<sub>2</sub>  
Acquired for Testing Against: CANCER

# National Cancer Institute Developmental Therapeutics Program

## In-Vitro Testing Results

NSC: D-709766-S/1	Experiment ID: 9907MD59-21	Test Type: 08	Units: Molar
Report Date: August 6, 1999	Test Date: July 12, 1999	QNS:	MC:
COMI: NU:UB 31	Stain Reagent: SRB Dual-P	SSPL: 0B6Z	

Panel/Cell Line	Time Zero	Ctrl	Mean Optical Densities					Log10 Concentration					Percent Growth		GI50	TGI	LC50
			-8.0	-7.0	-6.0	-5.0	-4.0	-8.0	-7.0	-6.0	-5.0	-4.0	-7.0	-6.0			
<b>Leukemia</b>																	
CCRF-CEM	0.300	0.776	0.841	0.816	0.769	0.284	0.083	114	108	99	-6	-72	2.93E-06	8.85E-06	4.63E-05		
HL-60(TB)	0.939	2.432	2.420	2.778	2.252	1.808	0.200	99	123	88	58	-79	1.15E-05	2.66E-05	6.17E-05		
K-562	0.157	0.916	0.934	0.939	0.890	0.083	0.028	102	103	97	-47	-82	2.11E-06	4.70E-06	1.21E-05		
MOLT-4	0.423	1.390	1.382	1.437	1.378	0.411	0.063	99	105	99	-3	-85	3.02E-06	9.38E-06	3.74E-05		
SR	1.084	2.934	2.930	2.985	2.998	1.136	0.247	100	103	103	3	-77	3.40E-06	1.08E-05	4.57E-05		
<b>Non-Small Cell Lung Cancer</b>																	
A549/ATCC	0.272	1.342	1.365	1.374	1.314	0.720	0.026	102	103	97	42	-90	7.14E-06	2.07E-05	4.95E-05		
EKVX	0.307	0.761	0.771	0.751	0.717	0.537	0.013	102	98	90	51	-96	1.01E-05	2.21E-05	4.86E-05		
HOP-62	0.362	0.815	0.829	0.812	0.781	0.529	0.051	103	99	92	37	-86	5.79E-06	1.99E-05	5.10E-05		
HOP-92	0.506	0.763	0.751	0.731	0.728	0.569	0.057	95	87	86	25	-89	3.87E-06	1.65E-05	4.54E-05		
NCI-H226	0.788	0.987	1.000	1.022	1.017	0.781	0.081	107	118	115	-1	-90	3.65E-06	9.81E-06	3.57E-05		
NCI-H23	0.291	0.877	0.902	0.934	0.889	0.614	0.028	104	110	102	55	-91	1.08E-05	2.39E-05	5.27E-05		
NCI-H460	0.341	1.989	2.019	1.912	1.981	0.788	0.075	102	95	100	27	-78	4.83E-06	1.81E-05	5.42E-05		
NCI-H522	0.267	0.811	0.825	0.853	0.837	0.441	0.024	103	108	105	32	-91	5.66E-06	1.82E-05	4.63E-05		
<b>Colon Cancer</b>																	
COLO 205	0.553	1.568	1.612	1.637	1.551	0.682	0.027	104	107	98	13	-95	3.66E-06	1.31E-05	3.81E-05		
HCC-2998	0.333	0.889	0.900	0.913	0.896	0.487	0.087	102	104	101	28	-74	4.96E-06	1.87E-05	5.80E-05		
HCT-116	0.119	0.991	0.948	0.929	0.938	0.218	0.002	95	93	94	11	-98	3.40E-06	1.27E-05	3.63E-05		
HCT-15	0.084	0.493	0.523	0.523	0.508	0.143	0.003	107	107	104	14	-97	4.00E-06	1.35E-05	3.79E-05		
HT29	0.381	1.555	1.581	1.495	1.526	0.492	0.029	102	95	98	9	-93	3.46E-06	1.24E-05	3.83E-05		
KM12	0.279	1.027	1.030	0.936	0.957	0.486	0.029	100	88	91	28	-90	4.41E-06	1.72E-05	4.58E-05		
SW-620	0.081	0.497	0.475	0.511	0.456	0.176	0.043	95	103	90	23	-48	3.94E-06	2.11E-05	>1.00E-04		
<b>CNS Cancer</b>																	
SF-268	0.251	1.025	1.043	1.047	1.043	0.729	0.085	102	103	102	62	-66	1.23E-05	3.03E-05	7.45E-05		
SF-295	0.622	1.767	1.829	1.816	1.721	1.146	0.076	105	104	96	46	-88	8.22E-06	2.20E-05	5.21E-05		
SNB-19	0.387	1.080	1.067	1.058	1.036	0.665	0.014	98	97	94	40	-97	6.53E-06	1.97E-05	4.57E-05		
SNB-75	0.418	0.615	0.660	0.668	0.651	0.476	0.205	123	127	118	29	-51	5.84E-06	2.31E-05	9.70E-05		
U251	0.268	1.377	1.304	1.342	1.308	0.807	0.013	93	97	94	49	-95	9.31E-06	2.18E-05	4.85E-05		
<b>Melanoma</b>																	
LOX IMVI	0.226	1.160	1.136	1.146	1.081	0.100	0.023	97	98	92	-56	-90	1.91E-06	4.18E-06	9.14E-06		
MALME-3M	0.319	0.795	0.822	0.811	0.816	0.667	0.031	106	103	104	73	-90	1.39E-05	2.80E-05	5.67E-05		
M14	0.402	1.514	1.484	1.408	1.472	0.137	0.043	97	90	96	-66	-89	1.93E-06	3.92E-06	7.96E-06		
SK-MEL-28	0.220	0.705	0.693	0.717	0.674	0.148	0.038	97	102	94	-33	-83	2.21E-06	5.49E-06	2.19E-05		
SK-MEL-5	0.703	1.609	1.653	1.669	1.610	0.898		105	107	100	21	-100	4.34E-06	1.50E-05	3.88E-05		
UACC-257	0.615	1.520	1.568	1.497	1.559	0.491	0.096	105	97	104	-20	-84	2.73E-06	6.89E-06	2.91E-05		
UACC-62	0.457	1.603	1.587	1.484	1.609	0.349	0.017	99	90	101	-24	-96	2.55E-06	6.45E-06	2.31E-05		
<b>Ovarian Cancer</b>																	
IGROV1	0.279	0.952	0.930	0.896	0.832	0.449	0.007	97	92	82	25	-97	3.67E-06	1.61E-05	4.10E-05		
OVCAR-3	0.534	0.815	0.808	0.822	0.774	0.525	0.072	97	102	85	-2	-87	2.54E-06	9.56E-06	3.71E-05		
OVCAR-4	0.510	1.231	1.212	1.244	1.111	0.736	0.037	97	102	83	31	-93	4.37E-06	1.79E-05	4.52E-05		
OVCAR-5	0.596	1.300	1.337	1.341	1.315	0.974	0.015	105	106	102	54	-97	1.06E-05	2.27E-05	4.85E-05		
OVCAR-8	0.230	0.755	0.753	0.729	0.727	0.395	0.019	100	95	95	31	-92	5.08E-06	1.80E-05	4.57E-05		
SK-OV-3	0.356	0.790	0.761	0.766	0.753	0.564	0.052	93	94	91	48	-85	8.90E-06	2.28E-05	5.42E-05		
<b>Renal Cancer</b>																	
786-0	0.429	1.712	1.689	1.707	1.654	0.904	0.012	98	100	95	37	-97	5.99E-06	1.89E-05	4.45E-05		
A498	0.991	1.665	1.634	1.648	1.624	1.308	0.095	95	97	94	47	-90	8.63E-06	2.20E-05	5.08E-05		
ACHN	0.341	1.273	1.270	1.260	1.186	0.582	-0.003	100	99	91	26	-100	4.23E-06	1.60E-05	4.00E-05		
CAKI-1	0.413	1.112	1.052	1.055	1.021	0.752	0.015	91	92	87	48	-96	9.11E-06	2.16E-05	4.78E-05		
RXF 393	0.583	1.244	1.242	1.184	1.152	0.802	0.196	100	91	86	33	-66	4.79E-06	2.15E-05	6.84E-05		
SN12C	0.302	0.931	1.002	0.940	0.941	0.511	0.009	111	101	102	33	-97	5.69E-06	1.80E-05	4.36E-05		
TK-10	0.520	1.308	1.324	1.287	1.396	0.901	0.092	102	97	111	48	-82	9.41E-06	2.34E-05	5.65E-05		
UO-31	0.526	1.220	1.238	1.205	1.147	0.627	0.016	103	98	90	14	-97	3.36E-06	1.35E-05	3.79E-05		
<b>Prostate Cancer</b>																	
PC-3	0.293	0.977	0.986	1.008	0.948	0.538	0.011	101	104	96	36	-96	5.80E-06	1.87E-05	4.46E-05		
DU-145	0.265	0.790	0.800	0.774	0.779	0.466	0.059	102	97	98	38	-78	6.35E-06	2.14E-05	5.76E-05		
<b>Breast Cancer</b>																	
MCF7	0.316	1.590	1.581	1.490	1.557	0.793	0.059	99	92	97	37	-81	6.17E-06	2.06E-05	5.44E-05		
NCI/ADR-RES	0.282	0.759	0.773	0.800	0.785	0.488	0.057	103	109	106	43	-80	7.76E-06	2.24E-05	5.72E-05		
MDA-MB-231/ATCC	0.391	0.888	0.909	0.924	0.839	0.548	0.060	104	107	90	32	-85	4.84E-06	1.87E-05	5.03E-05		
HS 578T	0.225	0.850	0.890	0.879	0.877	0.691	0.165	106	105	104	74	-27	1.75E-05	5.45E-05	>1.00E-04		
MDA-MB-435	0.297	1.132	1.080	1.100	1.067	0.483	0.026	94	96	92	22	-91	4.01E-06	1.57E-05	4.32E-05		
MDA-N	0.691	2.289	2.406	2.517	2.470	1.773	0.012	107	114	111	68	-98	1.28E-05	2.56E-05	5.12E-05		
BT-549	0.304	0.723	0.760	0.750	0.734	0.560	0.018	109	107	103	61	-94	1.18E-05	2.48E-05	5.19E-05		
T-47D	0.433	0.999	1.006	0.969	0.938	0.795	0.226	101	95	89	64	-48	1.33E-05	3.73E-05	>1.00E-04		

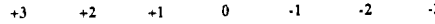
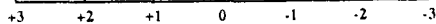
### Mean Graphs

Report Date: August 6, 1999

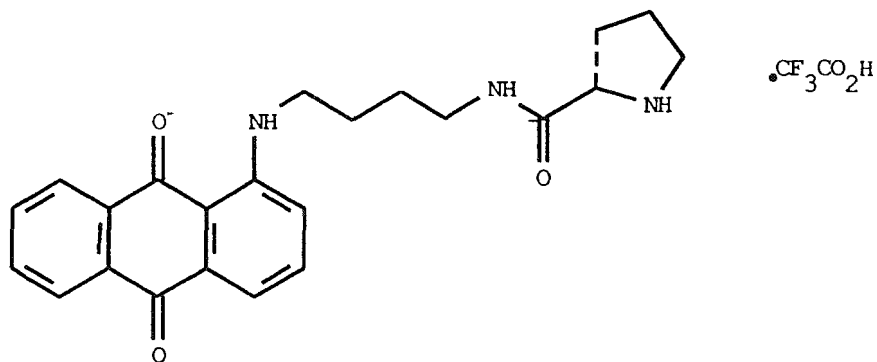
Test Date: July 12, 1999

Panel/Cell Line	Log <sub>10</sub> GI50	GI50	Log <sub>10</sub> TGI	TGI	Log <sub>10</sub> LC50	LC50
<b>Leukemia</b>						
CCRF-CEM	-5.53		-5.05		-4.33	
HL-60(TB)	-4.94		-4.58		-4.21	
K-562	-5.68		-5.33		-4.92	
MOLT-4	-5.52		-5.03		-4.43	
SR	-5.47		-4.97		-4.34	
<b>Non-Small Cell Lung Cancer</b>						
A549(ATCC)	-5.15		-4.68		-4.31	
EKVX	-5.00		-4.66		-4.31	
HOP-62	-5.24		-4.70		-4.29	
HOP-92	-5.41		-4.78		-4.34	
NCI-H226	-5.44		-5.01		-4.45	
NCI-H23	-4.97		-4.62		-4.28	
NCI-H460	-5.32		-4.74		-4.27	
NCI-H522	-5.25		-4.74		-4.33	
<b>Colon Cancer</b>						
COLO 205	-5.44		-4.88		-4.42	
HCC-2098	-5.30		-4.73		-4.24	
HCT-116	-5.47		-4.90		-4.44	
HCT-15	-5.40		-4.87		-4.42	
HT29	-5.46		-4.91		-4.42	
KM12	-5.36		-4.76		-4.34	
SW-620	-5.40		-4.68		> -4.00	
<b>CNS Cancer</b>						
SF-268	-4.91		-4.52		-4.13	
SF-295	-5.09		-4.66		-4.28	
SNB-19	-5.19		-4.71		-4.34	
SNB-75	-5.23		-4.64		-4.01	
U251	-5.03		-4.66		-4.31	
<b>Melanoma</b>						
LOX IMVI	-5.72		-5.38		-5.04	
MALME-3M	-4.86		-4.55		-4.25	
M14	-5.71		-5.41		-5.10	
SK-MEL-28	-5.66		-5.26		-4.66	
SK-MEL-5	-5.36		-4.82		-4.41	
UACC-257	-5.56		-5.16		-4.54	
UACC-62	-5.59		-5.19		-4.64	
<b>Ovarian Cancer</b>						
IGROV1	-5.44		-4.79		-4.39	
OVCAR-3	-5.60		-5.02		-4.43	
OVCAR-4	-5.36		-4.75		-4.34	
OVCAR-5	-4.97		-4.64		-4.31	
OVCAR-8	-5.29		-4.74		-4.34	
SK-OV-3	-5.05		-4.64		-4.27	
<b>Renal Cancer</b>						
786-0	-5.22		-4.72		-4.35	
A498	-5.06		-4.66		-4.29	
ACHN	-5.37		-4.80		-4.40	
CAKI-1	-5.04		-4.67		-4.32	
RXF 393	-5.32		-4.67		-4.16	
SN12C	-5.24		-4.74		-4.36	
TK-10	-5.03		-4.63		-4.25	
UO-31	-5.47		-4.87		-4.42	
<b>Prostate Cancer</b>						
PC-3	-5.24		-4.73		-4.35	
DU-145	-5.20		-4.67		-4.24	
<b>Breast Cancer</b>						
MCF7	-5.21		-4.69		-4.26	
NCI/ADR-RES	-5.11		-4.65		-4.24	
MDA-MB-231(ATCC)	-5.32		-4.73		-4.30	
HS 578T	-4.76		-4.26		> -4.00	
MDA-MB-435	-5.40		-4.80		-4.36	
MDA-N	-4.89		-4.59		-4.29	
BT-549	-4.93		-4.61		-4.28	
T-47D	-4.88		-4.43		> -4.00	
<b>MG_MID</b>	-5.27		-4.79		-4.35	
Delta	0.45		0.62		0.75	
Range	0.96		1.14		1.10	

*Handwritten note:* *partially*



NSC D- 709778



DRUG SYNTHESIS AND CHEMISTRY BRANCH, DTP, DCTD, NCI  
NSC NUMBER LIST

Dr. R. C. Harrison  
Pharmaceuticals Division  
British Technology Group  
101 Newington Causeway  
London SE1 6BU  
United Kingdom

Transmittal Letter or Collection Date: 01/26/99  
Supplier Compound ID: NU:UB 43  
NSC Number: D709778-H  
Molecular Formula: C<sub>23</sub>H<sub>25</sub>N<sub>3</sub>O<sub>3</sub>.C<sub>2</sub>H<sub>3</sub>F<sub>3</sub>O<sub>2</sub>  
Acquired for Testing Against: CANCER

# National Cancer Institute Developmental Therapeutics Program

## In-Vitro Testing Results

NSC: D-709778 -H / 1	Experiment ID: 9907MD58-36	Test Type: 08	Units: Molar
Report Date: August 5, 1999	Test Date: July 6, 1999	QNS:	MC:
COMI: NU:UB 43	Stain Reagent: SRB Dual-P	SSPL: 0B6Z	

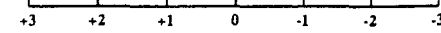
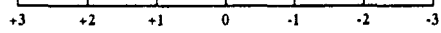
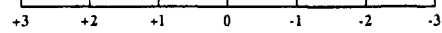
Panel/Cell Line	Time Zero	Log10 Concentration											GI50	TGI	LC50	
		Ctrl	-8.0	-7.0	-6.0	-5.0	-4.0	-8.0	-7.0	-6.0	-5.0	-4.0				
<b>Leukemia</b>																
CCR5-CEM	0.107	0.494	0.513	0.474	0.490	0.223	0.126	105	95	99	30	5	5.12E-06	>1.00E-04	>1.00E-04	
HL-60(TB)	0.246	1.118	1.277	1.197	1.196	0.174	0.142	118	109	109	-29	-42	2.66E-06	6.12E-06	>1.00E-04	
K-562	0.157	1.282	1.300	1.240	1.197	0.102	0.048	102	96	92	-35	-69	2.15E-06	5.29E-06	2.69E-05	
MOLT-4	0.149	0.680	0.666	0.665	0.631	0.159	0.044	97	97	91	2	-70	2.88E-06	1.06E-05	5.21E-05	
<b>Non-Small Cell Lung Cancer</b>																
A549/ATCC	0.198	0.996	1.011	1.025	1.020	0.522	0.029	102	104	103	41	-86	7.07E-06	2.10E-05	5.22E-05	
EKVX	0.630	1.403	1.442	1.368	1.364	1.195	0.085	105	95	95	73	-87	1.40E-05	2.87E-05	5.91E-05	
HOP-62	0.199	0.510	0.558	0.546	0.517	0.320	0.041	116	112	102	39	-79	6.69E-06	2.13E-05	5.94E-05	
HOP-92	0.394	0.932	0.948	0.935	0.921	0.809	0.084	103	101	98	77	-79	1.49E-05	3.13E-05	6.55E-05	
NCI-H23	0.301	0.965	0.973	0.972	0.963	0.797	0.012	101	101	100	75	-96	1.40E-05	2.74E-05	5.38E-05	
NCI-H322M	0.427	1.366	1.374	1.348	1.325	0.878	0.006	101	98	96	48	-99	9.08E-06	2.12E-05	4.66E-05	
NCI-H460	0.312	1.601	1.507	1.593	1.655	0.640	0.023	93	99	104	25	-93	4.88E-06	1.64E-05	4.35E-05	
NCI-H522	0.262	0.782	0.847	0.684	0.929	0.752	0.036	113	81	128	94	-86	1.76E-05	3.32E-05	6.29E-05	
<b>Colon Cancer</b>																
COLO 205	0.406	1.525	1.493	1.503	1.432	0.100	0.016	97	98	92	-75	-96	1.77E-06	3.53E-06	7.04E-06	
HCC-2998	0.360	0.698	0.687	0.688	0.671	0.098	0.006	97	97	92	-73	-98	1.80E-06	3.62E-06	7.26E-06	
HCT-116	0.254	1.571	1.585	1.511	1.461	0.495	0.010	101	95	92	18	-96	3.70E-06	1.45E-05	3.96E-05	
HCT-15	0.169	1.243	1.191	1.256	1.220	0.167	0.024	95	101	98	-1	-86	3.04E-06	9.73E-06	3.78E-05	
HT29	0.162	1.016	1.030	0.978	1.010	0.210	0.031	102	96	99	6	-81	3.35E-06	1.16E-05	4.37E-05	
KM12	0.286	1.237	1.242	1.310	1.263	0.697	0.047	101	108	103	43	-84	7.69E-06	2.19E-05	5.43E-05	
SW-620	0.066	0.549	0.564	0.551	0.577	0.219	0.077	103	100	106	32	2	5.65E-06	>1.00E-04	>1.00E-04	
<b>CNS Cancer</b>																
SF-268	0.250	1.003	1.091	1.041	1.027	0.855	0.060	112	105	103	80	-76	1.56E-05	3.26E-05	6.82E-05	
SF-295	0.454	1.272	1.251	1.196	1.242	0.797	0.060	97	91	96	42	-87	7.10E-06	2.12E-05	5.17E-05	
SF-539	0.568	1.211	1.171	1.250	1.235	0.374	0.033	94	106	104	-34	-94	2.45E-06	5.65E-06	1.83E-05	
SNB-19	0.335	1.055	1.054	1.043	1.035	0.519	0.040	100	98	97	26	-88	4.56E-06	1.68E-05	4.62E-05	
SNB-75	0.265	0.611	0.613	0.619	0.620	0.534	0.016	101	102	103	78	-94	1.45E-05	2.84E-05	5.54E-05	
U251	0.161	0.911	0.840	0.891	0.861	0.304	-0.006	90	97	93	19	-100	3.83E-06	1.43E-05	3.80E-05	
<b>Melanoma</b>																
LOX IMVI	0.085	0.835	0.895	0.887	0.863	0.058	0.039	108	107	104	-32	-55	2.48E-06	5.79E-06	6.16E-05	
MALME-3M	0.367	0.826	0.868	0.766	0.988	0.828	0.021	109	87	135	100	-94	1.81E-05	3.27E-05	5.91E-05	
M14	0.295	1.057	1.097	1.067	1.034	0.071	0.027	105	101	97	-76	-91	1.87E-06	3.64E-06	7.08E-06	
SK-MEL-2	0.257	0.675	0.647	0.676	0.676	0.193	0.002	93	100	100	-25	-99	2.52E-06	6.33E-06	2.17E-05	
SK-MEL-28	0.267	1.088	1.103	1.078	1.096	0.212	0.081	102	99	101	-21	-70	2.62E-06	6.75E-06	3.96E-05	
SK-MEL-5	0.428	1.801	1.788	1.810	1.828	0.554	0.004	99	101	102	9	-99	3.63E-06	1.21E-05	3.52E-05	
UACC-257	0.554	1.144	1.043	1.104	1.122	0.114	0.012	83	93	96	-79	-98	1.84E-06	3.53E-06	6.80E-06	
UACC-62	0.700	1.717	1.759	1.754	1.797	0.154	0.012	104	104	108	-78	-98	2.05E-06	3.80E-06	7.06E-06	
<b>Ovarian Cancer</b>																
IGROV1	0.110	0.737	0.744	0.771	0.763	0.437	0.030	101	105	104	52	-73	1.04E-05	2.61E-05	6.53E-05	
OVCA-3	0.446	0.821	0.847	0.816	0.819	0.668	0.075	107	99	99	59	-83	1.16E-05	2.60E-05	5.84E-05	
OVCA-4	0.265	0.752	0.765	0.742	0.790	0.595	0.028	103	98	108	68	-90	1.30E-05	2.70E-05	5.60E-05	
OVCA-5	0.774	1.698	1.646	1.673	1.638	1.605	0.029	94	97	94	90	-96	1.64E-05	3.04E-05	5.64E-05	
OVCA-8	0.121	0.888	0.856	0.929	0.895	0.529	0.056	96	105	101	53	-54	1.07E-05	3.13E-05	9.15E-05	
SK-OV-3	0.281	0.545	0.547	0.527	0.625	0.425	0.033	100	93	130	54	-88	1.07E-05	2.40E-05	5.39E-05	
<b>Renal Cancer</b>																
786-0	0.226	0.874	0.847	0.823	0.777	0.225	0.014	96	92	85	-1	-94	2.56E-06	9.82E-06	3.38E-05	
A498	0.848	1.426	1.469	1.393	1.453	1.265	0.044	107	94	105	72	-95	1.36E-05	2.70E-05	5.39E-05	
ACHN	0.237	0.867	0.891	0.888	0.894	0.500	-0.001	104	103	104	42	-100	7.37E-06	1.97E-05	4.44E-05	
CAKI-1	0.454	1.044	1.107	1.136	1.073	0.817	0.014	111	115	105	61	-97	1.18E-05	2.44E-05	5.06E-05	
RXF 393	0.359	0.697	0.720	0.608	0.674	0.482	0.030	107	74	93	36	-92	5.72E-06	1.92E-05	4.72E-05	
SN12C	0.377	0.989	0.960	0.940	0.923	0.692	0.019	95	92	89	51	-95	1.02E-05	2.24E-05	4.92E-05	
TK-10	0.529	1.165	1.069	1.171	1.153	0.913	0.013	85	101	98	60	-98	1.16E-05	2.41E-05	5.00E-05	
UO-31	0.242	0.664	0.632	0.654	0.678	0.159	0.009	92	98	103	-34	-96	2.44E-06	5.63E-06	1.79E-05	
<b>Prostate Cancer</b>																
PC-3	0.189	0.673	0.638	0.661	0.657	0.339	-0.003	93	97	97	31	-100	5.14E-06	1.72E-05	4.15E-05	
DU-145	0.211	0.680	0.693	0.630	0.689	0.541	0.003	103	89	102	70	-99	1.32E-05	2.61E-05	5.16E-05	
<b>Breast Cancer</b>																
MCF7	0.245	0.927	0.878	0.934	0.899	0.442	0.031	93	101	96	29	-87	4.84E-06	1.77E-05	4.77E-05	
NCI/ADR-RES	0.299	0.877	0.857	0.855	0.857	0.699	0.123	96	96	96	69	-59	1.41E-05	3.46E-05	8.50E-05	
MDA-MB-231/ATCC	0.322	0.858	0.812	0.830	0.852	0.580	0.005	91	95	99	48	-98	9.21E-06	2.13E-05	4.67E-05	
HS 578T	0.106	0.485	0.540	0.520	0.640	0.402	0.073	115	109	141	78	-32	1.80E-05	5.15E-05	>1.00E-04	
MDA-MB-435	0.279	0.964	0.987	0.969	1.016	0.211	0.016	103	101	108	-25	-94	2.73E-06	6.52E-06	2.31E-05	
MDA-N	0.352	1.414	1.408	1.374	1.347	0.236	0.008	99	96	94	-33	-98	2.21E-06	5.48E-06	1.83E-05	
BT-549	0.502	1.328	1.298	1.299	1.272	1.124	0.009	96	96	93	75	-98	1.40E-05	2.72E-05	5.27E-05	
T-47D	0.300	0.503	0.592	0.490	0.581	0.458	0.061	144	94	139	78	-80	1.51E-05	3.12E-05	6.48E-05	

Mean Graphs

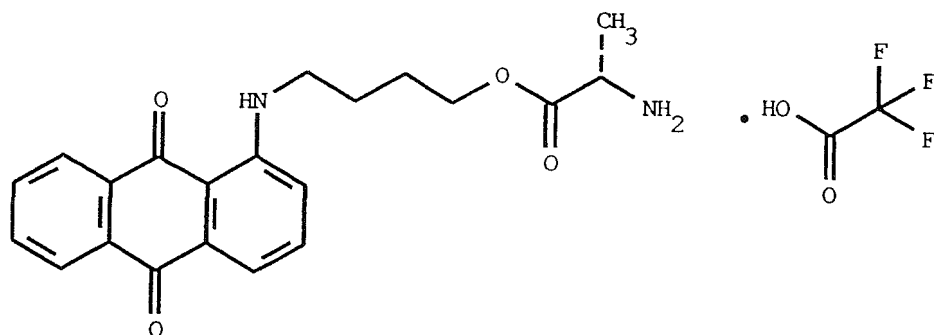
Report Date: August 5, 1999

Test Date: July 6, 1999

Panel/Cell Line	Log <sub>10</sub> GI50	GI50	Log <sub>10</sub> TGI	TGI	Log <sub>10</sub> LC50	LC50
<b>Leukemia</b>						
CCRF-CEM	-5.29		> -4.00		> -4.00	
HL-60(TB)	-5.58		-5.21		> -4.00	
K-562	-5.67		-5.28		-4.57	
MOLT-4	-5.54		-4.97		-4.28	
<b>Non-Small Cell Lung Cancer</b>						
A549/ATCC	-5.15		-4.68		-4.28	
EKVX	-4.85		-4.54		-4.23	
HOP-62	-5.17		-4.67		-4.25	
HOP-92	-4.83		-4.50		-4.18	
NCI-H23	-4.85		-4.56		-4.27	
NCI-H322M	-5.04		-4.67		-4.33	
NCI-H460	-5.31		-4.79		-4.36	
NCI-H522	-4.75		-4.48		-4.20	
<b>Colon Cancer</b>						
COLO 205	-5.75		-5.45		-5.15	
HCC-2998	-5.74		-5.44		-5.14	
HCT-116	-5.43		-4.84		-4.40	
HCT-15	-5.52		-5.01		-4.42	
HT29	-5.47		-4.94		-4.36	
KM12	-5.11		-4.66		-4.27	
SW-620	-5.25		> -4.00		> -4.00	
<b>CNS Cancer</b>						
SF-268	-4.81		-4.49		-4.17	
SF-295	-5.15		-4.67		-4.29	
SF-539	-5.61		-5.25		-4.74	
SNB-19	-5.34		-4.77		-4.34	
SNB-75	-4.84		-4.55		-4.26	
U251	-5.42		-4.84		-4.42	
<b>Melanoma</b>						
LOX IMVI	-5.61		-5.24		-4.21	
MALME-3M	-4.74		-4.49		-4.23	
M14	-5.73		-5.44		-5.15	
SK-MEL-2	-5.60		-5.20		-4.66	
SK-MEL-28	-5.58		-5.17		-4.40	
SK-MEL-5	-5.44		-4.92		-4.45	
UACC-257	-5.74		-5.45		-5.17	
UACC-62	-5.69		-5.42		-5.15	
<b>Ovarian Cancer</b>						
IGROV1	-4.98		-4.58		-4.19	
OVCAR-3	-4.94		-4.59		-4.23	
OVCAR-4	-4.89		-4.57		-4.25	
OVCAR-5	-4.79		-4.52		-4.25	
OVCAR-8	-4.97		-4.50		-4.04	
SK-OV-3	-4.97		-4.62		-4.27	
<b>Renal Cancer</b>						
786-0	-5.59		-5.01		-4.47	
A498	-4.87		-4.57		-4.27	
ACHN	-5.13		-4.71		-4.35	
CAKI-1	-4.93		-4.61		-4.30	
RXF 393	-5.24		-4.72		-4.33	
SN12C	-4.99		-4.65		-4.31	
TK-10	-4.94		-4.62		-4.30	
UO-31	-5.61		-5.25		-4.75	
<b>Prostate Cancer</b>						
PC-3	-5.29		-4.76		-4.38	
DU-145	-4.88		-4.58		-4.29	
<b>Breast Cancer</b>						
MCF7	-5.32		-4.75		-4.32	
NCI/ADR-RES	-4.85		-4.46		-4.07	
MDA-MB-231/ATCC	-5.04		-4.67		-4.33	
HS 578T	-4.74		-4.29		> -4.00	
MDA-MB-435	-5.56		-5.19		-4.64	
MDA-N	-5.66		-5.26		-4.74	
BT-549	-4.85		-4.57		-4.28	
T-47D	-4.82		-4.51		-4.19	
<b>MG_MID</b>						
Delta	0.53		0.66		0.78	
Range	1.01		1.45		1.17	



NSC D- 709768



DRUG SYNTHESIS AND CHEMISTRY BRANCH, DTP, DCTD, NCI  
NSC NUMBER LIST

Dr. R. C. Harrison  
Pharmaceuticals Division  
British Technology Group  
101 Newington Causeway  
London SE1 6BU  
United Kingdom

Transmittal Letter or Collection Date: 01/26/99  
Supplier Compound ID: NU:UB 73  
NSC Number: D709768-U  
Molecular Formula: C<sub>21</sub>H<sub>22</sub>N<sub>2</sub>O<sub>4</sub>.C<sub>2</sub>HF<sub>3</sub>O<sub>2</sub>  
Acquired for Testing Against: CANCER

# National Cancer Institute Developmental Therapeutics Program

## In-Vitro Testing Results

NSC: D-709768-U/1	Experiment ID: 9907MD59-23	Test Type: 08	Units: Molar
Report Date: August 6, 1999	Test Date: July 12, 1999	QNS:	MC:
COMI: NU:UB 73	Stain Reagent: SRB Dual-P	SSPL: 0B6Z	

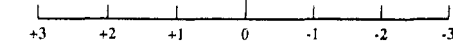
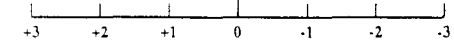
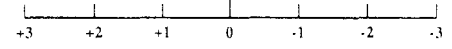
Panel/Cell Line	Time		Log10 Concentration						Percent Growth				GI50	TGI	LC50	
	Zero	Ctrl	-8.0	-7.0	-6.0	-5.0	-4.0	-8.0	-7.0	-6.0	-5.0	-4.0				
<b>Leukemia</b>																
CCRF-CEM	0.300	0.738	0.718	0.750	0.695	0.584	0.055	95	103	90	65	-82	1.26E-05	2.77E-05	6.08E-05	
HL-60(TB)	0.939	2.785	2.676	2.590	2.563	2.014	0.130	94	89	88	58	-86	1.14E-05	2.53E-05	5.62E-05	
K-562	0.157	0.917	0.917	0.907	0.864	0.602	0.233	100	99	93	58	10	1.49E-05	>1.00E-04	>1.00E-04	
MOLT-4	0.423	1.352	1.376	1.356	1.324	1.016	0.141	103	100	97	64	-67	1.28E-05	3.08E-05	7.45E-05	
SR	1.084	2.814	2.674	2.697	2.761	1.976	0.214	92	93	97	52	-80	1.03E-05	2.46E-05	5.89E-05	
<b>Non-Small Cell Lung Cancer</b>																
AS49/ATCC	0.272	1.156	1.165	1.149	1.126	0.989	0.059	101	99	97	81	-78	1.57E-05	3.23E-05	6.64E-05	
EKVX	0.307	0.788	0.796	0.794	0.759	0.623	0.076	102	101	94	66	-75	1.29E-05	2.92E-05	6.62E-05	
HOP-62	0.362	0.887	0.915	0.901	0.894	0.822	0.130	105	103	101	88	-64	1.77E-05	3.78E-05	8.07E-05	
HOP-92	0.506	0.777	0.778	0.760	0.794	0.720	0.150	100	94	106	79	-70	1.57E-05	3.38E-05	7.30E-05	
NCI-H226	0.788	1.073	1.098	1.007	1.085	0.965	0.201	109	77	104	62	-75	1.22E-05	2.84E-05	6.61E-05	
NCI-H23	0.291	0.931	0.985	0.986	0.980	0.894	0.026	108	108	108	94	-91	1.73E-05	3.22E-05	6.00E-05	
NCI-H460	0.341	1.964	1.968	1.963	1.968	1.603	0.120	100	100	100	78	-65	1.56E-05	3.51E-05	7.86E-05	
NCI-H522	0.267	0.830	0.855	0.831	0.816	0.694	0.082	104	100	98	76	-69	1.51E-05	3.33E-05	7.36E-05	
<b>Colon Cancer</b>																
COLO 205	0.553	1.737	1.760	1.658	1.752	1.517	0.030	102	93	101	81	-95	1.51E-05	2.90E-05	5.58E-05	
HCC-2998	0.333	0.868	0.867	0.849	0.897	0.828	0.037	100	96	105	93	-89	1.72E-05	3.23E-05	6.10E-05	
HCT-116	0.119	1.002	0.982	0.963	1.006	0.765	0.004	98	96	101	73	-97	1.37E-05	2.70E-05	5.31E-05	
HCT-15	0.084	0.536	0.519	0.524	0.541	0.378	-0.015	96	97	101	65	-100	1.23E-05	2.48E-05	4.98E-05	
HT29	0.381	1.766	1.774	1.838	1.824	1.493	0.010	101	105	104	80	-97	1.48E-05	2.83E-05	5.41E-05	
KML2	0.279	1.183	1.084	1.058	1.080	0.845	0.065	89	86	89	63	-77	1.23E-05	2.81E-05	6.42E-05	
SW-620	0.081	0.488	0.476	0.439	0.462	0.362	0.055	97	88	94	69	-32	1.55E-05	4.82E-05	>1.00E-04	
<b>CNS Cancer</b>																
SF-268	0.251	1.044	1.015	1.062	1.053	0.928	0.131	96	102	101	85	-48	1.84E-05	4.36E-05	>1.00E-04	
SF-295	0.622	1.959	1.974	2.025	1.969	1.721	0.089	101	105	101	82	-86	1.55E-05	3.09E-05	6.13E-05	
SNB-19	0.387	1.014	0.975	1.002	0.968	0.814	0.095	94	98	93	68	-75	1.34E-05	2.98E-05	6.65E-05	
SNB-75	0.418	0.628	0.644	0.636	0.623	0.547	0.155	107	104	98	61	-63	1.23E-05	3.11E-05	7.87E-05	
U251	0.268	1.358	1.293	1.276	1.271	1.006	0.038	94	92	92	68	-86	1.30E-05	2.76E-05	5.83E-05	
<b>Melanoma</b>																
LOX IMVI	0.226	1.280	1.229	1.229	1.264	0.934	0.081	95	95	99	67	-64	1.35E-05	3.25E-05	7.80E-05	
MALME-3M	0.319	0.803	0.808	0.797	0.791	0.768	0.111	101	99	98	93	-65	1.86E-05	3.86E-05	8.00E-05	
M14	0.402	1.267	1.239	1.310	1.303	1.203	0.068	97	105	104	93	-83	1.75E-05	3.37E-05	6.48E-05	
SK-MEL-28	0.220	0.679	0.677	0.686	0.679	0.600	0.067	100	101	100	83	-70	1.64E-05	3.49E-05	7.44E-05	
SK-MEL-5	0.703	1.676	1.708	1.616	1.747	1.571	0.005	103	94	107	89	-99	1.61E-05	2.97E-05	5.48E-05	
UACC-257	0.615	1.482	1.498	1.497	1.510	1.480	0.117	102	102	103	100	-81	1.89E-05	3.57E-05	6.74E-05	
UACC-62	0.457	1.630	1.651	1.666	1.567	1.328	0.029	102	103	95	74	-94	1.39E-05	2.77E-05	5.50E-05	
<b>Ovarian Cancer</b>																
IGROV1	0.279	1.021	1.029	0.992	1.005	0.790	0.068	101	96	98	69	-76	1.35E-05	2.99E-05	6.63E-05	
OVCAR-3	0.534	1.026	1.065	1.046	1.024	0.840	0.111	108	104	100	62	-79	1.22E-05	2.75E-05	6.21E-05	
OVCAR-4	0.510	1.249	1.252	1.269	1.178	0.941	0.131	100	103	90	58	-74	1.16E-05	2.75E-05	6.56E-05	
OVCAR-5	0.596	1.335	1.338	1.407	1.406	1.254	0.062	100	110	110	89	-90	1.65E-05	3.15E-05	6.00E-05	
OVCAR-8	0.230	0.832	0.821	0.795	0.792	0.662	0.077	98	94	93	72	-67	1.44E-05	3.30E-05	7.57E-05	
SK-OV-3	0.356	0.852	0.853	0.882	0.840	0.743	0.119	100	106	97	78	-67	1.56E-05	3.46E-05	7.67E-05	
<b>Renal Cancer</b>																
786-0	0.429	1.538	1.608	1.532	1.574	1.293	0.098	106	99	103	78	-77	1.51E-05	3.18E-05	6.68E-05	
A498	0.991	1.682	1.738	1.669	1.641	1.446	0.014	108	98	94	66	-99	1.25E-05	2.51E-05	5.06E-05	
ACHN	0.341	1.309	1.271	1.305	1.275	0.851	0.020	96	100	96	53	-94	1.04E-05	2.28E-05	5.00E-05	
CAKI-1	0.413	1.217	1.171	1.183	1.106	0.870	0.133	94	96	86	57	-68	1.13E-05	2.85E-05	7.18E-05	
RXF 393	0.583	1.220	1.180	1.139	1.139	0.927	0.226	94	87	87	54	-61	1.08E-05	2.94E-05	7.99E-05	
SN12C	0.302	1.001	0.990	0.970	1.033	0.827	0.045	98	96	105	75	-85	1.43E-05	2.94E-05	6.04E-05	
TK-10	0.520	1.310	1.328	1.389	1.405	1.141	0.080	102	110	112	79	-85	1.50E-05	3.03E-05	6.13E-05	
<b>Prostate Cancer</b>																
PC-3	0.293	0.904	0.930	0.931	0.932	0.812	0.039	104	104	105	85	-87	1.60E-05	3.12E-05	6.11E-05	
DU-145	0.265	0.833	0.833	0.766	0.808	0.610	0.082	100	88	96	61	-69	1.21E-05	2.93E-05	7.11E-05	
<b>Breast Cancer</b>																
MCF7	0.316	1.580	1.599	1.481	1.538	1.470	0.054	102	92	97	91	-83	1.72E-05	3.34E-05	6.46E-05	
NCI/ADR-RES	0.282	0.814	0.830	0.818	0.814	0.726	0.090	103	101	100	83	-68	1.66E-05	3.55E-05	7.60E-05	
MDA-MB-231/ATCC	0.391	0.833	0.813	0.860	0.829	0.721	0.074	95	106	99	75	-81	1.44E-05	3.01E-05	6.31E-05	
HS 578T	0.225	0.899	0.910	0.883	0.938	0.876	0.148	102	98	106	97	-34	2.27E-05	5.47E-05	>1.00E-04	
MDA-MB-435	0.297	1.271	1.246	1.217	1.165	0.971	0.019	97	95	89	69	-94	1.31E-05	2.66E-05	5.40E-05	
MDA-N	0.691	2.314	2.292	2.214	2.478	2.194	0.012	99	94	110	93	-98	1.67E-05	3.06E-05	5.59E-05	
BT-549	0.304	0.746	0.745	0.714	0.767	0.698	0.050	100	93	105	89	-84	1.69E-05	3.28E-05	6.39E-05	
T-47D	0.433	1.026	0.970	0.994	0.942	0.818	0.210	91	95	86	65	-52	1.34E-05	3.61E-05	9.69E-05	

### Mean Graphs

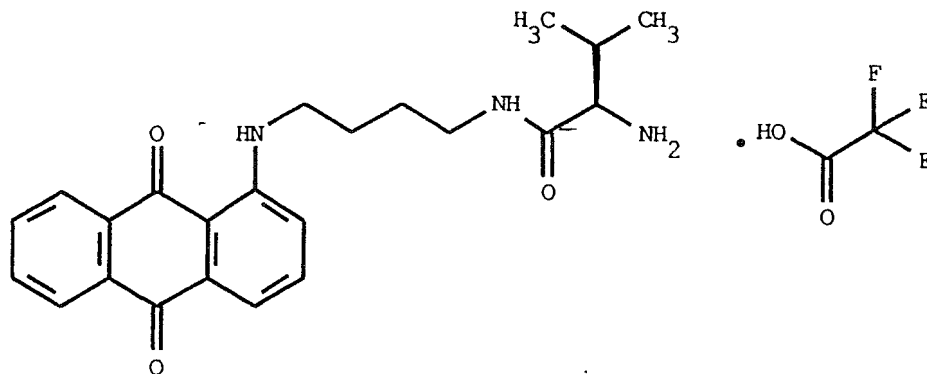
Report Date: August 6, 1999

Test Date: July 12, 1999

Panel/Cell Line	Log <sub>10</sub> GI50	GI50	Log <sub>10</sub> TGI	TGI	Log <sub>10</sub> LC50	LC50
<b>Leukemia</b>						
CCRF-CEM	-4.90		-4.56		-4.22	
HL-60(TB)	-4.94		-4.60		-4.25	
K-562	-4.83		> -4.00		> -4.00	
MOLT-4	-4.89		-4.51		-4.13	
SR	-4.99		-4.61		-4.23	
<b>Non-Small Cell Lung Cancer</b>						
A549/ATCC	-4.80		-4.49		-4.18	
EKVX	-4.89		-4.53		-4.18	
HOP-62	-4.75		-4.42		-4.09	
HOP-92	-4.80		-4.47		-4.14	
NCI-H226	-4.91		-4.55		-4.18	
NCI-H23	-4.76		-4.49		-4.22	
NCI-H460	-4.81		-4.45		-4.10	
NCI-H522	-4.82		-4.48		-4.13	
<b>Colon Cancer</b>						
COLO 205	-4.82		-4.54		-4.25	
HCC-2998	-4.76		-4.49		-4.21	
HCT-116	-4.86		-4.57		-4.27	
HCT-15	-4.91		-4.61		-4.30	
HT29	-4.83		-4.55		-4.27	
KM12	-4.91		-4.55		-4.19	
SW-620	-4.81		-4.32		> -4.00	
<b>CNS Cancer</b>						
SF-268	-4.74		-4.36		> -4.00	
SF-295	-4.81		-4.51		-4.21	
SNB-19	-4.87		-4.53		-4.18	
SNB-75	-4.91		-4.51		-4.10	
U251	-4.89		-4.56		-4.23	
<b>Melanoma</b>						
LOX IMVI	-4.87		-4.49		-4.11	
MALME-3M	-4.73		-4.41		-4.10	
M14	-4.76		-4.47		-4.19	
SK-MEL-28	-4.79		-4.46		-4.13	
SK-MEL-5	-4.79		-4.53		-4.26	
UACC-257	-4.72		-4.45		-4.17	
UACC-62	-4.86		-4.56		-4.26	
<b>Ovarian Cancer</b>						
IGROV1	-4.87		-4.52		-4.18	
OVCAR-3	-4.91		-4.56		-4.21	
OVCAR-4	-4.94		-4.56		-4.18	
OVCAR-5	-4.78		-4.50		-4.22	
OVCAR-8	-4.84		-4.48		-4.12	
SK-OV-3	-4.81		-4.46		-4.12	
<b>Renal Cancer</b>						
786-0	-4.82		-4.50		-4.18	
A498	-4.90		-4.60		-4.30	
ACHN	-4.98		-4.64		-4.30	
CAKI-1	-4.95		-4.55		-4.14	
RXF 393	-4.97		-4.53		-4.10	
SN12C	-4.84		-4.53		-4.22	
TK-10	-4.82		-4.52		-4.21	
<b>Prostate Cancer</b>						
PC-3	-4.80		-4.51		-4.21	
DU-145	-4.92		-4.53		-4.15	
<b>Breast Cancer</b>						
MCF7	-4.76		-4.48		-4.19	
NCI/ADR-RES	-4.78		-4.45		-4.12	
MDA-MB-231/ATCC	-4.84		-4.52		-4.20	
HS 578T	-4.64		-4.26		> -4.00	
MDA-MB-435	-4.88		-4.58		-4.27	
MDA-N	-4.78		-4.51		-4.25	
BT-549	-4.77		-4.48		-4.19	
T-47D	-4.87		-4.44		-4.01	
MG_MID	-4.84		-4.50		-4.17	
Delta	0.15		0.15		0.13	
Range	0.34		0.64		0.30	



NSC D- 709769



DRUG SYNTHESIS AND CHEMISTRY BRANCH, DTP, DCTD, NCI  
NSC NUMBER LIST

Dr. R. C. Harrison  
Pharmaceuticals Division  
British Technology Group  
101 Newington Causeway  
London SE1 6BU  
United Kingdom

Transmittal Letter or Collection Date: 01/26/99  
Supplier Compound ID: NU:UB 80  
NSC Number: D709769-V  
Molecular Formula: C<sub>23</sub>H<sub>27</sub>N<sub>3</sub>O<sub>3</sub>.C<sub>2</sub>HF<sub>3</sub>O<sub>2</sub>  
Acquired for Testing Against: CANCER

# National Cancer Institute Developmental Therapeutics Program In-Vitro Testing Results

NSC: D-709769 -V / 1	Experiment ID: 9907MD58-32	Test Type: 08	Units: Molar
Report Date: August 5, 1999	Test Date: July 6, 1999	QNS:	MC:
COMI: NU:UB 80	Stain Reagent: SRB Dual-P	SSPL: 0B6Z	

Panel/Cell Line	Time Zero	Log10 Concentration								Percent Growth				GI50	TGI	LC50
		Ctrl	-8.0	-7.0	-6.0	-5.0	-4.0	-8.0	-7.0	-6.0	-5.0	-4.0				
<b>Leukemia</b>																
CCRFL-CEM	0.107	0.456	0.417	0.425	0.435	0.059	0.013	89	91	94	-45	-88	2.06E-06	4.72E-06	1.28E-05	
HL-60(TB)	0.246	1.197	1.258	1.211	1.119	0.046	0.053	106	101	92	-81	-78	1.74E-06	3.39E-06	6.59E-06	
K-562	0.157	1.369	1.317	1.292	1.210	0.076	0.073	96	94	87	-52	-54	1.84E-06	4.23E-06	9.69E-06	
MOLT-4	0.149	0.640	0.615	0.678	0.596	0.120	0.076	95	108	91	-19	-49	2.35E-06	6.67E-06	>1.00E-04	
SR	0.136	0.415	0.437	0.445	0.407	0.171	0.185	108	111	97	13	17	3.61E-06	>1.00E-04	>1.00E-04	
<b>Non-Small Cell Lung Cancer</b>																
A549/ATCC	0.198	1.042	1.069	1.042	1.054	0.323	0.016	103	100	101	15	-92	3.92E-06	1.38E-05	4.05E-05	
EKVX	0.630	1.291	1.300	1.272	1.286	1.036	0.169	101	97	99	61	-73	1.22E-05	2.86E-05	6.73E-05	
HOP-62	0.199	0.476	0.448	0.459	0.466	0.165	0.042	90	94	96	-17	-79	2.56E-06	7.06E-06	3.39E-05	
NCI-H23	0.301	0.903	0.945	0.950	0.876	0.632	-0.022	107	108	96	55	-100	1.08E-05	2.26E-05	4.76E-05	
NCI-H322M	0.427	1.290	1.257	1.162	1.286	0.478	0.065	96	85	100	6	-85	3.38E-06	1.16E-05	4.13E-05	
NCI-H460	0.312	1.646	1.556	1.698	1.663	0.102	0.016	93	104	101	-67	-95	2.01E-06	3.99E-06	7.89E-06	
NCI-H522	0.262	0.804	0.782	0.813	0.802	0.065	0.018	96	102	100	-75	-93	1.92E-06	3.71E-06	7.16E-06	
<b>Colon Cancer</b>																
COLO 205	0.406	1.511	1.522	1.538	1.454	-0.005	0.015	101	102	95	-100	-96	1.70E-06	3.07E-06	5.54E-06	
HCC-2998	0.360	0.772	0.698	0.775	0.754	-0.005	-0.009	82	101	96	-100	-100	1.71E-06	3.08E-06	5.55E-06	
HCT-116	0.254	1.411	1.583	1.682	1.536	0.304	0.073	115	123	111	4	-71	3.72E-06	1.14E-05	5.23E-05	
HCT-15	0.169	1.108	1.085	1.173	1.107	0.168	0.010	98	107	100	-1	-94	3.13E-06	9.80E-06	3.36E-05	
HT29	0.162	0.995	1.001	0.960	0.989	0.084	0.033	101	96	99	-48	-80	2.16E-06	4.71E-06	1.14E-05	
KM12	0.286	1.186	1.190	1.206	1.137	0.305	0.073	100	102	95	2	-74	3.03E-06	1.07E-05	4.79E-05	
SW-620	0.066	0.457	0.477	0.438	0.463	0.035	-0.013	105	95	102	-48	-100	2.22E-06	4.79E-06	1.11E-05	
<b>CNS Cancer</b>																
SF-268	0.250	1.052	1.065	1.088	1.039	0.651	0.070	102	105	98	50	-72	1.00E-05	2.57E-05	6.60E-05	
SF-295	0.454	1.188	1.189	1.186	1.221	0.429	0.066	100	100	104	-6	-85	3.13E-06	8.91E-06	3.60E-05	
SF-539	0.568	1.051	1.050	1.122	1.094	0.037	0.001	100	115	109	-94	-100	1.95E-06	3.45E-06	6.09E-06	
SNB-19	0.335	1.015	1.022	1.063	1.003	0.332	0.020	101	107	98	-1	-94	3.06E-06	9.76E-06	3.35E-05	
SNB-75	0.265	0.572	0.565	0.546	0.565	0.387	0.057	98	91	98	40	-79	6.66E-06	2.17E-05	5.73E-05	
U251	0.161	0.972	0.908	0.955	0.928	0.118	0.015	92	98	95	-27	-91	2.33E-06	6.02E-06	2.31E-05	
<b>Melanoma</b>																
MALME-3M	0.367	0.861	0.876	0.884	0.920	0.053	-0.020	103	105	112	-86	-100	2.06E-06	3.69E-06	6.61E-06	
M14	0.295	1.043	1.062	1.072	1.055	0.036	-0.001	103	104	102	-88	-100	1.87E-06	3.44E-06	6.32E-06	
SK-MEL-2	0.257	0.729	0.652	0.733	0.679	0.058	-0.002	84	101	90	-78	-100	1.72E-06	3.43E-06	6.83E-06	
SK-MEL-28	0.267	0.960	0.950	0.938	0.969	0.065	0.018	99	97	101	-76	-93	1.95E-06	3.74E-06	7.16E-06	
SK-MEL-5	0.428	1.658	1.688	1.688	1.641	-0.014	-0.018	102	102	99	-100	-100	1.76E-06	3.14E-06	5.60E-06	
UACC-257	0.554	1.147	1.076	1.140	1.156	0.072	-0.007	88	99	102	-87	-100	1.88E-06	3.45E-06	6.36E-06	
UACC-62	0.700	1.598	1.603	1.596	1.696	0.045	-0.009	101	100	111	-94	-100	1.98E-06	3.48E-06	6.12E-06	
<b>Ovarian Cancer</b>																
OVCAR-3	0.446	0.779	0.766	0.763	0.748	0.307	0.102	96	95	91	-31	-77	2.16E-06	5.55E-06	2.56E-05	
OVCAR-4	0.265	0.729	0.732	0.716	0.691	0.296	0.112	101	97	92	7	-58	3.10E-06	1.27E-05	7.54E-05	
OVCAR-5	0.774	1.636	1.656	1.560	1.616	1.299	0.085	102	91	98	61	-89	1.18E-05	2.55E-05	5.49E-05	
SK-OV-3	0.281	0.506	0.499	0.504	0.505	0.190	0.040	97	99	99	-32	-86	2.37E-06	5.68E-06	2.13E-05	
<b>Renal Cancer</b>																
786-0	0.226	0.792	0.964	0.906	0.827	0.077	0.046	130	120	106	-66	-80	2.12E-06	4.13E-06	8.06E-06	
A498	0.848	1.398	1.404	1.394	1.392	1.143	0.011	101	99	99	54	-99	1.06E-05	2.25E-05	4.79E-05	
ACHN	0.237	0.828	0.843	0.858	0.848	0.257	-0.015	102	105	103	3	-100	3.42E-06	1.08E-05	3.28E-05	
CAKI-1	0.454	1.077	1.109	1.093	1.060	0.509	0.069	105	102	97	9	-85	3.42E-06	1.24E-05	4.24E-05	
RXF 393	0.359	0.824	0.795	0.790	0.779	0.225	0.053	94	93	90	-37	-85	2.07E-06	5.10E-06	1.84E-05	
SN12C	0.377	1.016	1.120	1.091	1.031	0.525	0.078	116	112	102	23	-79	4.59E-06	1.68E-05	5.18E-05	
TK-10	0.529	1.129	1.032	1.155	1.155	0.686	-0.006	84	104	104	26	-100	4.95E-06	1.61E-05	4.01E-05	
UO-31	0.242	0.694	0.626	0.693	0.788	0.090	0.010	85	100	121	-63	-96	2.43E-06	4.54E-06	8.50E-06	
<b>Prostate Cancer</b>																
PC-3	0.189	0.725	0.634	0.717	0.700	0.168	-0.002	83	98	95	-11	-100	2.66E-06	7.82E-06	2.73E-05	
DU-145	0.211	0.776	0.794	0.744	0.798	0.447	0.002	103	94	104	42	-99	7.36E-06	1.98E-05	4.48E-05	
<b>Breast Cancer</b>																
MCF7	0.245	0.888	0.851	0.870	0.895	0.121	0.009	94	97	101	-51	-97	2.17E-06	4.64E-06	9.91E-06	
NCI/ADR-RES	0.299	0.739	0.739	0.772	0.771	0.417	0.071	100	107	107	27	-76	5.14E-06	1.82E-05	5.56E-05	
MDA-MB-231/ATCC	0.322	0.937	0.879	0.927	0.885	0.338	0.003	91	98	91	3	-99	2.93E-06	1.06E-05	3.29E-05	
HS 578T	0.106	0.466	0.480	0.475	0.480	0.176	0.073	104	103	104	19	-31	4.34E-06	2.41E-05	>1.00E-04	
MDA-MB-435	0.279	0.952	1.003	0.911	0.926	0.094	0.045	108	94	96	-66	-84	1.92E-06	3.91E-06	7.94E-06	
MDA-N	0.352	1.246	1.405	1.378	1.352	0.265	0.047	118	115	112	-25	-87	2.83E-06	6.58E-06	2.55E-05	
BT-549	0.502	1.099	1.135	1.119	1.123	0.901	0.020	106	103	104	67	-96	1.27E-05	2.57E-05	5.22E-05	
T-47D	0.300	0.716	0.709	0.687	0.678	0.246	0.121	98	93	91	-18	-60	2.37E-06	6.83E-06	5.86E-05	

# National Cancer Institute Developmental Therapeutics Program

NSC: D-709769 -V / 1

Units: Molar

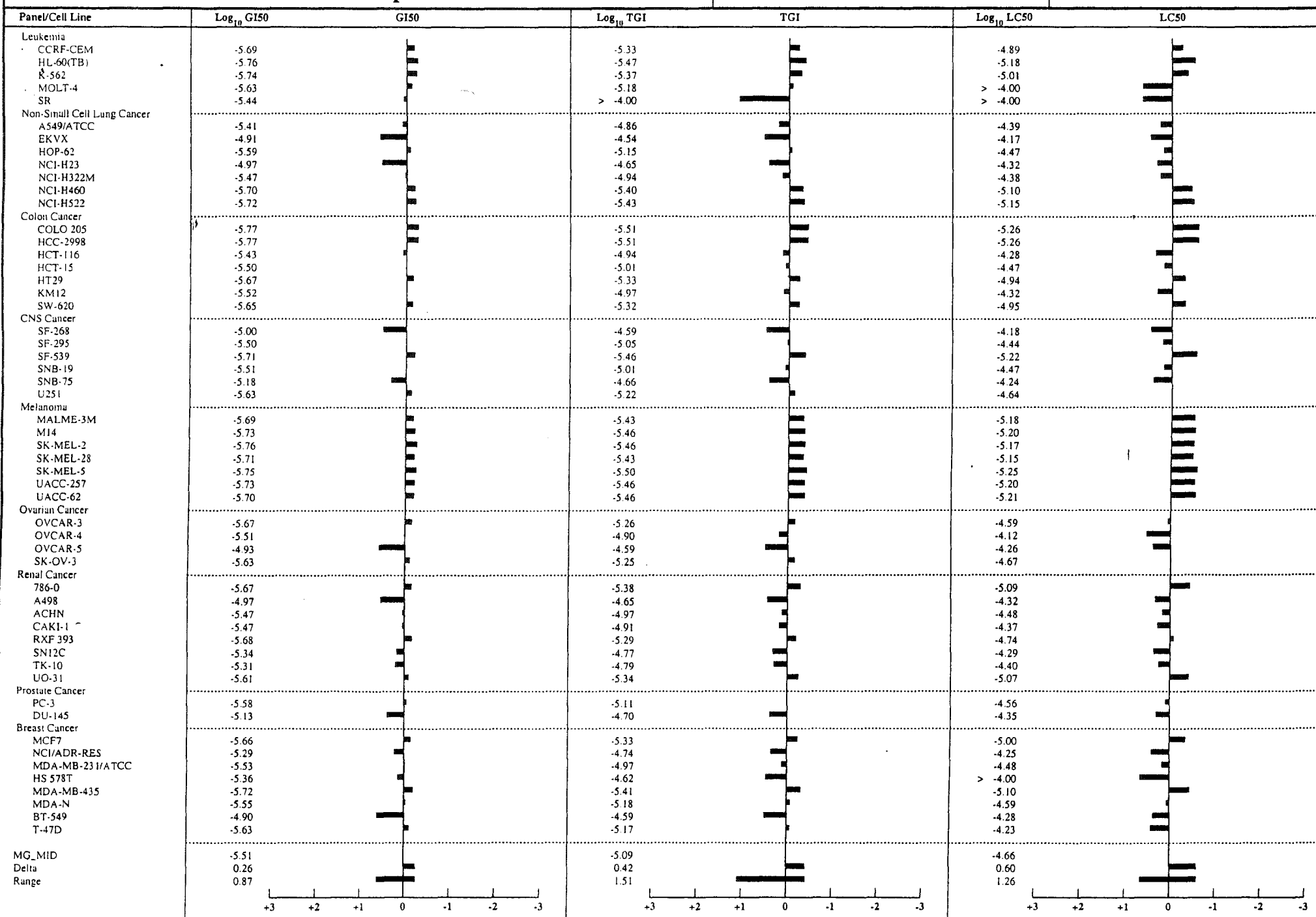
SSPL: 0B6Z

Exp. ID: 9907MD58-32

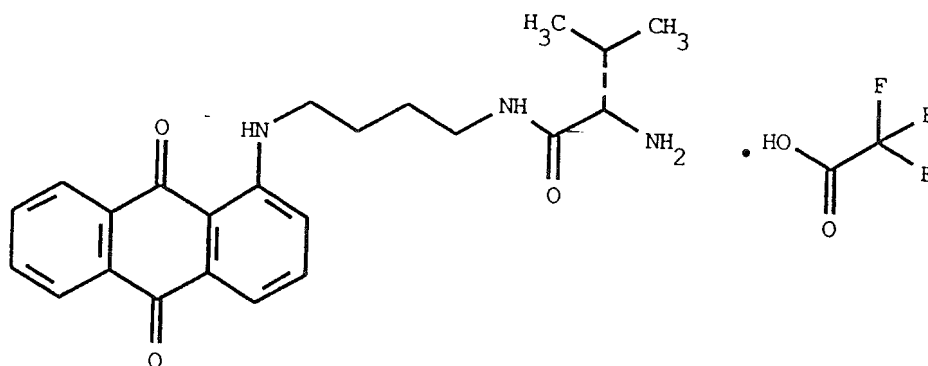
## Mean Graphs

Report Date: August 5, 1999

Test Date: July 6, 1999



NSC D- 709770



DRUG SYNTHESIS AND CHEMISTRY BRANCH, DTP, DCTD, NCI  
NSC NUMBER LIST

Dr. R. C. Harrison  
Pharmaceuticals Division  
British Technology Group  
101 Newington Causeway  
London SE1 6BU  
United Kingdom

Transmittal Letter or Collection Date: 01/26/99  
Supplier Compound ID: NU:UB 81  
NSC Number: D709770-W  
Molecular Formula: C<sub>23</sub>H<sub>27</sub>N<sub>3</sub>O<sub>3</sub>.C<sub>2</sub>H<sub>2</sub>F<sub>3</sub>O<sub>2</sub>  
Acquired for Testing Against: CANCER

# National Cancer Institute Developmental Therapeutics Program In-Vitro Testing Results

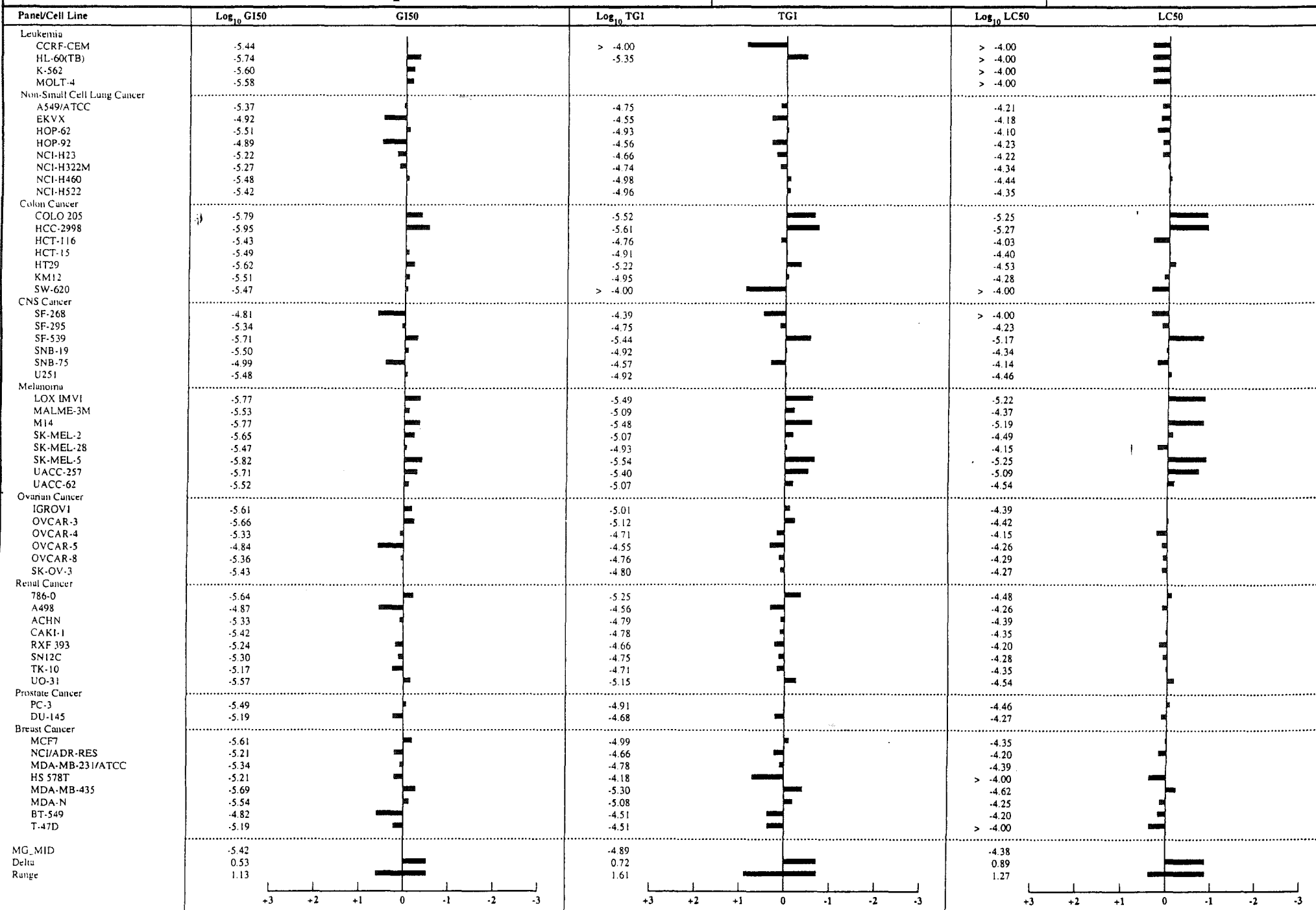
NSC: D-709770-W/1	Experiment ID: 9907MD58-33	Test Type: 08	Units: Molar
Report Date: August 5, 1999	Test Date: July 6, 1999	QNS:	MC:
COMI: NU:UB 81	Stain Reagent: SRB Dual-P	SSPL: 0B6Z	

Panel/Cell Line	Time		Mean Optical Densities					Percent Growth					GI50	TGI	LC50	
	Zero	Ctrl	-8.0	-7.0	-6.0	-5.0	-4.0	-8.0	-7.0	-6.0	-5.0	-4.0				
<b>Leukemia</b>																
CCRF-CEM	0.107	0.447	0.396	0.406	0.438	0.151	0.138	85	88	97	13	9	3.62E-06	>1.00E-04	>1.00E-04	
HL-60(TB)	0.246	1.066	0.908	0.886	0.937	0.136	0.184	81	78	84	-45	-25	1.84E-06	4.50E-06	>1.00E-04	
K-562	0.157	1.250	1.248	1.257	1.266	0.113	0.252	100	101	101	-28	9	2.49E-06		>1.00E-04	
MOLT-4	0.149	0.635	0.640	0.638	0.620	0.129	0.247	101	101	97	-14	20	2.66E-06		>1.00E-04	
<b>Non-Small Cell Lung Cancer</b>																
A549/ATCC	0.198	0.999	0.980	0.988	0.966	0.387	0.060	98	99	96	24	-70	4.31E-06	1.79E-05	6.12E-05	
EKVX	0.630	1.370	1.364	1.361	1.387	1.086	0.157	99	99	102	62	-75	1.21E-05	2.82E-05	6.55E-05	
HOP-62	0.199	0.534	0.498	0.553	0.513	0.214	0.088	89	106	94	4	-56	3.08E-06	1.18E-05	7.95E-05	
HOP-92	0.394	0.919	0.942	0.932	0.874	0.745	0.063	104	103	91	67	-84	1.29E-05	2.77E-05	5.94E-05	
NCI-H23	0.301	0.946	0.937	0.986	0.885	0.549	0.075	99	106	91	38	-75	5.98E-06	2.18E-05	6.01E-05	
NCI-H322M	0.427	1.358	1.308	1.354	1.333	0.730	0.031	95	100	97	33	-93	5.37E-06	1.82E-05	4.56E-05	
NCI-H460	0.312	1.582	1.623	1.515	1.599	0.337	0.031	103	95	101	2	-90	3.28E-06	1.05E-05	3.67E-05	
NCI-H522	0.262	0.690	0.705	0.761	0.759	0.275	0.057	103	116	116	3	-78	3.84E-06	1.09E-05	4.49E-05	
<b>Colon Cancer</b>																
COLO-205	0.406	1.459	1.309	1.335	1.360	0.010	-0.004	86	88	91	-98	-100	1.64E-06	3.03E-06	5.58E-06	
HCC-2998	0.360	0.667	0.676	0.671	0.537	0.037	0.024	103	101	58	-90	-93	1.13E-06	2.46E-06	5.38E-06	
HCT-116	0.254	1.538	1.388	1.508	1.465	0.463	0.123	88	98	94	16	-52	3.70E-06	1.73E-05	9.42E-05	
HCT-15	0.169	1.142	1.174	1.106	1.070	0.255	0.017	103	96	93	9	-90	3.23E-06	1.23E-05	3.94E-05	
HT29	0.162	0.999	0.977	0.963	0.985	0.118	0.040	97	96	98	-27	-75	2.42E-06	6.05E-06	2.96E-05	
KM12	0.286	1.218	1.125	1.191	1.159	0.324	0.084	90	97	94	4	-71	3.07E-06	1.13E-05	5.27E-05	
SW-620	0.066	0.525	0.484	0.540	0.484	0.126	0.069	91	103	91	13	1	3.35E-06	>1.00E-04	>1.00E-04	
<b>CNS Cancer</b>																
SF-268	0.250	0.940	0.926	0.914	0.893	0.748	0.133	98	96	93	72	-47	1.54E-05	4.04E-05	>1.00E-04	
SF-295	0.454	1.326	1.234	1.297	1.331	0.660	0.126	89	97	100	24	-72	4.53E-06	1.76E-05	5.85E-05	
SF-539	0.568	1.040	0.920	0.992	1.066	0.099	-0.003	75	90	105	-83	-100	1.97E-06	3.64E-06	6.70E-06	
SNB-19	0.335	1.023	0.996	1.046	0.977	0.382	0.068	96	103	93	7	-80	3.17E-06	1.20E-05	4.53E-05	
SNB-75	0.265	0.600	0.541	0.589	0.602	0.437	0.089	82	97	101	51	-67	1.02E-05	2.72E-05	7.23E-05	
U251	0.161	0.857	0.833	0.804	0.814	0.225	-0.001	97	92	94	9	-100	3.30E-06	1.21E-05	3.48E-05	
<b>Melanoma</b>																
LOX IMVI	0.085	0.817	0.827	0.797	0.757	0.009	0.034	101	97	92	-89	-60	1.70E-06	3.21E-06	6.06E-06	
MALME-3M	0.367	0.773	0.851	0.880	0.792	0.327	0.099	119	126	105	-11	-73	2.97E-06	8.05E-06	4.26E-05	
M14	0.295	1.065	1.058	1.046	0.988	0.052	0.046	99	97	90	-83	-84	1.70E-06	3.32E-06	6.48E-06	
SK-MEL-2	0.257	0.701	0.675	0.646	0.614	0.243	0.018	94	87	80	-6	-93	2.25E-06	8.60E-06	3.21E-05	
SK-MEL-28	0.267	1.070	1.025	1.070	1.073	0.304	0.108	94	100	100	5	-60	3.36E-06	1.18E-05	7.06E-05	
SK-MEL-5	0.428	1.634	1.483	1.530	1.408	0.023	-0.023	88	91	81	-95	-100	1.51E-06	2.90E-06	5.58E-06	
UACC-257	0.554	1.129	1.131	1.125	1.119	0.193	0.068	100	99	98	-65	-88	1.97E-06	3.99E-06	8.08E-06	
UACC-62	0.700	1.699	1.622	1.751	1.725	0.644	0.011	92	105	103	-8	-99	2.99E-06	8.45E-06	2.91E-05	
<b>Ovarian Cancer</b>																
IGROV1	0.110	0.786	0.777	0.754	0.673	0.109	0.020	99	95	83	-1	-82	2.48E-06	9.75E-06	4.04E-05	
OVCA-3	0.446	0.828	0.783	0.832	0.758	0.398	0.097	88	101	82	-11	-78	2.20E-06	7.65E-06	3.81E-05	
OVCA-4	0.265	0.816	0.757	0.792	0.807	0.408	0.098	89	96	98	26	-63	4.66E-06	1.96E-05	7.14E-05	
OVCA-5	0.774	1.725	1.693	1.718	1.680	1.500	0.042	97	99	95	76	-95	1.43E-05	2.80E-05	5.48E-05	
OVCA-8	0.121	0.875	0.924	0.889	0.835	0.308	0.024	107	102	95	25	-81	4.36E-06	1.72E-05	5.12E-05	
SK-OV-3	0.281	0.561	0.501	0.537	0.537	0.335	0.070	78	92	91	19	-75	3.74E-06	1.60E-05	5.42E-05	
<b>Renal Cancer</b>																
786-0	0.226	0.877	0.807	0.913	0.853	0.154	0.075	89	106	96	-32	-67	2.29E-06	5.62E-06	3.28E-05	
A498	0.848	1.443	1.389	1.451	1.516	1.272	0.068	91	101	112	71	-92	1.35E-05	2.73E-05	5.53E-05	
ACHN	0.237	0.853	0.820	0.847	0.835	0.403	0.002	95	99	97	27	-99	4.70E-06	1.63E-05	4.07E-05	
CAKI-1	0.454	1.154	1.008	1.126	1.048	0.630	0.047	79	96	85	25	-90	3.83E-06	1.65E-05	4.21E-05	
RXF 393	0.359	0.823	0.756	0.833	0.790	0.530	0.100	85	102	93	37	-72	5.80E-06	2.17E-05	6.25E-05	
SN12C	0.377	0.972	0.892	0.986	1.004	0.530	0.078	87	102	105	26	-79	4.96E-06	1.76E-05	5.25E-05	
TK-10	0.529	1.127	1.170	1.174	1.145	0.765	0.012	107	108	103	39	-98	6.81E-06	1.94E-05	4.49E-05	
UO-31	0.242	0.661	0.627	0.587	0.660	0.201	0.026	92	82	100	-17	-89	2.67E-06	7.16E-06	2.87E-05	
<b>Prostate Cancer</b>																
PC-3	0.189	0.653	0.642	0.630	0.615	0.234	-0.001	98	95	92	10	-100	3.23E-06	1.22E-05	3.50E-05	
DU-145	0.211	0.787	0.716	0.787	0.768	0.438	0.038	88	100	97	39	-82	6.53E-06	2.11E-05	5.43E-05	
<b>Breast Cancer</b>																
MCF7	0.245	0.911	0.869	0.821	0.786	0.249	0.057	94	86	81	1	-77	2.44E-06	1.02E-05	4.51E-05	
NCI/ADR-RES	0.299	0.889	0.908	0.860	0.873	0.518	0.085	103	95	97	37	-72	6.11E-06	2.19E-05	6.31E-05	
MDA-MB-231/ATCC	0.322	0.871	0.849	0.883	0.836	0.474	0.001	96	102	94	28	-100	4.59E-06	1.65E-05	4.07E-05	
HS 578T	0.106	0.465	0.413	0.426	0.451	0.241	0.097	85	89	96	38	-8	6.13E-06	6.54E-05	>1.00E-04	
MDA-MB-435	0.279	1.011	0.928	1.011	0.926	0.175	0.083	89	100	88	-37	-70	2.02E-06	5.04E-06	2.41E-05	
MDA-N	0.352	1.370	1.247	1.385	1.367	0.322	0.129	88	101	100	-9	-63	2.88E-06	8.32E-06	5.67E-05	
BT-549	0.502	1.171	1.186	1.250	1.181	1.027	0.089	102	112	101	78	-82	1.50E-05	3.08E-05	6.30E-05	
T-47D	0.300	0.725	0.663	0.714	0.698	0.469	0.175	85	98	94	40	-42	6.45E-06	3.07E-05	>1.00E-04	

Mean Graphs

Report Date: August 5, 1999

Test Date: July 6, 1999



## **APPENDIX 3**

## Assessment of *in vivo* drug activity

Pure strain NMRI mice of 6-8 weeks old (B+K Universal Ltd, UK) were used for the assessment of *in vivo* drug activity.

MAC 15A tumours were established from cells grown in culture. Cells were pelleted and resuspended in 2ml of HBSS. 0.2ml of cell suspension was injected subcutaneously into the flank of NMRI mice. Treatment of mice commenced approximately 4-5 days after cell implantation when tumours were visible and of a measurable size (4x5mm).

NU:UB compound was dissolved in a DMSO/arachis oil (1/10) mixture and administered at suitable concentrations of (e.g. NU:UB 31 at 100 (MTD), 67 and 33 mgkg<sup>-1</sup>). Camptothecin was given in DMSO/oil and administered at 10 mgkg<sup>-1</sup> (MTD). Controls were treated with DMSO/oil. Mitoxantrone was dissolved in saline and administered at 5 mgkg<sup>-1</sup> (MTD). All treatments were intraperitoneal (IP).

Tumours were measured daily using calipers and the tumour volume calculated using the formula below (Geran *et al.*, 1972)

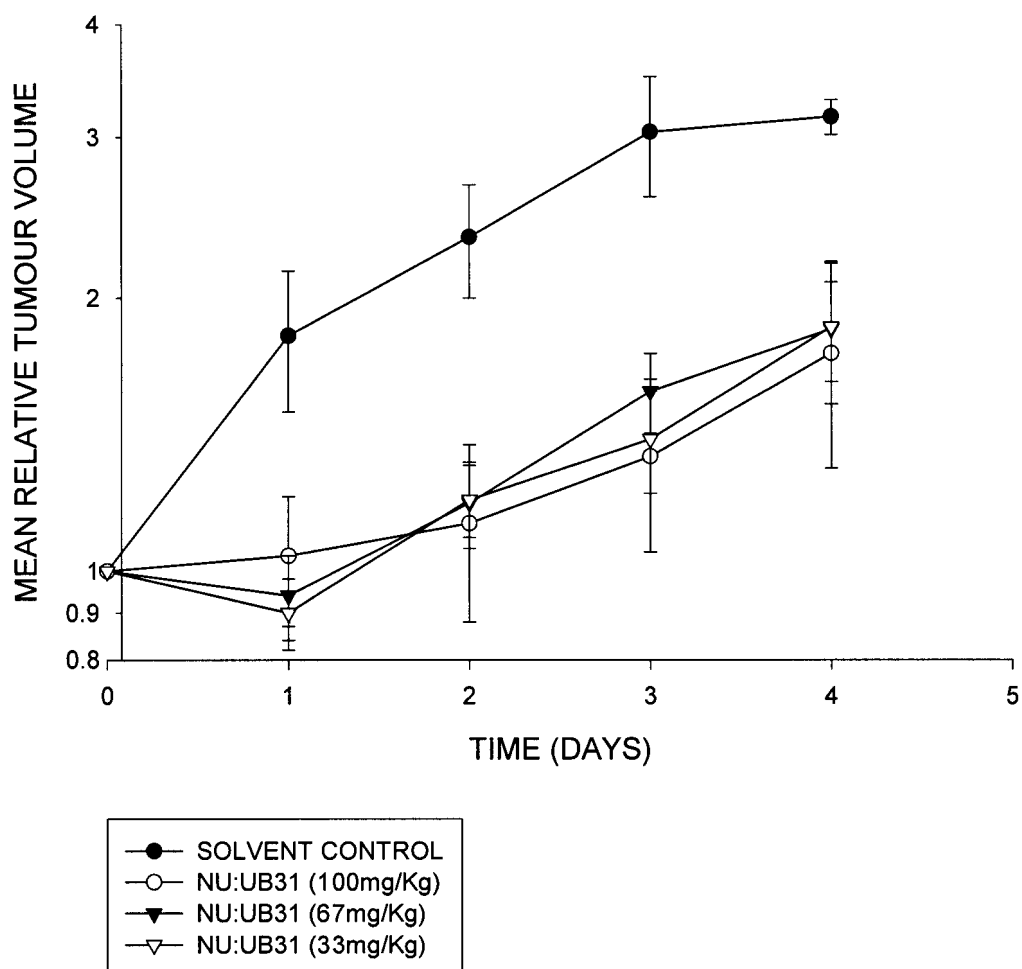
$$v = \frac{a^2 \times b}{2}$$

Where a = smaller diameter and b= larger diameter

The significance of any delays in tumour growth between control and treated groups of mice was determined by the use of the Mann-Whitney U-test using the time taken for the tumours to double in volume (RTV2).

Geran. R. I., Greenberg, N. H, and MacDonald, M. M. (1972). Protocols for screening chemical agents and natural products against tumours and other biological systems (third edition). *Cancer Chemotherapy Reports*, **3**:1-1033.

### MAC15A TUMOURS TREATED WITH NU:UB31

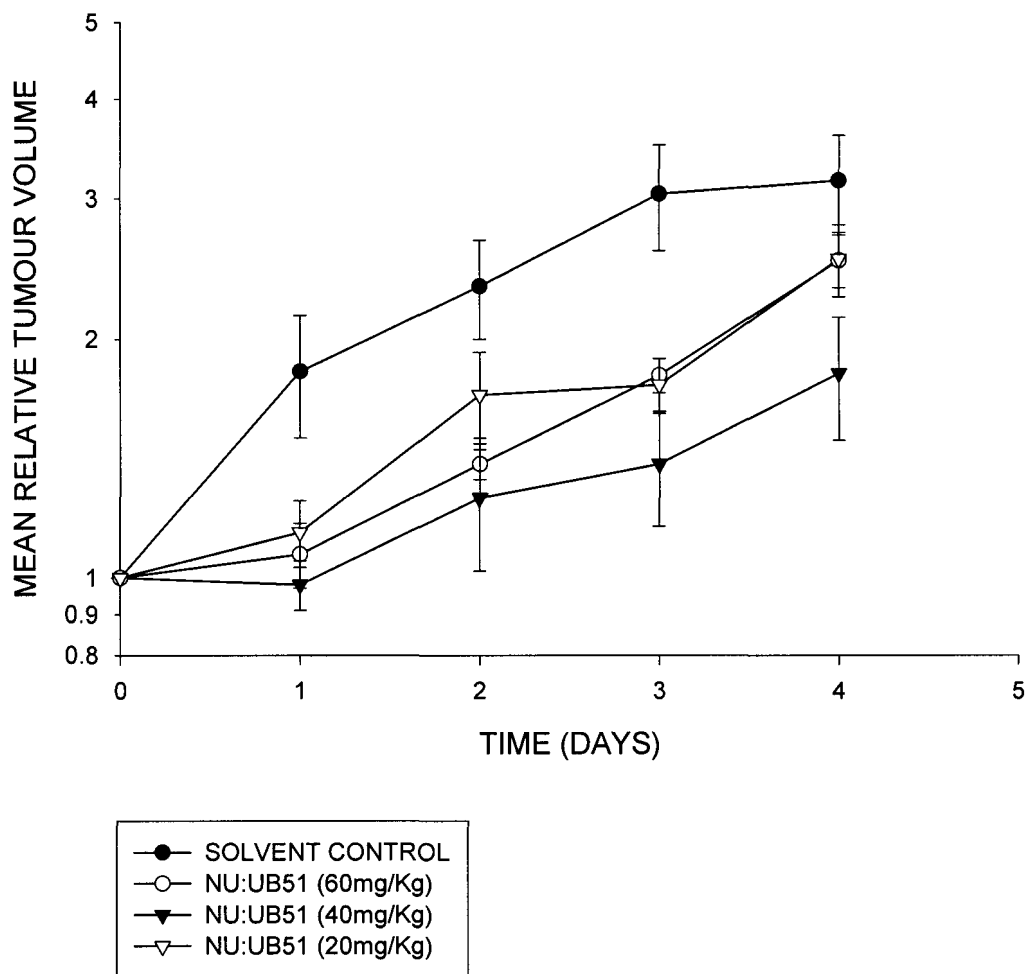


**Appendix 3, graph 1.** *In vivo* graph of relative tumour volume versus days for NU:UB 31.

DOSE (mg/Kg)	Growth delay (days)	Significance	% Weight loss
100	2.7	p<0.01	5.1%
67	4.3	p<0.01	2.3%
33	3.2	p<0.01	1.9%

**Appendix 3, table 1.** *In vivo* data of growth delay and weight loss relative to NU:UB 31 concentration.

## MAC15A TUMOURS TREATED WITH NU:UB51

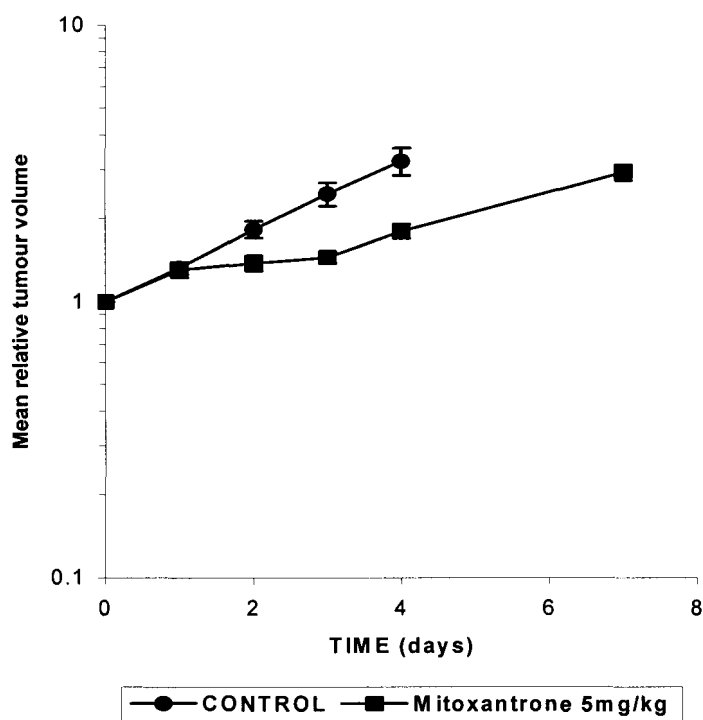


**Appendix 3, graph 2.** *In vivo* graph of relative tumour volume versus days for NU:UB 51.

DOSE (mg/Kg)	Growth delay (days)	Significance	% Weight loss
60	1.9	p<0.01	4.1%
40	3.5	p<0.05	3.2%
20	1.9	p<0.05	1.1%

**Appendix 3, table 2.** *In vivo* data of growth delay and weight loss relative to NU:UB 51 concentration.

## MAC15A TUMOURS TREATED WITH MITOXANTRONE

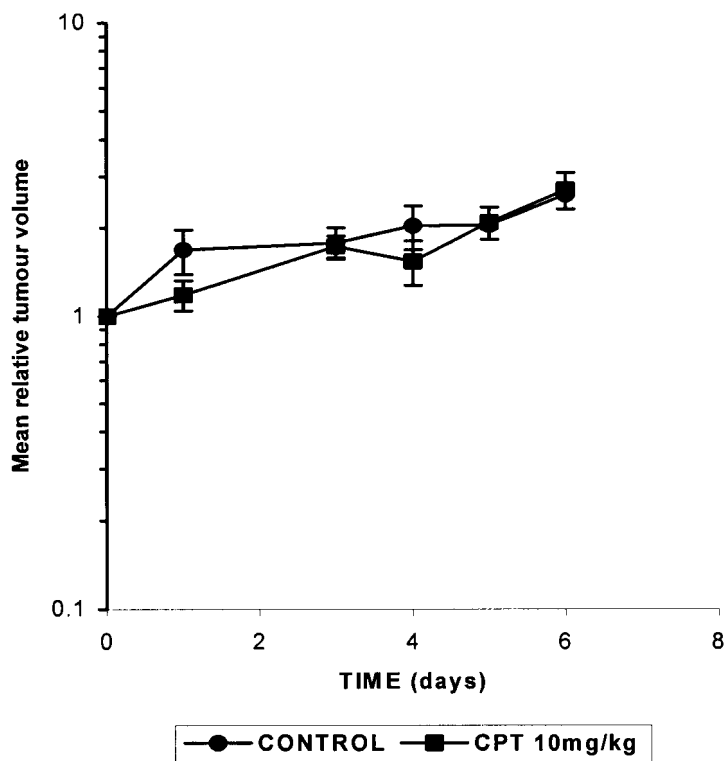


**Appendix 3, graph 3.** *In vivo* graph of relative tumour volume versus days of a single dose of mitoxantrone (mean  $\pm$ SEM, n=9).

Group	Mean time to RTV 2 (days)	Median time to RTV 2 (days)	Growth delay (days)	Significance	Maximum % weight loss
Control	2.5	2.6	-	-	10.5
Mitoxantrone 5mg/kg ip	5.0	4.9	2.3	P<0.01	20

**Appendix 3, table 3.** *In vivo* data of growth delay and weight loss relative to mitoxantrone concentration.

## MAC15A TUMOURS TREATED WITH CAMPTOTHECIN

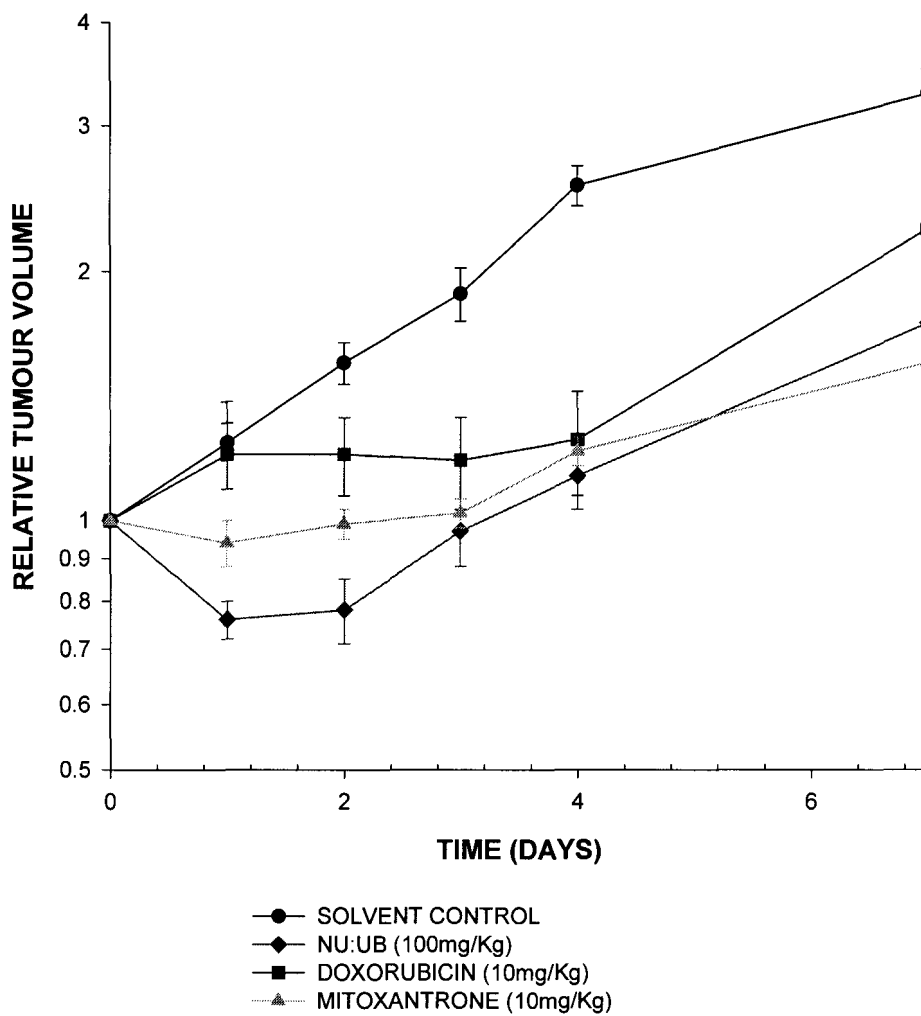


**Appendix 3, graph 4.** *In vivo* graph of relative tumour volume versus days of a single dose of camptothecin (mean  $\pm$ SEM, n=5).

Group	Mean time to RTV 2 (days)	Median time to RTV 2 (days)	Growth delay (days)	Significance	Maximum % weight loss
Solvent control (dms/oil)	2.9	3.5	-	-	-
Camptothecin 10mg/kg i.p	4.2	4.3	0.8	ns	8.6

**Appendix 3, table 4.** *In vivo* data of growth delay and weight loss relative to camptothecin concentration.

**Comparative *in vivo* data of NU:UB 31, doxorubicin and mitoxantrone against MAC15A adenocarcinoma of the colon**

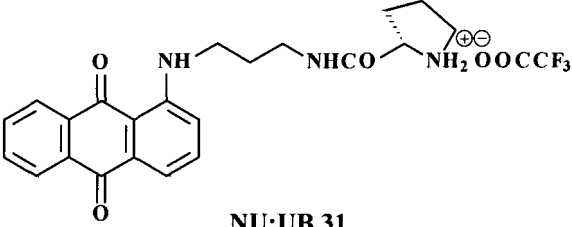


**Appendix 3, graph 5.** *In vivo* chemosensitivity against MAC15A adenocarcinoma of the colon, comparison of NU:UB 31, doxorubicin and mitoxantrone.

The anthraquinone NU:UB 31 showed a different behaviour to the anthraquinones mitoxantrone and doxorubicin. The latter induced a modest growth delay with no reduction in tumour volume whereas NU:UB 31 produced significant delay in this tumour model which is common with human clinical diseases is refractory to standard clinical agents. Thus, NU:UB 31 as well as NU:UB 51 was active *in vivo* in experimental colon cancer.

## **APPENDIX 4**

## Pharmacokinetics of NU:UB 31

 <b>NU:UB 31</b>			
IC <sub>50</sub> (μ M)[exposure] <i>in vitro</i> MAC 15A MTT assay	38 [1 h]	8 [24 h]	5 [96 h]
Stability: t <sub>1/2</sub> [hours] <i>in vitro</i>	> 100 h [ plasma]	75.1 h [culture medium]	25.7 h [whole blood]
Pharmacokinetics: t <sub>1/2</sub> <b>plasma</b> [hours] [i.p. at 100mgkg <sup>-1</sup> ]	2.2 hours and an AUC of 44.5 μg h ml <sup>-1</sup> [C <sub>max</sub> = 12 μg ml <sup>-1</sup> , at 30 min]		
Pharmacokinetics: t <sub>1/2</sub> <b>tumour</b> [hours] [i.p. at 100mgkg <sup>-1</sup> ]	6 hours and an AUC of 371 μg h g <sup>-1</sup> [C <sub>max</sub> = 39.5 μg g <sup>-1</sup> , at 2h]		
<b>CxT values</b>	176.2 μg hr ml <sup>-1</sup> [1 h]	82 μg hr ml <sup>-1</sup> [24 h]	18.8 μg hr ml <sup>-1</sup> [96 h]

**Appendix 4, table 1.** Pharmacokinetics data of NU:UB 31

IC<sub>50</sub> values for NU:UB 31 determined against MAC15A (murine adenocarcinoma) cells using MTT assay were 5μM, 8μM and 38μM for 96h, 24h and 1h exposures respectively.

A method has been developed to detect and analyse NU:UB 31 in biological samples using LC-MS. Assessment of the stability of NU:UB 31 *in vitro* gave t<sub>1/2</sub> values of 75.1 and 25.7 hours in tissue culture medium and whole murine blood respectively at 37°C. The compound was very stable in murine plasma with t<sub>1/2</sub> >100 hours.

Pharmacokinetic analysis of NU:UB 31 *in vivo* was assessed in MAC15A tumour bearing mice. NU:UB 31 was given i.p. at 100mgkg<sup>-1</sup> and plasma and tumour levels monitored over an 8 hour period. Drug concentration peaked in the plasma after 30 minutes (C<sub>max</sub> = 12 μg ml<sup>-1</sup>) with a t<sub>1/2</sub> value of 2.2 hours and an AUC of 44.5 μg h ml<sup>-1</sup>. Peak tumour concentrations exceeded those seen in the plasma by approximately 3-fold peaking at 2 hours (C<sub>max</sub> = 39.5 μg g<sup>-1</sup>) with a t<sub>1/2</sub> of 6 hours and an AUC of 371 μg h g<sup>-1</sup> (8-fold greater than plasma).

IC<sub>50</sub> values for the compound *in vitro* were converted to CxT values (taking into account the stability of the drug in tissue culture medium) giving values of 18.8, 82 and 176.2 μg hr/ml for

96h, 24h and 1h exposures respectively. The concentration of NU:UB 31 measured in MAC15A tumours *in vivo* therefore exceeds those of the *in vitro* IC<sub>50</sub> values. The concentration of NU:UB 31 in tumours and the long half life may go some way to explaining the good anti-tumour activity seen against MAC15A tumours.

## **APPENDIX 5**

<b>Compare Correlation LC<sub>50</sub></b>		
<b>NU:UB 31</b>		
Chemical Name	N	Pearson Corr. Coeff.
Bleomycin	60	0.509
Cyclopentenyl cytosine (M)	60	0.507
Brequinar (DUP785) (M)	60	0.486
Phosphotrienin	60	0.473
N-N-dibenzyl-daunomycin (T)	60	0.472
Anguidine	60	0.469
CCNU	60	0.452
Methyl CCNU	60	0.451
Topotecan (T)	60	0.439
D-tetrandrine	60	0.433
Amonafide (T)	60	0.424
<b>NU:UB 43</b>		
Aclacinomycin A (T)	57	0.663
Mitramycin	58	0.659
Deoxydoxorubicin (T)	58	0.653
5-Azacytidine	58	0.645
Cytembena	58	0.619
Anguidine	58	0.612
Bactobolin	58	0.607
Pancreatistatin (M)	58	0.604
Daunomycin (T)	58	0.598
Brequinar (DUP785) (M)	58	0.590
Thalicipine	58	0.583
<b>NU:UB 80</b>		
Aclacinomycin A (T)	57	0.630
Anguidine	58	0.625
Thalicipine	58	0.623
Pancreatistatin (M)	58	0.622
Mitomycin C	58	0.620
Adriamycin (T)	58	0.618
Triethylenemelamine	58	0.615
Daunomycin (T)	58	0.614
Mitramycin	58	0.610
Amonafide (T)	58	0.606
Actinomycin D (T)	58	0.602
<b>NU:UB 81</b>		
Brequinar (DUP785) (M)	58	0.720
Anguidine	58	0.669
Bactobolin	58	0.663
5-Azacytidine	58	0.658
Pancreatistatin (M)	58	0.650
Phyllanthoside	58	0.644
Amonafide (T)	58	0.641
Thalicipine	58	0.635
Aclacinomycin A (T)	57	0.632
Deoxydoxorubicin (T)	58	0.609
Cytembena	58	0.609

(T)-topoisomerase inhibitor, (M)-inhibitor of mitochondrial enzyme(s)